NATIONAL TECHNICAL UNIVERSITY OF ATHENS

SCHOOL OF CIVIL ENGINEERING

DEPARTMENT OF WATER RESOURCES AND ENVIRONMENTAL ENGINEERING

LABORATORY OF HARBOUR WORKS

Analysis of Coastal Storms for their Application in Harbours and Coastal Structures Design

PhD Thesis

Nikolaos Martzikos

Athens, July 2021

ΕΘΝΙΚΟ ΜΕΤΣΟΒΙΟ ΠΟΛΥΤΕΧΝΕΙΟ

ΣΧΟΛΗ ΠΟΛΙΤΙΚΩΝ ΜΗΧΑΝΙΚΩΝ

DEPARTMENT OF WATER ΤΟΜΕΑΣ ΥΔΑΤΙΚΩΝ ΠΟΡΩΝ ΚΑΙ ΠΕΡΙΒΑΛΛΟΝΤΟΣ

ΕΡΓΑΣΤΗΡΙΟ ΛΙΜΕΝΙΚΩΝ ΕΡΓΩΝ

Ανάλυση Παράκτιων Καταιγίδων για την Εφαρμογή τους στο Σχεδιασμό των Λιμενικών και Παράκτιων Έργων

ΔΙΔΑΚΤΟΡΙΚΗ ΔΙΑΤΡΙΒΗ

Για τον Επιστημονικό Τίτλο του «Διδάκτορα του ΕΜΠ»
στη Σχολή Πολιτικών Μηχανικών του Εθνικού Μετσόβιου Πολυτεχνείου

Νικόλαος Μαρτζίκος

Αθήνα, Ιούλιος 2021

NATIONAL TECHNICAL UNIVERSITY OF ATHENS

SCHOOL OF CIVIL ENGINEERING

DEPARTMENT OF WATER RESOURCES AND ENVIRONMENTAL ENGINEERING

LABORATORY OF HARBOUR WORKS

Analysis of Coastal Storms for their Application in Harbours and Coastal Structures Design

THESIS

submitted for the degree of Doctor of Philosophy

to the National Technical University of Athens

by

Nikolaos Martzikos

Defended in public, 19 July 2021

Athens, Greece

Members of the Examining Committee

Prof. Vasiliki Tsoukala	Sch. of Civil Eng. NTUA	*Supervisor*
Prof. Emer. Constantine Memos	Sch. of Civil Eng. NTUA	*Adv. Committee*
Prof. Panagiotis Prinos	Dep. of Civil Eng. AUTh	*Adv. Committee*
Prof. Dimitris Karlis	Dep. of Statistics AUEB	
Res. Director Takvor Soukissian	Inst. of Oceanography HCMR	
Assist. Prof. Vasiliki Katsardi	Dep. of Civil Eng. UTh	
Assoc. Prof. Aristeidis Nikoloulopoulos	Sch. of Computing Sciences UEA	

This doctoral thesis was implemented through a scholarship by State Scholarships Foundation (IKY), co-financed by Greece and the European Union (European Social Fund-ESF) through the Operational Programme «Human Resources Development, Education and Lifelong Learning» in the context of the project «Strengthening Human Resources Research Potential via Doctorate Research» (MIS-5000432).

You can never cross the ocean until you have the courage to lose sight of the shore.

Christopher Columbus

Let the knowledge be the boat, the sea to be your life and the coast on the other side to be always your dream. Even if you never dock, the view of the land will calm your restless mind. Ahoy!

Acknowledgements

This thesis is the harvest of a great mental effort that has monopolized my life over the last few years. This research is the consequence of a journey that I started at the Department of Mathematics (AUTH) and continued by adding the water element with a PhD in the School of Civil Engineering (NTUA) and a stopover at the School of Naval Architecture and Marine Engineering (NTUA) for my Master's degree. This thesis combines mathematics with the sea, two integral elements of my life, while applying the science in the field of Coastal Engineering.

I would like to express my gratitude to my supervisor and Director of Laboratory of Harbour Works (NTUA) Professor Vasiliki Tsoukala for giving me the opportunity to pursue this PhD and also learn a lot working by her side. I will always remember in my future career all the discussions and the exemplary collaboration with her. This PhD drastically changed my life, while evolving myself into a researcher and providing new opportunities, something that would never have happened without the full support and the faith of my supervisor.

My heartfelt thanks also go to the co-supervisors Professor Emeritus Constantine Memos and Professor Panagiotis Prinos. They were both aware of the progress of the PhD from the beginning, through establishing a very good collaboration that encouraged me. Their comments were always apt and their contribution was catalytic since I have learnt a lot from their experience.

I would also like to thank Professor Dimitris Karlis for our collaboration in the last year of my PhD and especially in the field of copulas. Our discussions have always been constructive and have helped me to be confident and to overcome statistical obstacles.

Special thanks also go to the rest examination committee, Research Director Dr Takvor Soukissian for giving me a lot of advice during my first steps of this journey, as well as Assistant Professor Vasiliki Katsardi and Associate Professor Aristeidis Nikoloulopoulos for their valuable comments and suggestions reviewing my thesis.

I am also grateful for the support that the research group of Laboratory of Harbour Works has provided to me and especially for the help that Vanesa, Andreas and Christina have offered during the writing of this thesis followed by many fruitful discussions. Also, I would like to thank Dimitra, Vasilis, Michalis, Tasos, and Maria-Eirini for the interaction and the collaboration all these years. I wish them all the best in their career.

I would also like to acknowledge the Puertos del Estado, as well as the Copernicus and the EMODnet databases for kindly providing me the wave data of this thesis. Many thanks also go to Dr Thomas Nagler and Dr Rick Katz for the useful comments regarding the “VineCopula” and “extRemes” packages respectively in R.

Most of all, I would like to thank my family for everything they have offered me over the years and my wife Nia, for their patience and the uninterrupted support to make my dreams come true.

This research was accomplished through a scholarship by the State Scholarships Foundation (IKY) which is appreciatively acknowledged.

Dedicated to my parents Trifonas & Eleni,

to my aunt Aggeliki,

to my godfather George

Contents

Abstract

Analysis of Coastal Storms for their Application in Harbours and Coastal Structures Design

by Nikolaos Martzikos

National Technical University of Athens
School of Civil Engineering
Department of Water Resources and Environmental Engineering
Laboratory of Harbour Works

The sea-level rise and the increase of storms severity are the major effects of climate change in coastal areas. Their impacts are of great importance for millions of people who live and work in coastal communities, also affecting the ports functionality and many other economic activities. In conjunction with the sea level, the astronomical and the meteorological tide, coastal storms cause extreme wave runup and overtopping phenomena in ports and coastal structures. Consequently, coastal storms threaten the reliability of infrastructure, the urban areas with coastal flooding, and the coasts from erosion.

The above reasons depict the importance of coastal storms analysis and its necessity before any technical study in coastal engineering. Such analyses provide valuable information for risk reduction, coastal management, harbour and coastal structures design.

Coastal storms as multivariate extreme events require a detailed multivariate analysis of many variables. A coastal storm analysis is accomplished by studying the wave height, the wave period, the duration, the calm period, and the storm energy, which are considered “coastal storm parameters” since they define a coastal storm event. The range of coastal storm parameters and how they are interrelating draw a rough outline of wave climate during coastal storm events. The analysis of these parameters is used to understand the coastal storm characteristics, their severity and improve their modelling.

The theory of copulas can be applied for coastal storm modelling, as it has already been implemented for other multivariate events in hydrology and finance.

This thesis focuses on the modelling of coastal storms through copulas, and secondly, in order to apply the proposed methodology, analyses 4008 coastal storms in the Mediterranean Sea, studying the activity of coastal storms in the last decades. More specifically, this thesis: a) describes the dependency of wave height (H) and the wave period (T) during a coastal storm investigating the best fit bivariate copulas, b) simulates the coastal storms in a given location applying a five-dimensional C-Vine copula, and c) estimates the return periods of coastal storms by using two- to five-dimensional copulas. In addition, for the description of energy, a comparison of coastal storm energy with energy flux is accomplished and the shape of coastal storms is also investigated.

The dependency of H and T is investigated among 40 copula families for 4008 coastal storms, presenting the two best-selected copulas and their properties. Three algorithms based on works of De Michele et al. (2007), Aas et al. (2009), and Stöber and Czado (2017) developed into five dimensions and compared for their efficiency in coastal storms simulation. To estimate the return periods, up to five-dimensional copulas are used for any combination of important coastal storm parameters. Moreover, the thresholds of coastal storm parameters, their identification, the frequency of their occurrence and the description of their characteristics are presented.

The Tawn and the Joe copulas are the most frequent best-selected bivariate copulas for modelling H and T during a coastal storm. The C-Vine copulas can be used to simulate the coastal storms efficiently and estimate high-dimensional return periods with extreme characteristics. The flexibility of C-Vines to describe better the tail dependencies makes this class of copulas an effective tool for coastal storm modelling. In addition, it can be said that Mediterranean coasts face around 10-14 coastal storms per year, with most of them occurring in winter. Their average duration is shorter than 30 hours, and 25% of them are consecutive events that hit twice a location in less than a day. Furthermore, the wave period and the main direction present no remarkable fluctuations during a coastal storm. The sharpness of coastal storms is not related to the wave period or the direction and they are not reaching their peak faster than they decay.

This thesis describes the use of copulas for the modelling of coastal storms. Besides, through a thorough analysis of Mediterranean coastal storms, a deeper understanding

of coastal storm severity is pursued, gaining knowledge about their past activity in order to be prepared in the future and protect the coastal areas. Consequently, all this information is helpful for their application in harbours and coastal structures design.

Extended Abstract *(in Greek)*

Ανάλυση Παράκτιων Καταιγίδων για την εφαρμογή τους στο Σχεδιασμό των Λιμενικών και Παράκτιων Έργων

Νικόλαος Μαρτζίκος

Σχολή Πολιτικών Μηχανικών
Τομέας Υδατικών Πόρων και Περιβάλλοντος
Εργαστήριο Λιμενικών Έργων

1. Εισαγωγή

1.1. Υπόβαθρο, κίνητρα και ερευνητικοί στόχοι

Οι καταιγίδες και οι φυσικές καταστροφές που συχνά προκαλούν, απασχολούν τον άνθρωπο από την αρχαιότητα. Στις μέρες μας, η σφοδρότητα των καταιγίδων είναι εντονότερη από αυτή του παρελθόντος και συνδέεται με την κλιματική αλλαγή. Οι επιπτώσεις των καταιγίδων στις ακτές και τις παράκτιες περιοχές θεωρείται ότι θα είναι ακόμη πιο καταστροφικές στο άμεσο μέλλον λόγω της κλιματικής αλλαγής (Knutson et al., 2015; Emanuel, 2017; Bhatia et al., 2018; IPCC, 2018, 2019), καθιστώντας πλέον επιτακτική τη συστηματική έρευνα και την ανάλυση των καταιγίδων.

Η ανάλυση των καταιγίδων συντελεί στη δημιουργία ενός ισχυρού επιστημονικού υπόβαθρου που είναι χρήσιμο για την καλύτερη κατανόηση του φαινομένου. Τα συμπεράσματα τέτοιων αναλύσεων είναι χρήσιμα για τους ερευνητές, αλλά και για τους οργανισμούς και τις κυβερνήσεις που επιθυμούν να αντιμετωπίσουν αποτελεσματικά τέτοιου είδους φαινόμενα, να προετοιμαστούν έγκαιρα και να προστατέψουν τους πολίτες (Hallegatte et al., 2011; Seneviratne et al., 2012; National Research Council, 2014; Gomes et al., 2015; Horton et al., 2015; Lane et al., 2015; Paton et al., 2017).

Οι καταιγίδες συχνά ταυτίζονται με τους κυκλώνες και τους τυφώνες, ενώ ουσιαστικά είναι μια ευρύτερη έννοια που περιγράφει τα ακραία υδρομετεωρολογικά γεγονότα. Ωστόσο, ο όρος των «παράκτιων καταιγίδων» χρησιμοποιείται ειδικότερα για να περιγράψει τις καταιγίδες που πλήττουν τις ακτές και έχουν διάφορες επιπτώσεις, όπως στη μορφολογία της ακτής, στη λειτουργικότητα και στην ευστάθεια των λιμενικών και παράκτιων έργων. Η επίδραση των παράκτιων καταιγίδων στη ζωή των ανθρώπων και

η φύση τους ως ακραία φαινόμενα ήταν τα αρχικά κίνητρα για την εκπόνηση της παρούσας διατριβής.

Για τον ορισμό και τον εντοπισμό των παράκτιων καταιγίδων χρησιμοποιούνται συνήθως οι ατμοσφαιρικές και οι κυματικές παράμετροι. Σύμφωνα με τη θεωρία των ακραίων τιμών, ορίζονται τα κατώφλια αυτών των παραμέτρων και εφαρμόζονται στον εντοπισμό των παράκτιων καταιγίδων ώστε στη συνέχεια να γίνει η ανάλυσή τους. Για την καλύτερη διερεύνηση των παράκτιων καταιγίδων απαιτείται η περιγραφή της σχέσης των μεταβλητών που τις ορίζουν και κατά συνέπεια η μοντελοποίηση τους. Η έρευνα των De Michele et al. (2007) εισήγαγε τη θεωρία των συζεύξεων στη μοντελοποίηση των καταιγίδων και επηρέασε σε μεγάλο βαθμό πολλές μεταγενέστερες έρευνες, όπως και την παρούσα διατριβή. Οι συζεύξεις αναπτύχθηκαν κυρίως στον τομέα της Στατιστικής και χρησιμοποιούνται ευρέως στα Οικονομικά (π.χ. τιμολόγηση, χρηματιστήρια, ανάλυση κινδύνου) και στην Υδρολογία (π.χ. ανάλυση ξηρασίας, πλημμύρας, βροχόπτωσης). Η εφαρμογή των συζεύξεων απαιτεί αρκετούς μαθηματικούς υπολογισμούς και χρειάζεται ιδιαίτερη προσοχή καθώς εύκολα μπορεί να οδηγήσει σε λάθος συμπεράσματα (όπως συνέβη στην οικονομική κρίση του 2007-2008 στις Η.Π.Α.). Αυτή η ιδιαιτερότητα των συζεύξεων κάνει την εφαρμογή τους ακόμη πιο ελκυστική.

Οι ερευνητικοί στόχοι της παρούσα διατριβής είναι οι εξής:

- Να ορίσει την παράκτια καταιγίδα και να αναπτύξει μια μεθοδολογία για τον εντοπισμό της, αλλά και την περιγραφή κάθε γεγονότος παράκτιας καταιγίδας μέσω των σημαντικών μεταβλητών.
- Να αναπτύξει τη θεωρία των συζεύξεων με σκοπό τη μοντελοποίηση των παράκτιων καταιγίδων: α) για την μελέτη της εξάρτησης του ύψους και της περιόδου κύματος κατά τη διάρκεια μιας παράκτιας καταιγίδας, β) για την προσομοίωση των παράκτιων καταιγίδων μιας περιοχής εφαρμόζοντας και συγκρίνοντας αλγορίθμους που υπήρχαν στη βιβλιογραφία (πέντε διαστάσεις), γ) για τον υπολογισμό των περιόδων επαναφοράς μιας παράκτιας καταιγίδας για διάφορους συνδυασμούς παραμέτρων (δυο-πέντε διαστάσεις).
- Να εντοπίσει και να μελετήσει γεγονότα παράκτιων καταιγίδων στη Μεσόγειο θάλασσα, ώστε να κατανοήσει τη δραστηριότητά τους, τα χαρακτηριστικά και τη συχνότητα εμφάνισής τους.
- Να εφαρμόσει τη μεθοδολογία για τη μοντελοποίηση των παράκτιων καταιγίδων μέσω των συζεύξεων στο δείγμα που έχει εντοπιστεί στη Μεσόγειο θάλασσα.

1.2. Πρωτότυπα στοιχεία

Η παρούσα διατριβή στηρίζεται στην ανάλυση των παράκτιων καταιγίδων και στην εφαρμογή των συζεύξεων για την μοντελοποίησή τους, για την προσομοίωση και την εκτίμηση των περιόδων επαναφοράς. Περιλαμβάνονται τα εξής πρωτότυπα στοιχεία:

- Οι μεταβλητές της παράκτιας καταιγίδας και τα απαιτούμενα κατώφλια διερευνώνται διεξοδικά, περιγράφοντας, για πρώτη φορά, μια αναλυτική μεθοδολογία για τον εντοπισμό των παράκτιων καταιγίδων.
- Η μεθοδολογία που αναπτύσσεται για τον εντοπισμό και την ανάλυση των παράκτιων καταιγίδων εφαρμόζεται σε πρωτογενή κυματικά δεδομένα και όχι σε δεδομένα προσομοιώσεων. Δεδομένα 30 διαφορετικών περιοχών αναλύονται για πρώτη φορά στη Μεσόγειο θάλασσα, αλλά και γενικότερα εκτός αυτής, προκειμένου να αναλυθούν οι παράκτιες καταιγίδες. Συνολικά, ανιχνεύονται 4008 παράκτιες καταιγίδες, καλύπτοντας την χρονική περίοδο 1985-2019. Παρουσιάζονται τα περιγραφικά στατιστικά στοιχεία αυτών των ακραίων γεγονότων, όπως και οι σημαντικές πληροφορίες για τη δραστηριότητα των παράκτιων καταιγίδων τις τελευταίες δεκαετίες.
- Ο εντοπισμός και η ανάλυση των παράκτιων καταιγίδων αναδεικνύει για πρώτη φορά στη βιβλιογραφία κάποια σημαντικά χαρακτηριστικά που αφορούν στη Μεσόγειο θάλασσα, όπως α) τη συμπεριφορά της ενέργειας των καταιγίδων και της ροής ενέργειας, σε σχέση με το ύψος και την περίοδο κύματος, β) τη διακύμανση της περιόδου του κύματος και της κατεύθυνσης κατά τη διάρκεια μιας παράκτιας καταιγίδας, και γ) τη μορφή του σχήματος των παράκτιων καταιγίδων σε σχέση με την κατεύθυνση και την περίοδο κύματος.
- Η βέλτιστη επιλογή της οικογένειας των συζεύξεων για το ύψος και την περίοδο κύματος κατά τη διάρκεια μιας παράκτιας καταιγίδας διερευνάται διεξοδικά, σε αντίθεση με την συνήθη πρακτική άλλων ερευνών που χρησιμοποιούν μια συγκεκριμένη οικογένεια (π.χ. Archimedean, Elliptical) χωρίς διερεύνηση. Συγκεκριμένα, εξετάζονται 40 οικογένειες συζεύξεων και παρουσιάζονται οι επικρατέστερες. Επιπλέον γίνεται διερεύνηση των δεύτερων βέλτιστων συζεύξεων σε μια προσπάθεια να εντοπιστούν ομοιότητες μεταξύ των διάφορων οικογενειών. Οι εξαρτήσεις ουράς και το εύρος των μεταβλητών διερευνώνται περαιτέρω, για πρώτη φορά, για τις παράκτιες καταιγίδες που μοντελοποιούνται μέσω μιας συγκεκριμένης οικογένειας σύζευξης.
- Η μεθοδολογία των C-Vine συζεύξεων εφαρμόζεται για πρώτη φορά στη μοντελοποίηση των παράκτιων καταιγίδων και επεκτείνεται μέχρι τις πέντε μεταβλητές, έναντι των τριών μεταβλητών που χρησιμοποιούνται συνήθως

στη βιβλιογραφία. Οι προτεινόμενες δομές των C-Vine συζεύξεων εφαρμόζονται στα δεδομένα της Malaga. Ωστόσο οι συγκεκριμένες C-Vine συζεύξεις μπορούν να εφαρμοστούν, χωρίς μεγάλες διαφορές, και σε άλλες περιοχές με παρόμοια χαρακτηριστικά αυτών της Malaga.

- Η μεθοδολογία των De Michele et al. (2007) για την προσομοίωση καταιγίδων στη θάλασσα, επεκτείνεται από τέσσερις μεταβλητές σε πέντε μεταβλητές και εφαρμόζεται στις παράκτιες καταιγίδες. Ο αλγόριθμος που αναπτύχθηκε συγκρίνεται με δυο αλγορίθμους που βασίστηκαν στη μεθοδολογία των Aas et al. (2009) και Stöber and Czado (2017) για πέντε μεταβλητές, ως προς τις προσομοιώσεις των παράκτιων καταιγίδων και εφαρμόζονται στα πραγματικά δεδομένα της Malaga.
- Οι περίοδοι επαναφοράς των παράκτιων καταιγίδων με τα πιο ακραία χαρακτηριστικά υπολογίζονται μέσω των συζεύξεων για δύο έως πέντε μεταβλητές, επεκτείνοντας τη μεθοδολογία που χρησιμοποιείται συνήθως στη βιβλιογραφία από τρεις, σε τέσσερις και πέντε μεταβλητές. Οι C-Vine συζεύξεις συγκρίνονται ως προς την αποτελεσματικότητά τους για τον υπολογισμό των περιόδων επαναφοράς με άλλες γνωστές συζεύξεις (π.χ. Gaussian, Gumbel, t).

2. Θεωρητικό υπόβαθρο στην ανάλυση παράκτιων καταιγίδων

Η απειλή των καταιγίδων ήταν ένας από τους λόγους που οι άνθρωποι οργάνωσαν τη ζωή τους δίνοντας προτεραιότητα στην προστασία και την ασφάλειά τους. Παράλληλα, οι άνθρωποι άρχισαν να αναζητούν τους λόγους που προκαλούν τέτοιου είδους ακραία φαινόμενα. Οι αναζητήσεις ήταν αρχικά θεολογικής υπόστασης, ενώ πολύ γρήγορα έστρεψαν την προσοχή τους στα σημάδια της φύσης που συνδέονταν με τις καταιγίδες. Οι κινήσεις των ουράνιων σωμάτων, η μορφή των νεφών, οι άνεμοι συγκεκριμένης κατεύθυνσης, η αλλαγή της στάθμης της θάλασσας αλλά και η συμπεριφορά των έμβιων όντων ήταν οιωνοί μιας σφοδρής καταιγίδας και των συνεπειών που θα προκαλούσε. Οι επιστημονικές προσεγγίσεις κάνουν την εμφάνιση τους μετά το 1880, σημειώνοντας μια ραγδαία και εντυπωσιακή αύξηση μετά το 2000 (Σχ. 1).

Η διερεύνηση των ιστορικών καταιγίδων δίνει σημαντικές πληροφορίες για την ένταση και τη συχνότητά τους, αναδεικνύοντας τις επιπτώσεις που έχουν στις ανθρώπινες κοινωνίες. Κυρίως όμως μέσα από τέτοιες έρευνες γίνεται αντιληπτό ότι η πρόληψη και η προετοιμασία είναι υψίστης σημασίας ειδικά για τις παράκτιες περιοχές. Η έρευνα των τελευταίων δεκαετιών επικεντρώνεται στη διαχείριση των καταιγίδων (Hissel et al., 2014; Spencer et al., 2015), στις προβλέψεις ακραίων γεγονότων (Madsen and Jakobsen, 2004; Lowe and Gregory, 2005; McInnes et al., 2007; Mattocks and Forbes, 2008; Rego and Li, 2009; Izaguirre et al., 2013) και στην εφαρμογή συστημάτων

έγκαιρης προειδοποίησης (Ciavola et al., 2011b, 2011a; Gall et al., 2013; Jones et al., 2017). Η διερεύνηση των καταιγίδων έχει εφαρμογή στην ολοκληρωμένη διαχείριση της παράκτιας ζώνης (Curtis, 2013; De la Torre et al., 2013; Hallegatte et al., 2013; Chadenas et al., 2014; Musereau and Regnauld, 2014; Jaranovic et al., 2017), και στο σχεδιασμό λιμενικών και παράκτιων έργων (Phan and Simiu, 2011; McCullough et al., 2013; Takahashi et al., 2014; Altomare et al., 2015; Burmeister et al., 2015; Basco, 2016; Do et al., 2016; Hatzikyriakou and Lin, 2017; Mooyaart and Jonkman, 2017; Mohd Anuar et al., 2018).

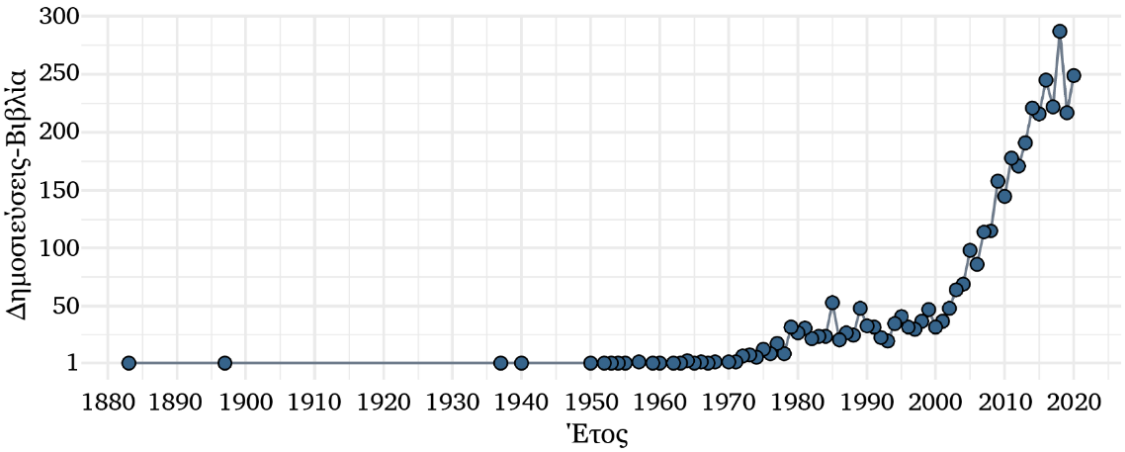

Σχήμα 1. Ο ετήσιος αριθμός βιβλίων ή δημοσιεύσεων που περιλαμβάνουν τους όρους «καταιγίδα», «παράκτια», «ακτή» στον τίτλο τους, την περίληψη ή στις λέξεις-κλειδιά, σύμφωνα με το Scopus.

Πιο συγκεκριμένα, η μελέτη των παράκτιων καταιγίδων περιλαμβάνει την ανάλυση των γεγονότων που συμβαίνουν σε πραγματικό χρόνο ή έχουν συμβεί στο παρελθόν, εστιάζοντας στα χαρακτηριστικά τους, στο εύρος των σημαντικών παραμέτρων, στη μεταξύ τους αλληλεπίδραση κατά τη διάρκεια ενός γεγονότος αλλά και στη μελέτη των επιπτώσεων τους στις παράκτιες περιοχές. Οι πληροφορίες αυτές δίνουν μια εικόνα του κυματικού κλίματος μιας περιοχής, κυρίως όμως είναι σημαντικές στη διαχείριση και στη μείωση του κινδύνου μιας επερχόμενης καταιγίδας καθώς μπορούν να χρησιμοποιηθούν για την πρόβλεψη της εμφάνισης καθώς και της εξέλιξης νέων γεγονότων, για την ανάπτυξη των μηχανισμών έγκαιρης προειδοποίησης καθώς και για τη λήψη μέτρων με σκοπό την αύξηση της ανθεκτικότητας των λιμενικών και παράκτιων έργων και των παράκτιων υποδομών. Σε γενικές γραμμές τα καίρια ζητήματα που εξετάζονται στην ανάλυση των παράκτιων καταιγίδων είναι: α) ο ορισμός τους, β) η μελέτη της σφοδρότητας, εξετάζοντας τα συνοπτικά συστήματα, την μετεωρολογική παλίρροια, την ανάλυση των χρονοσειρών των μεταβλητών και το δείκτη σφοδρότητας, γ) τα κατώφλια των μεταβλητών που ορίζουν μια παράκτια καταιγίδα, δ) οι επιπτώσεις τους στις ακτές, ε) η ταξινόμησή τους και τέλος στ) οι κοινωνικές διαστάσεις.

Η παρούσα διδακτορική διατριβή επικεντρώνεται κυρίως στον ορισμό των παράκτιων καταιγίδων, στον εντοπισμό τους και στη σφοδρότητά μέσω της ανάλυσης των σημαντικών τους μεταβλητών. Οι μεταβλητές που εξετάζονται είναι αυτές του ύψους και της περιόδου του κύματος κατά τη διάρκεια μιας παράκτιας καταιγίδας, όπως επίσης λαμβάνεται υπόψη η διάρκεια, το χρονικό διάστημα ηρεμίας και ο δείκτης σφοδρότητας για τον οποίο υπολογίζεται η ενέργεια και η ροή ενέργειας για κάθε παράκτια καταιγίδα. Για την περαιτέρω διερεύνηση της εξάρτησης των παραπάνω μεταβλητών επιδιώκεται η μοντελοποίηση των μεταβλητών και κατά συνέπεια των παράκτιων καταιγίδων. Για τη μοντελοποίηση των παράκτιων καταιγίδων, εφαρμόζεται η θεωρία των συζεύξεων που ενδείκνυται για φαινόμενα πολλών μεταβλητών. Οι συζεύξεις χρησιμεύουν στην κατασκευή ενός πολυμεταβλητού μοντέλου βάσει της εξάρτησης των μεταβλητών, το οποίο στη συνέχεια δίνει τη δυνατότητα: α) της μοντελοποίησης της εξάρτησης του ύψους και της περιόδου κύματος, β) της προσομοίωσης των παράκτιων καταιγίδων και γ) του υπολογισμού της κοινής πιθανότητας των μεταβλητών και της περιόδου επαναφοράς των παράκτιων καταιγίδων.

3. Μεθοδολογία για την ανάλυση και την μοντελοποίηση των παράκτιων καταιγίδων

Η μεθοδολογία για την ανάλυση και την μοντελοποίηση των παράκτιων καταιγίδων περιλαμβάνει τα εξής:

1. τον ορισμό και τον εντοπισμό της παράκτιας καταιγίδας, μέσω των μεταβλητών που την καθορίζουν,
2. τη θεωρία των συζεύξεων, για την μοντελοποίηση των παράκτιων καταιγίδων,
3. την εφαρμογή των συζεύξεων για την προσομοίωση των καταιγίδων, αναπτύσσοντας τρείς αλγορίθμους που βασίστηκαν στις μεθοδολογίες των De Michele et al. (2007), Aas et al. (2009) και Stöber and Czado (2017), επεκτείνοντάς αυτές σε πέντε μεταβλητές,
4. την εφαρμογή των συζεύξεων στον υπολογισμού της κοινής πιθανότητας κάθε συνδυασμού των μεταβλητών μιας παράκτιας καταιγίδας και τον υπολογισμό της περιόδου επαναφοράς μιας παράκτιας καταιγίδας όταν έχει ακραία χαρακτηριστικά.

Η μεθοδολογία της διατριβής για την ανάλυση και μοντελοποίηση των παράκτιων καταιγίδων εφαρμόζεται σε πρωτογενή δεδομένα κυματικών παραμέτρων, που προέρχονται από 30 πλωτούς μετρητές στη Μεσόγειο θάλασσα, για την περίοδο 1985-2019. Συνολικά εξετάζονται 4008 παράκτιες καταιγίδες στην Ελλάδα, την Ιταλία, την Γαλλία και την Ισπανία, μελετώντας τα χαρακτηριστικά τους και την δραστηριότητα τους.

3.1. Ορισμός και εντοπισμός παράκτιων καταιγίδων

Ως καταιγίδες ορίζονται οι διαταραγμένες καταστάσεις της ατμόσφαιρας, που επηρεάζουν την επιφάνεια της γης και συνδυάζονται με δυσμενείς και καταστροφικές καιρικές συνθήκες (AMS, 2019). Ωστόσο, για να οριστούν οι παράκτιες καταιγίδες θα πρέπει να γίνει αναφορά στο υδάτινο στοιχείο και στις επιπτώσεις που επιφέρουν οι καταιγίδες στις παράκτιες περιοχές. Στην παρούσα διατριβή ο ορισμός των παράκτιων καταιγίδων προκύπτει από το συνδυασμό των ορισμών των Harley (2017) και Ciavola et al. (2014), και επομένως ως παράκτιες καταιγίδες ορίζονται οι διαταραγμένες καταστάσεις της θάλασσας που προκαλούνται από μετεωρολογικές συνθήκες και μπορούν να επιφέρουν αλλαγές και καταστροφές στη μορφολογία των ακτών και στις κατασκευές.

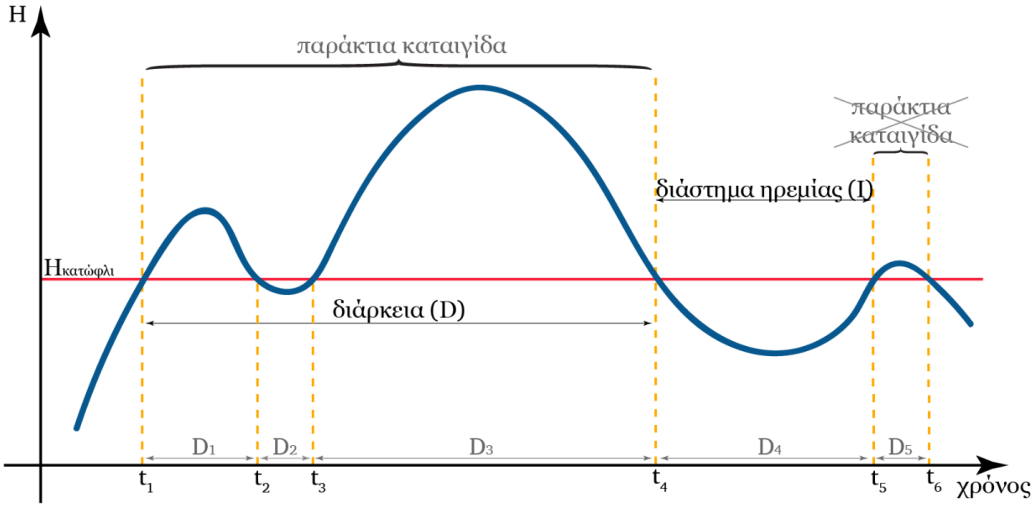

Σχήμα 2. Ο ορισμός της παράκτιας καταιγίδας μέσω των σημαντικότερων παραμέτρων.

Για την εντοπισμό των παράκτιων καταιγίδων είναι απαραίτητες οι μεταβλητές του σημαντικού ύψους κύματος (*H*), της διάρκειας (*D*) και του χρονικού διαστήματος ηρεμίας (*I* - calm period). Πιο συγκεκριμένα, για να εντοπιστεί μια παράκτια καταιγίδα, το ύψος κύματος πρέπει να ξεπερνάει ένα συγκεκριμένο κατώφλι (Σχ. 2) και να παραμένει πάνω από αυτό για ορισμένη χρονική περίοδο (Boccotti, 2000; De Michele et al., 2007; Li et al., 2014). Απαραίτητο είναι επίσης να οριστεί, η ελάχιστη διάρκεια μιας παράκτιας καταιγίδας ώστε η διερεύνηση να επικεντρώνεται στις καταιγίδες που διαρκούν περισσότερο και συνεπώς να μην αποτελούνται από χρονοσειρές μικρού μήκους. Επίσης σημαντικό είναι το χρονικό διάστημα ηρεμίας (calm period) (De Michele et al., 2007; Corbella and Stretch, 2013) που ορίζεται ως ο χρόνος που μεσολαβεί μεταξύ δυο διαδοχικών γεγονότων και χρησιμοποιείται για το διαχωρισμό τους. Στην περίπτωση που το διάστημα ηρεμίας είναι μικρό, τα διαδοχικά γεγονότα ενώνονται και θεωρούνται ως ένα με μεγαλύτερη διάρκεια. Για παράδειγμα, στο Σχήμα 2 οι διαδοχικές καταιγίδες έχουν διάρκεια D_1, D_3 και D_5. Οι δυο πρώτες μπορούν να θεωρηθούν ως ένα γεγονός,

λόγω του μικρού calm period (D_2) που μεσολαβεί, με τελική διάρκεια $D=t_4-t_1$. Αντίθετα, το επόμενο γεγονός με διάρκεια D_5 θεωρείται ανεξάρτητο από το προηγούμενο λόγω του μεγάλου calm period (D_4), αλλά δε θεωρείται παράκτια καταιγίδα καθώς η διάρκειά του (D_5) είναι μικρή.

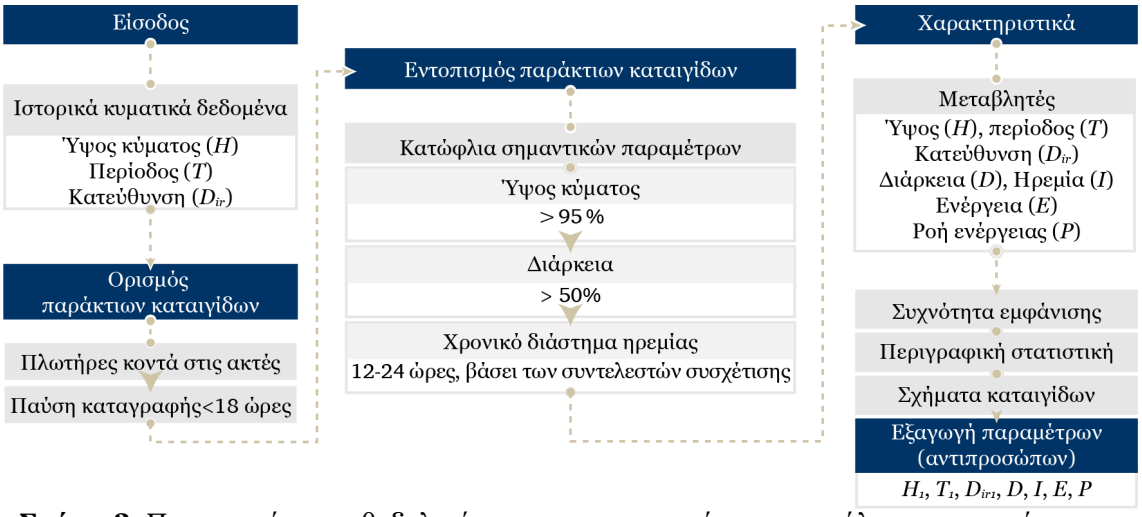

Σχήμα 3. Περιγραφή της μεθοδολογίας για τον εντοπισμό και την ανάλυση των παράκτιων καταιγίδων.

Στην παρούσα διατριβή η μεθοδολογία που αναπτύσσεται για τον εντοπισμό και την ανάλυση των παράκτιων καταιγίδων (Σχ. 3) στηρίζεται σε προηγούμενες έρευνες (De Michele et al., 2007; Corbella and Stretch, 2013; Li et al., 2014) και ειδικότερα για τον ορισμό των απαραίτητων κατωφλιών στηρίζεται στη θεωρία των ακραίων τιμών (Coles, 2001) και στη μέθοδο Peak Over Threshold (POT). Προκειμένου να γίνει διερεύνηση των παράκτιων καταιγίδων, επιλέγονται δεδομένα που προκύπτουν από μετρήσεις πλωτήρων που βρίσκονται στην πλησιέστερη απόσταση από την ακτή. Ενώ επίσης, δε λαμβάνονται υπόψη οι περιπτώσεις όπου η παύση καταγραφής των πλωτήρων ξεπερνάει τις 18 ώρες, θεωρώντας ότι είναι εκτός λειτουργίας. Ο εντοπισμός των παράκτιων καταιγίδων επιτυγχάνεται μέσω της εφαρμογής των κατωφλιών, τα οποία ορίζονται μοναδικά για κάθε περιοχή, καθώς εξαρτώνται από τα συνοπτικά μετεωρολογικά συστήματα, τη βαθυμετρία και το πόσο εκτίθεται μια περιοχή σε σφοδρούς ανέμους και υψηλά κύματα (Harley, 2017). Μετά τον εντοπισμό των παράκτιων καταιγίδων, υπολογίζονται και αναλύονται τα χαρακτηριστικά τους. Οι σημαντικότερες μεταβλητές υπολογίζονται για κάθε γεγονός, υπολογίζεται η συχνότητα εμφάνισης, τα περιγραφικά στατιστικά στοιχεία, γίνεται διερεύνηση του σχήματος των παράκτιων καταιγίδων και τέλος εξάγονται οι σημαντικές παράμετροι ως αντιπρόσωποι των μεταβλητών για την περιγραφή ενός γεγονότος.

Στην παρούσα διατριβή ο ορισμός των κατωφλιών επιτυγχάνεται μέσω περαιτέρω διερεύνησης. Ο ορισμός των κατωφλιών βασίζεται στα διαθέσιμα δεδομένα και σε

στατιστικές μεθόδους και το εύρος τους ποικίλει στη βιβλιογραφία. Για το σημαντικό ύψος κύματος λαμβάνεται ως κατώφλι (H_{thr}) το 95ο εκατοστημόριο, ώστε να εξετάζεται το 5% του δείγματος δηλαδή οι πιο ακραίες τιμές του ύψους κύματος σε κάθε περιοχή. Κάθε υπέρβαση του H_{thr} ομαδοποιείται και εξετάζεται ως παράκτια καταιγίδα. Για την ελάχιστη διάρκεια (D_{thr}), το κατώφλι ορίζεται πάνω από το 50% της διάρκειας όλων των καταιγίδων και μικρότερο από τη μέση τιμή αυτών. Το κατώφλι του διαστήματος ηρεμίας (I_{thr}) σχετίζεται με τη κυκλογένεση μιας περιοχής και συνήθως κυμαίνεται κοντά στις 24 ώρες για τη Μεσόγειο θάλασσα. Προκειμένου η επιλογή του I_{thr} να είναι πιο αντικειμενική, ελέγχονται επίσης οι συντελεστές συσχέτισης Spearman's rho (ρ), Kendall's tau (τ), και Pearson's r του ύψους και της περιόδου του κύματος μεταξύ των διαδοχικών γεγονότων κάθε περιοχής. Όταν οι τιμές των συντελεστών είναι κοντά στο μηδέν εξασφαλίζουν τη διαφορετικότητα των υπό εξέταση δειγμάτων και κατά συνέπεια παρέχουν μια επιπλέον πληροφορία για την ανεξαρτησία των διαδοχικών παράκτιων καταιγίδων. Τα αποτελέσματα ταξινομούνται ως προς τη συχνότητα εμφάνισης και η επικρατέστερη τιμή του διαστήματος ηρεμίας με αυτά τα χαρακτηριστικά ορίζεται ως το κατώφλι I_{thr} κάθε περιοχής.

3.2. Χαρακτηριστικά των παράκτιων καταιγίδων

Μετά τον εντοπισμό των παράκτιων καταιγίδων, υπολογίζονται τα χαρακτηριστικά τους. Πιο συγκεκριμένα, υπολογίζονται η συχνότητα εμφάνισης των παράκτιων καταιγίδων, το ύψος (H - significant wave height) και η περίοδος κύματος (T - spectral peak period), η διάρκεια (D - duration), το χρονικό διάστημα ηρεμίας (I - calm period), η κατεύθυνση, όπως επίσης η ενέργεια (E - storm energy) και η ροή ενέργειας (P - energy flux). Στη συνέχεια, για την κατανόηση της δραστηριότητας των παράκτιων καταιγίδων υπολογίζονται τα στατιστικά περιγραφικά στοιχεία των χαρακτηριστικών τους, ενώ ακόμη γίνεται διερεύνηση του σχήματος των παράκτιων καταιγίδων.

Η ενέργεια (E) και η ροή ενέργειας (P) κάθε γεγονότος υπολογίζονται για τον ορισμό του δείκτη της σφοδρότητας των παράκτιων καταιγίδων. Σύμφωνα με την Εξ. 1 των Dolan και Davis (1992) η ενέργεια υπολογίζεται ως εξής:

$$E = \int_{t_1}^{t_2} H^2 dt \,, \tag{1}$$

όπου t_1-t_2 θεωρείται η διάρκεια της παράκτιας καταιγίδας και H το σημαντικό ύψος κατά τη διάρκεια της. Η ροή ενέργειας (P) (Boccotti, 2015), η οποία συχνά χρησιμοποιείται για τη μελέτη των επιπτώσεων των καταιγίδων στις ακτές (Ruiz de Alegria-Arzaburu and Masselink, 2010; Harley et al., 2017; Molina et al., 2019; Wang et al., 2020), προκύπτει από την Εξ. 2:

$$P = E_u \cdot C_g \,, \tag{2}$$

όπου E_u η ενέργεια κύματος ανά μονάδα επιφάνειας και C_g η ταχύτητα ομάδας των κυμάτων που εξαρτάται από το βάθος, το μήκος και την περίοδο κύματος. Αντίστοιχα η ενέργεια κύματος ανά μονάδα επιφάνειας (E_u) υπολογίζεται από την Εξ. 3:

$$E_u = \frac{1}{8}\rho \cdot g \cdot H^2, \quad (3)$$

όπου g η επιτάχυνση της βαρύτητας και ρ η πυκνότητα του θαλασσινού νερού

Οι δυο μεταβλητές P και E συγκρίνονται σε σχέση με το ύψος και την περίοδο κύματος κατά τη διάρκεια μιας καταιγίδας. Η σύγκριση γίνεται με σκοπό να διερευνηθεί η επίδραση του ύψους και της περιόδου του κύματος στον υπολογισμό των P και E αλλά και για να επιλεγεί η καταλληλότερη μεταβλητή ως δείκτης σφοδρότητας της καταιγίδας.

Το σχήμα των παράκτιων καταιγίδων είναι ένα ακόμη χαρακτηριστικό τους που συχνά εξετάζεται στη βιβλιογραφία. Χρησιμεύει στη γραφική αναπαράσταση των καταιγίδων, στον υπολογισμό της ενέργειας (Dissanayake et al., 2015; Lin-Ye et al., 2016), κυρίως όμως απλοποιεί τη μορφή ενός γεγονότος και λειτουργεί ως μοντέλο για την κατασκευή συνθετικών καταιγίδων (De Michele et al., 2007; Corbella and Stretch, 2012a, 2013; Martín-Hidalgo et al., 2014; Boccotti, 2015; Martín Soldevilla et al., 2015; Laface and Arena, 2016; Duo et al., 2020; Marzeddu et al., 2020). Το σχήμα των καταιγίδων ποικίλει μεταξύ τριγωνικού, τραπεζοειδούς και παραβολικού, με επικρατέστερο το τριγωνικό λόγω της απλοποιημένης μορφής του. Δεδομένου ότι οι παράκτιες καταιγίδες της Μεσογείου θεωρούνται απότομες κατά την έναρξη μέχρι την κορύφωσή τους, ενώ φθίνουν ήπια μέχρι να φτάσουν στο τέλος τους (Lin-Ye et al., 2016), γίνεται διερεύνηση αν το ισοσκελές ή σκαληνό τριγωνικό σχήμα περιγράφει καλύτερα τις πραγματικές καταιγίδες και κατά πόσο η μορφή του εξαρτάται από την περίοδο και την κατεύθυνση του κύματος εντός της καταιγίδας.

Το τελευταίο βήμα της ανάλυσης των παράκτιων καταιγίδων περιλαμβάνει τον ορισμό των σημαντικών παραμέτρων H_1, T_1, D_{ir1}, D, I, E, P ως αντιπροσώπους των μεταβλητών H, T, D_{ir}, D, I, E, P αντίστοιχα, ώστε στη συνέχεια κάθε καταιγίδα να περιγράφεται από ένα σύνολο μοναδικών τιμών αυτών των μεταβλητών. Οι μεταβλητές D, I, E, P ορίζονται μοναδικά για κάθε παράκτια καταιγίδα, οπότε χρησιμοποιούνται ως έχουν. Η παράμετρος H_1 ορίζεται ως η μέση τιμή του ύψους κύματος κατά τη διάρκεια μιας παράκτιας καταιγίδας, ενώ ο ορισμός των παραμέτρων T_1, D_{ir1} γίνεται έπειτα από διερεύνηση του εύρους και της διακύμανσης των αντίστοιχων μεταβλητών κατά τη διάρκεια μιας παράκτιας καταιγίδας.

3.3. Μοντελοποίηση παράκτιων καταιγίδων μέσω συζεύξεων

3.3.1 Εισαγωγή στη θεωρία συζεύξεων και Vine συζεύξεων

Η θεωρία των συζεύξεων (copulas) θεμελιώθηκε στον τομέα της Στατιστικής και χρησιμοποιείται ευρέως τις τελευταίες δεκαετίες στην ανάλυση και μοντελοποίηση των πολυμεταβλητών φαινομένων, με εφαρμογές κυρίως στον τομέα των Οικονομικών (Frees and Valdez, 1998; Cherubini et al., 2004; McNeil et al., 2005; Trivedi and Zimmer, 2006; Aas et al., 2009; Embrechts, 2009; Genest et al., 2009) και στην Υδρολογία (Genest and Favre, 2007; Renard and Lang, 2007; Salvadori and De Michele, 2007; Serinaldi, 2015; Salvadori et al., 2016; Jäger and Nápoles, 2017; Jäger et al., 2019). Η θεωρία των συζεύξεων χρησιμοποιείται επίσης στη μοντελοποίηση των ακραίων κυματικών φαινομένων και των καταιγίδων (Corbella and Stretch, 2012a; Corbella and Stretch, 2013; De Michele et al., 2007; Li et al., 2014, 2018; Lin-Ye et al., 2016, 2018; Lira-Loarca et al., 2020; Salvadori et al., 2014).

Οι συζεύξεις παρουσιάστηκαν από τον Sklar (1959) και έπειτα από πολλά χρόνια εξετάστηκαν διεξοδικά από τον Joe (1997) και τον Nelsen (2006). Σύμφωνα με τον Nelsen (2006) οι συζεύξεις είναι α) συναρτήσεις που συνδέουν την πολυμεταβλητή συνάρτηση κατανομής δυο ή περισσότερων μεταβλητών με τις μονοδιάστατες περιθώριες κατανομές ή β) λειτουργούν οι ίδιες ως πολυμεταβλητές συναρτήσεις κατανομών αλλά στο πεδίο [0,1]. Οι συζεύξεις χρησιμοποιούνται για τη δημιουργία των πολυμεταβλητών κατανομών και τον υπολογισμό της κοινής πιθανότητας, ειδικά όταν οι μεταβλητές είναι εξαρτημένες και δεν ακολουθούν τις ίδιες κατανομές. Το κύριο πλεονέκτημά τους είναι ότι περιγράφουν την δομή εξάρτησής των εμπλεκόμενων μεταβλητών και θεωρούνται ένα αρκετά ευέλικτο μαθηματικό εργαλείο, ιδιαίτερα αποτελεσματικό όταν χρησιμοποιείται με προσοχή.

Η συνεισφορά των συζεύξεων είναι επίσης σημαντική στην ανάλυση και μοντελοποίηση των κυματικών παραμέτρων, όπου σε ερευνητικό τουλάχιστον επίπεδο κατά τη διάρκεια των χρόνων, οι κοινές πιθανότητες των κυματικών παραμέτρων (Longuet-Higgins, 1983; Memos, 1994; Ferreira and Guedes Soares, 2002) αντικαταστάθηκαν με τις δισδιάστατες συζεύξεις (Dong et al., 2015; Galiatsatou and Prinos, 2016; Jäger and Nápoles, 2017; Mazas and Hamm, 2017; Galiatsatou et al., 2019; Jäger et al., 2019) και στη συνέχεια με τις πολυμεταβλητές συζεύξεις για την περιγραφή πιο σύνθετων φαινομένων όπως είναι οι καταιγίδες (De Michele et al., 2007; Corbella and Stretch, 2013; Li et al., 2014, 2018; Wahl et al., 2016; Lin-Ye et al., 2020; Nadal-Caraballo et al., 2020).

Στις μέρες μας, οι διαφορετικές οικογένειες συζεύξεων και ο τρόπος κατασκευής τους αποτελούν αντικείμενο πολλών ερευνών, με την περίπτωση των Vine copulas να καθιερώνονται όλο και περισσότερο ως ένας εύκολος τρόπος για την κατασκευή πολυμεταβλητών συζεύξεων που απαιτεί μόνο τις δισδιάστατες συζεύξεις.

Σύμφωνα με το θεώρημα του Sklar (1959) αν X_1, X_2 δυο τυχαίες συνεχείς μεταβλητές με μονοδιάστατες περιθώριες κατανομές F_1, F_2 και $F_{12}\left(x_1, x_2\right)$ η κοινή συνάρτηση κατανομής για κάθε $x_1, x_2 \in \overline{\mathbb{R}}$, τότε υπάρχει μια σύζευξη C_{12}, τέτοια ώστε:

$$F_{12}\left(x_1, x_2\right) = C_{12}\left(F_1\left(x_1\right), F_2\left(x_2\right)\right). \tag{4}$$

Το θεώρημα επεκτείνεται αντίστοιχα για περισσότερες μεταβλητές, όπως για παράδειγμα στην Εξ. 5:

$$F\left(x_1, x_2, x_3, x_4, x_5\right) = C\left(F_1\left(x_1\right), F_2\left(x_2\right), F_3\left(x_3\right), F_4\left(x_4\right), F_5\left(x_5\right)\right). \tag{5}$$

Για λόγους καλύτερης προσαρμογής των συζεύξεων και της μελέτης της εξάρτησης των μεταβλητών, τα δεδομένα κανονικοποιούνται μέσω των ολοκληρωτικών μετασχηματισμών πιθανότητας. Πιο συγκεκριμένα, αν x_i μια τιμή της μεταβλητής X_i με περιθώρια κατανομή F_i, τότε ορίζεται η κανονικοποιημένη τιμή u_i ως εξής $u_i = F_i\left(x_i\right) = P\left(X_i \le x_i\right)$ για $i=1,\ldots,d$ με $u_i \in \left[0,1\right]$. Με αυτό τον τρόπο η κοινή πιθανότητα δυο μεταβλητών μπορεί να εκφραστεί ως εξής:

$$C_{12}\left(u_1, u_2\right) = F_{12}\left(F_1^{-1}\left(u_1\right), F_2^{-1}\left(u_2\right)\right) = F_{12}\left(x_1, x_2\right) = P\left(X_1 \le x_1, X_2 \le x_2\right). \tag{6}$$

Αντίστοιχα, η δεσμευμένη συνάρτηση κατανομής (ή δεσμευμένη πιθανότητα) δυο μεταβλητών ορίζεται επίσης με τη βοήθεια των συζεύξεων:

$$C_{1|2}\left(u_1 \middle| u_2\right) = P\left(U_1 \le u_1 \middle| U_2 = u_2\right) = \frac{\partial}{\partial u_2} C_{12}\left(u_1, u_2\right), \tag{7}$$

ενώ στη συνέχεια θα χρησιμοποιείται με τον όρο «*h-function*» (Aas et al., 2009; Czado, 2019), όπως για παράδειγμα:

$$h_{1|2}\left(u_1 \middle| u_2\right) = C_{1|2}\left(u_1 \middle| u_2\right) = \frac{\partial C_{12}\left(u_1, u_2\right)}{\partial u_2}. \tag{8}$$

Οι συζεύξεις κατηγοριοποιούνται σε διάφορες οικογένειες και κλάσεις, με κριτήριο την καλύτερη περιγραφή της εξάρτησης των μεταβλητών, τη συμπεριφορά των ουρών και των κατανομών που ακολουθούν (Nelsen, 2006; Salvadori et al., 2007; Joe, 2014; Durante and Sempi, 2015; Czado, 2019). Η αναλυτική τους μορφή είναι συχνά αρκετά πολύπλοκη, εξαρτάται από διάφορες παραμέτρους και διαφέρει μεταξύ οικογενειών. Οι πιο γνωστές συζεύξεις ανήκουν στην Αρχιμήδεια κλάση (π.χ. Clayton, Gumbel, Frank, Joe, Ali-Mikhail-Haq, BB1, BB6, BB7, BB8), την Ελλειπτική ή Μεταλλειπτική κλάση (π.χ. Gaussian, t), και την κλάση των Ακραίων συζεύξεων (π.χ. Gumbel, Tawn). Οι περιπτώσεις των BB1, BB6, BB7, BB8 είναι μικτές μορφές που έχουν προκύψει από το συνδυασμό των προηγούμενων συζεύξεων (Nikoloulopoulos et al., 2012; Joe, 2014). Ορίζονται επίσης κάποιες συζεύξεις εκ περιστροφής 90, 180, ή 270 μοιρών, ώστε να περιγράφουν κάθε μορφή εξάρτησης των εμπλεκομένων μεταβλητών.

Η ταυτόχρονη εμφάνιση πολύ χαμηλών ή υψηλών τιμών για δυο ή περισσότερες μεταβλητές έχει πολλές φορές καθοριστικό ρόλο στην επιλογή της κατάλληλης σύζευξης. Υπάρχουν συζεύξεις που αδυνατούν να περιγράψουν αυτή την εξάρτηση, ενώ άλλες είναι καταλληλότερες για τέτοιου είδους δεδομένα. Για τη διερεύνηση αυτής της εξάρτησης χρησιμοποιούνται οι συντελεστές ουρών λ_U και λ_L για την άνω και κάτω ουρά αντίστοιχα (Nelsen, 2006) βάσει των παρακάτω εξισώσεων:

$$\lambda_U = \lim_{t \to 1^-} \frac{1 - 2t + C(t,t)}{1 - t} \quad \text{και} \quad \lambda_L = \lim_{t \to 0^+} \frac{C(t,t)}{1 - t} \ . \tag{9}$$

Για την επέκταση των συζεύξεων σε περισσότερες από τρείς μεταβλητές, χρησιμοποιείται η μεθοδολογία της «κατασκευής ζευγών» (Pair Copula Construction - PCC) γνωστή και ως μέθοδος των Vine συζεύξεων. Αξίζει να σημειωθεί ότι ο όρος Vine χρησιμοποιείται τόσο για τη μεθοδολογία, όσο και για τις πολυδιάστατες συζεύξεις που δημιουργούνται από αυτή. Οι εργασίες των Aas et al. (2009) και De Michelle et al. (2007) επηρέασαν την έρευνα σε αυτό τον τομέα, ωστόσο η αρχική ιδέα είχε παρουσιαστεί πολύ νωρίτερα από τον Joe (1996) και τους Bedford and Cooke (2001, 2002). Οι Vine συζεύξεις είναι ιεραρχικές δομές που στηρίζονται στην εξάρτηση των μεταβλητών ανά ζεύγη, δίνοντας τη δυνατότητα να υπολογιστεί η κοινή συνάρτηση πυκνότητας f με τη βοήθεια των συζεύξεων (Aas et al., 2009) σύμφωνα με την Εξ.10:

$$f(x_1,\ldots,x_d) = \prod_{j=1}^{d-1}\prod_{i=1}^{d-j} c_{j,i+j;1,\ldots,j-1}\left(F_{x_j|x_1,\ldots,x_{j-1}}\left(x_j \middle| x_1,\ldots,x_{j-1}\right), F_{x_{i+j}|x_1,\ldots,x_{j-1}}\left(x_{i+j} \middle| x_1,\ldots,x_{j-1}\right)\right)\prod_{k=1}^{d} f_k\left(x_k\right). \tag{10}$$

Στη βιβλιογραφία εμφανίζονται τρεις παραλλαγές των Vine συζεύξεων (C-Vines, R-Vines, D-Vines), ωστόσο οι C-Vine συζεύξεις είναι η πιο απλοποιημένη εκδοχή τους.

Η δομή των Vine συζεύξεων περιγράφεται μέσω ενός δενδροειδούς δικτύου (Σχ. 4) που συνδυάζει ανά ζεύγος τις μεταβλητές, ενώ η ιεράρχηση των μεταβλητών στηρίζεται στην εξάρτηση τους. Η βέλτιστη επιλογή της κατάλληλης σύζευξης γίνεται μέσω των κριτηρίων πληροφορίας AIC και BIC όπως υπολογίζονται από τις Εξ. 11 και Εξ. 12 αντίστοιχα:

$$AIC = -2L + 2k\,, \tag{11}$$

$$BIC = -2L + \ln(n)\cdot k\,, \tag{12}$$

ενώ ο υπολογισμός των παραμέτρων της κάθε σύζευξης στηρίζεται στη μέγιστη πιθανοφάνεια, όπου υπολογίζεται με διαδοχικές εκτιμήσεις (sequential estimation) (Hobæk Haff, 2012, 2013; Dißmann et al., 2013).

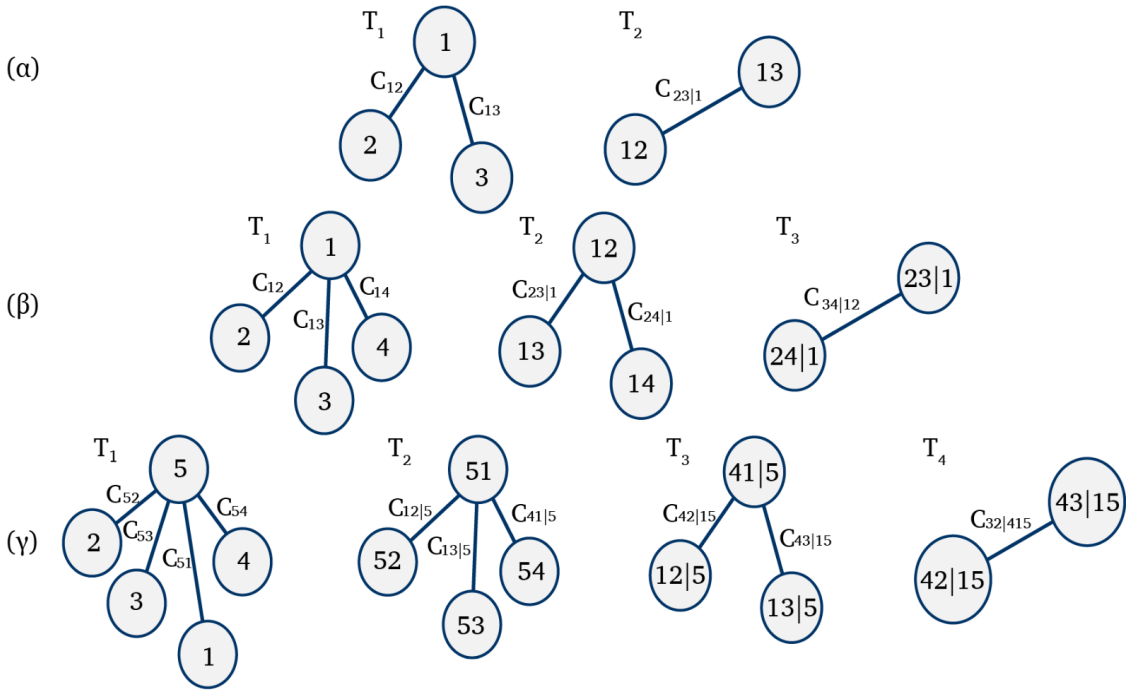

Σχήμα 4. Τυπικές δομές C-Vine συζεύξεων για τρεις (α), τέσσερις (β) και πέντε μεταβλητές (γ).

Για παράδειγμα, η κατασκευή μιας σύζευξης πέντε μεταβλητών μέσω των C-Vines (Σχ. 4γ), έχει ως αφετηρία το δέντρο T_1 και τη μεταβλητή (5) που παρουσιάζει τη μεγαλύτερη εξάρτηση μεταξύ των υπολοίπων. Η διαδικασία περιλαμβάνει την κατασκευή των δισδιάστατων συζεύξεων $C_{51}, C_{52}, C_{53}, C_{54}, C_{55}$, από το συνδυασμό των μεταβλητών, στη συνέχεια οι δισδιάστατες συζεύξεις χρησιμοποιούνται για την κατασκευή των δεσμευμένων δισδιάστατων συζεύξεων που αφορούν σε τρείς μεταβλητές του δέντρου T_2, $C_{12|5}, C_{13|5}, C_{41|5}$, αυτές με τη σειρά τους για τις δεσμευμένες συζεύξεις τεσσάρων μεταβλητών $C_{42|15}, C_{43|15}$ του δέντρου T_3 και στη συνέχεια για τη δεσμευμένη σύζευξη $C_{32|415}$ του δέντρου T_4 που συνδέει πέντε μεταβλητές. Η μετάβαση από δυο σε τρείς μεταβλητές κ.ο.κ. απαιτεί την κατασκευή των *h-functions* και μέσω αυτών την εύρεση της βέλτιστης σύζευξης όπως περιγράφεται στο Σχήμα 5, όπου X_i ($i=1,\ldots,5$) οι μεταβλητές, U_i οι κανονικοποιημένες μεταβλητές και F_i οι περιθώριες κατανομές. Η παραπάνω μεθοδολογία για την κατασκευή των Vine συζεύξεων μπορεί εύκολα να επεκταθεί σε περισσότερες μεταβλητές.

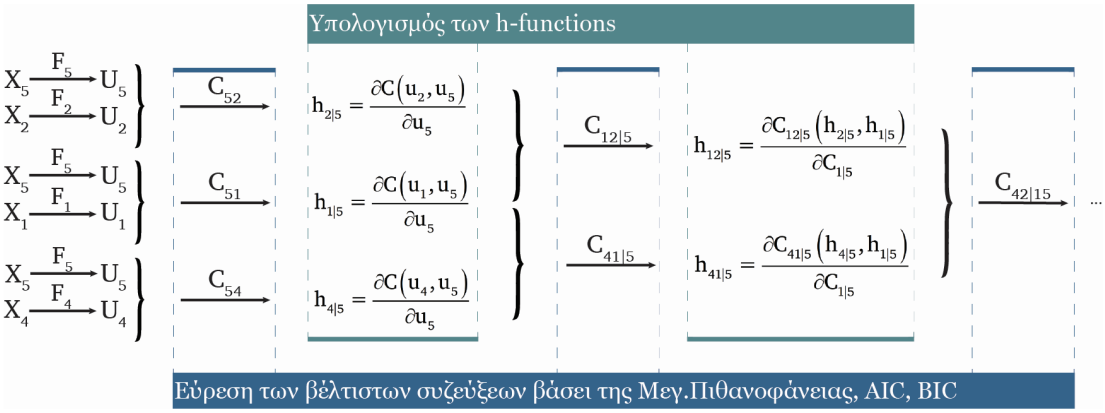

Σχήμα 5. Η διαδικασία κατασκευής ενός C-Vine μοντέλου για πέντε μεταβλητές.

Στη παρούσα διατριβή, οι απλές δισδιάστατες συζεύξεις χρησιμοποιούνται αρχικά για τη διερεύνηση της εξάρτησης του ύψους και της περιόδου κύματος κατά τη διάρκεια μιας παράκτιας καταιγίδας. Οι C-Vine συζεύξεις πέντε μεταβλητών (H_1, T_1, D, I, E) εφαρμόζονται στην προσομοίωση των παράκτιων καταιγίδων μιας περιοχής. Οι συζεύξεις δυο έως πέντε μεταβλητών διάφορων οικογενειών (π.χ. Gaussian, Gumbel και t) αλλά και οι C-Vine συζεύξεις τριών έως πέντε μεταβλητών χρησιμοποιούνται για την εύρεση των κοινών πιθανοτήτων και τον υπολογισμό των περιόδων επαναφοράς για τις καταιγίδες μιας περιοχής όταν αυτές χαρακτηρίζονται από υψηλές τιμές των παραμέτρων τους.

3.3.2. Προσομοίωση μέσω συζεύξεων

Η βέλτιστη σύζευξη δυο ή περισσότερων μεταβλητών λειτουργεί ως ένα μοντέλο που περιγράφει την εξάρτηση τους. Το μοντέλο αυτό μπορεί να χρησιμοποιηθεί για την προσομοίωση των μεταβλητών και κατά συνέπεια ενός φαινομένου που εξαρτάται από αυτές τις μεταβλητές. Η προσομοίωση δημιουργεί ένα νέο σύνολο δεδομένων που έχει παρόμοιες ιδιότητες με τα αρχικά δεδομένα.

Στην παρούσα διατριβή, η προσομοίωση δυο ή περισσότερων μεταβλητών επιτυγχάνεται μέσω των πολυδιάστατων συζεύξεων των γνωστών οικογενειών (π.χ. Gaussian, Joe, Gumbel) ή μέσω των C-Vines συζεύξεων και της μεθόδου PCC (για περισσότερες από τρείς μεταβλητές). Η μέθοδος PCC έχει εφαρμοστεί για την προσομοίωση των καταιγίδων στη θάλασσα από τους De Michele et al. (2007), χρησιμοποιώντας τέσσερις μεταβλητές, ενώ παρόμοιες προσεγγίσεις έχουν παρουσιαστεί στο τομέα των Οικονομικών όπως των Aas et al. (2009) και ακόμη πιο πρόσφατα των Stöber and Czado (2017). Βάσει των τριών μεθοδολογιών (De Michele et al., 2007; Aas et al., 2009; Stöber and Czado, 2017), αναπτύσσονται τρείς αλγόριθμοι που επεκτείνονται σε πέντε διαστάσεις και συγκρίνονται ως προς την

αποτελεσματικότητά τους για την προσομοίωση των παράκτιων καταιγίδων μιας περιοχής.

Πιο συγκεκριμένα, ξεκινώντας με ένα γνωστό δείγμα w=(w_1, w_2, w_3, w_4,,w_5) $\in [0,1]$ μπορεί να γίνει προσομοίωση ενός νέου δείγματος u=(u_1, u_2, u_3, u_4, u_5) μέσω των αλγορίθμων που βασίζονται στις μεθοδολογίες των Stöber and Czado (2017), Aas et al. (2009) και De Michele et al. (2007), όπου u,w$\sim U[0,1]$. Τα αρχικά στάδια των τριών αλγορίθμων παρουσιάζονται παρακάτω:

- **Αλγόριθμος Α,** βάσει της μεθοδολογίας των Stöber and Czado (2017)

$u_5 = v_{11} = w_5$

$v_{22} = w_4$

$v_{12} = h_{2|1}^{-1}\left(v_{22}\middle|v_{11}\right) = h^{-1}\left(w_4\middle|w_5\right) \Rightarrow u_4 = v_{12}$

$v_{33} = w_1$

$v_{23} = h_{3|2}^{-1}\left(v_{33}\middle|v_{22}\right) = h^{-1}\left(w_1\middle|w_4\right)$

$v_{13} = h_{3|1}^{-1}\left(v_{23}\middle|v_{11}\right) = h^{-1}\left(v_{23}\middle|w_5\right) \Rightarrow u_1 = v_{13}$

- **Αλγόριθμος Β**, βάσει της μεθοδολογίας των Aas et al. (2009):

$u_5 = v_{11} = w_5$

$v_{21} = w_4$

$v_{21} = h^{-1}\left(v_{21}\middle|v_{11}\right) = h_{4|5}^{-1}\left(w_4\middle|u_5\right) \Rightarrow u_4 = v_{21}$

$v_{22} = h\ \left(v_{21}\middle|v_{11}\right) = h_{4|5}\left(u_4\middle|u_5\right)$

$v_{31} = w_1$

$v_{31} = h^{-1}\left(v_{31}\middle|v_{22}\right) = h_{1|45}^{-1}\left(w_1\middle|v_{22}\right)$

$v_{31} = h^{-1}\left(v_{31}\middle|v_{11}\right) = h_{1|5}^{-1}\left(v_{31}\middle|u_5\right) \Rightarrow u_1 = v_{31}$

- **Αλγόριθμος Γ**, βάσει της μεθοδολογίας των De Michele et al. (2007)

u_1=w_1

$u_2 = h_{2|1}^{-1}\left(w_2\middle|w_1\right)$

$k_1 = h_{1|2}\left(w_1\middle|w_2\right) = \frac{\partial C_{12}(w_1, w_2)}{\partial w_2}, m_1 = h_{3|2}\left(w_3\middle|w_2\right) = \frac{\partial C_{23}(w_2, w_3)}{\partial w_2}$

$u_3 = h_{3|1}^{-1}\left(m_1\middle|k_1\right)$

Μετά την προσομοίωση, το παραγόμενο σύνολο δεδομένων $\left(u_1, u_2, u_3, u_4, u_5\right) \in [0,1]$ μετασχηματίζεται στο πραγματικό πεδίο των μεταβλητών $\left(x_1, x_2, x_3, x_4, x_5\right)$ χρησιμοποιώντας τον ολοκληρωτικό μετασχηματισμό πιθανότητας, τις αντίστροφες περιθώριες κατανομές ή τις εμπειρικές κατανομές όπως περιγράφεται στην Εξ. 14:

$$\left(x_1, x_2, x_3, x_4, x_5\right) = \left(F_1^{-1}\left(u_1\right), F_2^{-1}\left(u_2\right), F_3^{-1}\left(u_3\right), F_4^{-1}\left(u_4\right), F_5^{-1}\left(u_5\right)\right). \quad (14)$$

3.3.3. Περίοδοι επαναφοράς

Η περίοδος επαναφοράς είναι μια πιθανοτική εκτίμηση για την επανεμφάνιση ενός ακραίου γεγονότος. Έχει ευρεία χρήση στην ευστάθεια έργων και κυρίως σε διάφορους τομείς όπως στην Ακτομηχανική, στην Υδρολογία, στη Μετεωρολογία, στη Γεωλογία και αφορά σε φαινόμενα όπου η επανεμφάνισή τους μπορεί να είναι καταστροφική (π.χ. καταιγίδες, πλημμύρες, σεισμοί, τσουνάμι).

Η εφαρμογή των δισδιάστατων συζεύξεων στις περιόδους επαναφοράς χρησιμοποιείται ευρέως τα τελευταία χρόνια, με εφαρμογές στις κυματικές παραμέτρους (De Michele et al., 2007; Salvadori et al., 2014, 2015; Mazas and Hamm, 2017; Li and Liu, 2020; Orcel et al., 2021). Ομοίως, χρησιμοποιούνται στην Υδρολογία και για τρεις μεταβλητές (Latif and Mustafa, 2020; Mesbahzadeh et al., 2020; Saghafian and Sanginabadi, 2020; Tosunoglu et al., 2020; Zhang et al., 2021).

Στην περίπτωση των παράκτιων καταιγίδων, η περίοδος επαναφοράς είναι αρκετά σημαντική για το σχεδιασμό των λιμενικών και παράκτιων έργων καθώς η συχνή εμφάνιση ενός ακραίου κυματικού γεγονότος μπορεί να καθορίσει τη θέση του έργου, τη διάταξη, τις διαστάσεις, τη διάρκεια ζωής, καθώς και τα υλικά της κατασκευής του. Στο σχεδιασμό λιμενικών και παράκτιων έργων χρησιμοποιείται ως περίοδος επαναφοράς τα 100 έτη. Πιο συγκεκριμένα, τα χαρακτηριστικά μιας ακραίας κυματικής κατάστασης ή μιας παράκτιας καταιγίδας που έχει πιθανότητα 1/100 να συμβεί κατά τη διάρκεια ενός έτους καθορίζουν το κύμα σχεδιασμού των έργων.

Η περίοδος επαναφοράς μιας παράκτιας καταιγίδας με συγκεκριμένα χαρακτηριστικά (π.χ. $X_1>x_1$), όταν μ είναι ο μέσος χρόνος σε έτη μεταξύ δυο διαδοχικών γεγονότων, δίνεται από την Εξ. 15:

$$T_{(X_1>x_1)} = \frac{\mu}{P\left(X_1 > x_1\right)} = \frac{\mu}{1 - P\left(X_1 \le x_1\right)} = \frac{\mu}{1 - F_1\left(x_1\right)}. \quad (15)$$

Στη συγκεκριμένη εξίσωση η πιθανότητα $P(X_1>x_1)$ ορίζεται ως πιθανότητα υπέρβασης, ωστόσο μπορεί να χρησιμοποιηθεί οποιαδήποτε άλλη πιθανότητα που περιγράφει τα επιθυμητά χαρακτηριστικά μιας παράκτιας καταιγίδας. Η κοινή πιθανότητα των χαρακτηριστικών της καταιγίδας, υπολογίζεται με τη βοήθεια των συζεύξεων και στη συνέχεια μέσω αυτής και της Εξ. 15 υπολογίζεται οποιαδήποτε περίοδος επαναφοράς απαιτείται. Για τον υπολογισμό τους, χρησιμοποιούνται επίσης τα σύμβολα της ένωσης $\cup$ και τη τομής $\cap$ των συνόλων για την περιγραφή της ταυτόχρονης ή μη εμφάνισης των επιθυμητών χαρακτηριστικών.

Ο υπολογισμός των κοινών πιθανοτήτων μέσω των συζεύξεων για δυο και τρείς μεταβλητές έχει παρουσιαστεί στη βιβλιογραφία από διάφορους ερευνητές, ωστόσο η

επέκτασή τους σε περισσότερες μεταβλητές είναι αρκετά εύκολη. Ενδεικτικά αναφέρονται οι παρακάτω κοινές πιθανότητες (Serinaldi, 2015; Zhang and Singh, 2019a):

$$P\left(X_1 \le x_1, X_2 \le x_2\right) = C\left(u_1, u_2\right) \tag{16}$$

$$\begin{aligned} P\left(X_1 > x_1, X_2 > x_2\right) &= 1 - P\left(X_1 \le x_1\right) - P\left(X_2 \le x_2\right) + P\left(X_1 \le x_1, X_2 \le x_2\right) = \\ &= 1 - u_1 - u_2 + C\left(u_1, u_2\right). \end{aligned} \tag{17}$$

Συνεπώς, οι αντίστοιχες περίοδοι επαναφοράς προκύπτουν από τις παρακάτω εξισώσεις:

$$T_{\left(X_1 > x_1 \cap X_2 > x_2\right)} = \frac{\mu}{P\left(X_1 > x_1, X_2 > x_2\right)} = \frac{\mu}{1 - u_1 - u_2 + C\left(u_1, u_2\right)}, \tag{18}$$

$$T_{\left(X_1 > x_1 \cup X_2 > x_2\right)} = \frac{\mu}{1 - P\left(X_1 \le x_1, X_2 \le x_2\right)} = \frac{\mu}{1 - C\left(u_1, u_2\right)}, \tag{19}$$

και παρόμοια προκύπτουν όλοι οι υπόλοιποι συνδυασμοί για περισσότερες μεταβλητές.

Αξίζει να σημειωθεί ότι για τον υπολογισμό των δισδιάστατων περιόδων επαναφοράς, χρησιμοποιούνται οι βέλτιστες συζεύξεις των μεταβλητών X_1, X_2, έχοντας υπολογίσει και προσαρμόσει τις απαραίτητες παραμέτρους.

4. Αποτελέσματα και συζήτηση

4.1. Παράκτιες καταιγίδες στη Μεσόγειο θάλασσα

Η ανάλυση και η μοντελοποίηση των παράκτιων καταιγίδων εξετάζεται στη βιβλιογραφία σε μεμονωμένες περιοχές, χρησιμοποιώντας κυρίως δεδομένα προσομοιώσεων. Η παρούσα διατριβή στηρίζεται σε ένα σύνολο κυματικών δεδομένων από πλωτούς μετρητές σε 30 περιοχές στη Μεσόγειο θάλασσα (Σχ. 6) που καλύπτουν την περίοδο 1985-2019. Η επιλογή των περιοχών έγινε με κριτήριο την ελάχιστη δυνατή απόσταση από τις ευρωπαϊκές ακτές. Τα χαρακτηριστικά κάθε περιοχής είναι ανομοιογενή, ποικίλουν ως προς το βάθος και την απόσταση από την κοντινότερη ακτή, αναφέρονται σε διαφορετικές χρονικές περιόδους, και οι μετρήσεις έχουν συνήθως διαφορετικό χρονικό βήμα, με αποτέλεσμα οι διαδοχικές τιμές να απέχουν από 0.5-3 ώρες ανάλογα την περιοχή.

Εφαρμόζοντας τη μεθοδολογία για τον εντοπισμό των παράκτιων καταιγίδων, ορίζεται το κατώφλι του ύψους κύματος (H_{thr}) ως το 95^o εκατοστημόριο του σημαντικού ύψους κύματος κάθε περιοχής και εφαρμόζεται στα διαθέσιμα δεδομένα. Στη συνέχεια, ορίζεται η ελάχιστη διάρκεια των παράκτιων καταιγίδων (D_{thr}) στις εννέα ώρες, έπειτα από διερεύνηση του εύρους της διάρκειας και του διαστήματος καταγραφής (recording interval). Το κατώφλι της φάσης ηρεμίας (I_{thr}) ορίζεται σε κάθε περιοχή μεταξύ 12-24 ωρών, όπως συνήθως στη διεθνή βιβλιογραφία, λαμβάνοντας επίσης υπόψη τους

συντελεστές συσχέτισης Spearman's ρ, Kendall's τ και Pearson's r για τις μεταβλητές του ύψους και της περιόδου του κύματος μεταξύ διαδοχικών γεγονότων. Περιπτώσεις δεδομένων που ικανοποιούν τα προηγούμενα κριτήρια-κατώφλια, αλλά αποτελούνται από διαδοχικές τιμές που απέχουν χρονικά πάνω από 18 ώρες, δεν θεωρούνται καταιγίδες και εξαιρούνται.

Σχήμα 6. Οι 30 εξεταζόμενες περιοχές στη Μεσόγειο θάλασσα. Τα τετράγωνα πλαίσια στην αρίθμηση των περιοχών δηλώνουν τους πλωτήρες που είναι πλέον εκτός λειτουργίας.

4.1.1. Χαρακτηριστικά των παράκτιων καταιγίδων

Εφαρμόζοντας στα δεδομένα των 30 περιοχών τα κατώφλια H_{thr}, D_{thr}, I_{thr}, εντοπίζονται 4008 παράκτιες καταιγίδες και στη συνέχεια υπολογίζονται τα χαρακτηριστικά τους και εξάγονται τα περιγραφικά στατιστικά στοιχεία τους. Η συχνότητα εμφάνισης των παράκτιων καταιγίδων, οι μέγιστες, οι μέσες και οι ακραίες τιμές των εμπλεκόμενων μεταβλητών, το εύρος της περιόδου και της φάσης ηρεμίας όσο και το σχήμα παρουσιάζονται για να περιγράψουν τη δραστηριότητα τους στη Μεσόγειο θάλασσα.

Περιγραφική Στατιστική

Οι 4008 παράκτιες καταιγίδες που εντοπίζονται αντιστοιχούν συνολικά σε 41-127 γεγονότα ανά έτος στην Ελλάδα, στην Ιταλία, στη Γαλλία και στην Ισπανία. Σε επίπεδο χώρας, οι παράκτιες περιοχές αντιμετωπίζουν κατά μέσο όρο 10-14 καταιγίδες ετησίως. Πιο αναλυτικά, σε κάθε περιοχή συμβαίνουν 9-18 παράκτιες καταιγίδες ανά έτος (Σχ. 7), με τις περισσότερες να συμβαίνουν στην Ισπανία και την Γαλλία και κυρίως τους χειμερινούς μήνες (Σχ. 8), όπως αναμενόταν. Να σημειωθεί ότι τα δεδομένα της Ιταλίας, αναφέρονται σε μικρή χρονική περίοδο οπότε οι ετήσιες συχνότητες εμφάνισης δεν είναι άμεσα συγκρίσιμες και επομένως δεν παρουσιάζονται στο Σχήμα 7.

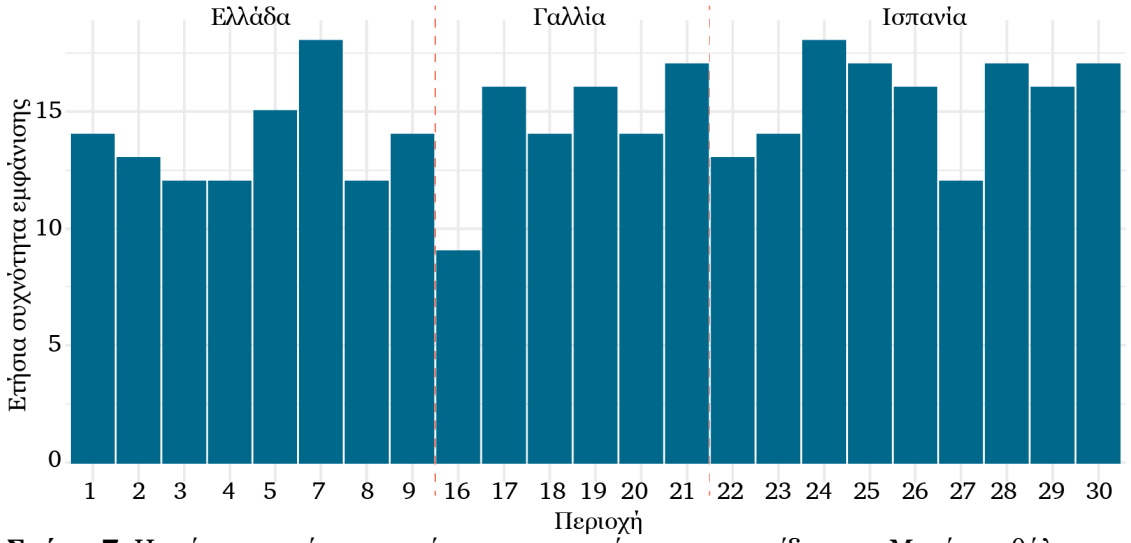

Σχήμα 7. Η ετήσια συχνότητα εμφάνισης των παράκτιων καταιγίδων στη Μεσόγειο θάλασσα.

Τα περιγραφικά στατιστικά στοιχεία εξάγονται από τις τιμές του ύψους (*H*) και της περιόδου (*T*) του κύματος κατά τη διάρκεια μιας καταιγίδας, όσο και από την τιμή της ενέργειας (*E*), της ροής ενέργειας (*P*) και της διάρκειας (*D*) οι οποίες αντιστοιχούν σε κάθε καταιγίδα. Στον Πίνακα 1, παρουσιάζονται οι μέσες (π.χ. m_H, m_T) και οι μέγιστες τιμές (π.χ. max_H, max_T) των παραπάνω μεταβλητών για όλες τις περιοχές. Οι ακραίες τιμές $m_{H5\%}$ $m_{T5\%}$, προκύπτουν από το μέσο όρο του 5% των υψηλότερων τιμών του ύψους και της περιόδου κύματος κατά τη διάρκεια της καταιγίδας. Σύμφωνα με τα αποτελέσματα, επιβεβαιώνεται ότι οι περιοχές που είναι εκτεθειμένες σε μεγάλα αναπτύγματα πελάγους (Cabo Begur, La Revellata, Palermo, Pylos) εμφανίζουν παράκτιες καταιγίδες με τα υψηλότερα κύματα και αντίθετα στις πιο προστατευμένες περιοχές (Kalamata, Venice, Nice και Tarragona) που συνήθως βρίσκονται σε μικρό βάθος, συμβαίνουν χαμηλότερης έντασης καταιγίδες βάσει του ύψους κύματος, της ενέργειας και της διάρκειας τους. Ιδιαίτερη σημασία έχουν τα χαρακτηριστικά των καταιγίδων στις περιοχές που είναι αρκετά κοντά στις ακτές (π.χ. Tarragona, Malaga, Son Bou) ή σε μικρό βάθος (Crotone και Nice) καθώς τα κυματικά χαρακτηριστικά που περιγράφονται στον Πίνακα 1 αφορούν στις παράκτιες περιοχές χωρίς να μεσολαβούν σημαντικές αλλοιώσεις λόγω θραύσης, περίθλασης ή ρήχωσης όπως συμβαίνει συνήθως στα κύματα που προέρχονται από τα βαθιά.

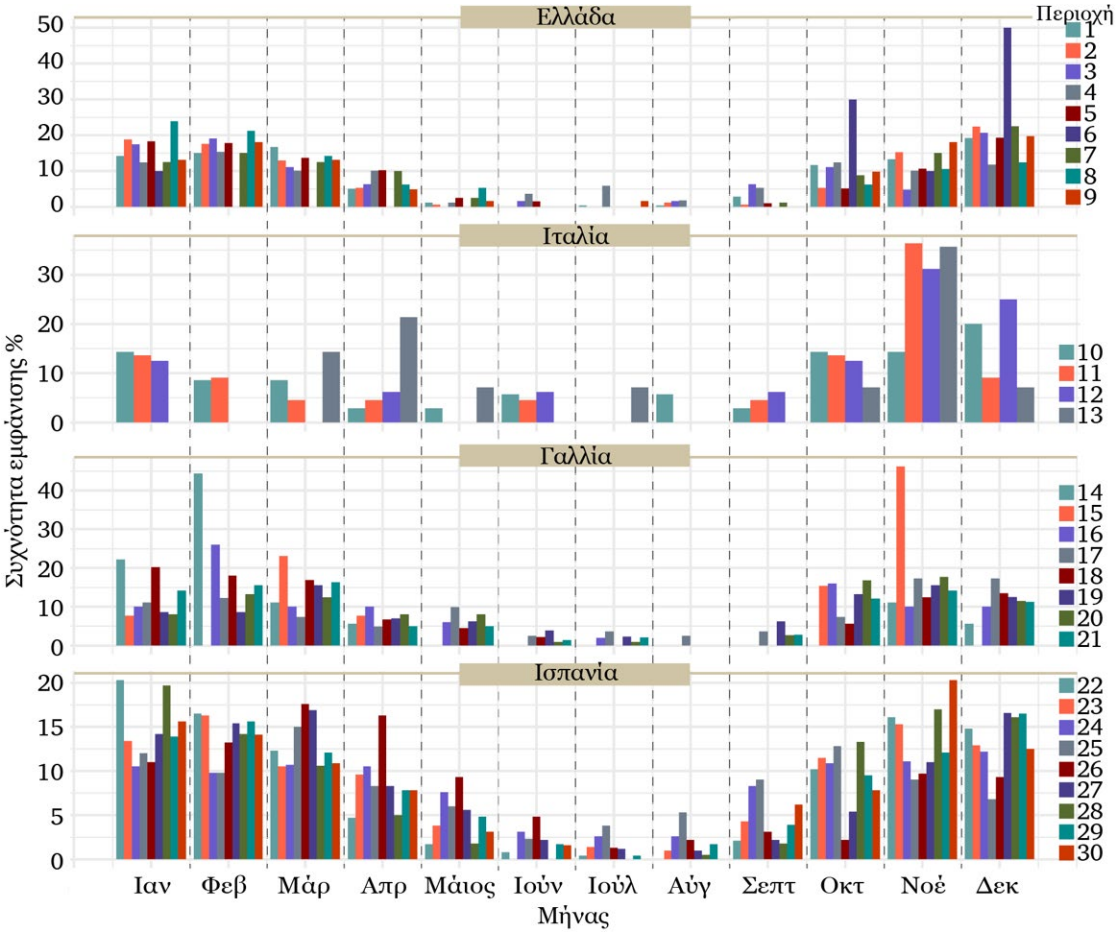

Σχήμα 8. Η μηνιαία συχνότητα εμφάνισης (%) των παράκτιων καταιγίδων στη Μεσόγειο θάλασσα.

Οι δυο προσεγγίσεις του δείκτη σφοδρότητας (ενέργεια καταιγίδας και ροή ενέργειας) αν και δεν είναι συγκρίσιμες έχουν παρόμοια συμπεριφορά, με τις μέγιστες τιμές να εμφανίζονται στις περιοχές όπου το ύψος, η περίοδος του κύματος και η διάρκεια της καταιγίδας έχουν υψηλές τιμές. Όλες οι μεταβλητές που παρουσιάζονται στον Πίνακα 1 είναι χρήσιμες για την κατανόηση των κυματικών χαρακτηριστικών των περιοχών κατά τη διάρκεια των καταιγίδων, αλλά και για τη σύγκριση της σφοδρότητάς τους σε κάθε περιοχή. Επιπλέον αναλύσεις, δείχνουν ότι η περίοδος κύματος κυμαίνεται μεταξύ 6-8 δευτερολέπτων όταν το ύψος κύματος ξεπερνάει το 90% του δείγματος σε κάθε περιοχή, με τις υψηλότερες τιμές να εμφανίζονται στις περιοχές της Πύλου και της Ζακύνθου.

Πίνακας 1
Στατιστικά στοιχεία των παράκτιων καταιγίδων στη Μεσόγειο θάλασσα.

	Περιοχή	m_H [m]	max_H [m]	m_T [s]	max_T [s]	m_E [m²hr]	m_P [Whr/m]	m_D [hr]	$m_{H5\%}$ [m]	$m_{T5\%}$ [s]
					Ελλάδα					
1	Athos	3.01	5.99	7.57	11.01	243.84	19850.37	27.06	4.01	9.05
2	Lesvos	2.43	4.92	7.13	10.56	169.71	14645.21	24.13	4.61	10.08
3	Skyros	3.01	5.45	7.82	10.04	248.04	20495.81	28.10	3.75	8.81
4	Mykonos	3.10	5.76	7.87	11.36	234.35	20860.71	27.38	5.13	9.47
5	Santorini	2.46	4.92	7.37	13.82	143.32	10966.83	24.51	3.08	9.16
6	Heraklion	2.47	4.25	7.33	10.04	191.64	16720.21	31.13	2.77	7.61
7	Kalamata	1.28	3.28	7.37	11.13	38.93	3049.20	24.31	1.76	9.13
8	Pylos	3.10	7.57	8.95	13.71	273.69	25949.15	28.64	4.05	10.21
9	Zakynthos	2.68	9.37	9.49	24.37	219.77	13874.17	28.82	4.62	18.37
					Ιταλία					
10	Venice	1.67	3.77	6.39	10.53	57.91	3956.21	20.23	2.34	8.34
11	Crotone	2.34	6.46	8.26	13.33	178.60	12565.84	29.09	3.41	9.67
12	Catania	2.21	4.96	8.57	12.50	131.63	10365.29	24.03	3.92	10.33
13	Palermo	2.85	5.49	8.99	13.33	152.46	15581.80	18.50	3.73	11.90
					Γαλλία					
14	Alistro	2.25	5.80	7.45	11.80	128.61	11851.22	23.31	3.45	9.12
15	La Revellata	3.94	7.70	9.65	13.30	374.49	33189.66	22.57	5.32	10.88
16	Nice	1.73	4.00	7.23	13.30	69.23	5042.72	22.45	2.24	10.82
17	Porquerolles	3.06	6.20	8.52	12.10	175.94	14482.73	19.09	3.85	10.07
18	Marseille	2.47	8.60	7.45	25.00	123.21	7947.60	20.57	3.10	8.94
19	Sete	2.36	5.90	7.41	11.80	162.38	10889.63	27.70	3.33	9.34
20	Leucate	2.33	9.10	7.40	28.60	164.50	11851.71	27.74	3.57	9.56
21	Banyuls	2.15	12.80	7.27	25.00	127.29	3901.43	25.77	3.17	9.80
					Ισπανία					
22	Cabo Begur	4.05	7.40	8.06	12.70	446.36	37867.01	26.98	5.11	9.91
23	Barcelona	2.03	5.20	7.56	12.30	118.88	10077.18	27.49	2.83	9.46
24	Tarragona	1.39	3.90	6.97	12.20	52.57	2024.92	25.02	1.81	7.09
25	Valencia	1.80	4.50	7.35	12.50	101.38	7684.43	29.51	2.42	9.57
26	Cabo De Gata	2.94	6.60	7.42	10.60	205.07	16190.26	23.47	3.76	8.77
27	Malaga	1.69	4.70	6.94	15.60	98.79	3720.91	30.37	2.47	6.83
28	Dragonera	3.27	6.30	8.24	12.80	269.30	26876.39	24.97	4.03	9.93
29	Capdepera	3.16	7.00	8.88	12.80	264.94	21296.32	25.88	4.16	10.09
30	Son Bou	1.73	4.98	5.33	8.52	89.94	1014.57	28.98	2.25	6.30

Διάρκεια και διάστημα ηρεμίας

Η διάρκεια και το διάστημα ηρεμίας των παράκτιων καταιγίδων εξετάζονται διεξοδικότερα σε κάθε περιοχή. Η μέση διάρκεια τους (Σχ. 9α) κυμαίνεται μεταξύ 18-31 ωρών, ενώ το 50% αυτών διαρκούν λιγότερο από 24 ώρες. Οι παράκτιες καταιγίδες της Ισπανίας εμφανίζουν τη μεγαλύτερη διάρκεια μέσα στο δείγμα. Η συχνότητα εμφάνισης των παράκτιων καταιγίδων συμπίπτει με αυτή των κυκλώνων στη Μεσόγειο θάλασσα σύμφωνα με τους Lionello et al. (2006), γεγονός που αποδεικνύει τη συσχέτιση των δυο φαινομένων και την επίδραση των μετεωρολογικών συνοπτικών συστημάτων στις παράκτιες καταιγίδες.

Το χρονικό διάστημα ηρεμίας (Σχ. 9β) μεταξύ δυο διαδοχικών παράκτιων καταιγίδων είναι κατά μέσο όρο μικρότερο από ένα μήνα. Τα περισσότερα διαδοχικά γεγονότα (75%) απέχουν λιγότερο από 750 ώρες (≈ 31 ημέρες), ενώ το 25% αυτών συμβαίνουν στην ίδια περιοχή σε λιγότερο από μια μέρα. Οι πληροφορίες για τη διάρκεια, το χρονικό διάστημα ηρεμίας σε κάθε περιοχή αλλά και για τις υπόλοιπες μεταβλητές είναι χρήσιμες

για περαιτέρω έρευνα σχετικά με τη διάβρωση των ακτών (Callaghan et al., 2008; Corbella and Stretch, 2012a; Dissanayake et al., 2015), όσο και για την αντοχή των κατασκευών και το σχεδιασμό τους (Salvadori et al., 2014; Lira-Loarca et al., 2020).

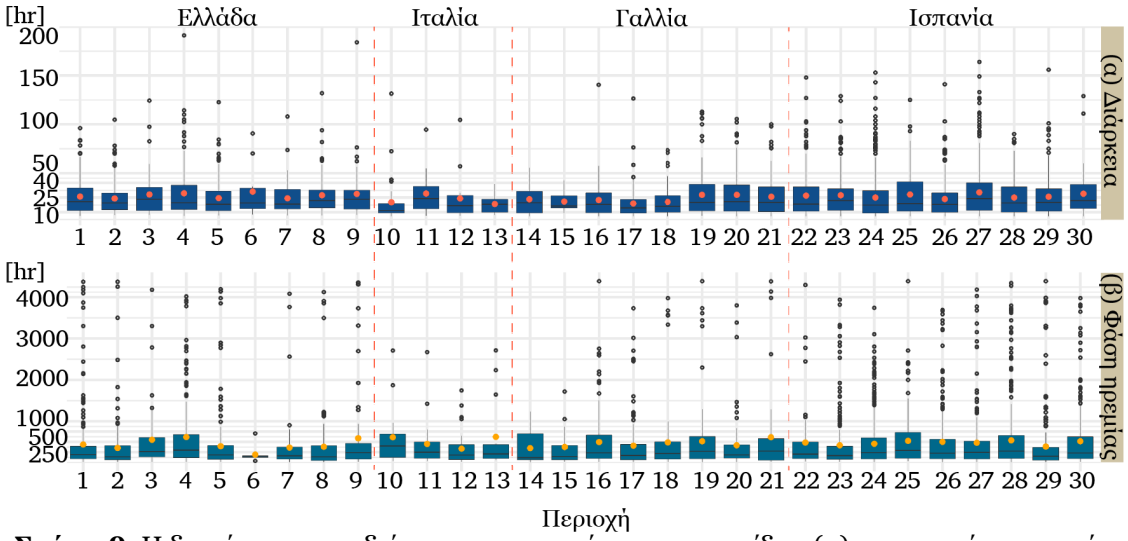

Σχήμα 9. Η διακύμανση της διάρκειας των παράκτιων καταιγίδων (α) και της φάσης ηρεμίας μεταξύ δυο γεγονότων (β).

Σχήμα παράκτιων καταιγίδων

Παρατηρώντας τα σχήματα των παράκτιων καταιγίδων σε οποιαδήποτε περιοχή, γίνεται εύκολα αντιληπτό ότι η μορφή τους ποικίλλει, όπως παρουσιάζεται συχνά στη βιβλιογραφία για τη μελέτη των συνθετικών καταιγίδων (Martín-Hidalgo et al., 2014; Martín Soldevilla et al., 2015; Duo et al., 2020; Marzeddu et al., 2020), παρά το γεγονός ότι το τριγωνικό σχήμα (Boccotti, 2015) έχει επικρατήσει στις μέρες μας λόγω απλότητας. Θεωρώντας λοιπόν ότι το τριγωνικό σχήμα περιγράφει καλύτερα τις παράκτιες καταιγίδες, εξετάζονται τρεις κατηγορίες ως προς την οξύτητα του τριγώνου, έτσι ώστε η κορυφή να είναι στο κέντρο (ισοσκελές τρίγωνο), αριστερά ή δεξιά από το μέσο της βάσης του (σκαληνό τρίγωνο) η οποία αντιπροσωπεύει τη διάρκεια της καταιγίδας. Οι τρείς κατηγορίες ελέγχονται ως προς τη σχέση τους με την κατεύθυνση και την περίοδο κύματος. Τα αποτελέσματα παρουσιάζονται στο Σχήμα 10 και είναι προφανές ότι δεν επικρατεί μια συγκεκριμένη μορφή τριγωνικού σχήματος στις παράκτιες καταιγίδες της Μεσογείου. Κατά συνέπεια, δεν επιβεβαιώνεται από το συγκεκριμένο δείγμα ότι οι παράκτιες καταιγίδες της Μεσογείου είναι πιο απότομες στην έναρξη τους, μέχρι να φτάσουν στην κορυφή και πιο ήπιες στη συνέχεια όπως έχουν υποστηρίξει οι Lin-Ye et al. (2016). Επιπλέον, η μορφή του τριγωνικού σχήματος δεν επηρεάζεται από την περίοδο κύματος ή την κατεύθυνση κατά τη διάρκεια μιας παράκτιας καταιγίδας, καθώς η διασπορά των χρωμάτων (Σχ. 10), που υποδηλώνουν τις κατηγορίες του τριγωνικού σχήματος, δεν ακολουθεί κάποιο μοτίβο.

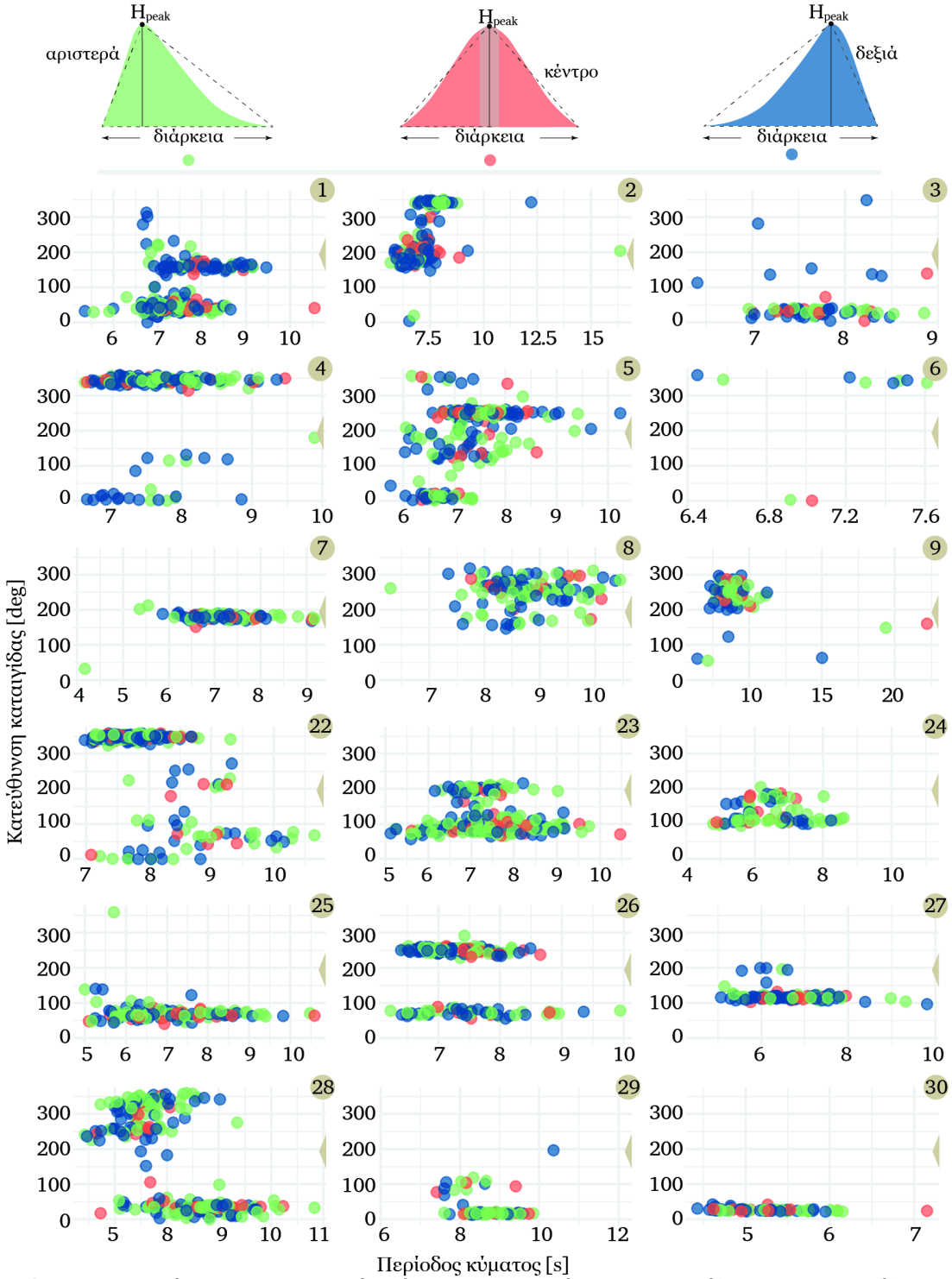

Σχήμα 10. Η σχέση του τριγωνικού σχήματος των παράκτιων καταιγίδων με την κατεύθυνση και την περίοδο κύματος.

3.1.2. Σημαντικές παράμετροι των παράκτιων καταιγίδων

Μετά τον εντοπισμό των παράκτιων καταιγίδων και την ανάλυση των χαρακτηριστικών τους, ορίζονται οι σημαντικές παράμετροι H_1, T_1, D_{ir1}, D, I, E, P ως αντιπρόσωποι κάθε γεγονότος. Για τον προσδιορισμό των παραμέτρων T_1, D_{ir1} υπολογίζεται ο συντελεστής

μεταβλητότητας (*CV*) της περιόδου (*T*) και η τυπική απόκλιση της κατεύθυνσης (D_{ir}) του κύματος κατά τη διάρκεια των παράκτιων καταιγίδων, ως δείκτες της διασποράς των μεταβλητών και το εύρος τους παρουσιάζεται στο Σχήμα 11.

Η περίοδος όσο και η κατεύθυνση κύματος διατηρείται σχεδόν σταθερή κατά τη διάρκεια μιας παράκτιας καταιγίδας, γεγονός που σημαίνει ότι η διασπορά των τιμών είναι μικρή και αρκετά κοντά στη μέση τιμή. Αυτό επιβεβαιώνεται από τις τιμές των συντελεστών μεταβλητότητας CV_T που είναι χαμηλότερες του 15% για όλες τις περιοχές και κατά μέσο όρο κάτω του 10% (Σχ. 11α), όσο και από το εύρος της τυπικής απόκλισης της κατεύθυνσης κύματος κατά τη διάρκεια μιας παράκτιας καταιγίδας (Σχ. 11β) που είναι μικρότερη των 20 μοιρών για τις περισσότερες παράκτιες καταιγίδες (75%) των περισσότερων περιοχών. Ως αποτέλεσμα, η μέση τιμή της περιόδου (T_1) και της κατεύθυνσης κύματος (D_{ir1}) θεωρείται ότι περιγράφουν ικανοποιητικά τις μεταβλητές *T* και D_{ir} μιας καταιγίδας, οπότε ορίζονται ως αντιπρόσωποι τους για κάθε γεγονός.

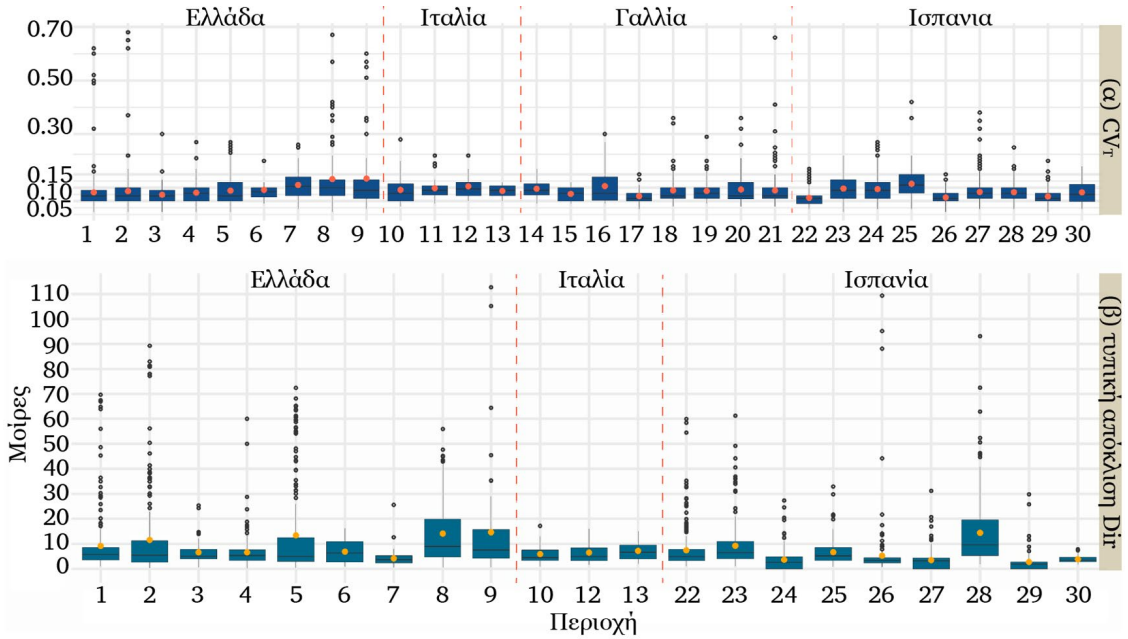

Σχήμα 11. Το εύρος του συντελεστή μεταβλητότητας για την περίοδο του κύματος CV_T (α) και της τυπικής απόκλισης της κατεύθυνσης του κύματος κατά τη διάρκεια μιας παράκτιας καταιγίδας (β).

Για τον δείκτη σφοδρότητας των παράκτιων καταιγίδων υπολογίζεται η ενέργεια της καταιγίδας *E* και η ροή ενέργειας *P*. Η συμπεριφορά των δυο μεταβλητών συγκρίνεται ώστε να φανεί η επίδραση του ύψους και της περιόδου κύματος στον υπολογισμό τους, καθώς και για να αποφασιστεί ποια μεταβλητή θα χρησιμοποιηθεί στη συνέχεια ως παράμετρος του δείκτη σφοδρότητας. Τα αποτελέσματα παρουσιάζονται σε σχέση με το ύψος κύματος (Σχ. 12), ενώ κάθε γεγονός (κουκίδα) κατηγοριοποιείται ως προς την περίοδο κύματος ($T<8$ s, $8\leq T<10$ s, και $T\geq 10$ s).

Οι δυο μεταβλητές *E* και *P* αφορούν μεγέθη με διαφορετικές μονάδες μέτρησης, ωστόσο είναι φανερό (Σχ. 12) ότι η συμπεριφορά τους ως προς το ύψος και την περίοδο

κύματος έχει πολλές ομοιότητες. Η διασπορά των μεταβλητών ακολουθεί το ίδιο μοτίβο στις περισσότερες περιοχές, χωρίς να είναι εφικτό να εξαχθεί κάποιο γενικό συμπέρασμα. Οι μέγιστες και ελάχιστες τιμές των δυο μεταβλητών προκύπτουν για παράκτιες καταιγίδες που έχουν ίδιο ύψος και περίοδο κύματος, με ελάχιστες εξαιρέσεις όπως αυτή της Πύλου (αρ. 8, Σχήμα 12). Ακόμη και όταν υπάρχουν παράκτιες καταιγίδες με ίδιο ύψος κύματος αλλά διαφορετική περίοδο δεν εντοπίζεται υποεκτίμηση των δυο μεταβλητών. Λόγω της παρόμοιας αυτής συμπεριφοράς των E και P, η Εξ. 1 των Dolan και Davis (1992) επιλέγεται για τον υπολογισμό του δείκτη σφοδρότητας των παράκτιων καταιγίδων όπως συνηθίζεται στη βιβλιογραφία μέχρι τις μέρες μας (Duo et al., 2020).

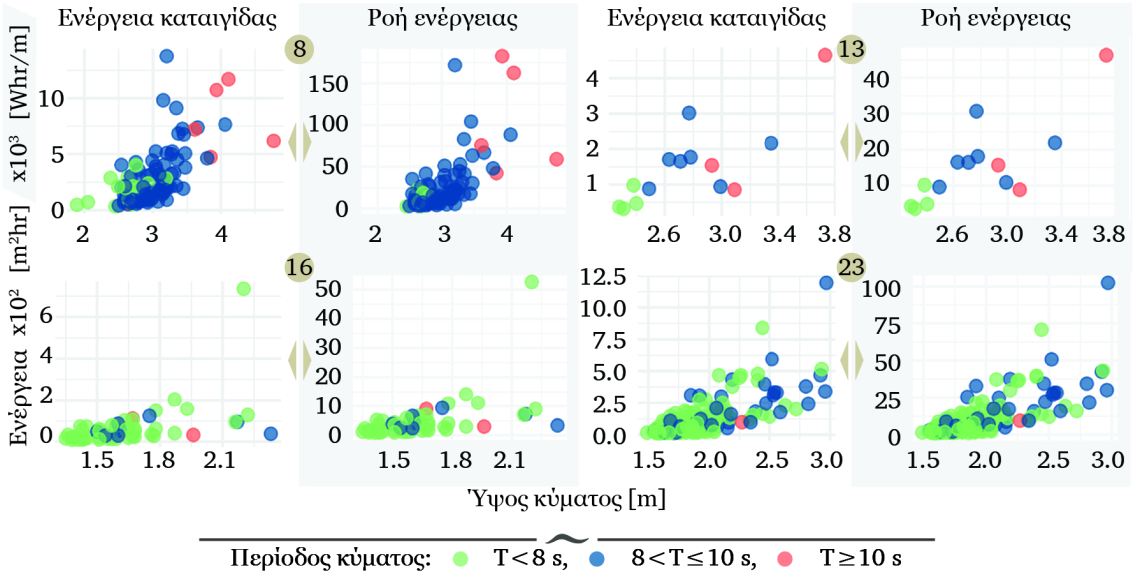

Σχήμα 12. Ενδεικτική σύγκριση της ενέργειας και της ροής ενέργειας των παράκτιων καταιγίδων σε σχέση με το ύψος και την περίοδο του κύματος στις περιοχές Pylos (8), Palermo (13), Nice (16), Barcelona (23).

Η παράμετρος H_1 για το ύψος κύματος μιας παράκτιας καταιγίδας συνήθως ορίζεται ως η μέγιστη τιμή του H κατά τη διάρκεια της παράκτιας καταιγίδας. Ωστόσο, η μέγιστη τιμή δεν αναφέρεται στη διάρκεια του γεγονότος, αλλά συνήθως σε κάποιες ώρες της διάρκειάς του. Συνεπώς, το μέσο ύψος κύματος (H_1) ορίζεται ως αντιπρόσωπος της καταιγίδας, ενώ η μέγιστη τιμή αλλά και όλο το φάσμα τιμών του ύψους κύματος λαμβάνονται υπόψη στον υπολογισμό της ενέργειας ώστε να μην γίνεται υποεκτίμηση της σφοδρότητας ενός γεγονότος.

Συνοψίζοντας, η μέση τιμή του ύψους (H_1), της περιόδου (T_1), της κατεύθυνσης του κύματος (D_{ir1}) κατά τη διάρκεια μια παράκτιας καταιγίδας, αλλά και η διάρκεια (D), το χρονικό διάστημα ηρεμίας (I) και η ενέργεια (E) που αντιστοιχεί σε ένα γεγονός ορίζονται ως αντιπρόσωποι των αντίστοιχων μεταβλητών. Στη συνέχεια, αναφέρονται ως σημαντικές παράμετροι μιας παράκτιας καταιγίδας και χρησιμοποιούνται για την περεταίρω έρευνα σε κάθε περιοχή.

4.2. Μοντελοποίηση παράκτιων καταιγίδων μέσω συζεύξεων

4.2.1. Συζεύξεις για το ύψος και την περίοδο του κύματος

Η βέλτιστη σύζευξη για την περιγραφή της εξάρτησης του ύψους (H) και της περιόδου κύματος (T) κατά τη διάρκεια μιας παράκτιας καταιγίδας επιλέγεται μεταξύ 40 διαφορετικών οικογενειών. Οι πιο γνωστές οικογένειες συζεύξεων εξετάζονται μέσω της R και της βιβλιοθήκης "VineCopula" (Nagler et al., 2021) και η επιλογή της βέλτιστης οικογένειας γίνεται βάσει της ελάχιστης τιμής των κριτηρίων πληροφορίας AIC και BIC. Προκειμένου η διερεύνηση να μην επηρεαστεί από τη χρονική εξάρτηση των τιμών των χρονοσειρών, υπολογίζεται η συνάρτηση αυτοσυσχέτισης για τις χρονοσειρές του H και αποφεύγονται οι περιπτώσεις που δεν ικανοποιούν αυτό το κριτήριο.

Οι επικρατέστερες οικογένειες συζεύξεων παρουσιάζονται στο Σχήμα 13. Ένα μεγάλο ποσοστό των εξεταζόμενων καταιγίδων παρουσιάζουν ανεξαρτησία μεταξύ του H και T για αυτό και οι ανεξάρτητες συζεύξεις (I) έχουν τη μεγαλύτερη συχνότητα εμφάνισης (Σχ. 13). Στη συνέχεια, οι πιο συνήθεις συζεύξεις είναι οι Tawn, Joe, Clayton και οι εκ περιστροφής μορφές τους. Οι οικογένειες Joe και Clayton ανήκουν στην Αρχιμήδεια κλάση και είναι ευρέως γνωστές κυρίως λόγω της απλοποιημένης μορφής τους (Corbella and Stretch, 2013; Martín Soldevilla et al., 2015; Lin-Ye et al., 2016; Li et al., 2018; Lira-Loarca et al., 2020). Ενδιαφέρον ωστόσο παρουσιάζουν οι συζεύξεις Tawn, που ανήκουν στην κλάση των Ακραίων συζεύξεων και φαίνεται να περιγράφουν ικανοποιητικά ακραία γεγονότα όπως είναι οι παράκτιες καταιγίδες. Η επιλογή των Tawn συζεύξεων θεωρείται βέλτιστη για αρκετές περιπτώσεις των παράκτιων καταιγίδων, όπως επίσης έχει συμβεί στο παρελθόν για την ανάλυση ξηρασίας (Sun et al., 2019; Botai et al., 2020). Γεγονός που αποδεικνύει ότι οι Tawn συζεύξεις πλεονεκτούν έναντι άλλων στην περιγραφή ακραίων γεγονότων και θα πρέπει να λαμβάνονται σοβαρά υπόψη στο μέλλον.

Δεδομένου ότι πολλές οικογένειες συζεύξεων μπορεί να είναι το ίδιο κατάλληλες για την μοντελοποίηση μιας σχέσης εξάρτησης, η βέλτιστη επιλογή είναι μια πολύπλοκη διαδικασία. Για την κατανόηση αυτής της διαδικασίας εξετάζονται τα χαρακτηριστικά των χρονοσειρών των H και T κατηγοριοποιώντας τα ως προς τις βέλτιστες οικογένειες συζεύξεων. Οι συντελεστές εξάρτησης των ουρών λ_L και λ_U επηρεάζουν την επιλογή της βέλτιστης σύζευξης. Το εύρος των συντελεστών λ_L και λ_U ποικίλει μεταξύ των συζεύξεων (Σχ. 14), ενώ κάποιες ομοιότητες που υπάρχουν είναι εύκολο να περιορίσουν τις επιλογές της βέλτιστης σύζευξης όταν οι συντελεστές λ_L και λ_U είναι ήδη γνωστοί. Αξίζει να σημειωθεί ότι η επιλογή της βέλτιστης σύζευξης είναι αρκετά δύσκολη όταν δυο ή περισσότερες οικογένειες παρουσιάζουν παρόμοια συμπεριφορά εξάρτησης των ουρών καθώς προσαρμόζονται το ίδιο καλά στα δεδομένα (Nikoloulopoulos and Karlis, 2008), όπως για παράδειγμα οι Clayton και survival Joe. Ως αποτέλεσμα η διερεύνηση της βέλτιστης σύζευξης μπορεί να περιοριστεί στις οικογένειες που έχουν διαφορετική συμπεριφορά στην εξάρτηση των ουρών (Nikoloulopoulos et al., 2012; Kadhem and Nikoloulopoulos, 2021).

Η διερεύνηση συνεχίζεται με τη διερεύνηση της διακύμανσης άλλων παραμέτρων, όπως είναι ο συντελεστής συσχέτισης Kendall's τ των H και T. Το εύρος τιμών του Kendall's τ διαφέρει μεταξύ των συζεύξεων (Σχ. 15). Πιο συγκεκριμένα, όταν οι μεταβλητές H και T έχουν αρνητική συσχέτιση οι βέλτιστες συζεύξεις είναι εκ περιστροφής 90 ή 270 μοιρών. Οι ανεξάρτητες συζεύξεις (I) κρίνονται βέλτιστες για τις παράκτιες καταιγίδες που οι μεταβλητές H και T έχουν συσχέτιση κοντά στο μηδέν. Οι συζεύξεις Tawn θεωρούνται βέλτιστες για συσχετίσεις που είναι λίγο μεγαλύτερες ή μικρότερες από το μηδέν, ενώ οι υψηλότερες συσχετίσεις ταιριάζουν με τις συζεύξεις Clayton , Gumbel, Frank και BB8.

Σχήμα 13. Οι επικρατέστερες συζεύξεις για το ύψος και την περίοδο του κύματος των παράκτιων καταιγίδων(στο κέντρο) και για κάθε χώρα (στις γωνίες).

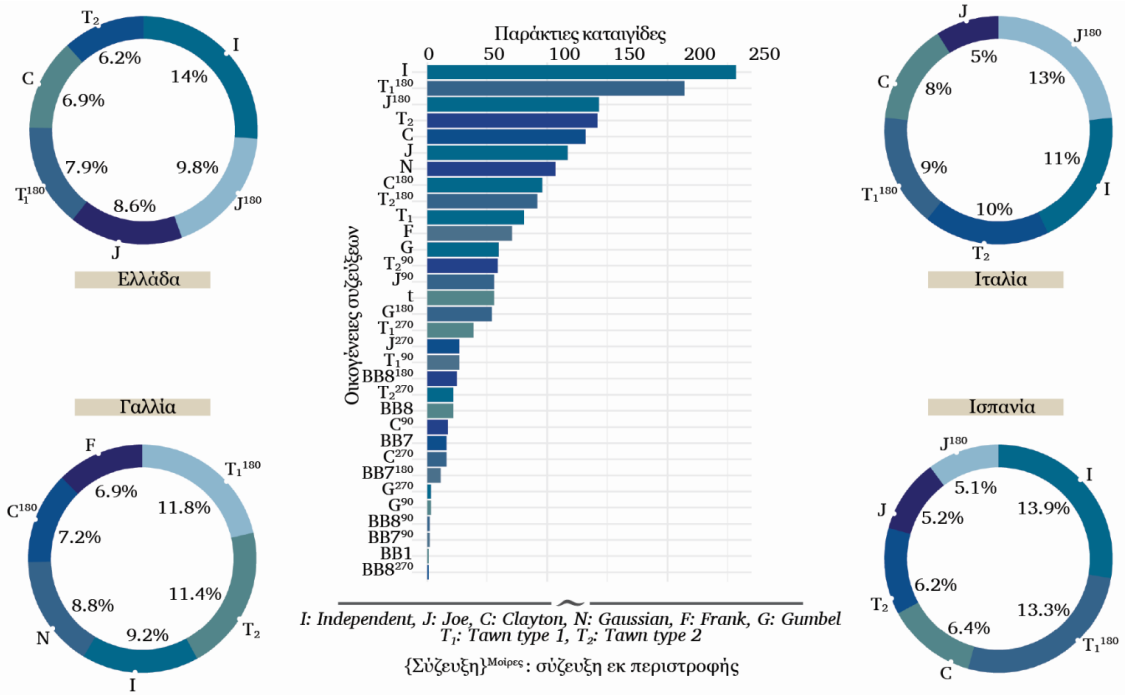

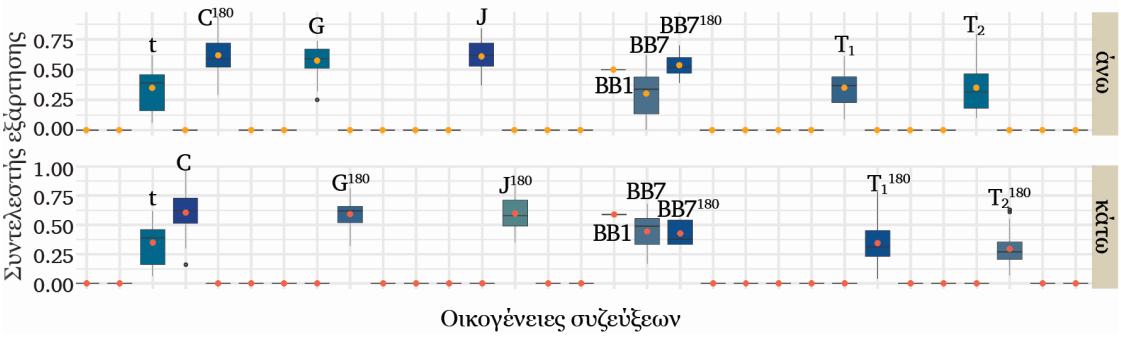

Σχήμα 14. Το εύρος των συντελεστών εξάρτησης των άνω και κάτω ουρών για τις διάφορες οικογένειες συζεύξεων.

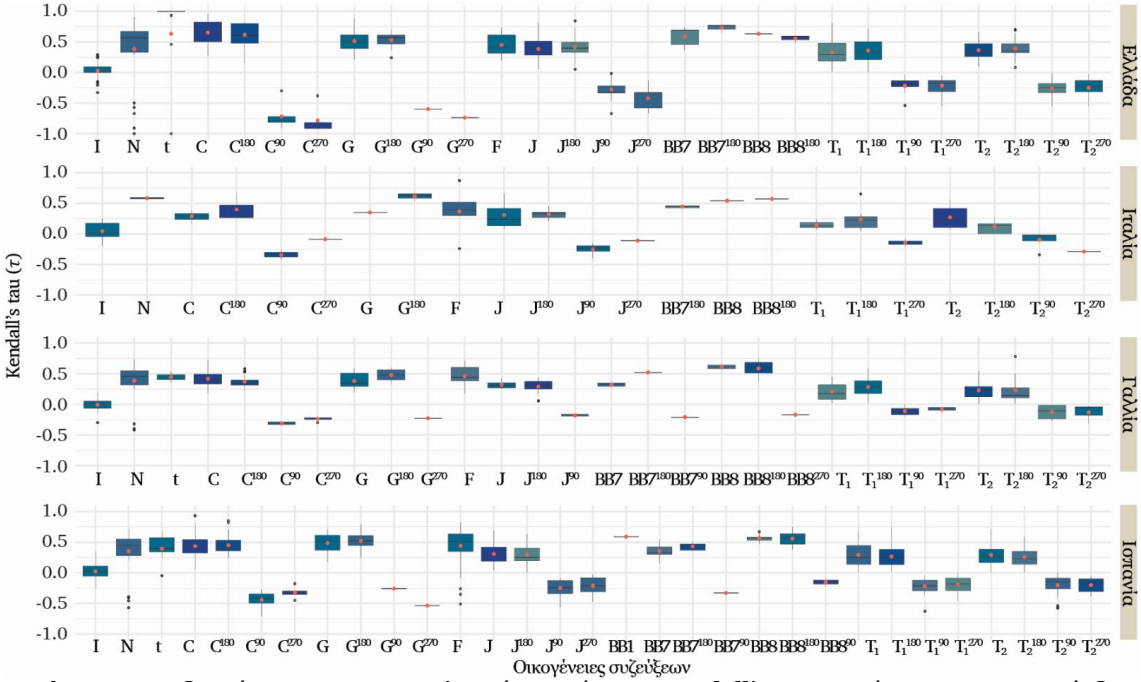

Σχήμα 15. Η διακύμανση του συντελεστή συσχέτισης Kendall's τ για το ύψος και την περίοδο του κύματος για κάθε οικογένεια σύζευξης

Η διερεύνηση της βέλτιστης επιλογής της σύζευξης προσεγγίζεται ακόμη με τη σύγκριση των χαρακτηριστικών των δυο επικρατέστερων συζεύξεων για κάθε ζεύγος των H και T μιας παράκτιας καταιγίδας. Για κάθε βέλτιστη σύζευξη υπολογίζονται οι τιμές των AIC, BIC και της μέγιστης πιθανοφάνειας και συγκρίνονται με τις τιμές που προκύπτουν αν επιλεγεί η δεύτερη καλύτερη σύζευξη (Πίνακας 2). Οι αποκλίσεις στις περισσότερες περιπτώσεις είναι μικρές, που αποδεικνύει ότι η βέλτιστη επιλογή μιας σύζευξης βάσει των κριτηρίων AIC και BIC δεν είναι κατά ανάγκη μοναδική. Η αμέσως επόμενη βέλτιστη σύζευξη μπορεί να έχει ελάχιστα μεγαλύτερες τιμές στα AIC και BIC και να είναι το ίδιο αποτελεσματική. Υπάρχουν επίσης οικογένειες συζεύξεων όπου αποτελούν την πρώτη και δεύτερη βέλτιστη επιλογή εναλλάξ, δείχνοντας ότι η μια οικογένεια μπορεί να αντικαταστήσει την άλλη και να είναι εξίσου αποτελεσματική. Για παράδειγμα ένα μεγάλο ποσοστό των περιπτώσεων έχουν βέλτιστη σύζευξη την Clayton και δεύτερη καλύτερη την Joe, ενώ αυτές που έχουν βέλτιστη σύζευξη την Joe έχουν ως δεύτερη βέλτιστη την Clayton, το ίδιο συμβαίνει και με τις οικογένειες Gumbel και Clayton, ενώ χαρακτηριστικό είναι ακόμη ότι όλες οι Tawn μορφές έχουν ως εναλλακτική επιλογή τις ανεξάρτητες συζεύξεις.

Πίνακας 2
Τα χαρακτηριστικά των δυο βέλτιστων συζεύξεων για το ύψος και την περίοδο του κύματος κατά τη διάρκεια μιας παράκτιας καταιγίδας.

Βέλτιστη σύζευξη			Απόλυτη διαφορά μέση τιμή			τυπική απόκλιση		
1η	2η	Εμφάνιση %	AIC	BIC	Μεγ. Πιθανοφάνεια	AIC	BIC	Μεγ. Πιθανοφάνεια
N	F	29.20	0.70	0.93	0.37	0.63	1.02	0.30
t	N	62.70	1.45	2.02	1.63	5.63	5.33	2.86
C	J^{180}	74.90	0.25	0.38	0.17	0.29	0.64	0.23
C^{180}	J	73.20	0.25	0.38	0.17	0.32	0.64	0.24
C^{90}	J^{270}	71.40	0.17	0.30	0.17	0.17	0.50	0.28
C^{270}	J^{90}	86.20	0.22	0.31	0.15	0.24	0.59	0.22
G	C^{180}	38.30	0.38	0.85	0.38	0.34	0.95	0.34
G^{180}	C	40.00	0.48	0.97	0.34	0.45	1.07	0.32
G^{90}	C^{270}	40.00	0.28	0.32	0.34	0.27	0.25	0.41
G^{270}	C^{90}	66.70	0.29	0.30	0.26	0.25	0.24	0.31
F	N	56.80	1.48	2.19	0.62	1.73	2.31	0.74
J	C^{180}	83.60	0.27	0.35	0.20	0.37	0.56	0.30
J^{180}	C	87.80	0.32	0.44	0.21	0.36	0.66	0.27
J^{90}	C^{270}	85.70	0.29	0.33	0.27	0.37	0.41	0.36
J^{270}	C^{90}	83.30	0.22	0.27	0.27	0.30	0.37	0.41
BB1	BB7	100.00	0.41	0.41	0.20	-	-	-
BB7	BB1	48.30	0.52	0.57	0.67	0.82	0.75	0.67
$BB7^{180}$	G	33.30	0.56	1.08	1.00	0.54	0.66	0.55
$BB7^{90}$	$BB1^{270}$	50.00	0.07	0.08	0.03	0.10	0.09	0.05
BB8	G	41.50	3.83	2.89	2.74	4.96	4.10	2.57
$BB8^{180}$	G^{180}	47.20	2.84	2.13	2.20	2.90	2.30	1.48
$BB8^{90}$	C^{270}	50.00	0.58	1.36	1.04	0.77	1.19	0.76
$BB8^{270}$	C^{90}	100.00	0.71	1.76	1.36	-	-	-
T_1	I	30.50	2.98	2.60	2.57	3.05	2.86	1.63
T_1^{180}	I	23.30	4.38	3.69	3.20	5.00	4.54	2.57
T_1^{90}	I	44.70	2.74	2.31	2.52	2.27	2.08	1.38
T_1^{270}	I	39.50	3.28	2.69	2.76	2.99	2.76	1.68
T_2	I	21.40	3.34	2.84	2.65	3.43	3.12	1.82
T_2^{180}	T_1	24.00	3.37	2.91	2.56	4.06	3.92	2.18
T_2^{90}	I	43.60	2.98	2.33	2.74	2.41	2.07	1.43
T_2^{270}	I	42.90	3.01	2.80	2.75	2.78	2.61	1.35

4.2.2. Συζεύξεις πέντε διαστάσεων για τις παράκτιες καταιγίδες μιας περιοχής

Οι συζεύξεις χρησιμοποιούνται επίσης για την μοντελοποίηση των παράκτιων καταιγίδων μιας περιοχής όταν οι σημαντικές παράμετροι H_1, T_1, D, I, E χρησιμοποιούνται ως μεταβλητές για την περιγραφή των γεγονότων. Χρησιμοποιώντας τη μεθοδολογία των C-Vine συζεύξεων, δημιουργείται ένα μοντέλο που δίνει τη δυνατότητα κατασκευής μιας σύζευξης πέντε διαστάσεων, συνδυάζοντας τις μεταβλητές σε δισδιάστατες συζεύξεις. Οι μεταβλητές αρχικά ελέγχονται για την ανεξαρτησία τους, κανονικοποιούνται στο πεδίο [0,1] και μέσω της δομής του Σχήματος 4γ και της διαδικασίας του Σχήματος 5 κατασκευάζεται το μοντέλο C-Vine πέντε διαστάσεων.

Η μεθοδολογία εφαρμόζεται στα δεδομένα της Malaga, όπου 409 καταιγίδες εντοπίζονται τη χρονική περίοδο 1985-2019. Το μοντέλο C-Vine (Πίνακας 3) έχει σαν βάση-αφετηρία την ενέργεια *E*, δεδομένου ότι είναι η μεταβλητή με τη μεγαλύτερη εξάρτηση σε σχέση με τις άλλες και στη συνέχεια με κριτήριο την εξάρτηση των

μεταβλητών ιεραρχούνται οι υπόλοιπο συνδυασμοί ώστε να κατασκευαστεί η σύζευξη πέντε μεταβλητών. Η επιλογή της βέλτιστης σύζευξης για κάθε συνδυασμό γίνεται σύμφωνα με τα κριτήρια πληροφορίας AIC και BIC, ενώ οι παράμετροι των συζεύξεων επιλέγονται βάσει της μέγιστης πιθανοφάνειας, όπως αναφέρθηκε και στην προηγούμενη παράγραφο (4.2.1) για τις δισδιάστατες συζεύξεις των *H* και *T*.

Το προτεινόμενο μοντέλο (Πίνακας 3), όπως την περίπτωση των δισδιάστατων συζεύξεων, δεν είναι κατά ανάγκη μοναδικό. Μικρές αλλαγές στην ιεραρχία των μεταβλητών ή στη βέλτιστη σύζευξη κάθε συνδυασμού μπορεί δημιουργήσει ένα εξίσου αποτελεσματικό μοντέλο. Η δομή του μοντέλου είναι παρόμοια και σε άλλες περιοχές της Μεσογείου, καθώς η εξάρτηση των μεταβλητών δε διαφέρει από περιοχή σε περιοχή. Να σημειωθεί επίσης ότι οι συνήθεις οικογένειες συζεύξεων (π.χ. Gaussian, Gumbel, t) έχουν τη δυνατότητα επέκτασης σε μεγαλύτερες διαστάσεις, χωρίς όμως να λαμβάνουν υπόψη τους την εξάρτηση των μεταβλητών στο βαθμό που αυτό γίνεται στις C-Vine συζεύξεις. Η ιδιαιτερότητα αυτή των C-Vine συζεύξεων καθιστά ιδιαίτερα αποτελεσματική την εφαρμογή τους στη μοντελοποίηση των παράκτιων καταιγίδων καθώς περιγράφουν καλύτερα αυτά τα φαινόμενα εμπεριέχοντας τη μεγαλύτερη δυνατή πληροφορία για την εξάρτηση των εμπλεκόμενων μεταβλητών.

Πίνακας 3
Τα χαρακτηριστικά της προτεινόμενης C-Vine σύζευξης.

Δέντρο	Ακμή	Σύζευξη	1η Παράμετρος	2η Παράμετρος	τ	Εξάρτηση ουρών	
						λ_U	λ_L
1	5,2	T_2	01.84	0.55	0.30	0.38	-
1	5,3	N	00.95	-	0.80	-	-
1	5,1	G	02.17	-	0.54	0.62	-
1	5,4	F	-00.99	-	-0.11	-	-
2	1,2|5	C	00.29	-	0.13	-	0.09
2	1,3|5	F	19.03	-	-0.81	-	-
2	1,4|5	F	-00.65	-	-0.07	-	-
3	4,2|1,5	T_2	01.21	0.28	0.08	0.11	-
3	4,3|1,5	F	-00.64	-	-0.07	-	-
4	2,3|4,1,5	T_2^{90}	-01.67	0.03	-0.03	-	-
1: H_1 • 2: T_1 • 3: D • 4: I • 5: E							

4.2.3. Προσομοίωση παράκτιων καταιγίδων

Η εφαρμογή των συζεύξεων στη μοντελοποίηση των παράκτιων καταιγίδων αφορά επίσης στη προσομοίωση των παράκτιων καταιγίδων. Η προσομοίωση μπορεί να επιτευχθεί μετά την κατασκευή του μοντέλου των C-Vine συζεύξεων που μοντελοποιεί τη σχέση των σημαντικών παραμέτρων της καταιγίδας H_1, T_1, D, I, E. Για τον σκοπό αυτό χρησιμοποιούνται τρείς διαφορετικοί αλγόριθμοι (Α, Β, Γ) βάσει των μεθοδολογιών των De Michele et al. (2007), Aas et al. (2009) και Stöber and Czado (2017) και συγκρίνονται μεταξύ τους ως προς την αποτελεσματικότητά τους.

Χρησιμοποιώντας το δείγμα της Malaga και τη μεθοδολογία των συζεύξεων, οι παραπάνω αλγόριθμοι εξάγουν ένα νέο σύνολο δεδομένων πέντε μεταβλητών και μήκους 409 καταιγίδων, που προσομοιώνουν τις σημαντικές παραμέτρους H_1, T_1, D, I, E, των παράκτιων καταιγίδων της περιοχής. Οι αλγόριθμοι των Aas et al. (2009) και Stöber and Czado (2017) ταυτίζονται ως προς τα αποτελέσματά τους, οπότε παρουσιάζονται από κοινού στη συνέχεια.

Οι προσομοιώσεις των παράκτιων καταιγίδων συγκρίνονται με τις κανονικοποιημένες τιμές των παραμέτρων, όπως έχουν προκύψει από τα αρχικά δεδομένα (Σχ. 16), με δυο τρόπους: α) γραφικά (Σχ. 16α) και β) μέσω των συντελεστών συσχέτισης Kendall's τ (Σχ. 16β). Η γραφική σύγκριση της σχέσης της εξάρτησης των μεταβλητών μεταξύ των δεδομένων που έχουν προκύψει από μετρήσεις και των προσομοιώσεων, παρουσιάζονται ανά ζεύγος στο Σχήμα 16α. Στη άνω τριγωνική πλευρά του Σχήματος 16α τα αποτελέσματα των Αλγορίθμων Α και Β παρουσιάζουν μικρές αποκλίσεις από τα αρχικά δεδομένα βλέποντας να ακολουθούν το ίδιο μοτίβο για κάθε συνδυασμό παραμέτρων. Αντίθετα, τα αποτελέσματα του Αλγόριθμου Γ στην κάτω τριγωνική πλευρά του Σχήματος 16α, παρουσιάζουν μεγάλες αποκλίσεις από τα αρχικά δεδομένα των παράκτιων καταιγίδων για κάποια ζεύγη (H_1-E, T_1-E, D-E, I-E). Τα συμπεράσματα είναι παρόμοια ακόμη κι αν συγκριθούν οι τιμές του συντελεστή συσχέτισης Kendall's τ (Σχ. 16β) για την εξάρτηση κάθε ζεύγους των μεταβλητών των αρχικών δεδομένων και των προσομοιώσεων. Οι συντελεστές Kendall's τ έχουν μικρές αποκλίσεις μεταξύ προσομοιώσεων και αρχικών δεδομένων στην περίπτωση των Αλγορίθμων Α και Β (άνω τριγωνική πλευρά), ενώ οι αποκλίσεις είναι μεγαλύτερες στην περίπτωση του Αλγορίθμου Γ (κάτω τριγωνική πλευρά), ειδικά για τα ζεύγη H_1-D, T_1-D, T_1-E, D-E.

Τα παραπάνω αποτελέσματα αναδεικνύουν την αποτελεσματικότητα της μεθοδολογίας των Aas et al. (2009) και Stöber and Czado (2017) και κατά συνέπεια των C-Vine συζεύξεων στην προσομοίωση των παράκτιων καταιγίδων έναντι του Αλγορίθμου Γ και επομένως της μεθοδολογίας των De Michele et al. (2007), που είχε αρχικά προταθεί για τέσσερις μεταβλητές. Γενικότερα οι Vine συζεύξεις θεωρούνται τα τελευταία χρόνια πολύ πιο αποτελεσματικές από άλλες μεθόδους (Jäger and Nápoles, 2017; Orcel et al., 2021) ενώ έχουν αποδειχτεί (Joe et al., 2010) αρκετά ευέλικτες στο να μοντελοποιούν την εξάρτηση των ουρών που συνήθως επηρεάζει την εφαρμογή τους.

Επιπλέον αξίζει να σημειωθεί ότι οι Αλγόριθμοι Α και Β που ακολουθούν τη δομή του μοντέλου C-Vine, είναι πιο εύχρηστοι, απαιτούν λιγότερες πράξεις, επεκτείνονται εύκολα σε μεγαλύτερες διαστάσεις και οι προσομοιώσεις που εξάγουν είναι πολύ κοντά στο αρχικό δείγμα. Ο Αλγόριθμος Γ που βασίζεται στη μεθοδολογία των De Michele et al. (2007) για την προσομοίωση των θαλάσσιων καταιγίδων, όπως αρχικά είχε προταθεί, απαιτεί πολλούς μαθηματικούς υπολογισμούς και είναι αρκετά δύσχρηστος, ειδικά όταν οι διαστάσεις αυξάνονται.

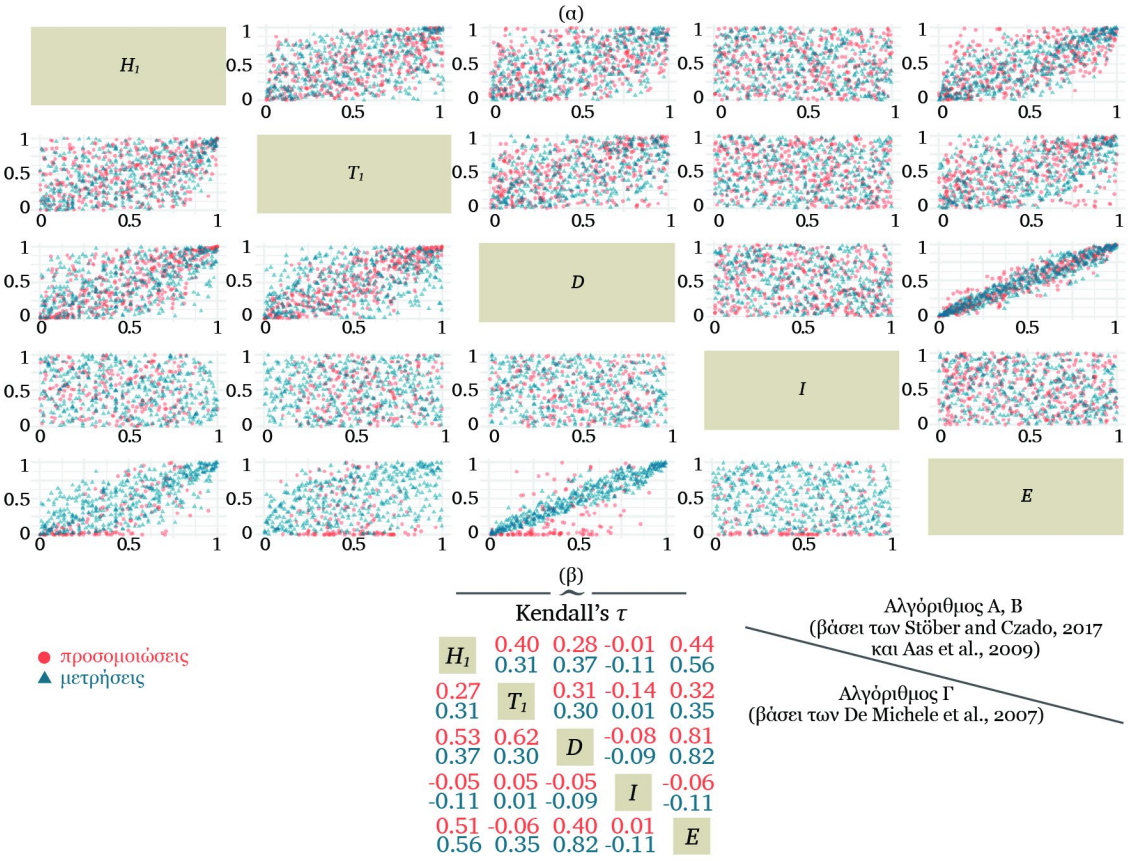

Σχήμα 16. (α) Σύγκριση των κανονικοποιημένων μετρήσεων και των προσομοιώσεων μέσω των αλγορίθμων Α και Β (άνω) και Γ (κάτω). (β) Σύγκριση των τριών αλγορίθμων μέσω του συντελεστή συσχέτισης Kendall's τ.

4.2.4. Περίοδοι επαναφοράς

Οι συζεύξεις χρησιμοποιούνται στον υπολογισμό της κοινής πιθανότητας πολλών μεταβλητών και κατά συνέπεια στον υπολογισμό των περιόδων επαναφοράς τροποποιώντας κατάλληλα την Εξ. 15. Οι κοινές πιθανότητες για τέσσερις και πέντε μεταβλητές μπορούν να κατασκευαστούν χρησιμοποιώντας τις C-Vine συζεύξεις ή και τις συνήθεις οικογένειες συζεύξεων (π.χ. Gaussian, Gumbel, t) και στη συνέχεια μέσω αυτών υπολογίζονται οι περίοδοι επαναφοράς των παράκτιων καταιγίδων για δυο έως πέντε μεταβλητές. Η μεθοδολογία εφαρμόζεται στις παράκτιες καταιγίδες της Malaga, ωστόσο μπορεί να χρησιμοποιηθεί για οποιαδήποτε περιοχή υπολογίζοντας εκ νέου τις κατάλληλες συζεύξεις.

Προκειμένου να υπολογιστούν οι περίοδοι επαναφοράς των παράκτιων καταιγίδων που έχουν ακραία χαρακτηριστικά, λαμβάνονται υπόψη οι υψηλότερες τιμές του δείγματος που αντιστοιχούν στο $90^{ο}$ έως $99^{ο}$ εκατοστημόριο των παραμέτρων H_1, T_1, D, E. Για τις χρονικό διάστημα ηρεμίας (I) λαμβάνονται υπόψη οι μικρότερες τιμές του δείγματος δηλαδή αυτές που αντιστοιχούν στο $1^{ο}$ έως $10^{ο}$ εκατοστημόριο, καθώς έχει αντίθετη ερμηνεία από τις υπόλοιπες παραμέτρους, δεδομένου ότι όσο πιο μικρό είναι το διάστημα ηρεμίας μιας παράκτιας καταιγίδας τόσο πιο ακραία θεωρείται και τόσο πιο σημαντικές είναι οι επιπτώσεις της στις ακτές.

Ο υπολογισμός των περιόδων επαναφοράς πραγματοποιείται για τον συνδυασμό δυο έως πέντε μεταβλητών. Για κάθε μια περίπτωση, επιλέγονται τρείς διαφορετικές συζεύξεις. Οι δισδιάστατες συζεύξεις επιλέγονται σύμφωνα με τα κριτήρια πληροφορίας AIC και BIC, ενώ για τις μεγαλύτερες διαστάσεις επιλέγονται οι C-Vine συζεύξεις και οι συζεύξεις κάποιας γνωστής οικογένειας (π.χ. Gaussian, Gumbel, t). Αξίζει να σημειωθεί, ότι ο υπολογισμός των παραμέτρων των συζεύξεων και η δομή των C-Vines προηγείται της εφαρμογής τους.

Τα αποτελέσματα των περιόδων επαναφοράς για κάθε συνδυασμό των παραμέτρων παρουσιάζονται παρακάτω (Σχ. 17-20 και Πιν. 4-11). Στις δισδιάστατες περιπτώσεις, η βέλτιστη επιλογή των συζεύξεων δεν επηρεάζει σημαντικά τον υπολογισμό της περιόδου επαναφοράς (Σχ. 17-20). Συνεπώς, δεν παρατηρούνται μεγάλες αποκλίσεις μεταξύ των δισδιάστατων συζεύξεων που επιλέγονται και ειδικά όταν οι παράμετροι αφορούν φυσικά μεγέθη που σχετίζονται μεταξύ τους (π.χ. ύψος και περίοδος κύματος). Επιπρόσθετα η βέλτιστη σύζευξη δεν παρουσιάζει ποτέ ακραίες εκτιμήσεις της περιόδου επαναφοράς σε σχέση με τις άλλες δυο συζεύξεις και συνήθως δίνει παρόμοια αποτελέσματα με τη δεύτερη βέλτιστη σύζευξη. Για τη βέλτιστη σύζευξη υπολογίζεται η περίοδος επαναφοράς για κάθε συνδυασμό ακραίων χαρακτηριστικών των παραμέτρων (Πιν. 4-7).

Στις μεγαλύτερες διαστάσεις (Πιν. 8-11), οι περίοδοι επαναφοράς που προκύπτουν από τα C-Vines ακολουθούν τη συμπεριφορά του αρχικού δείγματος που αφορά μια περίοδο καταγραφής περίπου 34 χρόνων. Για παράδειγμα, η περίοδος επαναφοράς μιας παράκτιας καταιγίδας όταν ισχύουν ταυτόχρονα H_1>2.39 m, T_1>8.18 s και D>102.21 h (Πιν. 8) υπολογίζεται 40.22 έτη, 8.19 έτη και 16.68 έτη μέσω των συζεύξεων C-Vines, Gumbel και t αντίστοιχα. Τα συγκεκριμένα χαρακτηριστικά δεν αντιστοιχούν σε παράκτια καταιγίδα που ανήκει στο δείγμα της Malaga, ωστόσο υπάρχει παράκτια καταιγίδα στο δείγμα της Malaga με παρόμοια χαρακτηριστικά που έχει συμβεί μια φορά στα 34 έτη. Σύμφωνα λοιπόν με τη συμπεριφορά του δείγματος τα αποτελέσματα των Gumbel και t συζεύξεων (8.19 και 16.68 έτη) θεωρείται ότι δεν είναι ρεαλιστικά, σε αντίθεση με την περίοδο επαναφοράς των C-Vines (40.22 έτη). Η παραπάνω ερμηνεία των αποτελεσμάτων δεν ενδείκνυται για την διερεύνηση της αποτελεσματικότητας των

συζεύξεων, ωστόσο είναι ένας τρόπος για την απόρριψη κάποιων αποτελεσμάτων και μεθόδων όπως στην περίπτωση του παραδείγματος.

Η επιλογή της κατάλληλης σύζευξης έχει καθοριστικό ρόλο στην εκτίμηση των περιόδων επαναφοράς για τρείς ή περισσότερες μεταβλητές, γεγονός που αναδεικνύει τη σημασία της διερεύνησης της βέλτιστης σύζευξης. Στην πράξη ωστόσο, μπορεί να χρησιμοποιηθεί ο μέσος όρος των περιόδων επαναφοράς που προκύπτουν από τις διάφορες συζεύξεις ως μια ενδιάμεση λύση, ελαχιστοποιώντας με αυτό τον τρόπο την αβεβαιότητα των διάφορων συζεύξεων.

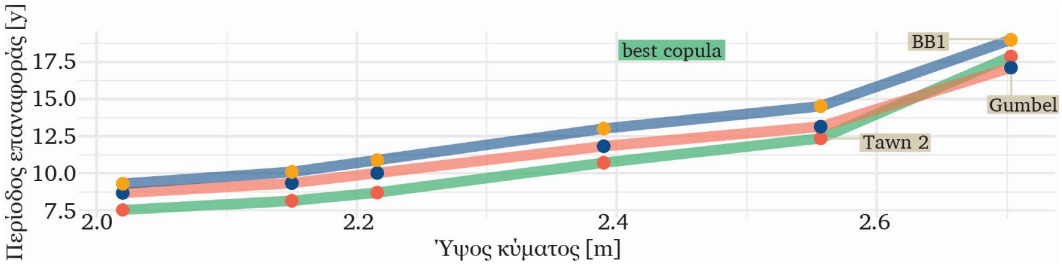

Σχήμα 17. Σύγκριση των περιόδων επαναφοράς όταν το H_1 κυμαίνεται μεταξύ των υψηλότερων τιμών (*90-99ο*) και το T_1 είναι μεγαλύτερο από 8.54 s (*99ο*).

Πίνακας 4
Οι περίοδοι επαναφοράς σε έτη για κάθε συνδυασμό των ακραίων τιμών των H_1 και T_1 μέσω της σύζευξης Tawn2.

			H_1 [m]					
AND case			*90ο*	*93ο*	*95ο*	*97ο*	*98ο*	*99ο*
			2.02	2.15	2.22	2.39	2.56	2.70
T_1 [s]	*90ο*	7.71	1.98	2.68	3.30	5.42	7.06	12.32
	93ο	7.84	2.31	3.02	3.65	5.82	7.52	12.93
	95ο	7.99	2.68	3.38	4.02	6.21	7.93	13.44
	97ο	8.18	3.79	4.47	5.08	7.26	8.99	14.61
	98ο	8.31	4.67	5.33	5.93	8.06	9.78	15.40
	99ο	8.54	7.53	8.15	8.71	10.72	12.36	17.87

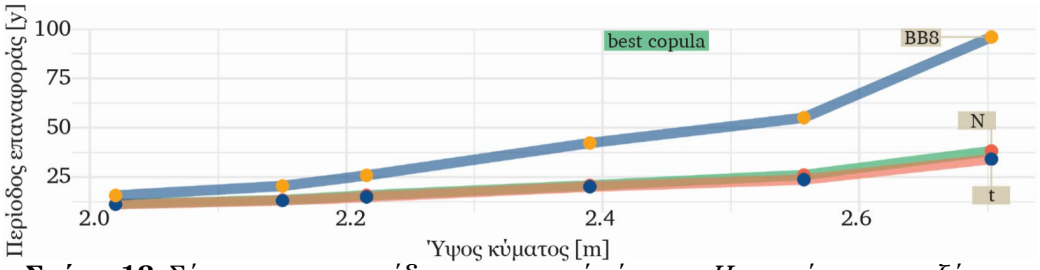

Σχήμα 18. Σύγκριση των περιόδων επαναφοράς όταν το H_1 κυμαίνεται μεταξύ των υψηλότερων τιμών (90-99ο) και το D είναι μεγαλύτερο από 127.38 h (*99ο*).

Πίνακας 5
Οι περίοδοι επαναφοράς σε έτη για κάθε συνδυασμό των ακραίων τιμών των H_1 και D μέσω της Gaussian σύζευξης.

	AND case		H_1 [m]					
			90ο	*93ο*	*95ο*	*97ο*	*98ο*	*99ο*
			2.02	2.15	2.22	2.39	2.56	2.70
D [h]	*90ο*	61.23	2.23	2.84	3.61	5.22	7.00	11.39
	93ο	72.24	2.87	3.61	4.52	6.42	8.51	13.57
	95ο	89.20	3.55	4.42	5.48	7.67	10.06	15.81
	97ο	102.21	5.49	6.68	8.13	11.10	14.29	21.83
	98ο	111.84	6.92	8.34	10.06	13.56	17.30	26.06
	99ο	127.38	11.26	13.33	15.81	20.81	26.06	38.22

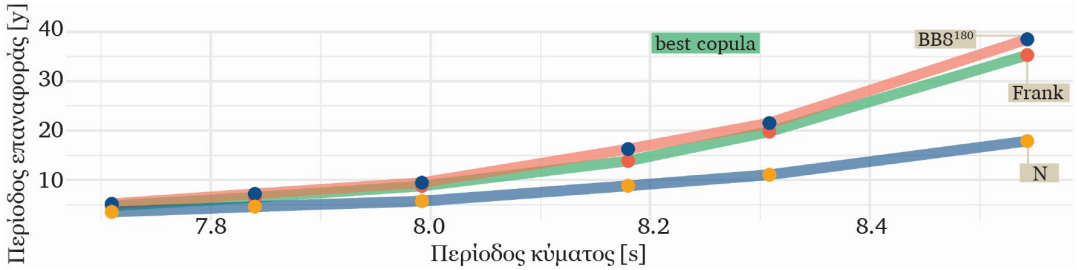

Σχήμα 19. Σύγκριση των περιόδων επαναφοράς όταν το T_1 κυμαίνεται μεταξύ των υψηλότερων τιμών (*90-99ο*) και το D είναι μεγαλύτερο από 127.38 h.

Πίνακας. 6
Οι περίοδοι επαναφοράς σε έτη για κάθε συνδυασμό των ακραίων τιμών των T_1 και D μέσω της σύζευξης Frank.

	AND case		T_1 [s]					
			90ο	*93ο*	*95ο*	*97ο*	*98ο*	*99ο*
			7.71	7.84	7.99	8.18	8.31	8.54
D [h]	*90ο*	61.23	3.33	4.56	6.17	9.76	13.96	24.86
	93ο	72.24	4.77	6.52	8.80	13.89	19.83	35.29
	95ο	89.20	6.04	8.24	11.11	17.52	25.01	44.48
	97ο	102.21	10.33	14.06	18.93	29.81	42.51	75.54
	98ο	111.84	13.66	18.59	25.01	39.37	56.12	99.71
	99ο	127.38	24.33	33.08	44.48	69.96	99.71	177.07

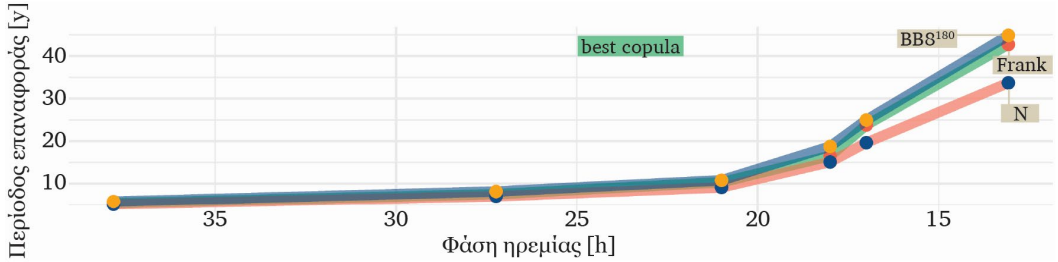

Σχήμα 20. Σύγκριση των περιόδων επαναφοράς όταν το I κυμαίνεται μεταξύ των χαμηλότερων τιμών και το E είναι μεγαλύτερο από 232.92 m^2h.

Πίνακας7
Οι περίοδοι επαναφοράς σε έτη για κάθε συνδυασμό των ακραίων τιμών των I και E μέσω σύζευξης Frank.

AND case			I[h]					
			10º	7º	5º	3º	2º	1º
			37.80	27.24	21.00	18.00	17.00	13.08
E[m²h]	90º	232.92	5.41	7.55	10.34	16.57	23.83	42.73
	93º	316.11	7.55	10.54	14.43	23.11	33.23	59.56
	95º	367.03	10.85	15.13	20.71	33.16	47.69	85.46
	97º	449.00	17.93	25.01	34.22	54.77	78.75	141.10
	98º	520.99	26.79	37.35	51.10	81.78	117.58	210.65
	99º	688.75	42.73	59.56	81.49	130.4	187.47	335.85

Πίνακας 8
Οι περίοδοι επαναφοράς σε έτη όταν H_1>2.39 m, T_1>8.18 s, D>102.21 h.

	C-Vine	Gumbel	t
AND case	40.22	8.19	16.68
OR case	1.08	1.26	1.17

Πίνακας 9
Οι περίοδοι επαναφοράς σε έτη όταν T_1>7.99 s, E> 367.03 m²h and I<21 h.

	C-Vine	Gumbel	t
AND case	57.64	23.73	22.98
OR case	0.62	0.65	0.64

Πίνακας 10
Οι περίοδοι επαναφοράς σε έτη όταν H_1>2.15 m, T_1>7.84 s, D>72.24 h, I<27.24 h.

	C-Vine	t	Gaussian
AND case	35.97	25.63	15.54
OR case	0.37	0.39	0.35

Πίνακας 11
Οι περίοδοι επαναφοράς σε έτη όταν H_1>2.39 m, T_1>8.18 s, D>102.21 h, I<18 h, E>449 m²h.

	C-Vine	t	Gaussian
AND case	57.99	76.25	7.65
OR case	0.82	0.88	0.76

4.3. Εφαρμογή την ανάλυσης των καταιγίδων στο σχεδιασμό λιμενικών και παράκτιων έργων.

Η ανάλυση των παράκτιων καταιγίδων στηρίζεται στην ανάλυση κυματικών παραμέτρων και κυρίως στη μελέτη των ιστορικών καταιγίδων που έχουν συμβεί σε μια περιοχή. Μέσω αυτής της μελέτης επιτυγχάνεται η καλύτερη κατανόηση του φαινομένου και ο τρόπος εντοπισμού των παράκτιων καταιγίδων. Η περιγραφική στατιστική ανάλυση, η μορφή του σχήματος των καταιγίδων, η μοντελοποίηση τους μέσω των συζεύξεων, η προσομοίωση και ο υπολογισμός των περιόδων επαναφοράς είναι στοιχεία

που βρίσκουν εφαρμογή στο σχεδιασμό λιμενικών και παράκτιων έργων και πλαισιώνουν την αντίστοιχη τεχνική μελέτη.

Πιο συγκεκριμένα, η περιγραφική στατιστική ανάλυση των ιστορικών παράκτιων καταιγίδων, συμπεριλαμβάνει τη συχνότητα εμφάνισης αλλά και τις μέσες, μέγιστες και ακραίες τιμές των μεταβλητών που ορίζουν ένα γεγονός. Οι πληροφορίες αυτές συμβάλλουν στην προκαταρκτική έρευνα μιας τεχνικής μελέτης, περιγράφοντας τα χαρακτηριστικά μιας ακραίας κατάστασης της θάλασσας στην περιοχή μελέτης προκειμένου να ληφθούν υπόψη στο σχεδιασμό, ο οποίος συνήθως στηρίζεται στις μέσες ετήσιες και στις μέγιστες τιμές των παραμέτρων.

Η προσομοίωση των παράκτιων καταιγίδων έχει ιδιαίτερη σημασία όταν δεν υπάρχουν διαθέσιμα δεδομένα, αλλά και για τη μελέτη ακραίων σεναρίων. Σε αυτό συμβάλλουν τα σχήματα καταιγίδων, καθώς χρησιμοποιούνται για την κατασκευή συνθετικών καταιγίδων που έχουν παρόμοια ή πιο ακραία συμπεριφορά από τις ιστορικές καταιγίδες. Οι συζεύξεις είναι ένας άλλος τρόπος για να επιτευχθεί η προσομοίωση των παράκτιων καταιγίδων. Οι συζεύξεις περιγράφουν και μοντελοποιούν την εξάρτηση των εμπλεκόμενων μεταβλητών, δίνοντας τη δυνατότητα της προσομοίωσης πολυμεταβλητών φαινομένων όπως είναι οι παράκτιες καταιγίδες. Οι προσομοιώσεις όπως και οι ιστορικές καταιγίδες μπορούν να χρησιμοποιηθούν για τη διερεύνηση της αντοχής των κατασκευών κάτω από ακραίες συνθήκες, ή να τροφοδοτήσουν αριθμητικά μοντέλα (π.χ. MIKE 21, XBeach) για τη μελέτη των κυματικών και παράκτιων διεργασιών.

Η συχνότητα εμφάνισης των ιστορικών καταιγίδων είναι χρήσιμη για τη μελέτη φόρτισης των κατασκευών. Στο ίδιο πλαίσιο, η περίοδος επαναφοράς είναι επίσης απαραίτητη καθώς εξετάζεται η επανεμφάνιση μιας παράκτιας καταιγίδας με συγκεκριμένα χαρακτηριστικά ακόμη και αν δεν έχει συμβεί ως ιστορική καταιγίδα. Ο υπολογισμός των περιόδων επαναφοράς πραγματοποιείται μέσω των συζεύξεων και χρησιμοποιείται για τον υπολογισμό της πιθανότητας αστοχίας μιας κατασκευής, την αξιοπιστία (Lira-Loarca et al., 2020) και το σχεδιασμό τους (Salvadori et al., 2014, 2015; Li et al., 2020; Orcel et al., 2021).

Η ανάλυση των παράκτιων καταιγίδων ανέδειξε τη σημασία της πολυμεταβλητής ανάλυσης στην κατανόηση τέτοιων ακραίων φαινομένων μέχρι και το σχεδιασμό των λιμενικών και παράκτιων έργων. Η εφαρμογή των συζεύξεων είναι καταλυτική σε τέτοιου είδους προβλήματα, ωστόσο η χρήση τους σε επίπεδο προδιαγραφών δεν είναι εξίσου διαδεδομένη. Οι κανονισμοί για το σχεδιασμό των κατασκευών (π.χ. Eurocode EN 1990, NORSOK N-003) συνιστούν τη μελέτη ταυτόχρονων ακραίων καταστάσεων, όπως οι καταιγίδες, και τον υπολογισμό των περιόδων επαναφοράς χωρίς όμως να αναφέρονται ακόμη στη χρήση των συζεύξεων.

5. Συμπεράσματα

Η δυναμική των παράκτιων καταιγίδων και οι σοβαρές επιπτώσεις που επιφέρουν στις παράκτιες περιοχές και τις τοπικές κοινωνίες στάθηκαν αφορμή για την παρούσα διατριβή. Το αντικείμενο της παρούσας διατριβής είναι η ανάλυση των παράκτιων καταιγίδων με κύριο στόχο τη μοντελοποίηση τους μέσω των συζεύξεων.

Σε σχέση με τους ερευνητικούς στόχους που τέθηκαν εκ των προτέρων σχετικά με τον ορισμό των παράκτιων καταιγίδων, τις σημαντικές μεταβλητές και τα απαραίτητα κατώφλια για τον εντοπισμό τους, στην παρούσα διατριβή ο ορισμός της παράκτιας καταιγίδας θεωρείται ότι εξαρτάται από τα χαρακτηριστικά μιας περιοχής και είναι συνήθως μοναδικός για κάθε τοποθεσία. Επομένως, ο εντοπισμός των παράκτιων καταιγίδων βασίζεται στα διαθέσιμα δεδομένα κάθε περιοχής και προκύπτει από τη διερεύνηση του ύψους, της διάρκειας και του διαστήματος ηρεμίας των παράκτιων καταιγίδων. Για τη μελέτη των παράκτιων καταιγίδων, ορίζονται οι εκπρόσωποι των σημαντικότερων μεταβλητών που περιγράφουν ένα γεγονός όπως: το ύψος, η περίοδος και η κατεύθυνση κύματος, καθώς και η διάρκεια, το διάστημα ηρεμίας και η ενέργεια της καταιγίδας.

Στα πλαίσια της διατριβής διερευνήθηκε η θεωρία των συζεύξεων και εφαρμόστηκε για την μοντελοποίηση των παράκτιων καταιγίδων. Οι συζεύξεις χρησιμοποιούνται για την περιγραφή της σχέσης των μεταβλητών που ορίζουν μια παράκτια καταιγίδα και εφαρμόζονται σε τρείς περιπτώσεις: α) για την μοντελοποίηση της σχέσης του ύψους και της περιόδου κύματος κατά τη διάρκεια μιας καταιγίδας, β) την προσομοίωση των παράκτιων καταιγίδων σε μια περιοχή, και γ) για τον υπολογισμό των περιόδων επαναφοράς των παράκτιων καταιγίδων.

Η εφαρμογή των συζεύξεων συνήθως περιορίζεται στις δυο μεταβλητές και σε συγκεκριμένες οικογένειες συζεύξεων. Σε αντίθεση, στην παρούσα διατριβή γίνεται διερεύνηση των καλύτερων συζεύξεων και η εφαρμογή τους γίνεται στις δυο έως πέντε διαστάσεις. Στην περίπτωση των δυο μεταβλητών η βέλτιστη σύζευξη επιλέγεται ανάμεσα σε 40 διαφορετικές οικογένειες συζεύξεων. Ελέγχεται το εύρος των παραμέτρων της παράκτιας καταιγίδας σε σχέση με τη βέλτιστη σύζευξη και επιπρόσθετα γίνεται διερεύνηση της δεύτερης βέλτιστης σύζευξης ως προς τις διαφορές της με την πρώτη και τις ομοιότητες που παρουσιάζουν ορισμένες οικογένειες. Η προσομοίωση των παράκτιων καταιγίδων πραγματοποιείται επίσης μέσω των συζεύξεων και των αλγορίθμων που αναπτύχθηκαν βάσει της μεθοδολογίας των De Michele et al. (2007), Aas et al., (2009) και Stöber and Czado, (2017) που επεκτάθηκαν στις πέντε μεταβλητές. Για τον υπολογισμό της περιόδου επαναφοράς των παράκτιων καταιγίδων χρησιμοποιούνται οι C-Vine συζεύξεις για τρείς έως πέντε μεταβλητές, καθώς και οι συνήθεις οικογένειες συζεύξεων(π.χ., Tawn, Frank, Gaussian, Gumbel, t) για δυο έως πέντε μεταβλητές.

Τα γενικά συμπεράσματα που εξάγονται από την εφαρμογή των συζεύξεων στη μοντελοποίηση των παράκτιων καταιγίδων συνοψίζονται στα εξής:

- Οι συζεύξεις Tawn και Joe είναι οι επικρατέστερες βέλτιστες για την μοντελοποίηση των H και T κατά τη διάρκεια μιας παράκτιας καταιγίδας. Οι καταιγίδες με ελαφριές ουρές έχουν σαν βέλτιστες τις Tawn συζεύξεις ενώ οι Joe συζεύξεις ταιριάζουν καλύτερα στις βαριές ουρές. Όσο αναφορά τη δεύτερη βέλτιστη σύζευξη, είναι σημαντικό ότι κάποιες συζεύξεις θεωρούνται εξίσου βέλτιστες με μικρή διαφορά στα χαρακτηριστικά τους (AIC, BIC, Loglik.) όπως οι συζεύξεις Joe και Clayton.
- Η C-Vine σύζευξη των πέντε μεταβλητών κατασκευάζεται μέσω του συνδυασμού των σημαντικών παραμέτρων ανά ζεύγη. Για την προσομοίωση των παράκτιων καταιγίδων, οι Αλγόριθμοι Α και Β που στηρίζονται στη μεθοδολογία των Stöber and Czado (2017) και Aas et al. (2009) αντίστοιχα, επεκτείνονται εύκολα στις πέντε μεταβλητές και ταυτίζονται ως προς τα αποτελέσματά τους που είναι αρκετά ικανοποιητικά. Σε αντίθεση, ο Αλγόριθμος Γ που αναπτύχθηκε βάσει της μεθοδολογίας των De Michele et al. (2007) είναι αρκετά δύσχρηστος και τα αποτελέσματα του αποκλίνουν από τα αρχικά δεδομένα σε πολλά ζεύγη των μεταβλητών.
- Οι δισδιάστατες περίοδοι επαναφοράς των παράκτιων καταιγίδων μπορούν να υπολογιστούν μέσω διάφορων συζεύξεων χωρίς μεγάλες αποκλίσεις στα αποτελέσματά τους. Για τις μεγαλύτερες διαστάσεις οι C-Vine συζεύξεις παρουσιάζουν περιόδους επαναφοράς που είναι πιο ρεαλιστικές σύμφωνα με τη συμπεριφορά του αρχικού δείγματος. Ωστόσο τα αποτελέσματα δεν είναι άμεσα συγκρίσιμα καθώς δεν είναι γνωστή η αποτελεσματικότητα της κάθε σύζευξης.

Η προτεινόμενη μεθοδολογία για την ανάλυση των παράκτιων καταιγίδων εφαρμόζεται σε ένα δείγμα κυματικών παραμέτρων από 30 περιοχές στη Μεσόγειο θάλασσα, στο οποίο εντοπίζονται 4008 παράκτιες καταιγίδες. Μέσω αυτής της ανάλυσης παρουσιάζεται η δραστηριότητα των παράκτιων καταιγίδων στην Ελλάδα, στην Ιταλία, στη Γαλλία και στην Ισπανία, περιγράφοντας σημαντικές πληροφορίες για τη συχνότητα εμφάνισης και τα χαρακτηριστικά των παράκτιων καταιγίδων. Συνεπώς, προκύπτουν κάποια δευτερεύουσας σημασίας συμπεράσματα για τις παράκτιες καταιγίδες στη Μεσόγειο θάλασσα, τα οποία συνοψίζονται στα εξής:

- 10 - 14 παράκτιες καταιγίδες συμβαίνουν ετησίως στη Μεσόγειο Θάλασσα στην Ελλάδα, στην Ιταλία, στη Γαλλία και στην Ισπανία.
- Πάνω από το 80% των παράκτιων καταιγίδων αναπτύσσονται στο διάστημα Οκτωβρίου-Μαρτίου, όπως αναμενόταν, ενώ οι περιοχές της Ισπανίας έχουν

εντονότερη δραστηριότητα τους καλοκαιρινούς μήνες σε σχέση με τις άλλες περιοχές.

- Οι παράκτιες καταιγίδες με τις υψηλότερες τιμές ύψους, περιόδου και ενέργειας εμφανίζονται, όπως αναμενόταν, στις περιοχές που είναι εκτεθειμένες σε υψηλά κύματα και βρίσκονται στα βαθιά νερά.
- Η μέση διάρκεια των παράκτιων καταιγίδων είναι μικρότερη από 30 ώρες και σχεδόν το 50% αυτών διαρκεί λιγότερο από 24 ώρες.
- Όσον αφορά το διάστημα ηρεμίας, το 25% των παράκτιων καταιγίδων πλήττουν δύο φορές μια συγκεκριμένη περιοχή σε λιγότερο από μια εβδομάδα.
- Η περίοδος και η κατεύθυνση κύματος έχουν μικρή διακύμανση κατά τη διάρκεια μιας παράκτιας καταιγίδας. Ο συντελεστής μεταβλητότητας της περιόδου κύματος είναι μικρότερος από 0.15 για τις περισσότερες παράκτιες καταιγίδες (75%), όπως και η τυπική απόκλιση της κατεύθυνσης είναι μικρότερη των 20 μοιρών για τα περισσότερα γεγονότα. Επομένως, η μέση τιμή της περιόδου και της κατεύθυνσης κύματος περιγράφουν αποτελεσματικά τις δύο αυτές μεταβλητές κατά τη διάρκεια μιας παράκτιας καταιγίδας.
- Η ροή ενέργειας και η ενέργεια παράκτιας καταιγίδας έχουν παρόμοια συμπεριφορά σε σχέση με το ύψος και την περίοδο κύματος. Οι παράκτιες καταιγίδες που έχουν ίδιο ύψος κύματος παρουσιάζουν επίσης υψηλές τιμές ενέργειας και ροή ενέργειας όταν η περίοδος κύματος είναι επίσης μεγάλη.
- Οι παράκτιες καταιγίδες της Μεσογείου αναπαρίστανται από τριγωνικά σχήματα, τα οποία μπορεί να είναι ισοσκελή ή σκαληνά και η μορφή τους δεν εξαρτάται από την κατεύθυνση ή την περίοδο κύματος.
- Σύμφωνα με προηγούμενες έρευνες οι παράκτιες καταιγίδες της Μεσογείου είναι πιο απότομες κατά την έναρξη τους και ηπιότερες προς τη λήξη τους. Ωστόσο, η συγκεκριμένη μορφή δεν επιβεβαιώνεται στο εξεταζόμενο δείγμα, καθώς το σκαληνό τριγωνικό σχήμα δεν επικρατεί.

Τα αποτελέσματα της παρούσας διατριβής είναι χρήσιμα κυρίως για την προσομοίωση των παράκτιων καταιγίδων και τον υπολογισμό των περιόδων επαναφοράς. Μέσω αυτών των διαδικασιών και γενικότερα της μοντελοποίησης των παράκτιων καταιγίδων μέσω των συζεύξεων η διατριβή επιδιώκει να συνεισφέρει στη βελτίωση της αξιοπιστίας του σχεδιασμού των λιμενικών και παράκτιων έργων. Συμπληρωματικά προς την κατεύθυνση αυτή λειτουργούν οι πληροφορίες σχετικά με τη δραστηριότητα των παράκτιων καταιγίδων στη Μεσόγειο θάλασσα, ενώ επίσης η μεθοδολογία που αναπτύσσεται για τον εντοπισμό και την ανάλυση των παράκτιων καταιγίδων αποτελεί έναν οδηγό για κάθε ανάλυση παράκτιων καταιγίδων στο μέλλον.

Οι περιορισμοί της παρούσας διατριβής αφορούν κυρίως στα δεδομένα που εξετάστηκαν. Παρά το γεγονός ότι το δείγμα ήταν αρκετά μεγάλο, η χρονική κάλυψη σε κάθε περιοχή δεν συμπίπτει, όπως και το χρονικό βήμα μεταξύ των μετρήσεων που κυμαίνεται από 0.5-3 ώρες. Λόγω αυτών των περιορισμών δεν μπορούν να εξαχθούν γενικά συμπεράσματα για την κλιματική αλλαγή, κάτι που θα είχε μεγάλο ενδιαφέρον. Η χρήση των C-Vine συζεύξεων αποδεικνύεται αποτελεσματική, η εφαρμογή τους όμως απαιτεί ιδιαίτερη προσοχή λόγω των πολλών μαθηματικών υπολογισμών.

Η ανάλυση των παράκτιων καταιγίδων και η μοντελοποίηση τους μέσω των συζεύξεων επιδέχεται φυσικά περεταίρω βελτίωση. Κάποιες προτάσεις για μελλοντικές έρευνες συνοψίζονται παρακάτω:

- Η μελέτη εφαρμογής για τον εντοπισμό των καταιγίδων μπορεί να βασιστεί σε ένα μεγαλύτερο σύνολο δεδομένων, με όσο το δυνατόν μικρότερο χρονικό βήμα (recording interval) μεταξύ των μετρήσεων. Ενώ παράλληλα μπορεί να γίνει διερεύνηση της επίδρασης του διαστήματος καταγραφής (recording interval) που κυμαίνεται μεταξύ 0.5 έως 3 ώρες τόσο στη διάρκεια όσο και στο διάστημα ηρεμίας.
- Πληροφορίες για τις επιπτώσεις των παράκτιων καταιγίδων στις ακτές όσο και στις κατασκευές, δορυφορικές εικόνες και επιπλέον μετεωρολογικά δεδομένα (π.χ. ατμοσφαιρική πίεση) μπορούν επίσης να συμπεριληφθούν για την καλύτερη ανάλυση των παράκτιων καταιγίδων.
- Οι συζεύξεις μπορούν να χρησιμοποιηθούν στις καταιγίδες που έχουν προσομοιωθεί και να υπολογιστεί η περίοδος επαναφοράς τους, ώστε να είναι εφικτή η σύγκριση τους με τις ιστορικές καταιγίδες.
- Η προτεινόμενη μεθοδολογία θα είχε ενδιαφέρον να εφαρμοστεί στο μέλλον σε περισσότερες περιοχές ώστε να μπορεί να γίνει μια καλύτερη σύγκριση των προσομοιώσεων αλλά και των περιόδων επαναφοράς.

Η πολυδιάστατη φύση των παράκτιων καταιγίδων και η πληθώρα των επιπτώσεων τους στις παράκτιες περιοχές επισημαίνουν την ανάγκη της ολοκληρωμένη προσέγγισης τους. Για την επίλυση αυτού του δύσκολου προβλήματος απαιτείται η μελέτη των ιστορικών καταιγίδων και δεύτερον η πολυμεταβλητή τους ανάλυση. Σε αυτήν την κατεύθυνση, η θεωρία του συζεύξεων είναι πολλά υποσχόμενη και αξίζει την προσοχή της επιστημονικής κοινότητας.

List of figures

List of tables

List of symbols

AIC	Akaike information criterion
ACF	Autocorrelation function
AND (or $\cap$)	AND case (or Intersection)
BB1	BB1 copula
BB6	BB6 copula
BB7	BB7 copula
BB8	BB8 copula
BIC	Bayesian information criterion
BM	Block Maxima
C	Clayton copula
C	Copula (or Copula distribution)
c	Copula density
$\bar{C}$	Survival copula
$C_{ij}(u_i,u_j)$ or $C(u_i,u_j)$	Bivariate copula of standardised variables U_i, U_j
$C_{12\ldots d}\left(u_1,u_2,\ldots,u_d\right)$ or $C\left(u_1,u_2,\ldots,u_d\right)$	Joint copula of $X_1,\ldots,X_d$
$C_{i\|j}\left(u_i \mid u_j\right)$	Conditional copula of U_i, U_j
CV_T	Coefficient of variation of wave period during a coastal storm
CV_H	Coefficient of variation of significant wave height during a coastal storm
CV_{Dir}	Coefficient of variation of coastal storm direction
D	Coastal storm duration
D_{ir}	Wave direction
D_{ir1}	Coastal storm direction
D_{thr}	Duration threshold
$\frac{\partial^d(\ldots)}{\partial\ldots}$	d-variate partial derivative

E	Coastal storm energy
EVT	Extreme Value Theory
F	Frank copula
$f(x)$	Probability density function of X
$f_i(x_i)$	Marginal density function of X_i
$f_{ij}(x_i, x_j)$	Joint density function of X_i, X_j
$f(x_1,\ldots,x_d)$	Joint density function of $X_1,\ldots,X_d$
$f_{i\|j}(x_i \mid x_j),\ i \neq j$	Conditional density function of X_i, X_j
$\overline{F_1}$	Survival distribution function
$F(x_i)$	Cumulative distribution function of X_i
$F_i(x_i)$	Marginal distribution function of X_i
$F_i^{-1}(x_i)$	Inverse marginal distribution function of X_i
$F_{ij}(x_i, x_j)$	Joint distribution function of X_i, X_j (or jcdf)
$F(x_1,\ldots,x_d)$	Joint distribution function of $X_1,\ldots,X_d$
$F_{i\|j}(x_i \mid x_j),\ i \neq j$	Conditional distribution function of X_i, X_j
{Family}$^{\text{Deg}}$	Rotated versions of copulas. e.g., T_2^{90} : Tawn 2 copula rotated copula by 90 degrees
G	Gumbel copula
$h_{i\|j}(u_i \mid u_j)$	h-function of U_i, U_j
H	Significant wave height
H_1	Coastal storm wave height
H_{thr}	Wave height threshold
I	Independence copula
I	Coastal storm calm period
I_{thr}	Calm period threshold
jcdf	joint cumulative distribution function
J	Joe copula

L or Loglik.	log-likelihood
m_H	mean of coastal storms significant wave height
m_T	mean of coastal storms wave peak period
m_E	mean of coastal storms energy
m_P	mean of coastal storms energy flux
m_D	mean of coastal storms duration
max_H	maximum of coastal storms significant wave height
max_T	maximum of coastal storms wave peak period
$m_{H5\%}$	mean of 5% highest coastal storms significant wave height
$m_{T5\%}$	mean of 5% highest coastal storms wave peak period
N	Gaussian copula
OR (or $\cup$)	OR case (or Union)
$P(\ldots)$	probability
POT	Peak over threshold
PCC	Pair copula construction
r	Pearson's r
t	Student copula
T	Wave peak period
T_1	Coastal storm peak period
T_1	Tawn 1 copula
T_2	Tawn 2 copula
T_i	C-Vines tree ($i=1,2,3,4$)
$T_{(X_i>x_i \cap X_j>x_j)}$	Return period in years for a coastal storm event with variable X_i, X_j exceeding simultaneously the values x_i, x_j respectively

$T_{(X_i>x_i \cup X_j>x_j)}$	Return period in years for a coastal storm event with variable X_i exceeding the value x_i, or the variable X_j exceeding the value x_j
u_i	Specific value of standardised variable U_i
U_i	Standardised variable based on X_i
U[0,1]	Uniform domain (variables range between 0 and 1)
X_i	ith random variable ($i=1,2,\ldots$)
x_i	Specific value of ith random variable
$\prod_{i=1}^{d}(\ldots)$	Product
θ	Copula parameters
λ_U	upper copula tail dependence coefficient
λ_L	lower copula tail dependence coefficient
ξ *or shape*	Shape parameter of generalised Pareto
ρ	Spearman's rho
σ^* *or scale*	Scale parameter of generalised Pareto
τ	Kendall's tau

Chapter 1

Introduction

1.1. Background, motivation and research objectives

Storms constitute one of the most common and destructive disasters that have posed barriers to human evolution throughout the years. Examples of storm events, such as the big storm that hit the Mayas' civilisation (Smyth et al., 2017) or the storm which Columbus faced during his fourth voyage in 1502 (Emanuel, 2005a), have provided significant knowledge to the subsequent generations about storm severity. Historical storms indicate their intertemporal presence in human life (Ludlum, 1963; Longshore, 2008), as well as the fact that efficient preparation against storms, including prevention actions, are needed since their avoidance is impossible.

Dealing with storms is nowadays imminent due to climate change, especially for better understanding these events and being prepared for the future (Michener et al., 1997; Lowe and Gregory, 2005; Bengtsson et al., 2006; Helman and Tomlinson, 2008; Wang et al., 2008; Hallegatte et al., 2011; Marcos et al., 2011; Seneviratne et al., 2012; Gomes et al., 2015; Horton et al., 2015). The term "climate change" is commonly accepted by the scientific community, even if a small part is more sceptical towards the matter (Brown, 2013; Capstick et al., 2015; Hornsey et al., 2016; Hartter et al., 2018; Taddicken et al., 2018).

The latest reports of the Intergovernmental Panel on Climate Change (IPCC) (2018, 2019) confirm this change and warn about how it could be even worse. In brief, the IPCC notes that human should act for climate during the next decade. The extreme weather events have been more severe and frequent after 2010. The sea level has risen

more than 20 cm since 1880, while an additional rise of 5 cm can cause severe coastal flooding that will affect more than 10 million people worldwide (IPCC, 2018, 2019). The coastal communities are at high risk since coastal areas have been recognised as one of the most vulnerable, exposed to high storm surges, extreme rainfall, inundation. The IPCC's statements are also confirmed by other scientists (Knutson et al., 2015; Emanuel, 2017; Bhatia et al., 2019) and constitute reasons to focus on coastal storm analysis and coastal storm hazards given the future's uncertainty.

Regarding their definition, storms are considered extreme hydro-meteorological events and in their broadest sense describe hurricanes and cyclones. More specifically, "coastal storm" is used to better describe the storms that cause severe impacts on coasts. Coastal storms indeed threaten the coastal structures, the ports, and the coastal communities. Storms' analysis is a crucial research topic for coastal engineering since it directly affects the resilience of coastal communities and the reliability of coastal structures. Therefore, the initial motivation for undertaking this thesis was shaped by the inherent connection of coastal storms and human well-being, their extreme nature, and the broad research field that they create.

In an attempt to sufficiently describe a coastal storm, important variables requiring investigation are emerging. Both atmospheric and wave characteristics of each location and the storm impacts on coastal zones are used to better approach this phenomenon. Going deeper into this topic, the work of De Michele et al. (2007) constituted a milestone for the formation of this thesis, since it created the basis for relating the barely known field of copula theory to coastal storms' modelling. In the last decades, the copulas have gained ground in multivariate analysis with applications in hydrology (e.g., droughts, extreme rainfall, floods) and in economics (e.g., pricing, stock markets, risk analysis). Their theory is considered demanding, combines calculus and statistics, and depends on many calculations. Besides, their indiscriminate use can sometimes lead to errors with catastrophic consequences (e.g., the financial crisis of 2007-2008 in the U.S.A.). This peculiarity makes their proper application even more attractive. The copulas describe the dependence of variables enabling the estimation of joint probabilities in high dimensions and can indeed simulate coastal storms.

The specific research objectives of this thesis are:

- To define the coastal storm and to develop a methodology for its identification, as well as the description of each event through the important variables.
- To develop the theory of copula in order to model coastal storms: a) concerning the dependence of wave height and wave period during a coastal storm, b) for the coastal storms simulation of a location by applying and comparing algorithms that proposed in the literature (five dimensions), c) for the estimation of coastal storm return periods for various combinations of parameters (two-five dimensions).
- To identify and study coastal storms in the Mediterranean Sea, in order to understand their activity, characteristics and frequency of occurrence.
- To apply the methodology for modelling coastal storms through copulas in the sample of the Mediterranean Sea, for understanding the best copula family for wave height and wave period modelling, for their simulation and their return period.

1.2. Innovative points and highlights

This thesis is based on the coastal storm analysis and the application of copulas for their modelling, mainly for their simulation and the estimation of coastal storm return periods. The following innovative aspects are included:

- The variables of a coastal storm and the required thresholds are described and explicitly investigated, providing, for the first time, a step-by-step methodology for coastal storm identification.
- The developed methodology for the identification and the analysis of coastal storms is validated via analysis of real wave data. Datasets from 30 different locations are analysed for the first time in the Mediterranean Sea, and in general also, for the study of coastal storms. In total, 4008 coastal storms are detected, covering, in general, a period from 1985 to 2019. The descriptive statistics of these extreme events are presented, providing significant information about coastal storm activity during the last decades.
- The analysis of detected coastal storms also highlights for the first time many important characteristics of Mediterranean coastal storms, concerning a) the

investigation of coastal storm energy and the energy flux, regarding the wave height and the wave period during a coastal storm, b) the variance of the wave period and the direction within a coastal storm, and c) the simplified shape of coastal storms concerning the wave direction and the wave period during an event.

- In comparison with the common practice that predetermines a single bivariate copula without investigation (e.g., Archimedean, Gaussian), in this thesis, the optimal selection of bivariate copulas for the wave height and the wave period during a coastal storm is thoroughly investigated. In particular, 40 copula families are examined, and the optimal copulas are presented. Furthermore, the second-best copulas are also investigated in an effort to identify similarities among copula families. Subsequently, the tail dependencies and the range of coastal storm parameters are further explored when the coastal storm dataset is modelled via a specific copula family.
- Following an overview of the C-Vine copulas methodology, this thesis elaborates on the extension of this particular methodology in five dimensions for coastal storm modelling. The proposed five-dimensional C-Vine structure is developed based on one of the 30 different datasets hereto analysed, namely Malaga's dataset. However, the developed C-vine copula can be applied in many other locations with similar characteristics.
- In the context of this thesis, the methodology of De Michele et al. (2007) for sea storm simulation is extended to five variables and an algorithm is developed so as to properly simulate coastal storms. The developed algorithm is compared to the ones proposed by Aas et al. (2009) and Stöber and Czado (2017). The simulation efficiency of the three algorithms is investigated through the detected coastal storms of Malaga's dataset.
- This research achieves to estimate the return periods of extreme coastal storms through copulas for two to five variables, extending conventional approaches that incorporate up to three variables. Furthermore, the C-Vines are compared to other well-known copulas (e.g., Gaussian, Gumbel, t).

1.3. Thesis structure

The main topic of this thesis is the analysis of coastal storms for their application in the design process of harbours and coastal structures. The primary research lines for coastal storm analysis are drawn following the review of recent literature and the description of key research issues (Chapter 2).

In Chapter 3, the methodology of this thesis regarding the analysis and the modelling of coastal storms is described. In particular, the storms' definition, the appropriate thresholds used to define them, their identification and their characteristics are investigated. Subsequently, the theory of coastal storm modelling through copulas is presented. The basic principles of copula theory, the construction of C-Vine copulas and their application in coastal storm simulation are described. Coastal storm activity can be simulated with three literature-based algorithms (De Michele et al., 2007; Aas et al., 2009; Stöber and Czado, 2017) incorporating five variables by extending the pre-existing methodologies. Their efficiency is investigated through the comparison of simulated and observed data for a particular case study in the Mediterranean Sea. Besides, the joint conditional functions are estimated through copulas and then they are used for the estimation of storms' return periods. In this context, a step-by-step methodology is provided, capable to properly analyse and simulate coastal storms.

Chapter 4 includes the results of the methodology presented in Chapter 3, as well as the results' discussion. Analysis of coastal storms of 30 locations in the Mediterranean Sea is conducted via descriptive statistics to provide not only an overview of their activity in the Mediterranean Sea over the last decades but also insights regarding their characteristics. The coastal storm characteristics include the duration, the calm period, the energy, the wave height, the wave period, the direction, and the shape of coastal storms are analysed. As far as the energy of coastal storms is concerned, two different approaches for the coastal storm severity index are analysed to identify which one can be included in coastal storm analysis. The application of bivariate copulas to model the significant wave height and wave period of 4008 detected coastal storms is described, and the two optimal copulas as well as their characteristics are presented. The five-dimensional C-Vine copula is described and subsequently, this proposed structure is applied to simulate coastal storms and estimate the return periods in the Malaga region. The simulated coastal storms are validated through comparison with observed data. At

the end of this Chapter, the application of copulas and coastal storm analysis in harbours and coastal structures design is discussed.

Finally, Chapter 5 contains the general conclusions of this thesis. Furthermore, the limitations encountered and the proposed suggestions for future research are also included in this Chapter.

Chapter 2

Theoretical background for coastal storm analysis

2.1. Key research issues of coastal storm analysis[1]

Throughout human history, priority has been given to protection against severe weather conditions, storms, and natural disasters (e.g., flooding, tsunamis, earthquakes, volcanoes). In an attempt to find answers, humans focused on how these natural phenomena happen and who is responsible. In ancient times, most cultures had gods or deities associated with natural disasters. Different gods were responsible for storms among different civilisations and eras; Hurakan for Mayas (Schwartz, 2015), Thor and Rán in Norse mythology, Susanoo in Japanese mythology, Indra in Indian religion, and Set in Ancient Egypt. In ancient Greece, Homer described Zeus to be responsible for storms while the sea had its own god, Poseidon, responsible for the storm surges (Hard, 2004; Taub, 2004).

As years went by, humans were more interested in "how" these phenomena occur, rather than "who" is responsible for their occurrence. For this reason, people became more sceptic and started to observe the signs of the sky and land, identify patterns and carefully prepare against extreme weather phenomena (Mölders and Kramm, 2014). Accurate explanations of these phenomena were given by philosophers, throughout the years, simply by analysing the changes and the movement of the clouds and the stars. However, it was not until 1880 that the first scientific approach for interpreting the nature, formation and impacts of storms appeared (Fig. 2.1). The science regarding this

[1] A part of this chapter has been published in Martzikos et al., (2021a).

topic remained scarce until the 1950s, when the topic started receiving attention, probably in alliance with the general post-World War II economic expansion, which required safety against extreme weather events. The research related to coastal storms started to raise significantly after 2000 (Fig. 2.1) and continue to rapidly increase till today.

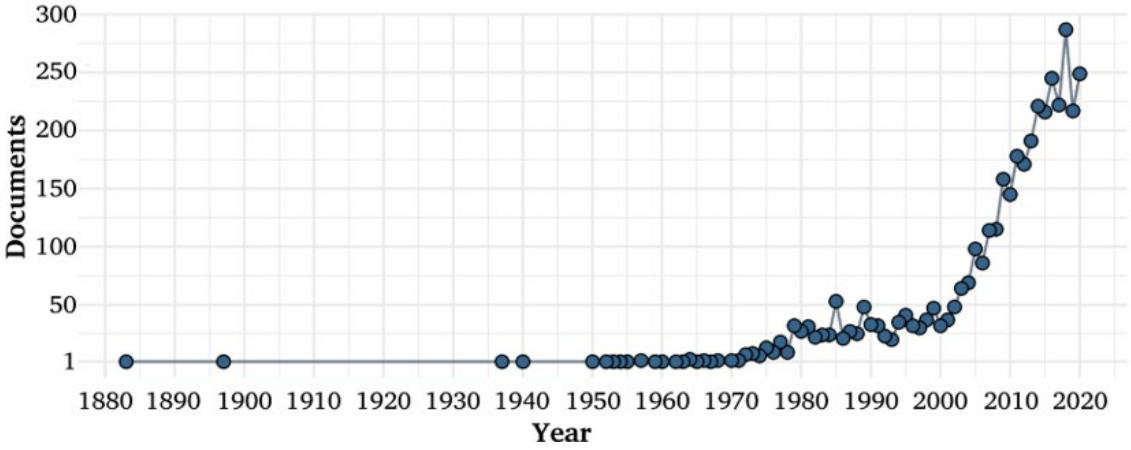

Figure 2.1. The annual number of documents-publications, including the term "storm" in the title, and the terms "coastal" or "coast" in the title, abstract or keywords, according to Scopus.

Several researchers have published their work concerning the accurate prediction of extreme storm events (Ferreira and Guedes Soares, 1998; Lowe and Gregory, 2005; McInnes et al., 2007; Izaguirre et al., 2013), the storm forecasting (Madsen and Jakobsen, 2004; Verlaan et al., 2005; Mattocks and Forbes, 2008; Rego and Li, 2009), and early warning techniques (Ciavola et al., 2011b, 2011a; Gall et al., 2013; Jones et al., 2017). In general, the nexus of extreme events and human preparation against their impacts attracts diachronically the research interest since the storm research provides information that improves not only the understanding of these extreme events but also the risk analysis of the related hazards.

Throughout human history, people tend to make settlements along the coasts. Currently, approximately 600 million people live in low elevation coastal zones (i.e., coastal regions less than 10 m above mean sea level) (Kirezci et al., 2020). Therefore, researchers primarily deal with storm management, which is vital for everyone who lives and works along the coasts and consequently focus on storm impacts in coastal areas (Hissel et al., 2014; Spencer et al., 2015). Considerable attention is given to research issues related to storm research, such as coastal zone management (Curtis,

2013; De la Torre et al., 2013; Hallegatte et al., 2013; Chadenas et al., 2014; Musereau and Regnauld, 2014; Jaranovic et al., 2017), the optimal design of port and coastal structures (Rao and Mandal, 2005; Phan and Simiu, 2011; McCullough et al., 2013; Takahashi et al., 2014; Altomare et al., 2015; Burmeister et al., 2015; Basco, 2016; Do et al., 2016; Van Doorslaer et al., 2017; Hatzikyriakou and Lin, 2017; Mooyaart and Jonkman, 2017; Mohd Anuar et al., 2018), and the rise of public awareness (National Research Council, 2014; Lane et al., 2015; Paton et al., 2017).

Apart from the implications of storms for coastal populations, and their inclusion in broader research topics, researchers also focus on the thorough investigation of coastal storms. For this reason, relevant research includes the analysis of historical events (Shand et al., 2011), the modelling of coastal storms (Massey et al., 2011; You, 2011; Kim and Suh, 2016; Pingree-Shippee et al., 2018) and the presence of storm surges (Bender et al., 2012; Naimaster et al., 2013; Allis et al., 2015; Yao et al., 2017; Pouzet et al., 2018). In addition, multiple publications are dedicated to describing the impacts of a coastal storm (Klemas, 2009; Hondula and Dolan, 2010; Barnard et al., 2014; Hartt, 2014) on sandy beaches (Rangel Buitrago and Anfuso, 2011a), the marine ecosystem (Sanchez-Vidal et al., 2012), the sediment transport (Aagaard and Kroon, 2017; Wang and Cheng, 2017; Swindles et al., 2018), the structures and their design (Benassai et al., 2009; Basco and Mahmoudpour, 2012), as well as the storm's implications with coastal erosion (Basco and Walker, 2010) and inundation (Wamsley et al., 2011; Barnard et al., 2014). Coastal storm research is inevitably linked to climate change (Sanuy et al., 2018) and provides in-depth information on the associated risk reduction. As a result, many risk assessments are found in the literature for different locations (Ferreira et al., 2009; Garnier et al., 2018), which subsequently help the forecasting (Flowerdew et al., 2010; Haerens et al., 2012) and the establishment of early warning systems (Valchev et al., 2014).

Coastal storm analysis is an integral part of coastal storm research, hence of paramount importance for scientists, organizations, and governments who wish to effectively deal with such phenomena, prepare in a timely manner and finally protect citizens. The general concept of coastal storm analysis is developed around the importance of learning from the past and prepare for the future, with regards to sufficient protection against an upcoming storm. The analysis is mostly based on identifying and understanding the variables involved while trying to properly describe

the event (e.g., wave height, wave period). However, due to the complexity and the number of variables, this effort is usually a complicated process.

In an attempt to simplify the entire process, a coastal storm analysis could be divided into three phases: before (*pre-storm*), during (*over-storm*) and after (*post-storm*) a storm event. Most research usually deals with one of these phases. The "pre-storm" phase entails studying past storm events and is based on oral evidence and historical data, i.e., measurements, models, satellite images, newspaper articles, photos, videos, old maps. This information is used to understand the wave climate conditions in a specific location. Moreover, they are valuable for studying storm consequences. Similarly to the "pre-storm" phase, the "over-storm" phase incorporates the offshore and onshore available real-time data, which are analysed to identify the storm event and understand its severity and its impacts. At the operational level, this analysis can be accomplished at the time of the storm's occurrence to predict its development and inform the society via the warning systems. The "post-storm" phase is focused on the consequences of coastal storms since it includes disasters' recording and analysis, as well as infrastructures' reliability, predictive models' efficiency of models and warning systems' accuracy during a storm.

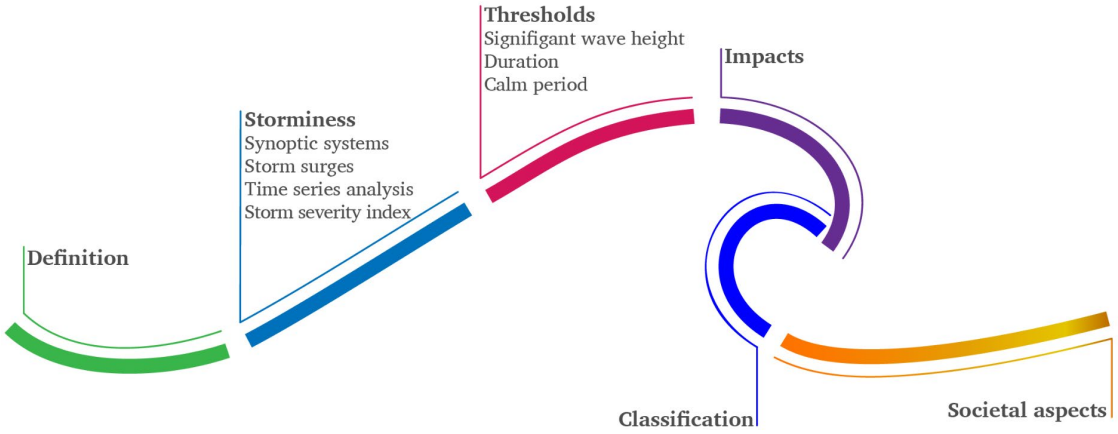

Figure 2.2. The most important key research issues of coastal storm analysis.

Further to the simplification of coastal storm analysis in temporal terms, this chapter seeks to shed light into the contextual components of a robust coastal storm analysis. In particular, the main pillars of such an analysis (Fig. 2.2) are the following: 1) the definition of a coastal storm, 2) the storminess' assessment, including the complete or partial analysis of synoptic systems, the storm surges, the wave characteristics with time series and the coastal storm severity index, 3) the identification of a coastal storm through thresholds' analysis, including the significant wave height, the duration and the

calm period, 4) the coastal storm impacts on the coasts, 5) the classification of the events, and 6) the societal aspects of a coastal storm. The proper assessment of the aforementioned components constitutes a prerequisite for a robust storm analysis and a guiding framework for undertaking the analysis. Furthermore, they highlight the multidimensional nature of coastal storms and the necessity for a holistic view of their approach.

2.2. Coastal storm definition

According to the Glossary of Meteorology of the American Meteorological Society (2019), a storm is “any disturbed state of the atmosphere, especially as affecting the earth’s surface, implying inclement and possibly destructive weather”. The term “storm” usually describes cyclonic systems (i.e., hurricanes, typhoons, cyclones) and, slightly more often, other storm types of thunder, snow, sand, rain, and winds. However, this definition is not sufficiently explanatory for the marine environment. In this direction, the definition should incorporate the water element, as well as the impacts of a coastal storm.

A first definition of storm is given by the Beaufort scale. (McIlveen, 2010; Beer, 2013; Hasse, 2015; Clements and Casani, 2016; WMO, 2017). The scale, as developed in its modern edition (Table 2.1) considers the wind speed and assess its effects on land and sea to describe the phenomena and associate them with one particular Beaufort number. According to this scale, the storm corresponds to Beaufort number 10 with the maximum number of 12 illustrating the roughest sea conditions (i.e., hurricane). The storm is presented as an event with very high waves, long crests, a white appearance at the sea surface and very low visibility. This scale is important for seafarers and it was more useful in the past for the ships sailing the ocean (Mather, 2005; Singleton, 2008). However, scale limitations related to the non-inclusion of a fully developed sea and swell dynamics result in limited use of this scale (Harley, 2017). Furthermore, the Beaufort scale is referred to the open sea, thus being insufficient for coastal areas since it cannot adequately inform coastal communities and protect them against the threats imposed by a storm regarding their health and well-being.

Table 2.1

The Beaufort Scale with observations for open sea according to WMO (2017).

Beaufort number	Description	Wind speed [ms^{-1}]	Specification for observations (open sea)	Probable maximum height of waves [m]
0	Calm	0-0.2	Sea like a mirror	-
1	Light air	0.3-1.5	Ripples with the appearance of scales are formed but without foam crests.	0.1
2	Light breeze	1.6-3.3	Small wavelets; still short but more pronounced; crests have a glassy appearance and do not break.	0.3
3	Gentle breeze	3.4-5.4	Large wavelets; crests begin to break; foam of glassy appearance; perhaps scattered white horses.	1.0
4	Moderate breeze	5.5-7.9	Small waves, becoming longer; fairly frequent white horses.	1.5
5	Fresh breeze	8-10.7	Moderate waves, taking a more pronounced long form; many white horses are formed (chance of some spray).	2.5
6	Strong breeze	10.8-13.8	Large waves begin to form; the white foam crests are more extensive everywhere (probably some spray).	4.0
7	Near gale	13.9–17.1	Sea heaps up and white foam from breaking waves begins to be blown in streaks along the direction of the wind	5.5
8	Gale	17.2–20.7	Moderately high waves of greater length; edges of crests begin to break into the spindrift; the foam is blown in well-marked streaks along the direction of the wind.	7.5
9	Strong gale	20.8–24.4	High waves; dense streaks of foam along the wind direction; crests of waves begin to topple, tumble and roll over; spray may affect visibility.	10.0
10	Storm	24.5–28.4	Very high waves with long overhanging crests; the resulting foam, in great patches, is blown in dense white streaks along the direction of the wind; on the whole, the surface of the sea takes a white appearance; the “tumbling” of the sea becomes heavy and shock-like; visibility affected.	12.5

Table 2.1 *(continue)*

The Beaufort Scale with observations for open sea according to WMO (2017).

Beaufort number	Description	Wind speed [ms^{-1}]	Specification for observations (open sea)	Probable maximum height of waves [m]
11	Violent storm	28.5–32.6	Exceptionally high waves (small and medium-sized ships might be for a time lost to view behind the waves); the sea is completely covered with long white patches of foam lying along the direction of the wind; everywhere the edges of the wave crests are blown into froth; visibility affected.	16.0
12	Hurricane	≥ 32.7	The air is filled with foam and spray; sea completely white with driving spray; visibility very seriously affected.	-

The specification of the term “storm” found in the Beaufort scale into “coastal storm” when describing a storm event that affects coastal areas is necessary. The term is firstly found in literature in 1950, but its common use commenced in the 1980s onwards (Fig. 2.3), constituting the main subject of many studies worldwide (Godschalk et al., 1989; Quevauviller, 2014; Quevauviller et al., 2017; Basco and Mahmoudpour, 2018; Vasseur et al., 2018). The research attention given to storm phenomena in relation to the marine environment spans from 1980 to 2020. However, the term “coastal storm” differs from the terms “sea storm” (Boccotti, 2000, 2015; De Michele et al., 2007; Beer, 2013; Corbella and Stretch, 2013) and “ocean storm”, which are referred to the open sea, rather than the coastal zone.

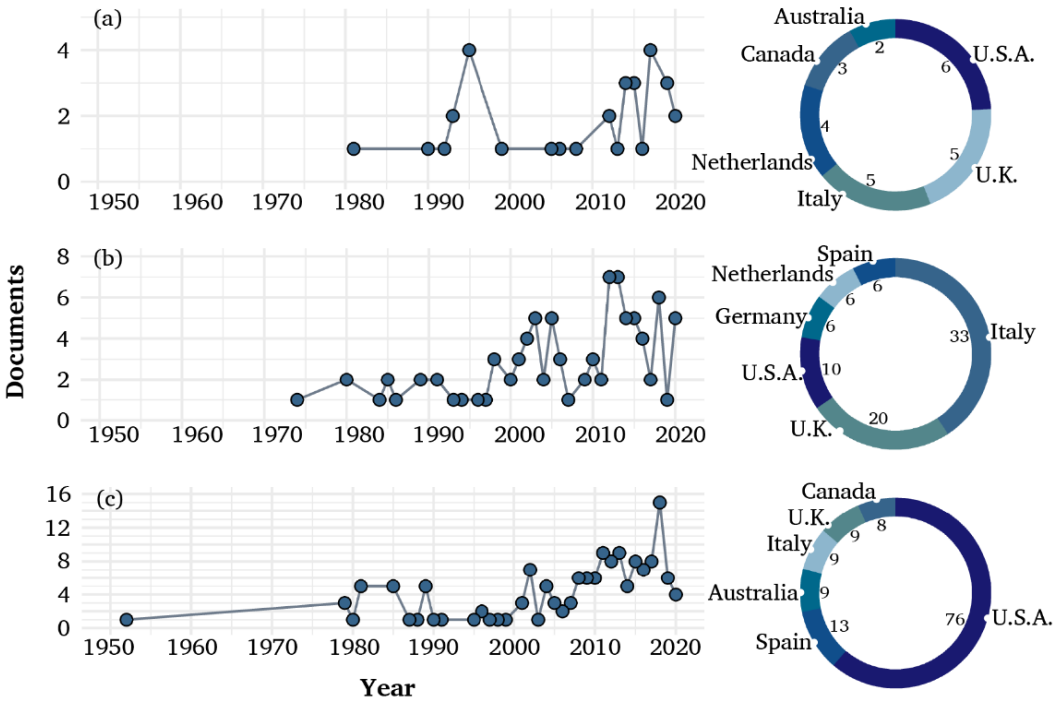

Figure 2.3. The annual quantity of documents-publications including the term (a) “ocean storm”, (b) “sea storm”, and (c) “coastal storm” in their title (on the left). The country of origin for the six highest documents counts (on the right), according to the Scopus database.

According to Harley (2017), the coastal storm definition is considered very challenging since it demands the combination of numerous parameters regarding the atmospheric conditions, the coastal environment, the total water level, the tidal cycle, the time that a storm begins as well as how long it is active. Mather et al. (1964) defined coastal storm many years ago, describing any synoptic situation that negatively affects

the coast and causes damages. Almost 20 years later, Dolan et al. (1988) referred to the coastal storm as any synoptic weather system which generates waves up to 1.6 metres in deep water (i.e., where depth is greater than half the wavelength). More recently, Ciavola et al. (2014) concluded that a coastal storm "can be considered as an anomalous set of meteorological conditions that have the potential to cause damage to the coastal zone and surrounding hinterland". Three years later, Harley (2017) provided an extensive definition for the coastal storm as a "meteorologically-induced disturbance to the local maritime conditions (i.e., waves and/or water levels) that has the potential to significantly alter the underlying morphology and expose the backshore to waves, currents and/or inundation".

Despite the evolution of the coastal storm definitions throughout the years, the identification of an extreme event as a coastal storm remains a complex procedure since it primarily depends on the local coastal environment. However, the accurate definition of a coastal storm and its connection to the properties of the coastal area that the storm occurs is the crucial first step of a robust coastal storm analysis.

2.3. Storminess

Another integral component of coastal storm analysis is the event's "storminess". The term is used to describe the coastal storm severity, the storm magnitude, or its strength, considering the coastal storm characteristics and mainly its duration and its impacts to the coastal zone. Therefore, the analysis of storminess is imperative while trying to understand how destructive a coastal storm is. Storminess assessment incorporates the critical examination of several aspects, including the meteorology and the synoptic systems, the existence of storm surges, the statistical analysis of the storm's characteristics and the investigation of coastal storm energy.

Synoptic systems

The relation of synoptic systems with the generation of storm events and their development have received research attention during the last decades (Trigo et al., 2002; Chen et al., 2010; Hopsch et al., 2010; Park et al., 2015; Machado and Calliari, 2016). Tropical cyclones and extra-tropical (or mid-latitude) cyclones constitute two synoptic systems that play a significant role in the formation of coastal storms that negatively affect the coastal zones.

A tropical cyclone is defined, according to the National Weather Service of NOAA (2019a), World Meteorological Organization (WMO) (2019), Met Office (2018) and (Zehnder, 2019), as a warm-core, non-frontal, low-pressure synoptic system, originating over tropical or subtropical oceans with organised deep convection and a cyclonic surface wind circulation. Tropical cyclones draw their energy from the tropics' warm and moist sea surface, while heat is released from cloud or rain formation. A tropical cyclone is formed during the upward movement of warm air when a low air pressure area forms over the sea. Consequently, the warm air cools off, clouds are shaped, and air from high air-pressure areas is entering the low air-pressure area over the sea. This process describes a continuous motion that feeds the cyclone. Therefore, tropical cyclones strengthen for as long as they are moving over water with high temperatures, and they fade when they move into cooler waters toward the poles and reach the coastline. The system moves from high to low air-pressure areas and rotates counter-clockwise when it follows a track between the North Pole and the equator, whereas the opposite is the case when a track is followed in the Southern Hemisphere. In parallel to the tropical cyclone phenomenon, strong winds which may exceed 240 km per hour also occur, leading to heavy rains and often an abnormal sea level rise. The combination of all these conditions is responsible for many hazards in coastal areas (Shepherd and Knutson, 2007; Harley, 2017). Different names (i.e., tropical depression, tropical storms, hurricanes, typhoons or cyclones) actually refer to the same weather phenomenon (i.e. tropical cyclone) (Ahrens and Henson, 2016), depending on the wind speed and the region where it occurs (Fig.2.4).

An extra-tropical cyclone is a cold core, low-pressure system in the middle or high latitudes of the earth beyond the tropics (Chan, 2019). It is characterised by and derives energy from significant horizontal variations of temperature, which are called fronts. An extra-tropical cyclone is developed at the interface of warm and cold air (Weisse and von Storch, 2010). It is also called middle-latitude, depression, or low cyclone (Ahrens and Henson, 2016). This type of cyclone is associated with strong winds causing severe damages, heavy rain leading to destructive flooding and thunderstorms responsible for remarkable temperature reduction. An extra-tropical cyclone is also responsible for extreme sea conditions and high storm surges. In contrast to the tropical ones, extra-tropical cyclones are static in terms of propagation, but they rotate counter-clockwise at the location of their occurrence. Even though they are less frequent and violent than

tropical cyclones, they can be more destructive for coastal zones as they remain over one area for a long period of time. A summary of tropical and extra-tropical cyclones and their main characteristics are presented in Table 2.2.

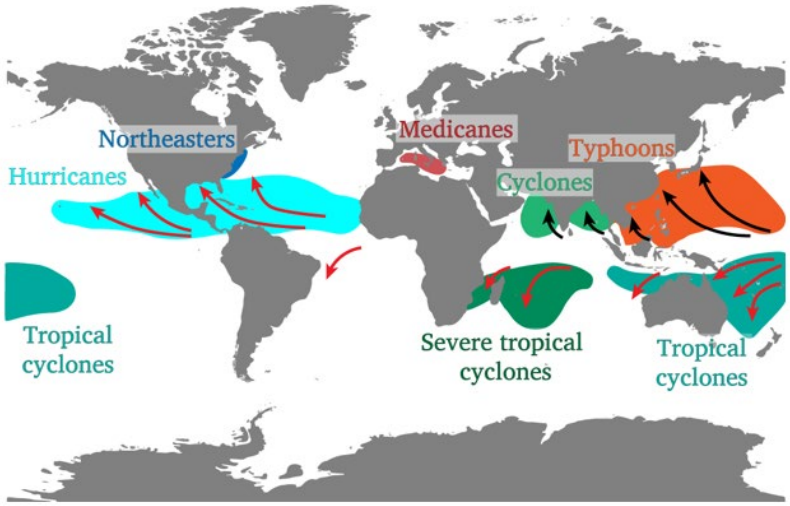

Figure 2.4. The different types of synoptic systems and the locations of their occurrence

Table 2.2
Main characteristics and names of tropical and extra-tropical cyclones based on WMO.

	Wind speed [m/s]	Names	Region	Occurring period
Tropical cyclones	<17	Tropical depression	-	-
	18-32	Tropical storm	-	-
	>32	Hurricane	Western North Atlantic, central and eastern North Pacific, Caribbean Sea and the Gulf of Mexico	June to November, with peaks in August and September
		Typhoon	Western North Pacific	May to November
		Cyclone	The Bay of Bengal and the Arabian Sea	April to June, and September to November
		Severe tropical cyclone	Western South Pacific and the southeast Indian Ocean	November to April
		Tropical Cyclone	Southwest Indian Ocean	November to April
Extra-Tropical cyclones		-	Middle latitudes of the Earth beyond tropics	-

A special focus is hereto given in two important synoptic systems: Northeasters and Medicanes which are generated from cyclonic systems. A Northeaster (or Nor'easter) is generated from a macro-scale extratropical cyclone, taking its name from its movement and the north-easterly direction of strong winds which are blowing in from the ocean over the east coast of North America and ahead of the storm (NOAA, 2013). These synoptic systems occur all year round but are usually characterised as winter storms, being more intense between September and April. They are associated with heavy snow, precipitation and extreme waves that cause severe damages in coastal areas, such as flooding and beach erosion (Davis et al., 1993; Komar and Allan, 2008; Horton et al., 2016; Lukens et al., 2018).

In the Mediterranean Sea, medium-scale tropical cyclones are developed, commonly known as Mediterranean hurricanes or as Medicanes (Cavicchia et al., 2014; Emanuel, 2005; Ernst and Matson, 1983; Pytharoulis et al., 2000; Romero and Emanuel, 2013). This type of system has recently attracted significant attention since they are becoming more frequent and hazardous (González-Alemán et al., 2019). They have a warm core and are accompanied by low pressure on sea level, intense cyclonic winds, and heavy rains. They are rare phenomena and mainly occur between late summer and autumn (Cavicchia and von Storch, 2012). They are usually weaker than tropical cyclones but are frequently responsible for property damage, negative impacts on marine transportation and loss of human life.

Storm Surges

The existence of storm surge at a given location and a specific timeframe constitutes an important component of storm analysis since its presence usually makes the coastal storm effects even more destructive. Storm surges are considered responsible for increased losses and mortality, according to IPCC (Collins et al., 2019) and are expected to become more threatening under sea-level rise projections. The nexus of storm surge and coastal storms has been investigated throughout the years (Needham and Keim, 2011; Booth et al., 2016), mainly regarding the storm surge disasters (Robertson et al., 2007; Tajima et al., 2014) and coastal flooding in particular (Burzel et al., 2010; Oumeraci et al., 2015; Prinos and Galiatsatou, 2018). Nevertheless, the storm surges' future evolution based on modelling that incorporates climate change (Woth et al., 2006; Boldingh Debernard and Petter Roed, 2008; Siek, 2011), as well as the

management of storm surges and the related coastal protection strategies (Kremer et al., 2013; Slobbe et al., 2013) have also been researched.

The storm surges and their characteristics are described thoroughly in Bertin et al. (2017), and Weisse and von Storch (2010), indicating that they depend on several processes. More specifically, the surge amplitude is affected by the storm intensity and the size, the central pressure, the propagation of the storm with forward speed, the wind direction, the angle of approach to the coast and the characteristics of the coastal zone (e.g., the shape of the coastline, the bathymetry, the width, and the slope of the seafloor).

The National Hurricane Center (NHC) of the National Oceanic and Atmospheric Administration (NOAA) defines the storm surge, also known as the meteorological tide (Sorensen, 2006), as an abnormal rise of water level generated by the aforementioned synoptic systems. A storm surge refers to the rise above the predicted astronomical sea tide. The surge height is basically the difference between the observed water level and the predicted astronomical tide, typically ranging from 1 to more than 5 metres (NOAA, 2019b). The reduced atmospheric pressure and the strong onshore winds of a tropical cyclone significantly contribute to the creation of storm surges by creating currents that accumulate water in shallow areas. Furthermore, winds that blow in a parallel direction to the coast, waves' interactions (i.e., wave breaking, runup, setup and overtopping) and the Ekman transport cause an additional rise in sea level. This rise is greater when a high tide exists or when the storm surges are affected by the Earth's rotation. Then, due to the Coriolis effect, an acceleration of water currents occurs, transporting more water toward the coast. A high storm surge implies a significant rise of the total water level, thus making a coastal storm very destructive since it causes higher wave overtopping and severe coastal floods.

Coastal storm analysis through time series

Studying and analysing wave climate data is another way to understand the storminess in a specific coastal location through the collection of information about the waves and the sea states during a coastal storm. Many studies have focused on time series analysis to detect the storm occurrence, with particular attention to their statistics for the investigation and the management of similar events in the future.

The time series theory is used for analysing separately or in combination the most important storm parameters as continuous random variables (i.e., the significant wave height, the wave period, the wave direction, the water level, the atmospheric pressure, the temperature, the wind velocity, the wind direction). Many studies analyse rather composite parameters, such as storm energy, the storm duration and the calm period or the interarrival time between two consecutive storm events (De Michele et al., 2007; Corbella and Stretch, 2013). A statistical analysis of coastal storms should include as many parameters as possible, but due to the process' complexity, the data availability and the research objectives, researchers tend to select some of these parameters to analyse for the location of interest.

Statistical analyses of extreme events are commonly found in literature since they constitute a useful tool for their understanding. In this direction, Coles' book (2001) about statistical modelling of extreme values provides a solid base for future related applications (e.g. Katz, 2010; Mannshardt and Gilleland, 2013; Cheng et al., 2014). However, many other books can be consulted for the statistical analysis of extreme events (e.g. Beirlant et al., 2004; Yakir, 2013; Chavez et al., 2015; Dey and Yan, 2015). Storms are regularly analysed through the incorporation of the Extreme Value Theory due to their extreme nature. The main methods used are the ones of the Peak Over Threshold (POT) and the Block Maxima (BM).

In the POT method, researchers use time series for predetermined important parameters. They define a threshold for each of them and subsequently study only the time series of the clusters that exceed the threshold. It should be noted that the selection of the optimal threshold in the POT method is a demanding process. For instance, Ross et al. (2018) use the POT method to analyse extreme storm surges in North Sea storms and estimate the associated return values. Similarly, Shao et al. (2019) analyse the wave heights of tropical cyclones in the South China Sea through the POT method.

In the BM method, several peaks for a certain time period (e.g., monthly, annual) are being taken as representatives constituting new time series, which are then examined for extreme event analysis. In literature, this method is applied for the return period estimation and the risk of coastal flooding by analysing the characteristics of extreme winds or waves (or storm surges). Applications have been conducted for the global scale (Muis et al., 2016), but also for the Colombian and the Caribbean Sea (Devis-Morales et al., 2017), as well as the Atlantic and the North Sea coasts of Europe (Calafat and

Marcos, 2020). The proper selection of the number of peaks is crucial for the efficiency of this method, but this number is determined through the rule of thumb without sufficient clarification and mostly ranges between one and three peaks annually (based on the r-largest method). However, the annual frequency of severe storm occurrence for each location might be useful for improving both the number of peaks used in the BM method and the threshold selection of the POT method.

In this direction, the incorporation of copulas has received significant research attention for the analysis and modelling of storms and extreme “metocean” events (Corbella and Stretch, 2012a; Corbella and Stretch, 2013; De Michele et al., 2007; Li et al., 2014, 2018; Lin-Ye et al., 2016, 2018; Lira-Loarca et al., 2020; Salvadori et al., 2014). The copula theory has been known in the last decades (Fig. 2.5), especially in the field of economics (Frees and Valdez, 1998; Cherubini et al., 2004; McNeil et al., 2005; Trivedi and Zimmer, 2006; Aas et al., 2009; Embrechts, 2009; Genest et al., 2009), where they are used in many complex problems of mathematical finance, concerning pricing, stock markets, and risk analysis. However, copula theory became also famous for its applications in hydrology, water resources and environmental engineering (Genest and Favre, 2007; Renard and Lang, 2007; Salvadori and De Michele, 2007; Serinaldi, 2015; Salvadori et al., 2016; Jäger and Nápoles, 2017; Jäger et al., 2019). They have been extensively used for the analysis of droughts (Shiau, 2006; Serinaldi et al., 2009; Kao and Govindaraju, 2010; Song and Singh, 2010; Seneviratne et al., 2012; De Michele et al., 2013; Xu et al., 2015; Chang et al., 2016), extreme rainfall (De Michele and Salvadori, 2003; Zhang and Singh, 2007; Bárdossy and Pegram, 2009; AghaKouchak et al., 2010) and floods (Salvadori, 2004; Salvadori and De Michele, 2004; Grimaldi and Serinaldi, 2006; Liu et al., 2015; Masina et al., 2015; Sraj et al., 2015; Sadegh et al., 2017).

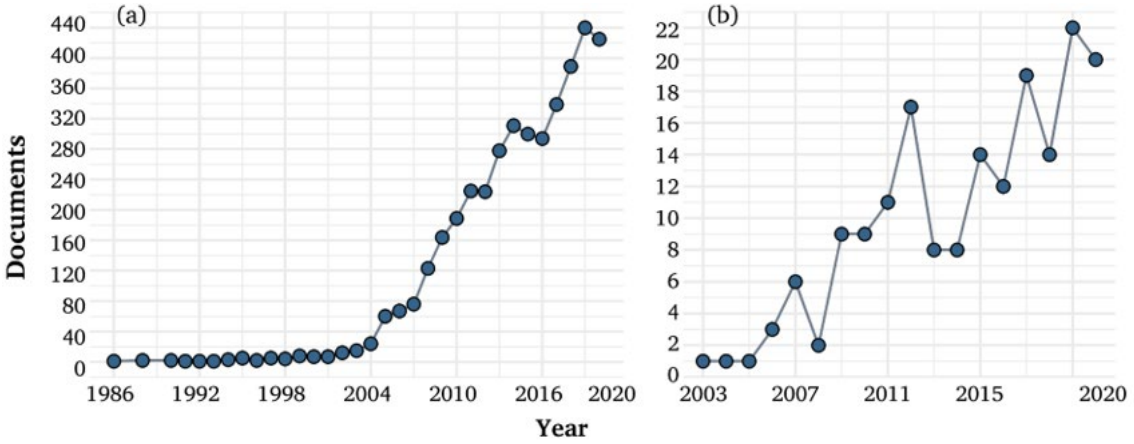

Figure 2.5. The annual quantity of documents-publications including the term "copulas" (a), and the terms "copulas" and "storm" (b) in the title, abstract, or keywords. The bibliometric analysis is carried out according to the Scopus database and is limited in relevant subject areas such as Engineering, Mathematics and Economics.

Coastal storm severity index

Assessing the storm severity is an integral part of a coastal storm analysis that can be estimated via the calculation of various quantitative properties such as the storm energy, the magnitude, the content of even a composite index. The storm energy is affected by the maximum wave height. Besides, the storm duration is important for damages and changes in beach morphology. In literature, different terms such as "storm magnitude" (De Michele et al., 2007), "energy content" (Mendoza et al., 2011; Duo et al., 2020) and "storm power index" (Dolan and Davis, 1992, 1994; Karunarathna et al., 2014; Dissanayake et al., 2015) are used to describe the severity of a coastal storm. As proposed by Dolan and Davis (1994, 1992) and also used by Mendoza et al. (2011), Rangel-Buitrago and Anfuso (2011b), the storm energy can be estimated by the Eq. 2.1,

$$E = \int_{t_1}^{t_2} H^2 dt \,, \tag{2.1}$$

where t_1 denotes the beginning of a storm event, t_2 is the end time and H is the significant wave height or the significant wave height over a threshold. De Michele et al. (2007), following the meaning of the storm energy, proposed the storm magnitude (M) (Eq. 2.2) such as the area of a triangle, where η represents the significant wave height threshold and D is the storm duration.

$$M = (H - \eta) \cdot \frac{D}{2}. \tag{2.2}$$

Corbella and Stretch (2013) extended this concept to obtain the wave power P (Eq. (2.3)) by incorporating the average wave energy E (Eq. 2.4), where g is gravitational acceleration, T is the maximum peak period and ρ is the density of salt water.

$$P = \left(\frac{gT}{4\pi}\right) \cdot E, \tag{2.3}$$

$$E = \frac{1}{8}\rho \cdot g \cdot H^2. \tag{2.4}$$

Karunarathna et al. (2014) calculated the storm power index (S_{pi}) by Eq. 2.5, but due to overestimation stemming from the use of the peak of wave height during a storm, Dissanayake et al. (2015) proposed the Eq. 2.6 referring, in a sense, to the equation of Dolan-Davis (Eq. 2.1), where ΔD and ΔH denote the duration and the storm wave height, respectively.

$$S_{pi} = D \cdot H_{peak}^2, \tag{2.5}$$

$$S_{pi} = \sum_{i=1}^{n}\left(\Delta D \cdot \Delta H_i^2\right). \tag{2.6}$$

Particularly for the Mediterranean Sea, Lin-Ye et al. (2016) highlighted that storms are sharp when they grow and milder when they decay. Therefore, they focused on the storm strength and proposed Eq. 2.7, where $E_{u,p}$ corresponds to the hourly storm energy around the peak.

$$E_{u,p} = \max_i(mean(E_{u,(i-1)} + E_{u,i} + E_{u,(i+1)})). \tag{2.7}$$

Furthermore, Basco and Mahmoudpour (2012, 2014, 2018) introduced the coastal storm impulse parameter (COSI). This index is also used for estimating the coastal storm strength, and it does consider the waves, the water levels, the currents, and the storm duration D as described in Eq. 2.8, where $f_{p(t)}$ denotes the storm surge momentum and $M(t)$ is the mean wave momentum flux that is the landward mass times velocity.

$$I = \int_0^D [f_{p(t)} + M(t)]dt. \tag{2.8}$$

The optimal choice of the method describing the storm severity is highly dependent on the researcher's preferences and depth of analysis. The latter is also the case for estimating the storminess as a whole. It is evident that storminess is better explored if all of its components are analysed, namely: the synoptic systems, the storm surges, the storm analysis with time series and the storm severity index. However, this holistic

analysis is rarely the case in related research due to data, resources, and time availability. However, the analysis of one of the aforementioned components, when properly conducted, is still capable to provide an accurate overview of the storminess.

2.4. Thresholds for coastal storm identification

Following the Extreme Value Theory (EVT), coastal storms as extreme and rare events can be described by specific parameters ranging above or below a threshold. In practice, this is a rather complex process as time series might fluctuate around a threshold and quite often many events are not significant enough to consider them as coastal storms. Therefore, researchers should review these thresholds based on the requirements of their research. The optimal selection of thresholds is not only a demanding procedure, but it is also somehow subjective since it is strongly related to the available data. The most common parameters for which thresholds are selected to define a storm are: the significant wave height, the storm duration, and the calm period, as shown in Figure 2.6. Their values are mostly site-dependent and vary widely between different locations (Table 2.3).

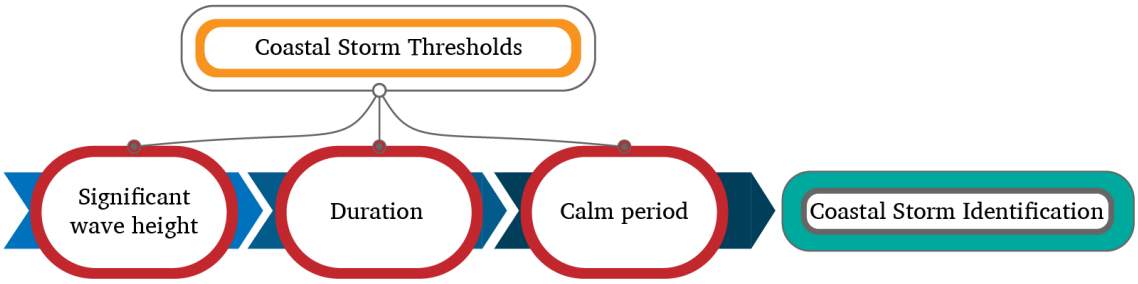

Figure 2.6. The most common thresholds which contribute to coastal storm identification.

Significant wave height

According to the inclusive and straightforward Boccotti's (2000) description, the sea storm is considered as a sequence of sea states with significant wave height (H) exceeding a specific threshold without falling below this threshold for a certain period of time. This threshold varies according to the location, the bathymetry, and the exposure to the open sea, as well as to the large fetches and consequently to the high waves. Generally, defining the thresholds which characterise coastal storms is more accurate if based on their effects, hence their impacts on the coast including beach

erosion, inundation or runup, rather than on a statistical rule. However, this information is not available at any location since it is both costly and time-consuming.

Dolan and Davis (1994, 1992) considered a threshold of H at 1.5 metres by assessing the remarkable erosion in the coast caused by waves in deep water higher than this threshold. From a statistical point of view, Almeida et al. (2011) defined their threshold as the mean H plus two times the standard deviation of their dataset. Based on extreme and generally the EVT. Many researchers who conduct their analysis based on EVT, or extreme wave analysis (Mendoza et al., 2011) use the 90^{th} percentile, or even greater one, to extract and analyse only the most extreme events (Dorsch et al., 2008; Rangel Buitrago and Anfuso, 2011a; Eastoe et al., 2013). A goodness of fit to the extreme value distributions (e.g., Generalised Pareto, Poisson or Weibull), the stability check of their parameters for a range of thresholds or a residual life plot as proposed by Coles (2001), are also used to define the threshold of significant wave height (Mazas and Hamm, 2011; Bernardara et al., 2014). In the same direction, Lin-Ye et al. (2016) relied on excess – over – thresholds plot for their analysis, whereas Li et al. (2014), as well as Duvat et al. (2016), proposed the root mean square error analysis among observed and fitted data which extracted from extreme value distribution of extreme data.

Boccotti (2000, 2015) suggested the threshold to be between 1.5 and 2 times the mean of annual significant wave height, using the concept of the equivalent triangular storm (ETS). The ETS substitutes the actual storm with a simplified equivalent storm, having a triangular shape with a height equal to the maximum wave height that corresponds to the storm intensity and the base of the triangle representing the duration of a storm. Many other permutations of ETS were presented to simplify the mathematical process and improve its efficiency (Martín-Hidalgo et al., 2014; Martín Soldevilla et al., 2015; Duo et al., 2020). Overall, the method to be used for defining the wave height threshold usually depends on the researchers' background and preferences.

Duration

The duration (D) of a coastal storm is the time period for which the significant wave height remains over a threshold. The duration is inherently linked to the time frame for which the storm impacts are noteworthy. However, the definition of a minimum duration is necessary in order to discard the shortest storm events. The minimum duration is defined in various ways (Table 2.3), having the most common values ranging

between 6 and 12 h (De Michele et al., 2007; Basco and Walker, 2010; Mendoza et al., 2011). These values are probably influenced by the minimum rainstorm duration and the hydrograph storm separation (Piest, 1963; Thorp and Scott, 1982). Rangel-Buitrago and Anfuso (2011a) considered the tidal duration for their location and defined the minimum duration required to observe storms that affect the coast during the tidal cycle. Lin-Ye et al. (2016) investigated the duration of 12 h, 24 h and 48 h and concluded that the duration of 12 h corresponds to more realistic storm events. The duration threshold can be alternatively defined according to the minimum duration of synoptic systems that contribute to the generation of storm events (i.e., tropical, and extratropical storms) at a given location. However, this approach is rather more complex since the synoptic systems are usually converted from one type to another as they grow (Harley, 2017).

In practice, the main constraint for properly defining the duration threshold is the elapsed time between consecutive measurements (also known as sampling or recording interval) usually ranging from 0.5 to 3 h. Therefore, the minimum storm duration should be over 3 h, and maybe over 6 h, to avoid identifying events that consist of short time series.

Calm period

The definition of the overall storm duration and the discretisation of consecutive storms, the term “calm period”, needs to be determined. The calm period denotes the time interval between the end and the start of two consecutive storms. According to De Michele et al. (2007) and Corbella et al. (2012a), the term is also known as inter-arrival time. In theory, a storm event ends when the significant wave height falls below the threshold for a while, whereas in practice, this is difficult to be observed since usually a storm event has more than one peak. For this reason, a calm period threshold is needed in order to separate different events, but also indirectly assess the severity of storm impacts on the coast, i.e. two consecutive events will be more destructive than occurring individually within a short time interval (Callaghan et al., 2008; Ferreira, 2005; Lee et al., 1998).

The threshold of the calm period is associated with the equilibrium conditions regarding the coastal profiles and the time of beach recovery (Dissanayake et al., 2015; Sénéchal et al., 2015), but is also related to the independence of the synoptic systems responsible for the storms. Indeed, the calm period threshold is site-dependent (as

shown in Table 2.3). This threshold ensures the discretisation of two events and it is generally useful to consider more events as a single one, especially when they are generated by one meteorological system. Piscopia et al. (2003) chose the independent events based on the autocorrelation function, while Corbella and Stretch (2012a, 2013) considered the calm period based on the decay of Spearman autocorrelation, confirming the statistical independence. It should be noted that following this method, Corbella and Stretch (2012a) set the calm period at 336 hours for the Durban region in Africa (i.e. the highest value in Table 2.3). The annual number of storms at a given location can also be useful for the definition of the calm period (Callaghan et al., 2008; Méndez et al., 2008; Davies et al., 2017). However, it is usually safe to consider this threshold as a fixed value, between 12-24 hours, as mostly used in literature, without further analysis.

Table 2.3

The storm thresholds in different locations.

Study area	Significant wave height [m]	Duration [hr]	Calm period [hr]	Authors
New South Wales, Australia	2.92	-	24	(Davies et al., 2017)
Adelaide, South Australia	1.00	-	30	(Dorsch et al., 2008)
Durban, Africa	3.50	-	336	(Corbella and Stretch, 2012a, 2013)
Yucatan, Mexico	1.50	24	-	(Mendoza et al., 2013)
North Carolina, USA	1.50	-	-	(Dolan and Davis, 1992)
North Carolina, USA	1.60	6	48	(Basco and Walker, 2010)
Liverpool Bay, UK	2.50	1	12	(Dissanayake et al., 2015)
Dutch coast, Netherlands	3.00	-	6	(Li et al., 2014)
Belgium	4.00	12	-	(Haerens et al., 2012)
Bordeaux, France	4.10	-	-	(Coco et al., 2014)
Biscarrosse, France	4.00	6	-	(Sénéchal et al., 2015)
Aveiro, Portugal	6.00	-	14	(Ferreira, 2005)
Faro, Portugal	3.00	-	-	(Almeida et al., 2012)
Cadiz, Spain	2.50	12	24	(Puig et al., 2016)
Andalusia, Spain	2.50	12	24	(Rangel Buitrago and Anfuso, 2011b)
Barcelona, Spain	2.20	12	-	(Lin-Ye et al., 2016)
Catalan Sea, Spain	2.00	6	72	(Mendoza et al., 2011)
Gulf of Lions, France	3.00	-	-	(Gervais et al., 2012)
Sardinia, Italy	2.00	6	-	(De Michele et al., 2007)

2.5. Coastal storm impacts

Once a coastal storm is defined according to the thresholds set out in advance, the strength of the storm should be linked to its impacts. This process is very important since the conclusions are useful to understand the storm severity but also to review the efficacy of the thresholds described in Section 2.4. The interconnection of storms and their impacts are regularly studied by researchers, with most of these studies concerning hurricane events, mainly due to the extensive damages they can cause. Collaborative works edited by Stone and Orford (2004), Ciavola and Stive (2012), van Dongeren et al. (2018) constitute a breakthrough in the research field because for the first time they incorporated storm impacts in coastal storm analysis in a coherent manner. Furthermore, the most recent updates regarding this research aspect are contained in the valuable books of Quevauviller (2014), Quevauviller et al. (2017), Ciavola and Coco (2017).

Coastal storm impacts primarily depend on the hydrodynamic regime of each location. However, the topography and the bathymetry also play an important role in the type and severity of the storm impacts. For the robust identification of these impacts, multiple elements have to be analysed. More specifically, information about past events and historical records is very useful. The meteorological and wave climate data, field observations, old maps, aerial photos before and after the storm are also needed to understand the effects on hydrometeorological conditions, sediment transport and infrastructure. The impacts can be also indirectly assessed via the coastal storm characteristics and the observation of other parameters (e.g., total water level, wave set-up). This part of a coastal storm analysis extends beyond the individual research and attempts to engage affected parties in order to accurately record storm impacts and prepare for the future. In this direction, a novel application named CoastSnap is based on public participation since coastal storm impacts are analysed through photos from citizens' smartphones at specific locations worldwide (Splinter et al., 2018; Harley et al., 2019), thus allowing for coasts' monitoring.

Researchers have shown an increased interest in the post-storm conditions, including the geomorphological changes of coastal systems. The impacts of coastal storms and the terrain of each examined location vary significantly around the world. These factors describe each coastal area, hence making each storm analysis unique. The coastal terrain (i.e., the sandy beaches, the barrier islands, the dunes, the cliffs, or the coral reefs)

affects the type and magnitude of the impacts. An overview of relevant investigations on storm impacts that have been performed worldwide is summarised in Table 2.4. Generally, coastal vulnerability depends on the equilibrium of storm frequency and the time which is needed for recovery after the event's occurrence (Coco et al., 2014). The coastal erosion, the changes in beach and dune morphology, the infrastructure (i.e., ports, coastal structures, buildings) damages, the overwash, the overtopping, and the flooding are some among the most significant coastal storm impacts.

Table 2.4

Overview of literature about storm impacts in coastal areas.

Study area	Impact	Terrain	Authors
Bordeaux, France	Erosion	Sandy beach - dunes	(Coco et al., 2014)
Varna, Bulgaria	Coastal morphology	Mixed	(Trifonova et al., 2012)
Belgium	Coastal morphology	Sandy beach	(Haerens et al., 2012)
Cadiz, Spain	Wave runup – erosion	Sandy beach	(Rangel Buitrago and Anfuso, 2011a; Del Río et al., 2012)
KwaZulu-Natal, South Africa	Shoreline recovery	-	(Corbella and Stretch, 2012)
Ria Formosa, Portugal	Overwash - runup - coastal damages - erosion - beach recovery	Sandy beach - barrier island - dunes	(Almeida et al., 2012; Vousdoukas et al., 2012; Plomaritis et al., 2018)
Bay of Biscay, France	Coastal flooding	Mixed	(Breilh et al., 2014; Huguet et al., 2018)
Catalan coast, Spain	Inundation - erosion - sand accumulation – ecosystem	Mixed	(Jiménez et al., 2012; Sanchez-Vidal et al., 2012)
Emilia-Romagna, Italy	Coastal structures - flooding - erosion	Dunes	(Armaroli et al., 2012; Armaroli and Duo, 2018)
Sefton Coast, England	Erosion	Dunes	(Esteves et al., 2012)
Dziwnow, Poland	Erosion	Dunes	(Furmańczyk et al., 2012)
Gulf of Lion, France	Morphological response -infrastructures	Sand barriers - dunes	(Gervais et al., 2012)
Dutch coast, The Netherlands	Erosion – flooding	Dunes	(den Heijer et al., 2012)
California, USA	Flooding - inundation - erosion	Mixed	(Fan et al., 2004; Barnard et al., 2014)
North Carolina, USA	Erosion - coastal structures - infrastructure	Barrier island	(Hondula and Dolan, 2010; Walker and Basco, 2011)
Gulf of Mexico, USA	Coastal erosion - sediment - overwash – flooding	Barrier island	(Stone et al., 2004; Wamsley et al., 2011)
New Jersey, USA	Overwash	Barrier beach	(Donnelly et al., 2004)
Southern Maine, USA	Coastal morphology - erosion	Sandy beach	(Hill et al., 2004)
Gulf of St. Lawrence, Canada	Inundation – erosion	Sandy barriers - dunes	(Forbes et al., 2004)

Table 2.4 *(continue)*

Overview of literature about storm impacts in coastal areas.

Study area	Impact	Terrain	Authors
Atlantic coasts of Europe	Erosion – flooding	-	(Lozano et al., 2004)
Western Ireland	Morphological changes - erosion	Sandy beach - dunes	(Cooper et al., 2004)
Western France	Erosion – accumulation	Beach - barriers	(Regnauld et al., 2004)
Norfolk, UK	Flooding - runup - financial - ecosystem - transport -sediment	Barriers - dunes	(Spencer et al., 2015; Christie et al., 2018; Swindles et al., 2018)
Charlottetown, Canada	Infrastructure	-	(Hartt, 2014)

2.6. Coastal storm classification

The classification of coastal storm events is crucial for coastal communities, as it allows people to compare coastal storms and stay alert. These classifications are useful for transferring this knowledge to everyone who lives and works around the coasts and enable communities to understand the storms' impacts and protect themselves and their properties from future events. Popular classifications such as Saffir-Simpson Scale for hurricanes (Clements and Casani, 2016; NHC, 2019) and the Dolan-Davis Scale (1994,1992) for northeasters have already been used for many years. With some improvements undertaken over the years, these storms scales are presented in Table 2.5 and Table 2.6.

Table 2.5
Dolan-Davis Scale for northeasters (Dolan and Davis, 1992, 1994).

Storm Class	Significant Wave Height [m]	Duration [hr]	Power [m^2hr]
1 Weak	2.0	8	≤71.63
2 Moderate	2.5	19	71.63-163.51
3 Significant	3.2	35	163.51-929.03
4 Severe	5.0	62	929.03-2322.58
5 Extreme	6.8	97	>2322.58

The Saffir-Simpson Scale is the most well-known, and its use is established by important intergovernmental organisations, such as IPCC and WMO. Besides, many other similar classification scales have been proposed to better cover particular marine areas, including the Western Pacific ocean proposed by India's Meteorological Department (WMO, 2015), the Indian ocean proposed by Hong Kong's Observatory (2009), and Australia presented by the Australian Bureau of Meteorology (2020). According to the storm severity, the scales discretise the storm events and briefly describe their characteristics as well as their impacts. This information is quite general and usually covers a wide area (i.e., an entire ocean); however, the use of small-scale classifications could be helpful for a specific location examined (Mendoza et al., 2011; Rangel Buitrago and Anfuso, 2011b; Martzikos et al., 2018).

Table 2.6

Saffir-Simpson Hurricane Scale according to National Hurricane Center (2019) and Clements and Casani (2016).

Category	Sustained Winds	Storm Surge	Anticipated damage
1 Minimal	74-95 mph 64-82 kt 119-153 km/h 33–42 m/s	4-5 ft 1.22-1.52 m	Very dangerous winds will produce some damage. Some coastal road flooding and minor pier damage.
2 Moderate	96-110 mph 83-95 kt 154-177 km/h 43–49 m/s	6-8 ft 1.83-2.13 m	Extremely dangerous winds will cause extensive damage. Coastal and low-lying escape routes flood 2–4 hours before the arrival of the hurricane centre. Small craft in unprotected anchorages breaks moorings.
3 Extensive	111-129 mph 96-112 kt 178-208 km/h 50–58 m/s	9-12 ft 2.74-3.66 m	Devastating damage will occur. Low-lying escape routes may be cut off by rising water 3–5 hours before hurricane centre arrival. Flooding near the coast destroys small structures. Large structures damaged by battering from floating debris. Terrain lower than 5 ft above mean sea level may be flooded inland 8 miles (13 km) or more. Evacuation of low-lying residences within blocks of the shoreline may be required.
4 Extreme	130-156 mph 113-136 kt 209-251 km/h 58–70 m/s	13-18 ft 3.96-5.47 m	Catastrophic damage will occur. Low-lying escape routes may be cut by rising water 3–5 hours before the arrival of the centre of the hurricane. Major damage to lower floors of structures near the shore. Terrain lower than 10 ft above sea level may be flooded, requiring massive evacuation of residential areas as far inland as 6 miles (10 km).
5 Catastrophic	≥157 mph ≥137 kt ≥252 km/h ≥ 70 m/s	>18 ft >5.47 m	Catastrophic damage will occur. Low-lying escape routes cut off by rising water 3–5 hours before hurricane centre arrival. Major damage to lower floors of all structures less than 15 ft above sea level and within 500 yards of the shoreline. Massive evacuation of residential areas on low ground within 5–10 miles (8–16 km) of the shoreline may be required.

The classification is usually developed with clustering analysis, considering the consecutive storm events as adjacent clusters. Clustering techniques seek to identify data patterns and separate them into groups with similar properties. The whole process is based on important storm parameters such as storm hydro-meteorological characteristics (e.g., wind speed, storm surge, central pressure) but also on their societal impacts (i.e., flooding and damages in homes, buildings, trees, roads).

The bulk of research is based on the algorithm of the hierarchical agglomerative clustering (Koutroumbas and Theodoridis, 2009) and especially on Ward's or the average linkage method, by using the euclidean distance and the energy content as a classification variable (Dolan and Davis, 1994, 1992; Mendoza et al., 2011). However, the adjustment of a clustering method according to the location examined is needed. In particular, the different indices, such as the degree of clusters association, the density of clusters and how well-separated they are, or the stability of clustering results, need to be evaluated and fit each location and dataset (Martzikos et al., 2018).

Another use of clustering algorithms results in storms' grouping, highlighting the importance of storm consequences (Besio et al., 2017). A group of storms that occur in a consecutive manner, with a short calm period between them, have similar effects compared to one storm event with high waves and more energy (Ferreira, 2006; Ferreira, 2005). Therefore, the storm grouping has significant impacts on beach response (Coco et al., 2014; Sénéchal et al., 2015, 2017; Godoi et al., 2018), beach erosion (Callaghan et al., 2008; Dissanayake et al., 2015; Ferreira, 2005; Karunarathna et al., 2014; Vousdoukas et al., 2012) and coastal flooding (Mendoza et al., 2013). Most recent studies combine cluster analysis and storm grouping with copula theory, improving, in this way, both storm (Lin-Ye et al., 2018) and coastal flooding (Pappadà et al., 2018) modelling.

2.7. Societal aspects of coastal storms

Finally, the key research issues of coastal storm analysis include the social effects of coastal storms or, in other words, how a coastal population is affected by such extreme events. Besides the mathematical representation of coastal storms, coastal populations actually organise their lives in coastal areas. Therefore, the impacts of coastal storms raised research attention early-on, since they affect human life and well-being.

Researchers try to analyse the social dimensions of this problem and provide solutions that improve social coherence. Further to the humans living close to the shoreline, coastal flora and fauna are also negatively affected by coastal storms (Baring et al., 2014; Maslo et al., 2019; Patrick et al., 2020).

Nowadays, communicating scientific issues to a broad audience is necessary. The rapid increase in published information about climate change has played a significant role in this shift. The most recent special reports of IPCC for "Global Warming of 1.5 °C" and about "The Ocean and Cryosphere in a Changing Climate" and especially the chapters by Hoegh-Gulbergh et al. (2018) and Oppenheimer et al. (2019), and the Fourth National Climate Assessment of U.S. Global Change Research Program (2018) are typical examples of science communication about the effects of climate change, the risk of extreme events and social vulnerability.

Over the last decade, there has also been a surge of interest for coastal communities outlined in many research projects. For instance, MICORE (Ciavola et al., 2011b), THESEUS (Zanuttigh, 2011), PEARL (Karavokiros et al., 2016) and RISC-KIT (van Dongeren et al., 2018) are some of the research projects in Europe which addressed and covered the societal aspect of hydrometeorological hazards and coastal risk management. In their attempt to protect the coasts and prepare the coastal communities from storms and other extreme events, they provided a scientific basis in this field, achieving global awareness and paving the way inter alia for a more detailed and multidisciplinary socially-oriented analysis in the future.

A positive impact of research in this field is the innovative environmental ideas to protect coasts from the threat of future storms or to transit the wave power to renewable energy. The reefs, mangroves, salt marshes and generally the coastal ecosystems that are severely affected by storms (Bazzichetto et al., 2020) can also contribute to the coastal defence and mitigate the storm impacts, acting as a buffer zone for a storm (Spalding et al., 2014; Gracia et al., 2018; Armitage et al., 2020; Hanley et al., 2020). On the other hand, the hybrid design of port and coastal structures has now gained ground, taking advantage of the storm strength. Many sophisticated systems that were proposed to be placed on the coastal structures can harness the wave or tidal power and convert it into energy (mostly electricity) (Roberts et al., 2016; Cascajo et al., 2019; Rosa-Santos et al., 2019; Vicinanza et al., 2019).

Living along the shoreline implies the constant threat of coastal storms (National Research Council, 2014; Bilkovic et al., 2017). Therefore, the acquisition of basic knowledge about the storms and how to be prepared is necessary (Petterson et al., 2006; Picou and Marshall, 2007; Shepherd and Knutson, 2007; Burton, 2010) to ensure health and well-being. The relationship between climate and society, as well as the social dimensions of climate change, should be the core of integrated coastal storm analysis (Nicholls et al., 2007; Stehr and Storch, 2009; Glavovic and Smith, 2014; Ranasinghe, 2016; Leal Filho, 2018). A careful study of storm severity is needed for acquiring useful information about the present and past activity of coastal storms. Risk assessments of storms in coastal zones allow for a better understanding of these extreme events and their impacts, but also of the size of an upcoming hazard, thus preparing appropriately the coastal communities (Hissel et al., 2014; Rangel Buitrago and Anfuso, 2015; Cuite et al., 2017; Ding, 2017; Quevauviller et al., 2017; Erikson et al., 2018; Garnier et al., 2018).

The research related to storm analysis is fundamental for decision making including: planning of coastal adaptation strategies (NOAA, 2010; Bathi and Das, 2016; Beavers et al., 2016; Cinner et al., 2018; Fouqueray et al., 2018; Leal Filho, 2018), infrastructure design, port resilience (Esteban et al., 2016; Smythe, 2016; Becker et al., 2018) and consequently cities' resilience (Glavovic and Smith, 2014; Mega, 2016; Balomenos and Padgett, 2018; Powell et al., 2019). The key in such analysis is to delve into the real needs of people living in coastal areas, and engage them through public discussions and interviews (Costas et al., 2015; Vasseur et al., 2018).

Chapter 3

Methodology for coastal storm analysis & modelling

This chapter contains the methodology for the analysis of coastal storms and their modelling through copulas. The definition of coastal storms and basic concepts regarding their identification arise from the combination of existed knowledge. The methodology is gathered and enriched by investigating the important thresholds, and as a general framework, it is presented to the reader.

In the same vein, the coastal storm characteristics such as the wave direction, the wave period, and the energy during a coastal storm are investigated. For the energy estimation, a correction is proposed, also taking into account the wave energy flux during an event, the coastal storm energy, and the shape of coastal storms.

The basic concepts in copula theory and the characteristics of bivariate copulas are gathered from introductory books in this field. The innovative aspects in this chapter include more complex cases and the extension of these concepts to higher dimensions. Hence, the important joint and conditional probabilities are expressed through copulas to more than two variables. The construction of a five-dimensional C-Vine is described. The methodology of De Michele et al. (2007) for sea storm simulation is extended explicitly to five dimensions and an algorithm is developed and consequently is compared to the algorithms of Aas et al. (2009) and Stöber and Czado (2017) that also extended to five dimensions. Similarly, the one to three-dimensional return periods in literature are expressed through copulas, and they are extended to four and five dimensions.

The Mediterranean coastal storms are used as a case study to both validate the proposed methodology and analyse coastal storms in the real world. Data from wave recordings from buoys at 30 locations over the Mediterranean Sea, in Greece, Italy, France and Spain are analysed. The data were obtained by the databases of Puertos del Estado (www.puertos.es), Copernicus (www.copernicus.eu) and EMODnet (www.emodnet.eu), covering in general, a time period since the 1980s. The 30 locations were selected based on the buoys' distance from the coast and were a selection of the closest available buoys on the European coasts, in order to analyse the coastal storms.

3.1. Coastal storm definition and identification[2]

Climate change and related extreme events causing infrastructure damages and resulting in human losses have turned coastal communities and consequently coastal storms into the centre of attention over the past decades. Many researchers focus on coastal storms to study their impacts, such as coastal flooding, beach erosion, and damages on ports, and they try to learn more about their severity, as presented in Section 2.1. The management of such events, the preparedness, and an informed coastal community, are of great importance and more urgent, especially nowadays in a changing climate.

In this context, the latest reports of the Intergovernmental Panel on Climate Change (IPCC, 2018, 2019), the United Nations Framework Convention on Climate Change meetings, such as the well-known "Paris Agreement" (UNFCC, 2016) and the Fourth National Climate Assessment of U.S. Global Change Research Program (USGCRP, 2018), give an incredible boost to the field of science communication regarding the climate change. This effort is enhanced by many research projects which are focused on the hazards and the risk management of extreme events in coastal communities. For Europe, the progress and the deliverables of these projects stand as a significant source of information for any researcher (Ciavola et al., 2011b; Zanuttigh, 2011; Van Dongeren et al., 2014; Karavokiros et al., 2016).

On the other hand, many extreme events hit coastal communities causing losses of billions of euros in the last two decades. Hurricane Sandy (22 October - 2 November 2012) (Rosenzweig and Solecki, 2014; Binder et al., 2015), Cyclone Xynthia (27 - 28 February 2010) (Bertin et al., 2012; Ferreira et al., 2017), Hurricane Katrina (23-31

[2] A part of this chapter has been published in Martzikos et al., (2021b)

August 2005) (Kates et al., 2006; Irish et al., 2008) are some of the most recent and among the costliest and deadliest storms in human history, which have changed the way the humans act, protect and prepare themselves within an everchanging environment.

Following the definitions of Harley (2017) and Ciavola et al. (2014), in this thesis the coastal storm is defined as "any meteorologically-induced disturbed sea state that causes changes and damages to the coastal zones, impinging the coastal morphology and the infrastructure".

For the description of coastal storms, their thresholds and their characteristics are required. As characteristics of coastal storms usually are taking into account the significant wave height (H), the duration (D), the calm period (I), the main direction (D_{ir}), the energy (E), as well as their mean and maximum values of them (Dissanayake et al., 2015; Lin-Ye et al., 2016). The significant wave height should exceed a certain threshold and remain over this for a time period (De Michele et al., 2007; Li et al., 2014). The minimum duration is also needed to focus only on the events that last longer. According to Corbella and Stretch (2013) and De Michele et al. (2007), the calm period (also known as inter-arrival time) separates the consecutive coastal storms describing the time between the start and the end of the upcoming and the previous event, respectively. If the calm period is too short, then the neighbouring storm events could be considered one, prolonging in this way the storm event and consequently extending the duration. For example, following the work of Wahl et al. (2016) and Li et al. (2014) in Figure 3.1, the consecutive events over the threshold have duration D_1, D_3 and D_5. The first two of them could be considered as one storm event, due to their short calm period (D_2), with final storm duration $D = t_4 - t_1$. The next event with duration D_5 is independent of the previous, due to the long calm period (D_4), but it is not a storm event because of its short duration (D_5).

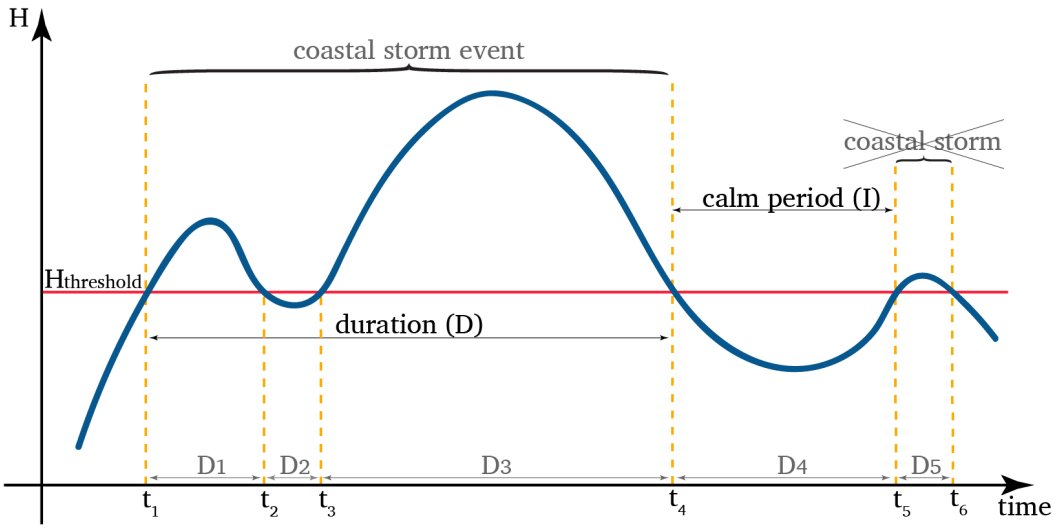

Figure 3.1. Definition of the coastal storm event and the description of important parameters.

The identification of coastal storms, the frequency of their occurrence and their severity require a large dataset of wave climate. However, the time series of coastal storm characteristics acquired from buoys measurements are rarely used due to their spatial availability and limitation in temporal data coverage. The majority of the wave data are not available before 1978 (Caires and Sterl, 2005). Even nowadays, data are only available for specific locations and not everywhere. According to the interactive map of EMODnet - the European marine observation and data network - (http://emodnet-physics.eu/Map/), in the Mediterranean Sea, Spain and France have a dense network of buoys to record the wave climate of their seas, in contrast with the other European countries, which have very few (i.e., Greece, Italy, Bulgaria and Romania) and other countries that have none at all. However, the buoys are frequently out of order, or their position is changing over the years. The available datasets are usually non-continuous and with many gaps. Hence, a lot of research is based on model and satellite data before or after a reanalysis (Kistler et al., 2001; Dee et al., 2011; Sartini et al., 2017), which are operationally more efficient and cost-effective.

Significant research has been conducted for the wave climate and storm events along European coasts. Usually, the conducted research is not limited to the Mediterranean Sea (Almeida et al., 2011; Ciavola et al., 2011b), it is based on model data (Lionello et al., 2008, 2012; Androulidakis et al., 2015; Vousdoukas et al., 2016) and often examines storms from the climatology viewpoint, investigating the characteristics and the frequency of occurrence for cyclones or medicanes in the Mediterranean region

(Cavicchia et al., 2014a; Emanuel, 2005; González-Alemán et al., 2019; Lionello et al., 2016, 2006).

The Extreme Value Theory (EVT) is adopted to analyse coastal storms as extreme hydrometeorological events. The EVT is widespread in the last decades and has become increasingly popular through Coles (2001), describing the theoretical background of this field thoroughly. Since then, numerous works and applications in EVT have a high impact on coastal engineering (Caires and Sterl, 2005; Méndez et al., 2006; Menéndez et al., 2009; Ruggiero et al., 2010; Mazas and Hamm, 2011; Vinoth and Young, 2011). The Block Maxima (BM) and the Peak Over Threshold (POT) methods are both the fundamental approaches in EVT but differ in their application (Jarušková and Hanek, 2006; Arns et al., 2013; Bezak et al., 2014). In brief, the BM method is based on the analysis of maximum values of a dataset or within a specific block, and alternatively, BM takes the r-largest order statistics (Coles, 2001; Dey and Yan, 2015). Therefore, the BM is not recommended when the reference period is only a few years or decades (Caires and Sterl, 2005). The POT method analyses time series which are extracted from the initial dataset when they exceed a specific threshold (Ferreira and Guedes Soares, 1998; Coles, 2001).

As a follow-up of previous works, the methodology of this thesis for coastal storm analysis is primarily based on the input data. It incorporates the coastal storm definition, the identification, the analysis of their characteristics and the storm activity (Fig. 3.2.). For the definition of coastal storms, the closest buoys from the coast are taken discarding the events with a measurement gap greater than 18 hours (at the phase of data cleaning).

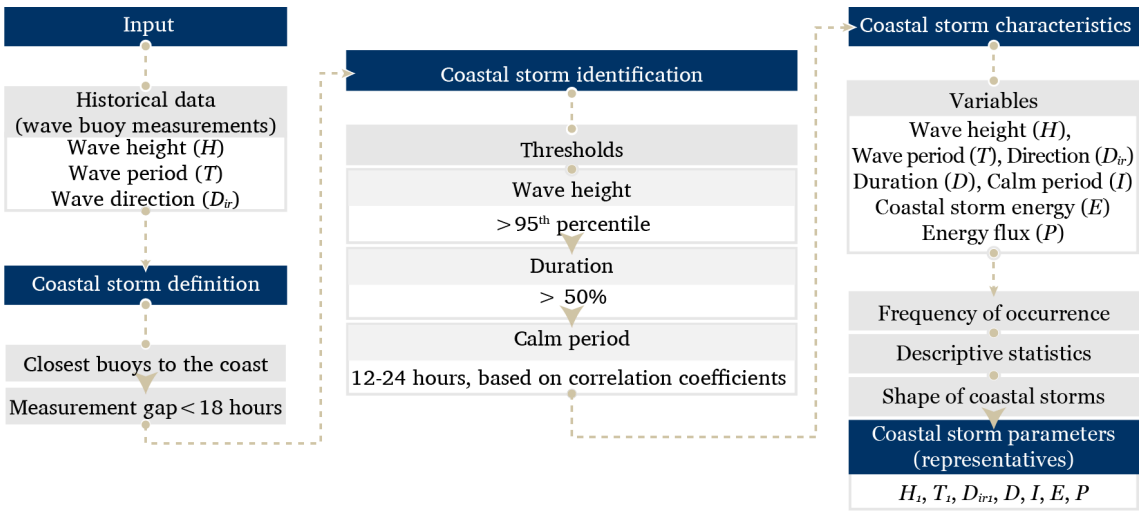

Figure 3.2. Description of the methodology for coastal storm identification and analysis.

The coastal storms are identified by applying the EVT to define the H threshold to extract the most extreme values, and consequently, the data are filtered by the thresholds of duration and calm period. The identification is conducted through the thresholds of the significant wave height, the duration, and the calm period in each location. The coastal storm thresholds are site-specific and they depend on the synoptic systems, the bathymetry, the local characteristics, and the exposure of a location to the winds and the big waves (Harley, 2017). In literature, storm thresholds are defined in different ways but mainly depend on available data.

3.1.1. Significant wave height threshold

The threshold of significant wave height H_{thr} could be selected by a) defining a specific value as representative for a specific location (Corbella and Stretch, 2012), b) following the stability check for the parameters of extreme value distribution as it was described by Coles (2001), c) using a high percentile of the data set, usually over 90%, to describe and analyse only the most extreme events (Rangel Buitrago and Anfuso, 2011b; Masselink et al., 2014; Tsoukala et al., 2016; Davies et al., 2017; Duo et al., 2020), or d) taking a linear equation between the mean value and the standard deviation of an important parameter. The last methodology was proposed by Yevjevich (1967) for the drought analysis but is also used similarly by Almeida et al. (2011) for the storms.

Given the short reference period of data, in this thesis, the significant wave height threshold H_{thr} can be defined by applying the stability check (b) or by taking a high threshold following the POT method (c). For the stability check, if the significant wave height of a dataset follows Weibull distribution, then the EVT implies that generalised Pareto distribution adequately approaches the upper tail above a threshold. Thus, after fitting a generalised Pareto for different thresholds (Gilleland and Katz, 2016), the parameters of scale (σ^*) and shape (ξ) are estimated to detect if a further increase does not affect their values and hence to define the H_{thr}. The H_{thr} can also be defined as the 95^{th} percentile of the significant wave height at each location, examining the grouped exceedances over the threshold as coastal storm events.

3.1.2. Duration and calm period thresholds

Investigating the storm duration and calm period for each country, both thresholds of the minimum duration (D_{thr}) and the calm period (I_{thr}) of consecutive coastal storms are defined based on the range of these parameters. The storm duration is defined as the time period in which the significant wave height remains over the threshold (Boccotti, 2000). Through boxplots and trying to analyse the most severe events, the minimum duration (D_{thr}) is considered appropriate to be higher than the median, investigating the longest events (upper 50% in storm duration), but without exceeding the mean value. Consequently, the events with storm duration shorter than the D_{thr} are ignored.

A sequence of storm events causes extensive damages to coastal zones, affecting the coastal morphology and could be more destructive than isolated events in many cases (Dissanayake et al., 2015; Ferreira, 2005; Sénéchal et al., 2017). Coastal storms with a long calm period might occur in different seasons, and they are certainly not related to each other. The short calm period means more dependent events that usually could be unified. Therefore, in this thesis, the range of the calm period is first investigated, and subsequently, focuses only on the closest consecutive events that have a calm period shorter than three months (approximately 2190 hours).

Two coastal storm events are independent from a meteorological perspective if they are developed in different synoptic systems. On the other hand, the consecutive coastal storms which belong to the same synoptic system could have similar characteristics and be dependent. It is entirely rational for the dependent events to belong to the same weather system, but it is conceivable that this may also happen in different systems. The threshold of calm period I_{thr} can be determined better in a physical way, as the mean calm period between consecutive synoptic systems (tropical or extratropical cyclones). The concurrent weather satellite images and weather maps could be beneficial, but all this information is difficult to get up to now. Corbella et al. (2015) link the atmospheric circulation patterns with the spectral characteristics of ocean waves, trying to improve the identification of statistically independent storm events. In extreme value analysis of rainfall and flooding events, the independence of consecutive events is ensured by using the minimum inter-event period (Jean et al., 2018; Freitas et al., 2020). Similarly, the independence of coastal storms is usually approached by taking a fixed value of the calm period (e.g., 12, 24, 36 hours) between coastal storms.

Here, the independence of coastal storms means that the consecutive events are separated by a sufficient calm period without having similar characteristics. The definition of calm period threshold I_{thr} is approached by estimating the correlation coefficients based on available wave measurements. More specifically, the coefficients of Spearman's rho (ρ), Kendall's tau (τ), and Pearson's (*r*) are estimated, trying to understand the behaviour of *H* or the *T* within consecutive coastal storms.

The Spearman's rho (ρ), Kendall's tau (τ), and Pearson's (*r*) coefficients measure the association strength between two numeric variables. The three coefficients are usually used for the independence of different variables (Kereszturi et al., 2016; Williams et al., 2016) and the correlation between different samples of the same variable. Two samples are strongly associated when ρ, τ, *and r* values are close to 1 or -1. On the contrary, both samples are considered independent when the coefficients are close to zero. The correlation coefficients vary in their effectiveness, and usually one of them is more appropriate than the other (Ferguson et al., 2000); thus, all of them are estimated to get a better overview.

The Spearman's rho (ρ) is estimated based on Eq. 3.1 (Hollander et al., 2015) when the samples have no ties. The R_i and S_i are the ranks of X_i and Y_i variables (when both samples are in ascending order). Here, X_i and Y_i represent the *H* or *T* of consecutive coastal storm events.

$$\rho = 1 - \frac{6\sum_{i=1}^{n}(S_i - R_i)^2}{n\left(n^2 - 1\right)}. \tag{3.1}$$

The Kendall's tau (τ) statistic, or the Kendall rank correlation coefficient, is used primarily when the data do not necessarily come from a bivariate normal distribution. The estimation is done according to Eqs. 3.2 and 3.3 (Hollander et al., 2015) for two different samples, with the same length *n* and without ties.

$$\tau = \frac{2\sum_{i=1}^{n-1}\sum_{j=i+1}^{n} Q\left((X_i, Y_i),(X_j, Y_j)\right)}{n(n-1)}, \tag{3.2}$$

$$Q\left((X_i, Y_i),(X_j, Y_j)\right) = \begin{cases} 1, \text{ if } (Y_j - Y_i)(X_j - X_i) > 0 \\ -1, \text{ if } (Y_j - Y_i)(X_j - X_i) > 0 \end{cases}, \text{ for } 1 \le i \le j \le n. \tag{3.3}$$

The Pearson's (*r*) statistic is given by Eq. 3.4 for two samples or variables $X=(X_1,..,X_n)$, $Y=(Y_1,..,Y_n)$, with mean values $\overline{X}, \overline{Y}$.

$$r = \frac{\sum_{i=1}^{n}\left(X_i - \overline{X}\right)\left(Y_i - \overline{Y}\right)}{\sqrt{\sum_{i=1}^{n}\left(X_i - \overline{X}\right)^2 \sum_{i=1}^{n}\left(Y_i - \overline{Y}\right)^2}}. \tag{3.4}$$

The coefficients ρ, τ, and r are estimated for H and T for all the consecutive events at each location, considering only the values which are close to zero. It is optimal to analyse the longest coastal storms, working with a lot of data, but coastal storms often consist of short length time series. For the best performance, a small extension is accomplished whenever an event consists of less than ten values by taking some additional values of H or T before the first event and after the end of the second event.

In literature, the calm period threshold usually ranges around 24 hours. Hence the analysis is used to provide more information for selecting the optimal threshold. Finally, the calm period threshold is set as the minimum calm period, which ensures a weak correlation of H samples, based on ρ, τ, and r, for the most consecutive coastal storms (and similarly for T). The results are classified by the calm period into 15 classes, from 12 to 96 hours. The representative of each class is the upper boundary and is set as a multiple of 6, dividing a day into quartiles. However, the first class is 12 hours, and all the previous classes are merged into one, setting a half-day milestone for the calm period.

The general framework of this methodology for thresholds' definition is very common in literature (Corbella and Stretch, 2013; Bernardara et al., 2014; Lin-Ye et al., 2016; Lira-Loarca et al., 2020), as also described in Section 2.4, but differs in the way the thresholds are set. Contrary to previous works, where the thresholds are defined based on literature (De Michele et al., 2007; Li et al., 2014, 2018) or without describing the following procedure, in this thesis the thresholds are selected after investigation.

3.2. Coastal storm characteristics

After the storm identification, the storm characteristics are estimated to describe coastal storm activity. Hence the frequency of occurrence of coastal storms, the significant wave height (H) and the spectral peak wave period (T), or simply wave height and wave period during a coastal storm, as well as the duration (D), the direction (D_{ir}), the calm period (I) and the coastal storm severity index through the energy (E) and the energy

flux (*P*) of each event, are estimated. In addition, the triangular shape of a coastal storm is also investigated.

The wave height (*H*) and the wave period (*T*) during a coastal storm are derived from the respective variables' time series when the previously mentioned thresholds H_{thr}, D_{thr}, I_{thr} (Sections 3.1.1 and 3.1.2) are applied. The duration (*D*), the direction (D_{ir}), the calm period (*I*) are unique values for each coastal storm and they are estimated at the identification stage (Section 3.1) following Figure 3.1.

The coastal storm severity is approached by the estimation of the energy (*E*) and the energy flux (*P*). The coastal storm energy (*E*) is estimated for each event by using Eq. 3.5, as it was proposed by Dolan and Davis (1992), where t_1 and t_2 denote the beginning and the end of an event, respectively.

$$E = \int_{t_1}^{t_2} H^2 dt \,. \tag{3.5}$$

For the energy estimation, the coastal storm duration and the sampling interval may need to be corrected. Whenever the first value of *H* during a coastal storm is not equal to the threshold, a correction is applied to estimate the duration. More specifically, the properties of "similar triangles" in Geometry are used to approximate the storm duration better, considering a more linear shape of a storm. Following this simplified version, the *H* threshold is set at the first and the last value for each storm event, extending the duration by adding a short time period s_4 before and after the initially estimated duration, as described in Figure 3.3(a). Consequently, the corrected duration is considered as the storm duration (*D*). Also, when the sampling interval (*dt*) is non-constant during a coastal storm, the *H* values are distributed uniformly according to the duration (Fig. 3.3b), and hence the storm energy is estimated based on a new average time step (*dt*).

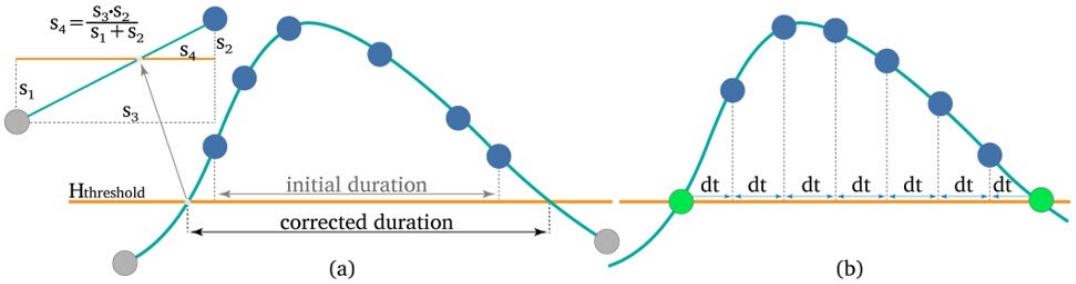

Figure 3.3. (a) The correction of storm duration when the first and the last value of H are not equal to the threshold, extending by s_4 the storm duration, according to properties of similar triangles. (b) The values of H are distributed uniformly by dt when the sampling interval (dt) is not constant during a coastal storm.

The coastal storms affect sediment transport and can consequently cause beach erosion. Many researchers widely use the wave energy flux (P) (Boccotti, 2015) as the most accurate indicator for understanding these impacts (Ruiz de Alegria-Arzaburu and Masselink, 2010; Harley et al., 2017; Molina et al., 2019; Wang et al., 2020). The energy flux can be estimated by Eq. 3.6, as follows:

$$P = E_u \cdot C_g , \tag{3.6}$$

where C_g denotes the group velocity that includes other wave parameters such as the wave period, the wave length and depends on the water depth (i.e., shallow, intermediate, deep waters) and E_u is the wave energy (E_u) per unit surface area that can be estimated by Eq. 3.7:

$$E_u = \frac{1}{8} \rho \cdot g \cdot H^2 , \tag{3.7}$$

where g is the gravitational acceleration and ρ denotes the water density. The energy flux is estimated at each hour of storm duration, and then the coastal storm energy flux is calculated by adding the hourly values. Both approaches of coastal storm severity index (Eqs. 3.5-3.6) are investigated further based on their relationship to the wave period and the direction.

The shape of coastal storms is another important characteristic that is usually analysed. The shape of coastal storms is used for their graphical representation and the energy estimation (Dissanayake et al., 2015; Lin-Ye et al., 2016). The shape of coastal

storms is useful for simplifying and constructing synthetic storms by considering an equivalent storm model. The equivalent triangular storm model (ETS) or other storm models (De Michele et al., 2007; Corbella and Stretch, 2012a, 2013; Martín-Hidalgo et al., 2014; Boccotti, 2015; Martín Soldevilla et al., 2015; Laface and Arena, 2016; Duo et al., 2020; Marzeddu et al., 2020) intend to simulate an actual storm event considering an equivalent (synthetic) storm event with a similar potential. The proposed storm shapes are mostly triangular, trapezoid or parabolic and their efficiency is frequently investigated (Martín-Hidalgo et al., 2014; Martín Soldevilla et al., 2015; Duo et al., 2020; Marzeddu et al., 2020). The triangles are the most common due to their simplicity, and they are usually considered scalene or isosceles. The storms in the Mediterranean Sea are also considered sharp while they grow until reaching their peak and milder when they decay (Lin-Ye et al., 2016). Regarding the shape of coastal storms, the samples of 4008 detected coastal storms are used, with the intent to find out if the triangular shape is the most dominant for real storms. Secondly, assuming that a triangle describes better the shape of a coastal storm, both isosceles and scalene are investigated about their efficiency in real-world coastal storms.

3.3. Coastal storm parameters

After identifying the coastal storms and investigating the coastal storm characteristics, information about the start, the end date, and the variables H, T, D, I, E, P, D_{ir} are used to describe each event. The variables D, I, E, P, are described by unique values for a coastal storm and they are also used as coastal storms parameters in the following analysis. Regarding the variables H, T, D_{ir}, the representative values H_1, T_1, D_{ir1} should be defined in order to describe sufficiently a coastal storm.

In literature, the maximum value of wave height (H) during a coastal storm is preferred as representative rather than the average. However, this value corresponds to the peak of a coastal storm. To describe the whole event, the average wave height H_1 within a coastal storm is selected as a coastal storm parameter. Furthermore, the highest values of H are included while estimating the wave energy to avoid any underestimation of extreme events.

The coastal storm direction and wave period representatives, D_{ir1}, T_1, are respectively estimated through the standard deviation and the coefficient of variation (CV_T) (Eq. 3.8),

$$CV = \frac{s}{\bar{x}}. \tag{3.8}$$

Both statistics are used to measure the dispersion of the wave period and direction. More specifically, CV_T shows the homogeneity of wave period describing how normally is spread around the mean during a coastal storm. It should be noted that the circular standard deviation (Jammalamadaka and SenGupta, 2001) has been used for the direction. CV_T is estimated for all the coastal storms, dividing for each variable the standard deviation (s) with the mean value ($\bar{x}$).

The seven parameters H_1, T_1, D, I, E, P, D_{ir1} will be mentioned below as coastal storm parameters without being confused with the associated parameters of distributions in statistics and probability theory.

3.4. Coastal storm modelling through copulas

Copula: noun /ˈkɒp.jə.lə/

a word that joins or couples two different things

3.4.1. Introduction to copula theory

The copulas and their theory have been established in the field of statistics and have been utilized frequently in the last two decades for the analysis of multivariate extreme events. The copulas were introduced by Sklar (1959) and, after many years, were examined thoroughly by Joe (1997) and Nelsen (2006). According to Nelsen (2006), copulas are a) functions that join the multivariate distribution functions of two or more variables to their one-dimensional marginal distribution functions, but also b) stand as multivariate distributions. Their advantage is detected in their competence to describe and model the dependence of involved variables. The use of copulas prevails over joint distributions in multivariate analysis when the variables are not independent, are not normally distributed, and their marginal distributions are different (Nelsen, 2006; Salvadori et al., 2007). Thus, over the years in coastal engineering research, the joint probabilities of wave parameters (Longuet-Higgins, 1983; Memos, 1994; Ferreira and Guedes Soares, 2002) are replaced by bivariate copulas (Dong et al., 2015; Galiatsatou and Prinos, 2016; Jäger and Nápoles, 2017; Mazas and Hamm, 2017; Galiatsatou et al., 2019; Jäger et al., 2019) and then by multivariate copulas which allow us to study multivariate events such as storms and coastal storms (De Michele et al., 2007; Corbella

and Stretch, 2013; Li et al., 2014, 2018; Wahl et al., 2016; Lin-Ye et al., 2020; Nadal-Caraballo et al., 2020), and finally to estimate their return periods and better approach the risk analysis (Salvadori et al., 2014, 2015).

Many books set the scientific background of copula theory, providing the basic knowledge and fundamental concepts (Joe, 2014; Durante and Sempi, 2015; Mai and Scherer, 2017; Úbeda Flores et al., 2017) for their application in finance (Mai and Scherer, 2014; Ruppert and Matteson, 2015; Cherubini et al., 2016), and their contribution to engineering concerning the analysis of the extreme events (Salvadori et al., 2007; Salvadori and De Michele, 2013; Chen and Guo, 2019; Zhang and Singh, 2019b).

The different copula families and the construction methods of a copula, especially for dimensions higher than two, are the most attractive topics in this field. The class of vine copulas is indicated for high-dimensional data, enabling an easy-way extension of their construction based on bivariate copulas and the univariate marginal distributions. The construction of Vine copula is based on the decomposition of multivariate probability density using the bivariate copulas. The dependence of the associated variables is the decisive factor in this structure which is described through a nested set of trees. The selection of the best bivariate copula for each pair of variables and their combination for a higher dimension copula make vine copulas quite flexible. This kind of construction is known as “pair copula construction” and became extremely popular after the works of De Michele et al. (2007) and Aas et al. (2009) in the field of coastal engineering and economics, respectively. The books of Kurowicka and Joe (2010) and Czado (2019) are devoted entirely to vine copulas. Valuable information can also be found in specific chapters of the books of Joe (2014), Mai and Scherer (2017), and Zhang and Singh (2019b). A practical guide of copulas and many examples of their use in a programming environment, especially in R, can be found in the books of Ruppert and Matteson (2015), Hofert et al. (2018), and Czado (2019).

The application of copula theory to coastal storms is described by presenting first the theoretical background of copulas. Therefore, the basic concepts in probability theory, the copula definition, the basic concepts in copula theory, the copula construction, the copula families, and the estimation of important probabilities are described below.

Consequently, the best bivariate copula families are investigated for the dependence of significant wave height and the wave period during coastal storms. The estimation of important probabilities and the five-dimensional copulas are used for the coastal storm simulation and the estimation of return periods. These topics have attracted the scientific community's attention in the past, but rarely in combination and mainly for few variables. In addition, the effectiveness of these approaches will be evaluated by a dataset of Mediterranean coastal storms for the bivariate case and consequently to a specific location for the case of five dimensions.

Basic concepts in probability theory

To better understand the copulas, it is appropriate to provide a concise description of the most fundamental concepts in Probability theory.

Considering $X_1,X_2,\ldots,X_d$ as d continuous random variables or as a d-dimensional continuous random vector $(X_1,X_2,\ldots,X_d)$, the **probability density function** f of X_1 (pdf) satisfies the following properties:

$$\int_{-\infty}^{\infty} f(x)dx = 1,\ \ P(a \le X_1 \le b) = \int_{a}^{b} f(x)dx, \text{ and } f(x) \ge 0\,. \tag{3.9}$$

The **cumulative distribution function** F of X_1 (cdf)**,** denotes the probability of X_1 to be less than or equal to a certain value x_1.

$$F(x_1) = P(X_1 \le x_1) = \int_{-\infty}^{x_1} f(x)dx\,. \tag{3.10}$$

The **joint cumulative distribution function** F of X_1 and X_2 (jcdf) is defined by:

$$F(x_1,x_2)\ \ or\ \ F_{12}(x_1,x_2) = P(X_1 \le x_1, X_2 \le x_2) = \int_{-\infty}^{x_2}\int_{-\infty}^{x_1} f(x,y)dx\,dy\,. \tag{3.11}$$

And similarly for higher dimensions, when $x_1,x_2,\ldots,x_d$ are specific values of $X_1,X_2,\ldots,X_d$ respectively, the jcdf is given by:

$$F(x_1,x_2,\ldots,x_d) = P(X_1 \le x_1, X_2 \le x_2,\ldots,X_d \le x_d) = \int_{-\infty}^{x_1}\ldots\int_{-\infty}^{x_d} f(x,y,\ldots,z)dx\,dy\ldots dz\,. \tag{3.12}$$

The **joint density function** f of X_1 and X_2 can be expressed as:

$$f(x_1,x_2)\ or\ f_{12}(x_1,x_2) = \frac{\partial^2 F_{12}(x_1,x_2)}{\partial x_1 \partial x_2}\ . \tag{3.13}$$

And similarly, for higher dimensions

$$f\left(x_1, x_2 ..., x_d\right) = \frac{\partial^d F\left(x_1, x_2, ..., x_d\right)}{\partial x_1 \partial x_2 ... \partial x_d} \quad . \tag{3.14}$$

Based on the joint functions, the univariate pdf and cdf stated as marginal" pdf and cdf. The **marginal distribution function** F_1 of X_1 is defined as follows:

$$F_1\left(x_1\right) = F\left(x_1, \infty\right) = P\left(X_1 \le x_1, X_2 \le \infty\right) = \int_{-\infty}^{x_1} \int_{-\infty}^{\infty} f_{12}\left(x, y\right) dx\, dy = P\left(X_1 \le x_1\right). \tag{3.15}$$

The **marginal density function** f_1 of X_1 is given by:

$$f_1\left(x\right) = \frac{dF_1\left(x\right)}{dx} = \int_{-\infty}^{\infty} f_{12}\left(x, y\right) dy \, . \tag{3.16}$$

The **conditional probability density function** $f_{1|2}$ of X_1 given that $X_2 = x_2$ is defined as follows:

$$f_{1|2}\left(x_1 \middle| x_2\right) = \frac{f_{12}\left(x_1, x_2\right)}{f_2\left(x_2\right)}. \tag{3.17}$$

The **conditional probability distribution function** $F_{1|2}$ of X_1 given that $X_2 = x_2$ is defined as follows:

$$F_{1|2}\left(x_1 \middle| x_2\right) = P\left(X_2 \le x_1 \middle| X_2 = x_2\right) = \frac{\frac{\partial}{\partial x_2} F_{12}\left(x_1, x_2\right)}{f_2\left(x_2\right)}. \tag{3.18}$$

The **survival function** $\overline{F}$ of X_1 (or marginal survival function) denotes the probability of X_1 to be greater than a certain value x_1.

$$\overline{F}\left(x_1\right) = P\left(X_1 > x_1\right) = 1 - F_1\left(x_1\right). \tag{3.19}$$

And for higher dimensions, is defined as follows:

$$\overline{F}\left(x_1, x_2, ..., x_n\right) = P\left(X_1 > x_1, X_2 > x_2, ..., X_d > x_d\right) = 1 - F\left(x_1, x_2, ..., x_d\right). \tag{3.20}$$

Table 3.1

Important symbols and abbreviations of basic concepts in Probability theory for one and two continuous random variables.

	Density Function	Distribution Function
Marginal	f_1	$F_1 = P\left(X_1 \le x_1\right)$
Survival	-	$\overline{F_1} = P\left(X_1 > x_1\right)$
Joint	f_{12}	$F_{12} = P\left(X_1 \le x_1, X_2 \le x_2\right)$ *or "jcdf"*
Conditional	$f_{1\|2}$	$F_{1\|2} = P\left(X_1 \le x_1 \middle\| X_2 = x_2\right)$

Copula Definition

A copula can be defined as a multivariate distribution function with uniform marginal distribution functions or in a different aspect as the dependence structure between random variables. However, their meaning becomes more accessible to everyone through Sklar's theorem (Sklar, 1959), which introduced and established these functions in the scientific community. The coupling of univariate marginal distributions with the joint distribution function justifies the selection of the term "copula" (Eq. 3.21). The proof of this theorem and many other aspects of the theoretical background of copulas can be found in Nelsen (2006) and Joe (2014).

Sklar's theorem. Let X_1, X_2 be random continuous variables with univariate marginal distribution functions F_1, F_2 and the joint distribution function $F_{12}\left(x_1,x_2\right)$ for all $x_1,x_2 \in \overline{\mathbb{R}} = \left[-\infty,+\infty\right]$. Then there exists a copula C_{12}, such that

$$F_{12}\left(x_1,x_2\right) = C_{12}\left(F_1\left(x_1\right),F_2\left(x_2\right)\right) \tag{3.21}$$

When F_1 and F_2 are continuous then the copula C_{12} is unique. On the contrary, if F_1 and F_2 are distribution functions of X_1, X_2 and C_{12} a copula, then the joint distribution function F_{12} with marginals F_1 and F_2 is given by the Eq. 3.21.

Standardisation of data is needed using the probability integral transformation to understand the dependence of different variables in a dataset and compare them properly. If a continuous random variable X follows a distribution function F with an observed value x, then $u=F(x)$ is the **probability integral transform** at x. In short, if $X \sim F$ then $F\left(X\right) \sim U\left(0,1\right)$. Similarly, the d-dimensional can be stated by defining $u_i = F_i\left(x_i\right) = P\left(X_i \le x_i\right)$ for $i=1,\ldots,d$ with $u_i \in \left[0,1\right]$ and consequently the Sklar's theorem can be stated for d-dimensions (Czado, 2019). After this stage, the dependence of associated variables is investigated through the correlation coefficients, the scatterplots, or other graphical methods. For this purpose, the K-plot (Kendall plot) and the chi-plot (Genest and Favre, 2007; Zhang and Singh, 2019a) which are based on Kendall's τ and the chi-square statistic are widely used.

Sklar's Theorem. Let $X_1,X_2,\ldots,X_d$ be d random continuous variables with marginal distribution functions $F_1,F_2,\ldots,F_d$, then there exists a copula C, where the joint distribution function $F\left(x_1,x_2,\ldots,x_d\right)$ for all $x_1,x_2,\ldots,x_d\in\overline{\mathbb{R}}=\left[-\infty,+\infty\right]$ can be expressed as follows:

$$F\left(x_1,x_2,\ldots,x_d\right)=C\left(F_1\left(x_1\right),F_2\left(x_2\right),\ldots,F_d\left(x_d\right)\right), \tag{3.22}$$

and the density function f can be written

$$f\left(x_1,x_2,\ldots,x_d\right)=c\left(F_1\left(x_1\right),F_2\left(x_2\right),\ldots,F_d\left(x_d\right)\right)f_1\left(x_1\right)f_2\left(x_2\right)\ldots f_d\left(x_d\right),$$

$$\text{or } c\left(F_1\left(x_1\right),F_2\left(x_2\right),\ldots,F_d\left(x_d\right)\right)=\frac{f\left(x_1,x_2,\ldots,x_d\right)}{f_1\left(x_1\right)f_2\left(x_2\right)\ldots f_d\left(x_d\right)}. \tag{3.23}$$

When $F_1,F_2,\ldots,F_n$ are all continuous then the copula C is unique. Conversely, if $F_1,F_2,\ldots,F_d$ are marginal distribution functions of a joint distribution function F, then a copula C can be defined as:

$$C\left(u_1,u_2,\ldots,u_d\right)=F\left(F_1^{-1}\left(u_1\right),F_2^{-1}\left(u_2\right),\ldots,F_d^{-1}\left(u_d\right)\right), \tag{3.24}$$

and **the copula density function** is defined as follows:

$$c\left(u_1,\ldots,u_d\right)=\frac{\partial^n C\left(u_1,\ldots,u_d\right)}{\partial u_1\ldots\partial u_d}=\frac{f\left(x_1,\ldots,x_d\right)}{f_1\left(x_1\right)\ldots f_d\left(x_d\right)}=\frac{f\left(F_1^{-1}\left(u_1\right),\ldots,F_d^{-1}\left(u_d\right)\right)}{f_1\left(F_1^{-1}\left(u_1\right)\right)\ldots f_d\left(F_d^{-1}\left(u_d\right)\right)}. \tag{3.25}$$

Briefly, it can be stated that each multivariate copula with marginal distributions stands as multivariate distribution limited to the domain U[0,1] and on the other hand, a multivariate distribution can be written as a multivariate copula based on associated marginal distributions.

Basic concepts in copula theory

Considering the probability integral transformations $u_i=F_i\left(x_i\right)=P\left(X_i\le x_i\right)$ for $i=1,\ldots,d$ with $u_i\in\left[0,1\right]$.

Based on Eq. 3.23, the bivariate density function can be written as:

$$f_{12}\left(x_1,x_2\right)=c_{12}\left(F_1\left(x_1\right),F_2\left(x_2\right)\right)f_1\left(x_1\right)f_2\left(x_2\right). \tag{3.26}$$

Because

$$f_{12}\left(x_1,x_2\right)=\frac{\partial^2 F_{12}\left(x_1,x_2\right)}{\partial x_1\partial x_2}=\frac{\partial^2 C_{12}\left(F_1\left(x_1\right),F_2\left(x_2\right)\right)}{\partial x_1\partial x_2}$$
$$=\frac{\partial^2 C_{12}\left(F_1\left(x_1\right),F_2\left(x_2\right)\right)}{\partial F_1\left(x_1\right)\partial F_2\left(x_2\right)}\frac{\partial F_1\left(x_1\right)}{\partial x_1}\frac{\partial F_2\left(x_2\right)}{\partial x_2}=\frac{\partial^2 C_{12}\left(u_1,u_2\right)}{\partial u_1\partial u_2}f_1\left(x_1\right)f_2\left(x_2\right) \tag{3.27}$$
$$=c_{12}\left(F_1\left(x_1\right),F_2\left(x_2\right)\right)f_1\left(x_1\right)f_2\left(x_2\right)=c_{12}\left(u_1,u_2\right)f_1\left(x_1\right)f_2\left(x_2\right).$$

Similarly, the **bivariate copula density function** c_{12} is

$$c_{12}\left(u_1,u_2\right)=\frac{\partial^2 C_{12}\left(u_1,u_2\right)}{\partial u_1\partial u_2}=\frac{f_{12}\left(F_1^{-1}\left(u_1\right),F_2^{-1}\left(u_2\right)\right)}{f_1\left(F_1^{-1}\left(u_1\right)\right)\,f_2\left(F_2^{-1}\left(u_2\right)\right)}=\frac{f_{12}\left(x_1,x_2\right)}{f_1\left(x_1\right)\,f_2\left(x_2\right)}. \tag{3.28}$$

The **joint distribution functions** in terms of their copula can be expressed as:

$$C_{12}\left(u_1,u_2\right)=F_{12}\left(F_1^{-1}\left(u_1\right),F_2^{-1}\left(u_2\right)\right)=F_{12}\left(x_1,x_2\right)=P\left(X_1\le x_1,X_2\le x_2\right). \tag{3.29}$$

And similarly, for three dimensions

$$C\left(u_1,u_2,u_3\right)=P\left(X_1\le x_1,X_2\le x_2,X_3\le x_3\right)=F\left(F_1^{-1}\left(u_1\right),F_2^{-1}\left(u_2\right),F_3^{-1}\left(u_3\right)\right). \tag{3.30}$$

The conditional density function $f_{1|2}$ of X_1 given that $X_2 = x_2$ is associated with **conditional copula density function** c_{12} and can be stated as:

$$f_{1|2}\left(x_1\mid x_2\right)=c_{12}\left(F_1\left(x_1\right),F_2\left(x_2\right)\right)f_2\left(x_2\right) \tag{3.31}$$

but also, in bivariate case, satisfies

$$c_{1|2}\left(u_1\mid u_2\right)=c_{12}\left(u_1,u_2\right). \tag{3.32}$$

The **conditional distribution function** $F_{1|2}$ is described as:

$$F_{1|2}\left(x_1\middle|x_2\right)=\frac{\partial}{\partial u_2}C_{12}\left(F_1\left(x_1\right),u_2\right)=\frac{\partial}{\partial F_2\left(x_2\right)}C_{12}\left(F_1\left(x_1\right),F_2\left(x_2\right)\right)= \tag{3.33}$$
$$=C_{1|2}\left(F_1\left(x_1\right)\middle|F_2\left(x_2\right)\right)$$

and thus $C_{1|2}\left(u_1\middle|u_2\right)=P\left(U_1\le u_1\middle|U_2=u_2\right)=\frac{\partial}{\partial u_2}C_{12}\left(u_1,u_2\right).$ (3.34)

The bivariate conditional distribution function $C_{1|2}$ is also known as ***h-function*** (Aas et al., 2009; Czado, 2019) and can be expressed as:

$$h_{1|2}\left(u_1\middle|u_2\right)=C_{1|2}\left(u_1\middle|u_2\right)=\frac{\partial C_{12}\left(u_1,u_2\right)}{\partial u_2} \tag{3.35}$$

and $h_{2|1}\left(u_2\middle|u_1\right)=C_{2|1}\left(u_2\middle|u_1\right)=\frac{\partial C_{12}\left(u_1,u_2\right)}{\partial u_1}.$ (3.36)

Regarding the abbreviation, it should be noted that $C_{12}\left(u_1,u_2\right)$ or $C\left(u_1,u_2\right)$ denotes the copula of u_1, u_2. For higher dimensions, $C_{123}\left(u_1,u_2,u_3\right)$ denotes the copula of u_1, u_2, u_3, but for brevity, $C\left(u_1,u_2,u_3\right)$ is used and similarly the other cases are defined, unless it is deemed necessary.

Table 3.2
Important symbols and abbreviations of basic concepts in copula theory for univariate and bivariate cases.

	Density function	Distribution Function
Marginal	c_1	$C_1 = P\left(U_1 \le u_1\right)$
Joint	c_{12}	$C_{12} = P\left(U_1 \le u_1, U_2 \le u_2\right)$
Conditional	$c_{1\|2}$	$C_{1\|2} = P\left(U_1 \le u_1 \middle\| U_2 = u_2\right)$ *or* $h_{1\|2}$

Copula construction

As stated in Sklar's theorem (Eq. 3.24), a copula can be constructed on the inversion method and the probability integral transformation, when the joint distribution function F is known for the associated variables $X_1, X_2, \ldots, X_n$, as follows:

$C\left(u_1,u_2,\ldots,u_d\right) = F\left(F_1^{-1}\left(u_1\right),F_2^{-1}\left(u_2\right),\ldots,F_d^{-1}\left(u_d\right)\right)$, where $u_1 = F_1\left(x_1\right),\ldots,u_d = F_d\left(x_d\right)$.

Another method uses the generator functions φ (Table 3.5) to construct a copula by the following procedure:

$$\begin{aligned} \varphi\left(F\left(x_1,\ldots,x_d\right)\right) &= \varphi\left(F_1\left(x_1\right)\right) + \ldots + \varphi\left(F_d\left(x_d\right)\right) \\ \Rightarrow \varphi\left(C\left(u_1,\ldots,u_d\right)\right) &= \varphi\left(u_1\right) + \ldots + \varphi\left(u_d\right) \\ \Rightarrow C\left(u_1,\ldots,u_d\right) &= \varphi^{-1}\left(\varphi\left(u_1\right) + \ldots + \varphi\left(u_d\right)\right). \end{aligned} \tag{3.37}$$

The copulas can also be constructed by a combination of bivariate copulas following the pair-copula construction method (Bedford and Cooke, 2001, 2002; Joe, 2014) by extending the extreme value theory from one to higher dimensions (Czado, 2019) or by using geometric and algebraic methods (Zhang and Singh, 2019a). Further information about copulas' construction can be found in any introductory book in copula theory, such as Nelsen's (2006) and Joe's (2014). Based on these methods, a d-variate joint copula distribution, or shortly a "copula" can be constructed depending on the copula families which are used.

Copula families

As multivariate joint distributions, copulas are grouped into different copula families (Nelsen, 2006; Salvadori et al., 2007; Mai and Scherer, 2017) with a similar meaning and a variety of univariate distribution functions. The different families better describe the dependence of variables, the tails behaviour and the asymmetries of distributions (Nelsen, 2006; Salvadori et al., 2007; Joe, 2014; Durante and Sempi, 2015; Czado, 2019). A non-exhaustive list of these copulas includes the class of Archimedean copulas (Clayton, Gumbel, Frank, Joe, Ali-Mikhail-Haq, BB1, BB6, BB7, BB8), the class of Meta-elliptical copulas (Gaussian, t), and the class of Extreme value copulas (Gumbel, Tawn).

The BB1, BB6, BB7, BB8 are mixed copulas, arising from a combination of other copula families; hence the Clayton-Gumbel copula is known as BB1, the Joe-Gumbel copula as BB6, the Joe-Clayton copula as BB7, the Joe-Frank copula as BB8 (Nikoloulopoulos et al., 2012; Joe, 2014). Nowadays, the classes of Archimedean and meta-elliptical copulas are widely used in hydrology and coastal engineering. The Archimedean copulas are preferred due to their simple form and their properties while, on the other hand, the meta-elliptical copulas are mainly applied to multivariate data. The basic characteristics of the copula families are described below in Table 3.4 (Nelsen, 2006; Salvadori et al., 2007; Joe, 2014; Durante and Sempi, 2015; Czado, 2019).

Furthermore, the rotated versions of copulas by 90, 180, or 270 degrees have been defined for many copula families (Mai and Scherer, 2017), extending their properties for any tail dependencies (Table 3.3). The copula that arises from the rotation of 180° (C^{180}) is also known as the survival copula of C. The **survival copula** $\bar{C}$, following Sklar's theorem couples the marginal survival functions, where $\bar{F}_i\left(x_i\right) = P\left(X_i > x_i\right) = 1 - F\left(x_i\right), i = 1,...,d$, to the joint survival function $\bar{F}$. For the bivariate case, a survival copula satisfies (Nelsen, 2006):

$$\bar{C}\left(u_1,u_2\right) = u_1 + u_2 - 1 + C\left(1-u_1,1-u_2\right) \tag{3.38}$$

and similarly, $\bar{C}\left(1-u_1,1-u_2\right) = 1 - u_1 - u_2 + C\left(u_1,u_2\right)$. (3.39)

Table 3.3

The copula density for the bivariate case of rotated versions.

copula density	copula distribution function
$c^{90}\left(u_1,u_2\right)=c\left(1-u_1,u_2\right)$	$C^{90}\left(u_1,u_2\right)=u_2-C\left(1-u_1,u_2\right)$
$c^{180}\left(u_1,u_2\right)=c\left(1-u_1,1-u_2\right)$	$C^{180}\left(u_1,u_2\right)=C\left(1-u_1,1-u_2\right)+u_1+u_2-1$
$c^{270}\left(u_1,u_2\right)=c\left(u_1,1-u_2\right)$	$C^{270}\left(u_1,u_2\right)=u_1-C\left(u_1,1-u_2\right)$

The tail dependence (Nelsen, 2006) or, in other words, the probability of the joint occurrence of extremely high or extremely small values of associated variables, can be described by the (λ_U) and the lower (λ_L) tail dependence coefficients (Czado, 2019) given as :

$$\lambda_U=\lim_{t\to 1^-}\frac{1-2t+C\left(t,t\right)}{1-t}\text{ and }\lambda_L=\lim_{t\to 0^+}\frac{C\left(t,t\right)}{1-t}. \tag{3.40}$$

Table 3.4

Characteristics of Bivariate Copulas.

Class	Family	Bivariate Copula	Domain of Parameters	independence
	Independent	$C(u_1,u_2)=u_1u_2$	-	-
Elliptical	Gaussian	$C(u_1,u_2)=\Phi_\rho\left(\Phi^{-1}(u_1),\Phi^{-1}(u_2)\right)$ Φ_ρ: distribution function of standard Gaussian N(0,1) with correlation ρ Φ^{-1}: inverse univariate distribution function of standard Gaussian N(0,1) $\Phi(x)=\frac{1}{\sqrt{2\pi}}\int_{-\infty}^{x}e^{\frac{-y^2}{2}}dy$	$\rho\in[-1,1]$	-
	t	$C(u_1,u_2)=t_{\rho,\nu}\left(t_\nu^{-1}(u_1),t_\nu^{-1}(u_2)\right)$ $t_{\rho,\nu}$: bivariate distribution function of Student's t with correlation ρ and ν degrees of freedom t_ν^{-1}: inverse univariate distribution function of Student's t	$\rho\in[-1,1]$ $\nu>2$	-
Archimedean	Clayton	$C(u_1,u_2)=\left(u_1^{-\theta}+u_2^{-\theta}-1\right)^{\frac{-1}{\theta}}$	$\theta\in[-1,+\infty)-\{0\}$	$\theta\to 0$
	Gumbel	$C(u_1,u_2)=e^{-\left[(-\ln u_1)^\theta+(-\ln u_2)^\theta\right]^{\frac{1}{\theta}}}$	$\theta\geq 1$	$\theta\to 1$
	Frank	$C(u_1,u_2)=-\frac{1}{\theta}\ln\left(1-\frac{\left(1-e^{-\theta u_1}\right)\left(1-e^{-\theta u_2}\right)}{1-e^{-\theta}}\right)$	$\theta\neq 0$	$\theta\to 0$
	Joe	$C(u_1,u_2)=1-\left(\left(1-u_1\right)^\theta+\left(1-u_2\right)^\theta-\left(1-u_1\right)^\theta\left(1-u_2\right)^\theta\right)^{\frac{1}{\theta}}$	$\theta\geq 1$	$\theta\to 1$

Table 3.4 *(continue)*

Characteristics of Bivariate Copulas.

Class	Family	Bivariate Copula	Domain of Parameters	independence
Archimedean	BB1	$C(u_1,u_2)=\left[1+\left(\left(u_1^{-\theta}-1\right)^{\delta}+\left(u_2^{-\theta}-1\right)^{\delta}\right)^{\frac{1}{\delta}}\right]^{\frac{-1}{\theta}}$	$\theta>0,\ \delta\geq 1$	$\theta\to 0,\ \delta\to 1$
	BB6	$C(u_1,u_2)=1-\left[1-e^{-\left[\left(-\ln\left(1-(1-u_1)^{\theta}\right)\right)^{\delta}+\left(-\ln\left(1-(1-u_2)^{\theta}\right)\right)^{\delta}\right]^{\frac{1}{\delta}}}\right]^{\frac{1}{\theta}}$	$\theta,\ \delta\geq 1$	$\theta\to 1,\ \delta\to 1$
	BB7	$C(u_1,u_2)=1-\left[1-\left(\left(1-(1-u_1)^{\theta}\right)^{-\delta}+\left(1-(1-u_2)^{\theta}\right)^{-\delta}-1\right)^{\frac{-1}{\delta}}\right]^{\frac{1}{\theta}}$	$\theta\geq 1,\ \delta>0$	$\theta\to 1,\ \delta\to 0$
	BB8	$C(u_1,u_2)=\frac{1}{\delta}\left(1-\left[1-\left(1-\left(1-\delta\right)^{\theta}\right)^{-1}\left(1-\left(1-\delta u_1\right)^{\theta}\right)\left(1-\left(1-\delta u_2\right)^{\theta}\right)\right]^{\frac{1}{\theta}}\right)$	$\theta\geq 1,\delta\in(0,1]$	$\theta\to 1,\ \delta\to 0$
Extreme	**Tawn**	$C(u_1,u_2)=e^{\ln(u_1u_2)A\left(\frac{\ln(u_1)}{\ln(u_1u_2)}\right)}$ $A(t)=(1-\psi_1)(1-t)+(1-\psi_2)t+\left[\left(\psi_1(1-t)\right)^{\theta}+\left(\psi_2 t\right)^{\theta}\right]^{\frac{1}{\theta}}$ Tawn Type 1: $\psi_1=1$ • Tawn Type 2: $\psi_2=1$	$t,\ \psi_1,\ \psi_2\in[0,1]$ $\theta\in[1,+\infty)$	$\theta\to 1$ $\psi_1\to 1,\psi_2\to 1$

* ***Gumbel*** *family also belongs to the Extreme class.*

Table 3.5

The generator functions $\varphi(t)$ of Archimedean copulas, according to Nelsen (2006) and Joe (2014).

Family	φ(t)
Clayton	$\frac{t^{-\theta} - 1}{\theta}$
Gumbel	$\left(-\ln t\right)^{\theta}$
Frank	$-\ln\frac{e^{-\theta t} - 1}{e^{-\theta} - 1}$
Joe	$-\ln\left(1 - \left(1 - t\right)^{\theta}\right)$
BB1	$\left(t^{-\theta} - 1\right)^{\delta}$
BB6	$-\ln\left(1 - \left(1 - t\right)^{\theta}\right)$
BB7	$\left(1 - \left(1 - t\right)^{\theta}\right)^{-\delta} - 1$
BB8	$1 - \left(1 - \delta t\right)^{\theta}$

Estimation of important probabilities

The estimation of important joint probabilities is a prerequisite step in coastal storm modelling and especially for the simulation of coastal storms and the estimation of return periods. The joint probabilities for bivariate and trivariate cases are presented by many authors, and they are easy to understand even by using Venn diagrams. An indication of these probabilities (Serinaldi, 2015; Zhang and Singh, 2019a) is given below:

$$P\left(X_1 > x_1, X_2 > x_2\right) = 1 - P\left(X_1 \le x_1\right) - P\left(X_2 \le x_2\right) + P\left(X_1 \le x_1, X_2 \le x_2\right) = \\ = 1 - u_1 - u_2 + C\left(u_1, u_2\right). \tag{3.41}$$

$$P\left(X_1 > x_1, X_2 \le x_2\right) = P\left(X_2 \le x_2\right) - P\left(X_1 \le x_1, X_2 \le x_2\right) = u_2 - C\left(u_1, u_2\right). \tag{3.42}$$

$$P\left(X_1 \le x_1, X_2 > x_2\right) = P\left(X_1 \le x_1\right) - P\left(X_1 \le x_1, X_2 \le x_2\right) = u_1 - C\left(u_1, u_2\right). \tag{3.43}$$

$$\begin{aligned} P\left(X_1 > x_1, X_2 > x_2, X_3 > x_3\right) &= 1 - P\left(X_1 \le x_1\right) - P\left(X_2 \le x_2\right) - P\left(X_3 \le x_3\right) \\ &+ P\left(X_1 \le x_1, X_2 \le x_2\right) + P\left(X_1 \le x_1, X_3 \le x_3\right) + P\left(X_2 \le x_2, X_3 \le x_3\right) \\ &- P\left(X_1 \le x_1, X_2 \le x_2, X_3 \le x_3\right) = \\ &1 - u_1 - u_2 - u_3 + C_{12}\left(u_1, u_2\right) + C_{13}\left(u_1, u_3\right) + C_{23}\left(u_2, u_3\right) - C\left(u_1, u_2, u_2\right). \end{aligned} \tag{3.44}$$

In the context of this thesis, the joint probabilities are extended to four and five dimensions and they can be expressed as follows:

$$\begin{aligned} &P\left(X_1 > x_1, X_2 > x_2, X_3 > x_3, X_4 > x_4\right) = 1 - P\left(X_1 \le x_1\right) - P\left(X_2 \le x_2\right) \\ &- P\left(X_3 \le x_3\right) - P\left(X_4 \le x_4\right) + P\left(X_1 \le x_1, X_2 \le x_2\right) + P\left(X_1 \le x_1, X_3 \le x_3\right) \\ &+ P\left(X_2 \le x_2, X_3 \le x_3\right) + P\left(X_2 \le x_2, X_4 \le x_4\right) + P\left(X_3 \le x_3, X_4 \le x_4\right) \\ &- P\left(X_1 \le x_1, X_2 \le x_2, X_3 \le x_3\right) - P\left(X_1 \le x_1, X_2 \le x_2, X_4 \le x_4\right) \\ &- P\left(X_1 \le x_1, X_3 \le x_3, X_4 \le x_3\right) - P\left(X_2 \le x_2, X_3 \le x_3, X_4 \le x_4\right) \\ &+ P\left(X_1 \le x_1, X_2 \le x_2, X_3 \le x_3, X_4 \le x_4\right) \\ &= 1 - u_1 - u_2 - u_3 - u_4 + C_{12}\left(u_1, u_2\right) + C_{13}\left(u_1, u_3\right) + C_{23}\left(u_2, u_3\right) + C_{24}\left(u_2, u_4\right) \\ &+ C_{34}\left(u_3, u_4\right) - C\left(u_1, u_2, u_3\right) - C\left(u_1, u_2, u_4\right) - C\left(u_1, u_3, u_4\right). \\ &- C\left(u_2, u_3, u_4\right) + C\left(u_1, u_2, u_3, u_4\right) \end{aligned} \tag{3.45}$$

$$
\begin{aligned}
&P\left(X_1 > x_1, X_2 > x_2, X_3 > x_3, X_4 > x_4, X_5 > x_5\right) = \\
&\quad 1 - P\left(X_1 \le x_1, X_2 \le x_2, X_3 \le x_3, X_4 \le x_4, X_5 \le x_5\right) = \\
&\quad 1 - P\left(X_1 \le x_1\right) - P\left(X_2 \le x_2\right) - P\left(X_3 \le x_3\right) - P\left(X_4 \le x_4\right) - P\left(X_5 \le x_5\right) \\
&\quad + P\left(X_1 \le x_1, X_2 \le x_2\right) + P\left(X_1 \le x_1, X_3 \le x_3\right) + P\left(X_1 \le x_1, X_4 \le x_4\right) \\
&\quad + P\left(X_1 \le x_1, X_5 \le x_5\right) + P\left(X_2 \le x_2, X_3 \le x_3\right) + P\left(X_2 \le x_2, X_4 \le x_4\right) \\
&\quad + P\left(X_2 \le x_2, X_5 \le x_5\right) + P\left(X_3 \le x_3, X_4 \le x_4\right) + P\left(X_3 \le x_3, X_5 \le x_5\right) \\
&\quad + P\left(X_4 \le x_4, X_5 \le x_5\right) - P\left(X_1 \le x_1, X_2 \le x_2, X_3 \le x_3\right) \\
&\quad - P\left(X_1 \le x_1, X_2 \le x_2, X_4 \le x_4\right) - P\left(X_1 \le x_1, X_2 \le x_2, X_5 \le x_5\right) \\
&\quad - P\left(X_1 \le x_1, X_3 \le x_3, X_4 \le x_4\right) - P\left(X_1 \le x_1, X_3 \le x_3, X_5 \le x_5\right) \\
&\quad - P\left(X_1 \le x_1, X_4 \le x_4, X_5 \le x_5\right) - P\left(X_2 \le x_2, X_3 \le x_3, X_4 \le x_4\right) \\
&\quad - P\left(X_2 \le x_2, X_3 \le x_3, X_5 \le x_5\right) - P\left(X_2 \le x_2, X_4 \le x_4, X_5 \le x_5\right) \\
&\quad - P\left(X_3 \le x_3, X_4 \le x_4, X_5 \le x_5\right) + P\left(X_1 \le x_1, X_2 \le x_2, X_3 \le x_3, X_4 \le x_4\right) \\
&\quad + P\left(X_1 \le x_1, X_2 \le x_2, X_3 \le x_3, X_5 \le x_5\right) \\
&\quad + P\left(X_1 \le x_1, X_2 \le x_2, X_4 \le x_4, X_5 \le x_5\right) \\
&\quad + P\left(X_1 \le x_1, X_3 \le x_3, X_4 \le x_4, X_5 \le x_5\right) \\
&\quad + P\left(X_2 \le x_2, X_3 \le x_3, X_4 \le x_4, X_5 \le x_5\right) \\
&\quad - P\left(X_1 \le x_1, X_2 \le x_2, X_3 \le x_3, X_4 \le x_4, X_5 \le x_5\right).
\end{aligned}
\tag{3.46}
$$

or by using the copulas:

$$
\begin{aligned}
&P\left(X_1 > x_1, X_2 > x_2, X_3 > x_3, X_4 > x_4, X_5 > x_5\right) = \\
&\quad 1 - u_1 - u_2 - u_3 - u_4 - u_5 + C\left(u_1, u_2\right) + C\left(u_1, u_3\right) + C\left(u_1, u_4\right) + C\left(u_1, u_5\right) \\
&\quad + C\left(u_2, u_3\right) + C\left(u_2, u_4\right) + C\left(u_2, u_5\right) + C\left(u_3, u_4\right) + C\left(u_3, u_5\right) + C\left(u_4, u_5\right) \\
&\quad - C\left(u_1, u_2, u_3\right) - C\left(u_1, u_2, u_4\right) - C\left(u_1, u_2, u_5\right) - C\left(u_1, u_3, u_4\right) \\
&\quad - C\left(u_1, u_3, u_5\right) - C\left(u_1, u_4, u_5\right) - C\left(u_2, u_3, u_4\right) - C\left(u_2, u_3, u_5\right) \\
&\quad - C\left(u_2, u_4, u_5\right) - C\left(u_3, u_4, u_5\right) + C\left(u_1, u_2, u_3, u_4\right) + C\left(u_1, u_2, u_3, u_5\right) \\
&\quad + C\left(u_1, u_2, u_4, u_5\right) + C\left(u_1, u_3, u_4, u_5\right) \\
&\quad + C\left(u_2, u_3, u_4, u_5\right) - C\left(u_1, u_2, u_3, u_4, u_5\right).
\end{aligned}
\tag{3.47}
$$

And briefly, for other more complex cases:

$$
\begin{aligned}
&P\left(X_1 \le x_1, X_2 > x_2, X_3 > x_3, X_4 > x_4, X_5 > x_5\right) = \\
&\qquad u_1 - C\left(u_1, u_2\right) - C\left(u_1, u_5\right) + C\left(u_1, u_2, u_5\right).
\end{aligned}
\tag{3.48}
$$

$$
\begin{aligned}
&P\left(X_1 > x_1, X_2 \le x_2, X_3 \le x_3, X_4 \le x_4, X_5 \le x_5\right) = \\
&\qquad C\left(u_2, u_3, u_4, u_5\right) - C\left(u_1, u_2, u_3, u_4, u_5\right).
\end{aligned}
\tag{3.49}
$$

$$
\begin{aligned}
&P\left(X_1 > x_1, X_2 > x_2, X_3 \le x_3, X_4 \le x_4, X_5 \le x_5\right) = \\
&\quad C\left(u_3, u_4, u_5\right) - C\left(u_2, u_3, u_4, u_5\right) - C\left(u_1, u_3, u_4, u_5\right) - C\left(u_1, u_2, u_3, u_4, u_5\right).
\end{aligned}
\tag{3.50}
$$

Based on the probability theory and the joint probabilities, the conditional probabilities can be expressed as conditional copula distribution functions. For instance,

$$P\left(X_1 \le x_1 \middle| X_2 \le x_2\right) = \frac{F_{12}\left(x_1, x_2\right)}{F_2\left(x_2\right)} = C_{12}\left(U_1 \le u_1 \middle| U_2 \le u_2\right) = \frac{C\left(u_1, u_2\right)}{u_2}. \tag{3.51}$$

$$P\left(X_1 > x_1 \middle| X_2 \le x_2\right) = 1 - P\left(X_1 \le x_1 \middle| X_2 \le x_2\right) = 1 - \frac{C\left(u_1, u_2\right)}{u_2}. \tag{3.52}$$

$$P\left(X_2 > x_2 \middle| X_1 = x_1\right) = 1 - P\left(X_2 \le x_2 \middle| X_1 = x_1\right) = 1 - \frac{\partial C\left(u_1, u_2\right)}{\partial u_1}. \tag{3.53}$$

$$P\left(X_1 \le x_1 \middle| X_2 > x_2\right) = \frac{P\left(X_1 \le x_1, X_2 > x_2\right)}{P\left(X_2 > x_2\right)} = \frac{u_1 - C\left(u_1, u_2\right)}{1 - u_2}. \tag{3.54}$$

$$P\left(X_1 \le x_1, X_2 \le x_2 \middle| X_3 = x_3\right) = C_{12|3}\left(U_1 \le u_1, U_2 \le u_2 \middle| U_3 = u_3\right) = \frac{\partial C\left(u_1, u_2, u_3\right)}{\partial u_3}. \tag{3.55}$$

$$\begin{aligned} P\left(X_1 \le x_1 \middle| X_2 = x_2, X_3 = x_3\right) &= \frac{\dfrac{\partial^2 F\left(x_1, x_2, x_3\right)}{\partial x_2 \partial x_3}}{\dfrac{\partial^2 F\left(x_2, x_3\right)}{\partial x_2 \partial x_3}} = \\ &= C_{1|23}\left(U_1 \le u_1 \middle| U_2 = u_2, U_3 = u_3\right) = \frac{\dfrac{\partial^2 C\left(u_1, u_2, u_3\right)}{\partial u_2 \partial u_3}}{\dfrac{\partial^2 C\left(u_2, u_3\right)}{\partial u_2 \partial u_3}}. \end{aligned} \tag{3.56}$$

And their extensions to four and five variables are the following:

$$\begin{aligned} &P\left(X_5 \le x_5 \middle| X_1 = x_1, X_2 = x_2, X_3 = x_3, X_4 = x_4\right) = \\ &C\left(U_5 \le u_5 \middle| U_1 = u_1, U_2 = u_2, U_3 = u_3, U_4 = u_4\right) = \frac{\dfrac{\partial^4 C\left(u_1, u_2, u_3, u_4, u_5\right)}{\partial u_1 \partial u_2 \partial u_3 \partial u_4}}{\dfrac{\partial^4 C\left(u_1, u_2, u_3, u_4\right)}{\partial u_1 \partial u_2 \partial u_3 \partial u_4}}. \end{aligned} \tag{3.57}$$

$$\begin{aligned} P\left(X_5 > x_5 \middle| X_1 = x_1, X_2 = x_2, X_3 = x_3, X_4 = x_4\right) &= \\ = C\left(U_5 > u_5 \middle| U_1 = u_1, U_2 = u_2, U_3 = u_3, U_4 = u_4\right) &= \\ = 1 - C\left(U_5 \le u_5 \middle| U_1 = u_1, U_2 = u_2, U_3 = u_3, U_4 = u_4\right) &= \\ = 1 - \frac{\dfrac{\partial^4 C\left(u_1, u_2, u_3, u_4, u_5\right)}{\partial u_1 \partial u_2 \partial u_3 \partial u_4}}{\dfrac{\partial^4 C\left(u_1, u_2, u_3, u_4\right)}{\partial u_1 \partial u_2 \partial u_3 \partial u_4}}. \end{aligned} \tag{3.58}$$

$$\begin{aligned} &P\left(X_1 \le x_1, X_2 \le x_2, X_3 \le x_3, X_4 \le x_4 \middle| X_5 \le x_5\right) = \\ &= \frac{P\left(X_1 \le x_1, X_2 \le x_2, X_3 \le x_3, X_4 \le x_4, X_5 \le x_5\right)}{F_5\left(x_5\right)} = \frac{C\left(u_1, u_2, u_3, u_4, u_5\right)}{u_5}. \end{aligned} \tag{3.59}$$

$$P\left(X_5 \le x_5 \middle| X_1 \le x_1, X_2 \le x_2, X_3 \le x_3, X_4 \le x_4\right) = \frac{F\left(x_1, x_2, x_3, x_4, x_5\right)}{F\left(x_1, x_2, x_3, x_4\right)} = \\ = C\left(U_5 \le u_5 \middle| U_1 \le u_1, U_2 \le u_2, U_3 \le u_3, U_4 \le u_4\right) = \frac{C\left(u_1, u_2, u_3, u_4, u_5\right)}{C\left(u_1, u_2, u_3, u_4\right)}. \tag{3.60}$$

$$\begin{aligned} P\left(X_5 > x_5 \middle| X_1 \le x_1, X_2 \le x_2, X_3 \le x_3, X_4 \le x_4\right) &= \\ &= C\left(U_5 > u_5 \middle| U_1 \le u_1, U_2 \le u_2, U_3 \le u_3, U_4 \le u_4\right) \\ &= 1 - C\left(U_5 \le u_5 \middle| U_1 \le u_1, U_2 \le u_2, U_3 \le u_3, U_4 \le u_4\right) \\ &= 1 - \frac{C\left(u_1, u_2, u_3, u_4, u_5\right)}{C\left(u_1, u_2, u_3, u_4\right)}. \end{aligned} \tag{3.61}$$

Table 3.6

Summing up the relationship of conditional probabilities and the associated copula distribution functions in the bivariate case.

$P\left(U_1 \le u_1 \middle\| U_2 = u_2\right) = \frac{\partial C\left(u_1, u_2\right)}{\partial u_2}$	$P\left(U_2 \le u_2 \middle\| U_1 = u_1\right) = \frac{\partial C\left(u_1, u_2\right)}{\partial u_1}$
$P\left(U_1 > u_1 \middle\| U_2 = u_2\right) = 1 - \frac{\partial C\left(u_1, u_2\right)}{\partial u_2}$	$P\left(U_2 > u_2 \middle\| U_1 = u_1\right) = 1 - \frac{\partial C\left(u_1, u_2\right)}{\partial u_1}$
$P\left(U_1 \le u_1 \middle\| U_2 \le u_2\right) = \frac{C\left(u_1, u_2\right)}{u_2}$	$P\left(U_2 \le u_2 \middle\| U_1 \le u_1\right) = \frac{C\left(u_1, u_2\right)}{u_1}$
$P\left(U_1 > u_1 \middle\| U_2 > u_2\right) = 1 - \frac{u_1 - C\left(u_1, u_2\right)}{1 - u_2}$	$P\left(U_2 > u_2 \middle\| U_1 > u_1\right) = 1 - \frac{u_2 - C\left(u_1, u_2\right)}{1 - u_1}$

3.4.2. Vine copulas

The extension of copulas construction from bivariate to higher dimensions is a demanding procedure that has been presented by Nelsen (2006) and since then, it is an important topic in copula theory. For many copula families, a high-dimensional copula can be constructed through various proposed methods as described in the previous sub-section. The pair copula construction (PCC) is an effective, easy, and flexible method to build multivariate copulas based on the bivariate copulas as well as the conditional and the marginal distributions. In this direction, the work of Aas et al. (2009) and of De Michelle et al. (2007) are very important, but the general idea was described by Joe (1996) and by Bedford and Cooke (2001, 2002). The vine copulas are constructed by the pair copula method; hence, the PCC method is also known as Vine copulas construction.

Vine copulas are hierarchical structures that are based on pairs' dependence, covering a great variety of dependence and tail behaviour between variables since they combine different univariate distributions and copula families (Joe, 2014; Zhang and Singh, 2019c). The decomposition of the d-dimension density function to $\frac{d(d-1)}{2}$ bivariate density functions and the conditional density functions are needed for their construction. It should be noted that the conditional distribution function differs from the conditional copula. For instance, the copula $C_{12|3}(x_1, x_2 | x_3)$ has univariate marginal distributions and is associated with the bivariate conditional distribution $F(X_1 \le x_1, X_2 \le x_2 | X_3 = x_3)$. On the other hand, the conditional distribution function $C_{12|3}(u_1, u_2 | u_3)$ denotes the conditional distribution function of (U_1, U_2) given that $U_3 = u_3$ and has a density function $c_{12|3}(u_1, u_2 | u_3)$.

The joint density function can be factorized as follows:

$$f(x_1, x_2, ..., x_d) = f(x_d | x_1, ..., x_{d-1}) ... f(x_2 | x_1) f(x_1), \tag{3.62}$$

which is not unique and provides different forms regarding the order of variables. For instance, the trivariate case could be written as:

$$f(x_1, x_2, x_3) = f_{2|13}(x_2 | x_1, x_3) f_{3|1}(x_3 | x_1) f_1(x_1). \tag{3.63}$$

Applying Sklar's theorem and Eq. 3.31 (Czado, 2019), this decomposition leads to the **pair copula construction** of a joint trivariate density function, which is described by the following equation:

$$\begin{aligned} f(x_1, x_2, x_3) = c_{12|3}(F_{1|3}(x_1 | x_3), F_{2|3}(x_2 | x_3); \theta_{12|3}) c_{13}(F_1(x_1), F_3(x_3); \theta_{13}) \\ c_{23}(F_2(x_2), F_3(x_3); \theta_{23}) f_3(x_3) f_2(x_2) f_1(x_1), \end{aligned} \tag{3.64}$$

where $\theta_{12|3}, \theta_{23}, \theta_{13}$ are the associated copula parameters and similarly, the pair copula construction of a joint trivariate copula density function can be stated as:

$$c(u_1, u_2, u_3) = c_{12|3}(C_{1|3}(u_1 | u_3), C_{2|3}(u_2 | u_3); \theta_{12|3}) c_{13}(u_1, u_3; \theta_{13}) c_{23}(u_2, u_3; \theta_{23}). \tag{3.65}$$

In general, the d-dimensional probability density function, with no reference to the parameters θ, through PCC (Aas et al., 2009) is given by the following Eq. 3.66:

$$f(x_1, ..., x_d) = \prod_{j=1}^{d-1} \prod_{i=1}^{d-j} c_{j,i+j;1,...,j-1}(F_{x_j | x_1,....,x_{j-1}}(x_j | x_1, ..., x_{j-1}), F_{x_{i+j} | x_1,....,x_{j-1}}(x_{i+j} | x_1, ..., x_{j-1})) \prod_{k=1}^{d} f_k(x_k).$$

The Vine copulas are distinguished in the drawable D-Vines (Fig.3.4), the regular R-Vines (Fig. 3.5) and the canonical C-Vines (Fig. 3.6). Their structure is described through a network of trees T_i ($i=1,\ldots$). The three-dimensional vines have a similar structure, but some differences are identified in higher dimensions. The D-Vines are more accessible in their application, while they are based on variables interaction without a specific order (Fig. 3.4). However, the C-Vines are more sensitive in the dependence, having the most dependent variable at the base of their structure. Due to a better description of dependence and their simplicity, this thesis focuses only on C-Vines.

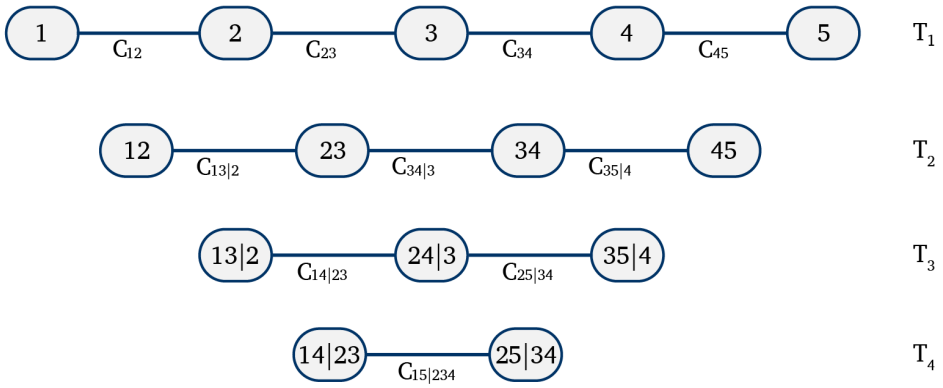

Figure 3.4. Typical structures of D-Vines for five variables (Aas et al., 2009).

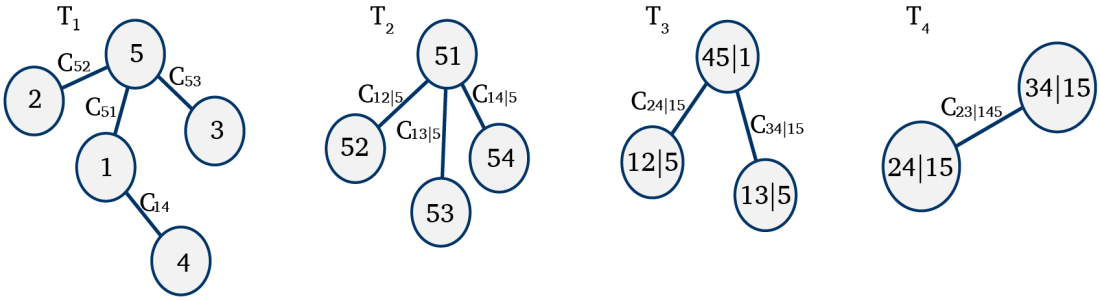

Figure 3.5. Typical structure of R-Vines for five variables.

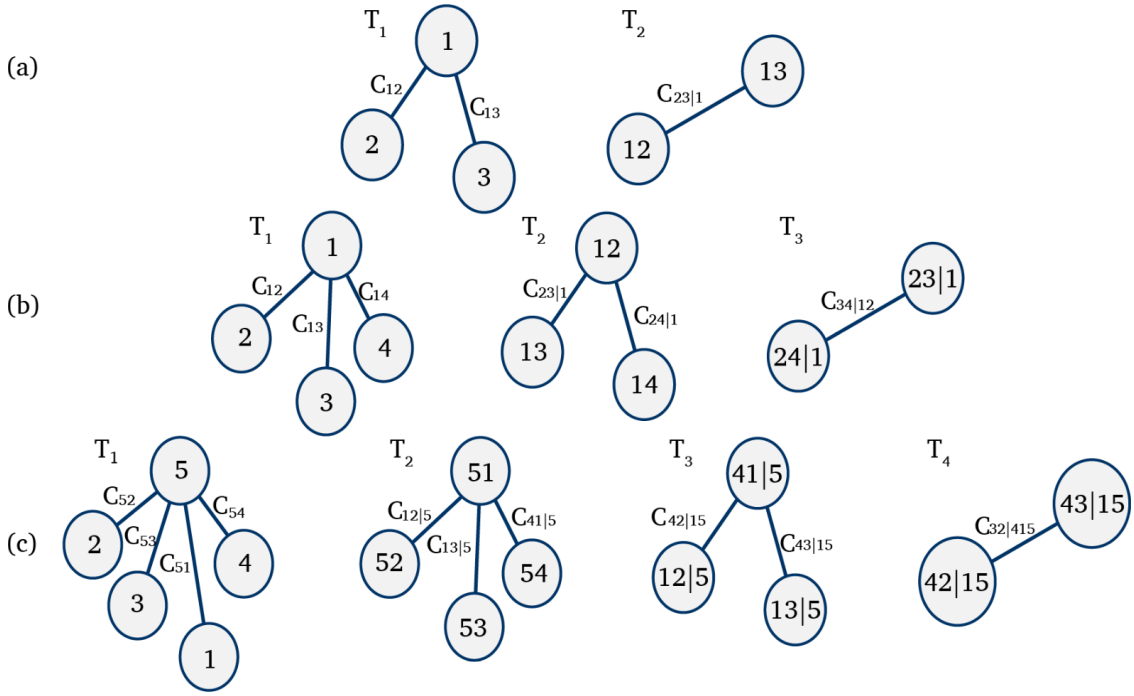

Figure 3.6. Typical structures of C-Vines for three (a), four (b) and five variables (c).

In five dimensions (Fig. 3.6c) the C-Vine structure consists of ten copulas and four trees T_i (i = 1,…,4) with parameters θ. The primary variable is the variable with the strongest dependency on the others, which is confirmed by their correlation according to Kendall's tau (τ). The dependence of pairs is examined at each edge of trees, and similarly, different bivariate copula families are investigated and can be selected for each pair of variables after applying an independence test at a 5% significance level. The selection of the best copula family is evaluated among others according to minimum Akaike information criterion (AIC) or the Bayesian information criterion (BIC) by using the following equations, where n is the sample size and k is the number of parameters:

$$AIC = -2L + 2k\,. \tag{3.67}$$

$$BIC = -2L + ln\left(n\right)\cdot k\,. \tag{3.68}$$

The selection of an appropriate copula family is important when a strong dependence exists, while on the contrary, the impact is less at weak dependence (Joe, 2017). The corresponding copula parameters θ are selected by maximizing the likelihood by using sequential estimates as initial values, also known as sequential estimation of maximum likelihood (Hobæk Haff, 2012, 2013; Dißmann et al., 2013).

For example, the construction of the five-dimensional C-Vine (Fig. 3.6c) starts from the tree T_1 taking as input the standardised variables U_1, U_2, U_3, U_4, U_5. The variable with the strongest dependence among the others (U_5) is set at the start of the tree and the bivariate copulas $C_{51}, C_{52}, C_{53}, C_{54}, C_{55}$, are constructed after the investigation of the best copula family and the estimation of associated parameters. Then the conditional copulas $C_{12|5}, C_{13|5}, C_{41|5}$ of tree T_2 are constructed through the bivariate ones and so on so forth since the copula $C_{32|415}$ of T_4 be constructed. The transition from two to three and higher dimensions requires the construction of *h-functions* and through them the investigation of the optimal copula at each stage as described in Figure 3.7, where X_i ($i=1,\ldots,5$) the variables, U_i the standardised variables and F_i the marginal distribution functions of each variable. It should be mentioned that the above methodology for the construction of a C-Vine copula for five variables can be easily extended to more variables.

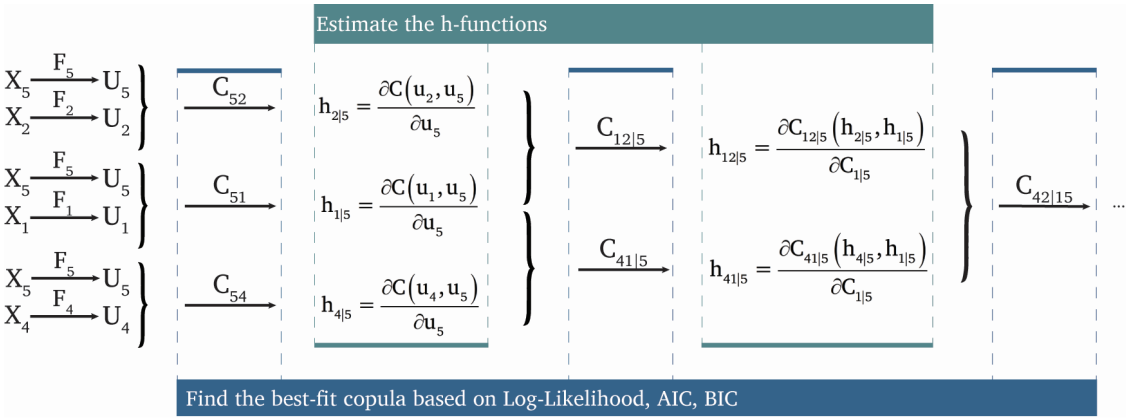

Figure 3.7. A typical building procedure of C-Vine structure.

All the required copulas C and their parameters θ are summarized in two triangular matrices, as below (Eq. 3.69), where the i^{th} line corresponds to the copulas and the parameters of the corresponding tree (T_i) in vine structure.

$$C = \begin{pmatrix} 0 & C_{52} & C_{53} & C_{51} & C_{54} \\ 0 & 0 & C_{12|5} & C_{13|5} & C_{41|5} \\ 0 & 0 & 0 & C_{42|15} & C_{43|15} \\ 0 & 0 & 0 & 0 & C_{32|415} \\ 0 & 0 & 0 & 0 & 0 \end{pmatrix} \begin{matrix} \rightarrow T_1 \\ \rightarrow T_2 \\ \rightarrow T_3 \\ \rightarrow T_4 \\ \end{matrix} \qquad \Theta = \begin{pmatrix} 0 & \theta_{12} & \theta_{13} & \theta_{14} & \theta_{15} \\ 0 & 0 & \theta_{23} & \theta_{24} & \theta_{25} \\ 0 & 0 & 0 & \theta_{34} & \theta_{35} \\ 0 & 0 & 0 & 0 & \theta_{45} \\ 0 & 0 & 0 & 0 & 0 \end{pmatrix} \begin{matrix} \rightarrow T_1 \\ \rightarrow T_2 \\ \rightarrow T_3 \\ \rightarrow T_4 \\ \end{matrix} \quad (3.69)$$

Respectively, the joint trivariate density distribution, according to Figure 3.6 and Eq. 3.66 can be described as:

$$f\left(x_1,x_2,x_3\right)=c_{23|1}\left(F_{2|1}\left(x_2|x_1\right),F_{3|1}\left(x_3|x_1\right);\theta_{23}\right)c_{13}\left(F_1\left(x_1\right),F_3\left(x_3\right);\theta_{13}\right)\\ c_{12}\left(F_1\left(x_1\right),F_2\left(x_2\right);\theta_{12}\right)f_3\left(x_3\right)f_2\left(x_2\right)f_1\left(x_1\right) \tag{3.70}$$

and it could be extended to four variables as follows:

$$f\left(x_1,x_2,x_3,x_4\right)=\\ c_{34|12}\left(F_{3|12}\left(x_3|x_1,x_2\right),F_{4|12}\left(x_4|x_1,x_2\right);\theta_{35}\right)c_{24|1}\left(F_{2|1}\left(x_2|x_1\right),F_{4|1}\left(x_4|x_1\right);\theta_{24}\right)\\ c_{23|1}\left(F_{2|1}\left(x_2|x_1\right),F_{3|1}\left(x_3|x_1\right);\theta_{23}\right)c_{14}\left(F_1\left(x_1\right),F_4\left(x_4\right);\theta_{14}\right)\\ c_{13}\left(F_1\left(x_1\right),F_3\left(x_3\right);\theta_{13}\right)c_{12}\left(F_1\left(x_1\right),F_2\left(x_2\right);\theta_{12}\right)f_4\left(x_4\right)f_3\left(x_3\right)f_2\left(x_2\right)f_1\left(x_1\right), \tag{3.71}$$

and similarly, to five variables:

$$f\left(x_1,x_2,x_3,x_4,x_5\right)=\\ c_{23|145}\left(F_{2|145}\left(x_2|x_1,x_4,x_5\right),F_{3|145}\left(x_3|x_1,x_4,x_5\right);\theta_{45}\right)\\ c_{35|12}\left(F_{3|12}\left(x_3|x_1,x_2\right),F_{5|12}\left(x_5|x_1,x_2\right);\theta_{35}\right)\\ c_{24|15}\left(F_{2|15}\left(x_2|x_1,x_5\right),F_{4|15}\left(x_4|x_1,x_5\right);\theta_{34}\right)\\ c_{14|5}\left(F_{1|5}\left(x_1|x_5\right),F_{4|5}\left(x_4|x_5\right);\theta_{25}\right)c_{13|5}\left(F_{2|5}\left(x_1|x_5\right),F_{3|5}\left(x_3|x_5\right);\theta_{24}\right)\\ c_{12|5}\left(F_{1|5}\left(x_1|x_5\right),F_{2|5}\left(x_2|x_5\right);\theta_{23}\right)c_{54}\left(F_5\left(x_5\right),F_4\left(x_4\right);\theta_{15}\right)c_{53}\left(F_5\left(x_5\right),F_3\left(x_3\right);\theta_{14}\right)\\ c_{52}\left(F_5\left(x_5\right),F_2\left(x_2\right);\theta_{13}\right)c_{51}\left(F_5\left(x_5\right),F_1\left(x_1\right);\theta_{12}\right)\\ f_5\left(x_5\right)f_4\left(x_4\right)f_3\left(x_3\right)f_2\left(x_2\right)f_1\left(x_1\right). \tag{3.72}$$

3.4.3. Simulation through copulas

Once the best copula is constructed, a new sample can be generated that validates this model and simulates the associated variables. The methodology of simulation through copulas is based on Rosenblatt transform and can be described through the methodologies of De Michele et al. (2007), Aas et al. (2009) and the most recent work of Stöber and Czado (2017) by following the PCC method and the C-Vine copulas. Following these methodologies and starting with a known sample $w_i=(w_1,\ldots,w_d)$ a new sample $u_i=(u_1,\ldots,u_d)$ is generated through the copulas, where $u_i,w_i \sim U\left[0,1\right]$, $i=1,\ldots,d$. In the case of coastal storms, the application of simulation is accomplished in five dimensions by using the coastal storm parameters (H, T, D, I, E) for a specific location.

The three methodologies (De Michele et al.,2007; Aas et al., 2009; Stöber and Czado, 2007) are based on the pair copula construction method. Therefore, similarly to the construction method of C-Vine (Fig. 3.7), they construct the high-dimensional copulas

through the combination of low-dimensional copulas and the *h-functions*. More specifically, for the above three simulation algorithms the conditional distribution functions (Czado, 2019; Zhang and Singh, 2019c) are described by the following Equation:

$$F\left(x_j\middle|x_1,...,x_{j-1}\right)=\frac{\partial C_{j,j-1|1,...,j-2}\left(F\left(x_j\middle|x_1,...,x_{j-2}\right),F\left(x_{j-1}\middle|x_1,...,x_{j-2}\right)\right)}{\partial F\left(x_{j-1}\middle|x_1,...,x_{j-2}\right)}\ . \tag{3.73}$$

The ascending order of variables is not mandatory but depends on the vine structure (Fig. 3.6), for instance:

$$F_{4|15}\left(x_4\middle|x_1,x_5\right)=\frac{\partial}{\partial F_{1|5}\left(x_1,x_5\right)}C_{41|5}\left(F_{4|5}\left(x_4,x_5\right),F_{1|5}\left(x_1,x_5\right)\right), \tag{3.74}$$

and similarly, for the copula distribution function:

$$\begin{aligned}C_{4|15}\left(u_4\middle|u_1,u_5\right)&=\frac{\partial}{\partial C_{1|5}\left(u_1,u_5\right)}C_{41|5}\left(C_{4|5}\left(u_4,u_5\right),C_{1|5}\left(u_1,u_5\right)\right)\\&=\frac{\partial}{\partial h_{1|5}\left(u_1,u_5\right)}C_{41|5}\left(h_{4|5}\left(u_4\middle|u_5\right),h_{1|5}\left(u_1\middle|u_5\right)\right)=h_{4|15}\left(h_{4|5}\left(u_4\middle|u_5\right)\middle|h_{1|5}\left(u_1\middle|u_5\right)\right),\end{aligned} \tag{3.75}$$

where $h_{1|5}\left(u_1\middle|u_5\right)=\frac{\partial C_{51}\left(u_1,u_5\right)}{\partial u_5}$, $h_{4|5}\left(u_4\middle|u_5\right)=\frac{\partial C_{54}\left(u_4,u_5\right)}{\partial u_5}$.

Therefore, for higher dimensions, we have the following:

$$\begin{aligned}C_{3|415}\left(u_3\middle|u_4,u_1,u_5\right)&=h_{3|415}\left(C_{3|15}\left(u_3\middle|u_1,u_5\right)\middle|C_{4|15}\left(u_4\middle|u_1,u_5\right)\right)\\&=h_{3|415}\left(h_{3|15}\left(h_{3|5}\left(u_3\middle|u_5\right)\middle|h_{1|5}\left(u_1\middle|u_5\right)\right)\middle|C_{4|15}\left(u_4\middle|u_1,u_5\right)\right).\end{aligned} \tag{3.76}$$

$$\begin{aligned}&C_{2|3415}\left(u_2\middle|u_3,u_4,u_1,u_5\right)=h_{2|3415}\left(C_{2|415}\left(u_2\middle|u_4,u_1,u_5\right)\middle|C_{3|415}\left(u_3\middle|u_4,u_1,u_5\right)\right)=\\&h_{2|3415}\left(h_{2|415}\left(h_{2|15}\left(h_{2|5}\left(u_2\middle|u_5\right)\middle|h_{1|5}\left(u_1\middle|u_5\right)\right)\middle|C_{4|15}\left(u_4\middle|u_1,u_5\right)\right)\middle|C_{3|415}\left(u_3\middle|u_4,u_1,u_5\right)\right).\end{aligned}$$

(3.77)

The required conditional distributions are estimated, as described above, and they are used by the simulation algorithms to reach the simulation of variables $u_i=(u_1,\ldots,u_5)$. In practice, three algorithms (A, B, and C) are developed extending in five dimensions the work of De Michele et al., (2007), Aas et al. (2009), and Stöber and Czado (2007). The three simulation algorithms are presented with distinct steps, as described below, and require a lot of mathematical computations. These computations are less for the algorithms of Aas et al. (2009) and Stöber and Czado (2007) that follow the C-Vine copula (Fig. 3.6c) instead of the third algorithm based on the work of De Michele et al., (2007) that is more complicated.

Algorithm A, which is the extension of the simulation algorithm of Stöber and Czado (2017) in five dimensions, is expanded as follows (given the parameters of Eq. 3.69) :

$$\begin{aligned} &\Rightarrow u_5 = v_{11} = w_5 \\ &\quad v_{22} = w_4 \\ &\qquad v_{12} = h_{2|1}^{-1}\left(v_{22}\middle|v_{11}\right) = h^{-1}\left(w_4\middle|w_5,\theta_{12}\right) \Rightarrow u_4 = v_{12} \end{aligned} \tag{3.78}$$

$$\begin{aligned} &v_{33} = w_1 \\ &\qquad v_{23} = h_{3|2}^{-1}\left(v_{33}\middle|v_{22}\right) = h^{-1}\left(w_1\middle|w_4,\theta_{23}\right) \\ &\qquad v_{13} = h_{3|1}^{-1}\left(v_{23}\middle|v_{11}\right) = h^{-1}\left(v_{23}\middle|w_5,\theta_{13}\right) \Rightarrow u_1 = v_{13} \end{aligned} \tag{3.79}$$

$$\begin{aligned} &v_{44} = w_3 \\ &\qquad v_{34} = h_{4|3}^{-1}\left(v_{44}\middle|v_{33}\right) = h^{-1}\left(w_3\middle|w_1,\theta_{34}\right) \\ &\qquad v_{24} = h_{4|2}^{-1}\left(v_{34}\middle|v_{22}\right) = h^{-1}\left(v_{34}\middle|w_4,\theta_{24}\right) \\ &\qquad v_{14} = h_{4|1}^{-1}\left(v_{24}\middle|v_{11}\right) = h^{-1}\left(v_{24}\middle|w_5,\theta_{14}\right) \Rightarrow u_3 = v_{14} \end{aligned} \tag{3.80}$$

$$\begin{aligned} &v_{55} = w_2 \\ &\qquad v_{45} = h_{5|4}^{-1}\left(v_{55}\middle|v_{44}\right) = h^{-1}\left(w_2\middle|w_3,\theta_{45}\right) \\ &\qquad v_{35} = h_{5|3}^{-1}\left(v_{45}\middle|v_{33}\right) = h^{-1}\left(v_{45}\middle|w_1,\theta_{35}\right) \\ &\qquad v_{25} = h_{5|2}^{-1}\left(v_{35}\middle|v_{22}\right) = h^{-1}\left(v_{35}\middle|w_4,\theta_{25}\right) \\ &\qquad v_{15} = h_{5|1}^{-1}\left(v_{25}\middle|v_{11}\right) = h^{-1}\left(v_{25}\middle|w_5,\theta_{15}\right) \Rightarrow u_2 = v_{15}\,. \end{aligned} \tag{3.81}$$

The *h-functions* are described in Eqs. 3.35, 3.36 and by following Czado (2019) can be given as follows:

$$h_{i|j}\left(u_i\middle|u_j;\theta_{ij}\right) = \frac{\partial C_{ij}\left(u_i,u_j;\theta_{ij}\right)}{\partial u_j} \text{ and } h_{j|i}\left(u_j\middle|u_i;\theta_{ij}\right) = \frac{\partial C_{ij}\left(u_i,u_j;\theta_{ij}\right)}{\partial u_i}\,. \tag{3.82}$$

Using the same abbreviation for copula parameters (Eq. 3.69), the **Algorithm B** is the extension of the simulation algorithm of Aas et al. (2009) and described as:

$$\begin{aligned} &\Rightarrow u_5 = v_{11} = w_5 \\ &\quad v_{21} = w_4 \\ &\qquad v_{21} = h^{-1}\left(v_{21}\middle|v_{11}\right) = h_{4|5}^{-1}\left(w_4\middle|u_5,\theta_{12}\right) \Rightarrow u_4 = v_{21} \\ &\qquad v_{22} = h\ \left(v_{21}\middle|v_{11}\right) = h_{4|5}\left(u_4\middle|u_5,\theta_{12}\right) \end{aligned} \tag{3.83}$$

$$\begin{aligned} &v_{31} = w_1 \\ &\qquad v_{31} = h^{-1}\left(v_{31}\middle|v_{22}\right) = h_{1|45}^{-1}\left(w_1\middle|v_{22},\theta_{23}\right) \\ &\qquad v_{31} = h^{-1}\left(v_{31}\middle|v_{11}\right) = h_{1|5}^{-1}\left(v_{31}\middle|u_5,\theta_{13}\right) \Rightarrow u_1 = v_{31} \\ &\qquad v_{32} = h\ \left(v_{31}\middle|v_{11}\right) = h_{1|5}\left(u_1\middle|u_5,\theta_{13}\right) \\ &\qquad v_{33} = h\ \left(v_{32}\middle|v_{22}\right) = h_{1|45}\left(v_{32}\middle|v_{22},\theta_{23}\right) \end{aligned} \tag{3.84}$$

$$
\begin{aligned}
&v_{41} = w_3 \\
&\quad v_{41} = h^{-1}\left(v_{41}\middle|v_{33}\right) = h^{-1}_{3|415}\left(w_3\middle|v_{33},\theta_{34}\right) \\
&\quad v_{41} = h^{-1}\left(v_{41}\middle|v_{22},\theta_{24}\right) \\
&\quad v_{41} = h^{-1}\left(v_{41}\middle|v_{11}\right) = h^{-1}_{3|5}\left(v_{41}\middle|u_5,\theta_{14}\right) \Rightarrow u_3 = v_{41} \\
&\quad v_{42} = h\ \left(v_{41}\middle|v_{11}\right) = h_{3|5}\left(u_3\middle|u_5,\theta_{14}\right) \\
&\quad v_{43} = h\ \left(v_{42}\middle|v_{22},\theta_{24}\right) \\
&\quad v_{44} = h\ \left(v_{43}\middle|v_{33},\theta_{34}\right)
\end{aligned}
\tag{3.85}
$$

$$
\begin{aligned}
&v_{51} = w_2 \\
&\quad v_{51} = h^{-1}\left(v_{51}\middle|v_{44}\right) = h^{-1}_{2|3415}\left(w_2\middle|v_{44},\theta_{45}\right) \\
&\quad v_{51} = h^{-1}\left(v_{51}\middle|v_{33},\theta_{35}\right) \\
&\quad v_{51} = h^{-1}\left(v_{51}\middle|v_{22},\theta_{25}\right) \\
&\quad v_{51} = h^{-1}\left(v_{51}\middle|v_{11}\right) = h^{-1}_{2|5}\left(w_2\middle|u_5,\theta_{15}\right) \Rightarrow u_2 = v_{51}.
\end{aligned}
\tag{3.86}
$$

Finally, following the copula theory and the properties of bivariate copula derivatives (Schepsmeier and Stöber, 2014), the **Algorithm C** based on the work of De Michele et al. (2007) is described as follows:

1st variable: $\Rightarrow u_1 = w_1$

2nd variable: $\Rightarrow u_2 = h^{-1}_{2|1}\left(w_2\middle|w_1\right) = G^{-1}_2\left(w_2\middle|w_1\right),$ (3.87)

given that $G_2\left(w_2\middle|w_1\right) = P\left(W_2 \le w_2\middle|W_1 = w_1\right) = \dfrac{\partial C_{12}\left(w_1,w_2\right)}{\partial w_1} = h_{2|1}\left(w_2\middle|w_1\right).$ (3.88)

3rd variable: $k_1 = h_{1|2}\left(w_1\middle|w_2\right) = \dfrac{\partial C_{12}(w_1,w_2)}{\partial w_2},$ (3.89)

$$m_1 = h_{3|2}\left(w_3\middle|w_2\right) = \frac{\partial C_{23}(w_2,w_3)}{\partial w_2}. \tag{3.90}$$

$$\Rightarrow u_3 = h^{-1}_{3|1}\left(m_1\middle|k_1\right) = G^{-1}_3\left(w_3\middle|w_1,w_2\right), \tag{3.91}$$

given that $G_3\left(w_3\middle|w_1,w_2\right) = P\left(W_3 \le w_3\middle|W_1 = w_1, W_2 = w_2\right) =$

$$\frac{\dfrac{\partial^2 C(w_1,w_2,w_3)}{\partial w_1 \partial w_2}}{\dfrac{\partial^2 C_{12}(w_1,w_2)}{\partial w_1 \partial w_2}} = \frac{\varphi}{\dfrac{\partial^2 C_{12}(w_1,w_2)}{\partial w_1 \partial w_2}} = \frac{\partial C_{13}\left(k_1,m_1\right)}{\partial k_1} = h_{3|1}\left(m_1\middle|k_1\right) \tag{3.92}$$

and $\varphi = \dfrac{\partial^2 C(w_1,w_2,w_3)}{\partial w_1 \partial w_2} = \dfrac{\partial C_{13}\left(\dfrac{\partial C_{12}(w_1,w_2)}{\partial w_2}, \dfrac{\partial C_{23}(w_2,w_3)}{\partial w_2}\right)}{\partial u_1} =$

$$= \frac{\partial C_{13}\left(k_1, m_1\right)}{\partial u_1} = \frac{\partial C_{13}\left(k_1, m_1\right)}{\partial k_1} \cdot \frac{\partial k_1}{\partial u_1} = \frac{\partial C_{13}\left(k_1, m_1\right)}{\partial k_1} \cdot \frac{\partial^2 C_{12}(w_1, w_2)}{\partial w_1 \partial w_2}. \tag{3.93}$$

4th variable: $\psi_1 = \dfrac{\partial^2 C(w_1, w_2, w_3)}{\partial w_2 \partial w_3} = \dfrac{\partial C_{13}\left(\dfrac{\partial C_{12}(w_1, w_2)}{\partial w_2}, \dfrac{\partial C_{23}(w_2, w_3)}{\partial w_2}\right)}{\partial w_3} =$

$$\frac{\partial C_{13}\left(k_1, m_1\right)}{\partial w_3} = \frac{\partial C_{13}\left(k_1, m_1\right)}{\partial m_1} \frac{\partial m_1}{\partial w_3} = h_{1|3}\left(k_1 \middle| m_1\right) \frac{\partial^2 C_{23}\left(w_2, w_3\right)}{\partial w_2 \partial w_3} = h_{1|3}\left(k_1 \middle| m_1\right) \frac{\partial h_{3|2}\left(w_3 \middle| w_2\right)}{\partial w_3}. \tag{3.94}$$

$$m_2 = \frac{\partial C_{23}(w_2, w_3)}{\partial w_3} = h_{2|3}\left(w_2 \middle| w_3\right), \tag{3.95}$$

$$k_2 = \frac{\partial C_{34}(w_3, w_4)}{\partial w_3} = h_{4|3}\left(w_4 \middle| w_3\right), \tag{3.96}$$

$$\psi_2 = \frac{\partial^2 C(w_2, w_3, w_4)}{\partial w_2 \partial w_3} = \frac{\partial C_{24}\left(\dfrac{\partial C_{23}(w_2, w_3)}{\partial w_3}, \dfrac{\partial C_{34}(w_3, w_4)}{\partial w_3}\right)}{\partial w_2} = \frac{\partial C_{24}\left(m_2, k_2\right)}{\partial w_2} = \tag{3.97}$$

$$\frac{\partial C_{24}\left(m_2, k_2\right)}{\partial m_2} \frac{\partial m_2}{\partial w_2} = h_{4|2}\left(k_2 \middle| m_2\right) \frac{\partial^2 C_{23}\left(w_2, w_3\right)}{\partial w_2 \partial w_3} = h_{4|2}\left(k_2 \middle| m_2\right) \frac{\partial h_{2|3}\left(w_2 \middle| w_3\right)}{\partial w_2}$$

$$\Rightarrow u_4 = h_{4|1}^{-1}\left(\psi_2 \middle| \psi_1\right) = G_4^{-1}\left(w_4 \middle| w_1, w_2, w_3\right), \tag{3.98}$$

given that $G_4\left(w_4 \middle| w_1, w_2, w_3\right) = P\left(W_4 \le w_4 \middle| W_1 = w_1, W_2 = w_2, W_3 = w_3\right) =$

$$\frac{\dfrac{\partial^3 C\left(w_1, w_2, w_3, w_4\right)}{\partial w_1 \partial w_2 \partial w_3}}{\dfrac{\partial^3 C\left(w_1, w_2, w_3\right)}{\partial w_1 \partial w_2 \partial w_3}} = \frac{\dfrac{\partial^3 C\left(w_1, w_2, w_3, w_4\right)}{\partial w_1 \partial w_2 \partial w_3}}{\dfrac{\partial}{\partial w_3}\left(\dfrac{\partial^2 C\left(w_1, w_2, w_3\right)}{\partial w_1 \partial w_2}\right)} = \frac{\psi}{\dfrac{\partial \varphi}{\partial w_3}} = \tag{3.99}$$

$$\frac{\partial C_{14}\left(\psi_1, \psi_2\right)}{\partial \psi_1} = h_{4|1}\left(\psi_2 \middle| \psi_1\right),$$

and $\psi = \dfrac{\partial^3 C\left(w_1, w_2, w_3, w_4\right)}{\partial w_1 \partial w_2 \partial w_3} = \dfrac{\partial C_{14}\left(\dfrac{\partial^2 C(w_1, w_2, w_3)}{\partial w_2 \partial w_3}, \dfrac{\partial^2 C(w_2, w_3, w_4)}{\partial w_2 \partial w_3}\right)}{\partial w_1}$

$$= \frac{\partial C_{14}\left(\psi_1, \psi_2\right)}{\partial w_1} = \frac{\partial C_{14}\left(\psi_1, \psi_2\right)}{\partial \psi_1} \cdot \frac{\partial \psi_1}{\partial w_1} = \tag{3.100}$$

$$\frac{\partial C_{14}\left(\psi_1, \psi_2\right)}{\partial \psi_1} \cdot \frac{\partial}{\partial w_1}\left(\frac{\partial^2 C(w_1, w_2, w_3)}{\partial w_2 \partial w_3}\right) = \frac{\partial C_{14}\left(\psi_1, \psi_2\right)}{\partial \psi_1} \cdot \frac{\partial \varphi}{\partial w_3}.$$

5th variable: $$q_1 = \frac{\partial^3 C(w_1,w_2,w_3,w_4)}{\partial w_2 \partial w_3 \partial w_4} = \frac{\partial C_{14}\left(\frac{\partial^2 C(w_1,w_2,w_3)}{\partial w_2 \partial w_3}, \frac{\partial^2 C(w_2,w_3,w_4)}{\partial w_2 \partial w_3}\right)}{\partial w_4}$$

$$= \frac{\partial C_{14}\left(\psi_1,\psi_2\right)}{\partial w_4} = \frac{\partial C_{14}\left(\psi_1,\psi_2\right)}{\partial \psi_2}\frac{\partial \psi_2}{\partial w_4} = h_{1|4}\left(\psi_1\middle|\psi_2\right)\frac{\partial^2 C_{24}(m_2,k_2)}{\partial w_2 \partial w_4}. \quad (3.101)$$

$$g_1 = \frac{\partial^2 C(w_2,w_3,w_4)}{\partial w_3 \partial w_4} = \frac{\partial C_{24}\left(\frac{\partial C_{23}(w_2,w_3)}{\partial w_3}, \frac{\partial C_{34}(w_3,w_4)}{\partial w_3}\right)}{\partial w_4} = \frac{\partial C_{24}\left(m_2,k_2\right)}{\partial w_4} \quad (3.102)$$
$$= \frac{\partial C_{24}\left(m_2,k_2\right)}{\partial k_2}\frac{\partial k_2}{\partial w_4} = h_{2|4}\left(m_2\middle|k_2\right)\frac{\partial^2 C_{34}(w_3,w_4)}{\partial w_3 \partial w_4} = h_{2|4}\left(m_2\middle|k_2\right)\frac{\partial h_{4|3}\left(w_4\middle|w_3\right)}{\partial w_3}$$

$$k_3 = \frac{\partial C_{34}(w_3,w_4)}{\partial w_4} = h_{3|4}\left(w_3\middle|w_4\right) \quad (3.103)$$

$$m_3 = \frac{\partial C_{45}(w_4,w_5)}{\partial w_4} = h_{5|4}\left(w_5\middle|w_4\right) \quad (3.104)$$

$$g_2 = \frac{\partial^2 C(w_3,w_4,w_5)}{\partial w_3 \partial w_4} = \frac{\partial C_{35}\left(\frac{\partial C_{34}(w_3,w_4)}{\partial w_4}, \frac{\partial C_{45}(w_4,w_5)}{\partial w_4}\right)}{\partial w_3} = \frac{\partial C_{35}\left(k_3,m_3\right)}{\partial w_3} \quad (3.105)$$
$$= \frac{\partial C_{35}\left(k_3,m_3\right)}{\partial k_3}\frac{\partial k_3}{\partial w_3} = h_{5|3}\left(m_3\middle|k_3\right)\frac{\partial^2 C_{34}(w_3,w_4)}{\partial w_3 \partial w_4} = h_{5|3}\left(m_3\middle|k_3\right)\frac{\partial h_{3|4}\left(w_3\middle|w_4\right)}{\partial w_3},$$

$$q_2 = \frac{\partial^3 C(w_2,w_3,w_4,w_5)}{\partial w_2 \partial w_3 \partial w_4} = \frac{\partial C_{25}\left(\frac{\partial^2 C(w_2,w_3,w_4)}{\partial w_3 \partial w_4}, \frac{\partial^2 C(w_3,w_4,w_5)}{\partial w_3 \partial w_4}\right)}{\partial w_2} = \quad (3.106)$$
$$= \frac{\partial C_{25}\left(g_1,g_2\right)}{\partial w_2} = \frac{\partial C_{25}\left(g_1,g_2\right)}{\partial g_1}\frac{\partial g_1}{\partial w_2} = h_{5|2}\left(g_2\middle|g_1\right)\frac{\partial^2 C_{24}(m_2,k_2)}{\partial w_2 \partial w_4}.$$

$$\Rightarrow u_5 = h_{5|1}^{-1}\left(q_2\middle|q_1\right) = G_5^{-1}\left(w_5\middle|w_1,w_2,w_3,w_4\right), \quad (3.107)$$

given that $G_5\left(w_5\middle|w_1,w_2,w_3,w_4\right) = P\left(W_5 \le w_5\middle|W_1 = w_1, W_2 = w_2, W_3 = w_3, W_4 = w_4\right)$

$$= \frac{\frac{\partial^4 C\left(w_1,w_2,w_3,w_4,w_5\right)}{\partial w_1 \partial w_2 \partial w_3 \partial w_4}}{\frac{\partial^4 C\left(w_1,w_2,w_3,w_4\right)}{\partial w_1 \partial w_2 \partial w_3 \partial w_4}} = \frac{\frac{\partial^4 C\left(w_1,w_2,w_3,w_4,w_5\right)}{\partial w_1 \partial w_2 \partial w_3 \partial w_4}}{\frac{\partial}{\partial w_4}\left(\frac{\partial^3 C\left(w_1,w_2,w_3,w_4\right)}{\partial w_1 \partial w_2 \partial w_3}\right)} \quad (3.108)$$
$$= \frac{q}{\frac{\partial \psi}{\partial u_4}} = \frac{\partial C_{15}\left(q_1,q_2\right)}{\partial q_1} = h_{5|1}\left(q_2\middle|q_1\right)$$

$$\text{and } q=\frac{\partial^4 C\left(w_1,w_2,w_3,w_4,w_5\right)}{\partial w_1\partial w_2\partial w_3\partial w_4}=\frac{\partial C_{15}\left(\dfrac{\partial^3 C(w_1,w_2,w_3,w_4)}{\partial w_2\partial w_3\partial w_4},\dfrac{\partial^3 C(w_2,w_3,w_4,w_5)}{\partial w_2\partial w_3\partial w_4}\right)}{\partial w_1}$$

$$\begin{aligned}&=\frac{\partial C_{15}\left(q_1,q_2\right)}{\partial w_1}=\frac{\partial C_{15}\left(q_1,q_2\right)}{\partial q_1}\frac{\partial q_1}{\partial w_1}\\&=\frac{\partial C_{15}\left(q_1,q_2\right)}{\partial q_1}\frac{\partial}{\partial w_1}\left(\frac{\partial^3 C(w_1,w_2,w_3,w_4)}{\partial w_2\partial w_3\partial w_4}\right)=\frac{\partial C_{15}\left(q_1,q_2\right)}{\partial q_1}\frac{\partial \psi}{\partial w_4}.\end{aligned}\tag{3.109}$$

The three simulation algorithms are applied to five coastal storm parameters comparing their efficiency. After simulation, the final produced sample $u=\left(u_1,u_2,u_3,u_4,u_5\right)\in\left[0,1\right]$ should be transformed in the real domain $\left(x_1,x_2,x_3,x_4,x_5\right)$ using the probability integral transform and the inverse of marginal distribution functions or the empirical distribution functions, as described below:

$$\left(x_1,x_2,x_3,x_4,x_5\right)=\left(F_1^{-1}\left(u_1\right),F_2^{-1}\left(u_2\right),F_3^{-1}\left(u_3\right),F_4^{-1}\left(u_4\right),F_5^{-1}\left(u_5\right)\right).\tag{3.110}$$

3.4.4. Joint conditional functions

Considering the conditional probabilities of Eqs. 3.51 - 3.61, the high-dimensional conditional distributions $F\left(x_i\middle|x_1,\ldots,x_{i\text{-}1}\right)=P\left(X_i\le x_i\middle|X_1\le x_1,\ldots,X_{i\text{-}1}\le x_{i\text{-}1}\right)$ can be estimated through copulas and especially through C-Vine copulas. Similarly, the joint distribution function is described as follows:

$$F\left(x_1,\ldots,x_d\right)=P\left(X_1\le x_1,\ldots,X_d\le x_d\right)=C\left(U_1\le u_1,\ldots,U_d\le u_d\right).\tag{3.111}$$

The joint conditional functions are estimated and consequently, they are incorporated into the coastal storm return periods.

The **joint conditional distribution function** (jcdf) is easily described through the pair-copula decomposition and the selected C-Vine structure (Fig. 3.6). The jcdf up to five dimensions are described thoroughly by Zhang and Singh (2019c). In the case of two variables X_1, X_2, the jcdf are defined as follows:

$F\left(x_1,x_2\right)=P\left(X_2\le x_2\middle|X_1\le x_1\right)F_1\left(x_1\right)$ or $P\left(X_1\le x_1\middle|X_2\le x_2\right)F_2\left(x_2\right)$ where the associated conditional probabilities are estimated according to Eq. 3.51. For three or four variables, a possible C-vine structure is described in Figure 3.6(a) and 3.6(b), respectively. According to the trees T_1, T_2, T_3, the joint distributions $F\left(x_1,x_2,x_3\right)$ and

$F\left(x_1,x_2,x_3,x_4\right)$ can be estimated through the lower dimension probabilities. Since the procedure is repeated, only the case of five variables is presented below.

For instance, starting with the first tree T_1 of a typical C-Vine (Fig. 3.6c), the bivariate conditional probabilities can be estimated based on Eq. 3.51 as follows:

$$\begin{aligned} &P\left(X_1 \le x_1 \middle| X_5 \le x_5\right) = \frac{C_{51}\left(u_1,u_5\right)}{u_5},\ P\left(X_2 \le x_2 \middle| X_5 \le x_5\right) = \frac{C_{52}\left(u_2,u_5\right)}{u_5}, \\ &P\left(X_3 \le x_3 \middle| X_5 \le x_5\right) = \frac{C_{53}\left(u_3,u_5\right)}{u_5},\ P\left(X_4 \le x_4 \middle| X_5 \le x_5\right) = \frac{C_{54}\left(u_4,u_5\right)}{u_5}. \end{aligned} \tag{3.112}$$

For brevity, these equations can be simplified without mentioning the associated parameters θ, as follows:

$$P_{1|5} = \frac{C\left(u_1,u_5\right)}{u_5},\ P_{2|5} = \frac{C\left(u_2,u_5\right)}{u_5},\ P_{3|5} = \frac{C\left(u_3,u_5\right)}{u_5},\ P_{4|5} = \frac{C\left(u_4,u_5\right)}{u_5}. \tag{3.113}$$

Based on tree T_2 and following the same abbreviation, the probability distributions can be estimated:

$$\begin{aligned} P_{12|5} &= P\left(X_1 \le x_1, X_2 \le x_2 \middle| X_5 \le x_5\right) = C_{12|5}\left(U_1 \le u_1, U_2 \le u_2 \middle| U_5 \le u_5\right) = \\ &C_{12|5}\left(C_{1|5}\left(U_1 \le u_1 \middle| U_2 \le u_2\right), C_{2|5}\left(U_2 \le u_2 \middle| U_5 \le u_5\right)\right) = C_{12|5}\left(P_{1|5}, P_{2|5}\right). \end{aligned} \tag{3.114}$$

And similarly,

$$P_{13|5} = P\left(X_1 \le x_1, X_3 \le x_3 \middle| X_5 \le x_5\right) = C_{13|5}\left(P_{1|5}, P_{3|5}\right), \tag{3.115}$$

$$P_{41|5} = P\left(X_4 \le x_4, X_1 \le x_1 \middle| X_5 \le x_5\right) = C_{41|5}\left(P_{4|5}, P_{1|5}\right). \tag{3.116}$$

Based on the above conditional copulas, other probability distributions for three variables can be estimated:

$$\begin{aligned} P_{2|15} &= P\left(X_2 \le x_2 \middle| X_1 \le x_1, X_5 \le x_5\right) = C_{2|15}\left(U_2 \le u_2 \middle| U_1 \le u_1, U_5 \le u_5\right) = \\ &\frac{C_{12|5}\left(\frac{C_{51}\left(u_1,u_5\right)}{u_5}, \frac{C_{52}\left(u_2,u_5\right)}{u_5}\right)}{\frac{C_{51}\left(u_1,u_5\right)}{u_5}} = \frac{C_{12|5}\left(P_{1|5},P_{2|5}\right)}{P_{1|5}}. \end{aligned} \tag{3.117}$$

$$\begin{aligned} P_{3|15} &= P\left(X_3 \le x_3 \middle| X_1 \le x_1, X_5 \le x_5\right) \\ &= C_{3|15}\left(U_3 \le u_3 \middle| U_1 \le u_1, U_5 \le u_5\right) = \frac{C_{13|5}\left(P_{1|5},P_{3|5}\right)}{P_{1|5}}. \end{aligned} \tag{3.118}$$

$$P_{4|15} = P\left(X_4 \le x_4 \middle| X_1 \le x_1, X_5 \le x_5\right) = C_{4|15}\left(U_4 \le u_4 \middle| U_1 \le u_1, U_5 \le u_5\right) = \frac{C_{41|5}\left(P_{4|5}, P_{1|5}\right)}{P_{1|5}}. \tag{3.119}$$

Based on the tree T_3, we have the following

$$\begin{aligned} P_{42|15} &= P\left(X_4 \le x_4, X_2 \le x_2 \middle| X_1 \le x_1, X_5 \le x_5\right) \\ &= C_{42|15}\left(U_4 \le u_4, U_2 \le u_2 \middle| U_1 \le u_1, U_5 \le u_5\right) \\ &= C_{42|15}\left(C_{4|15}\left(U_4 \le u_4 \middle| U_1 \le u_1, U_5 \le u_5\right), C_{2|15}\left(U_2 \le u_2 \middle| U_1 \le u_1, U_5 \le u_5\right)\right) \\ &= C_{42|15}\left(P_{4|15}, P_{2|15}\right). \end{aligned} \tag{3.120}$$

$$\begin{aligned} P_{3|415} &= P\left(X_3 \le x_3 \middle| X_4 \le x_4, X_1 \le x_1, X_5 \le x_5\right) \\ &= C_{43|15}\left(P\left(X_3 \le x_3 \middle| X_1 \le x_1, X_5 \le x_5\right), P\left(X_4 \le x_4 \middle| X_1 \le x_1, X_5 \le x_5\right)\right) \\ &= C_{43|15}\left(P_{3|15}, P_{4|15}\right). \end{aligned} \tag{3.121}$$

$$\begin{aligned} P_{2|415} &= P\left(X_2 \le x_2 \middle| X_4 \le x_4, X_1 \le x_1, X_5 \le x_5\right) \\ &= C_{42|15}\left(P\left(X_2 \le x_2 \middle| X_1 \le x_1, X_5 \le x_5\right), P\left(X_4 \le x_4 \middle| X_1 \le x_1, X_5 \le x_5\right)\right) \\ &= C_{42|15}\left(P_{2|15}, P_{4|15}\right). \end{aligned} \tag{3.122}$$

Finally, for five variables and according to the tree T_4, we have the following:

$$\begin{aligned} P_{32|415} &= P\left(X_3 \le x_3, X_2 \le x_2 \middle| X_4 \le x_4, X_1 \le x_1, X_5 \le x_5\right) = \\ &C_{32|415}\left(\begin{array}{l} P\left(X_3 \le x_3 \middle| X_4 \le x_4, X_1 \le x_1, X_5 \le x_5\right), \\ \qquad C_{2|415}\left(X_2 \le x_2 \middle| X_4 \le x_4, X_1 \le x_1, X_5 \le x_5\right) \end{array}\right) \\ &= C_{32|415}\left(P_{3|415}, P_{2|415}\right). \end{aligned} \tag{3.123}$$

Hence **the joint distribution function for five dimensions** can be described as follows

$$\begin{aligned} F\left(x_1, x_2, x_3, x_4, x_5\right) &= P\left(X_1 \le x_1, X_2 \le x_2, X_3 \le x_3, X_4 \le x_4, X_5 \le x_5\right) \\ &= P\left(X_3 \le x_3, X_2 \le x_2 \middle| X_4 \le x_4, X_1 \le x_1, X_5 \le x_5\right) \cdot P\left(x_4, x_1, x_5\right) \\ &= P_{32|415} \cdot P\left(x_4, x_1, x_5\right) \end{aligned} \tag{3.124}$$

where,

$$\begin{aligned} &F\left(x_4, x_1, x_5\right) = P\left(x_4, x_1, x_5\right) = \\ &P\left(X_4 \le x_4, X_1 \le x_1, X_5 \le x_5\right) = P\left(X_4 \le x_4, X_1 \le x_1 \middle| X_5 \le x_5\right) P\left(x_5\right) = P_{41|5} \cdot u_5. \end{aligned} \tag{3.125}$$

$$\begin{aligned} &F\left(x_1, x_2, x_4, x_5\right) = P\left(X_1 \le x_1, X_2 \le x_2, X_4 \le x_4, X_5 \le x_5\right) = \\ &P\left(X_4 \le x_4, X_2 \le x_2 \middle| X_5 \le x_5, X_1 \le x_1\right) \cdot P\left(x_5, x_1\right) = P_{42|15} \cdot C_{51}\left(u_5, u_1\right) \end{aligned} \tag{3.126}$$

$$\begin{aligned} &\text{and } F\left(x_1, x_3, x_4, x_5\right) = \\ &P\left(X_4 \le x_4, X_3 \le x_3 \middle| X_5 \le x_5, X_1 \le x_1\right) \cdot P\left(x_5, x_1\right) = P_{43|15} \cdot C_{51}\left(u_5, u_1\right). \end{aligned} \tag{3.127}$$

3.4.5. Return periods

The return period denotes the reoccurrence of an event or the average time interval between an upcoming event and the previous one with specific characteristics. It is widely used for events that reoccur, such as cyclones, tsunamis, rainfalls, floods, and storms. In coastal engineering, coastal storms affect the coastal zones, the reliability, and the lifetime of coastal structures. Hence, the return periods of coastal storms are essential for the design, and they are generally valuable for risk analysis (Corbella and Stretch, 2012b).

Copulas are indicated for the estimation of return periods of multivariate events. Their application in coastal engineering is very common, especially for two variables (De Michele et al., 2007; Salvadori et al., 2014, 2015; Mazas and Hamm, 2017; Li and Liu, 2020; Orcel et al., 2021). Recently, copulas are also used to estimate three-dimensional return periods in hydrology for droughts and floods (Latif and Mustafa, 2020; Mesbahzadeh et al., 2020; Saghafian and Sanginabadi, 2020; Tosunoglu et al., 2020; Zhang et al., 2021). Extending this methodology to four and five dimensions, the high-dimensional return periods of coastal storms can be efficiently estimated through copulas.

The **return period** of an event, with specific characteristics regarding their parameters (e.g., $X_1 > x_1$) and the average time interval (μ) in years between two events, is given by the following equation:

$$T_{(X_1>x_1)} = \frac{\mu}{P\left(X_1 > x_1\right)} = \frac{\mu}{1 - P\left(X_1 \le x_1\right)} = \frac{\mu}{1 - F_1\left(x_1\right)}. \tag{3.128}$$

Hence, the exceedance probability of such event is

$$P\left(X_1 > x_1\right) = \frac{\mu}{T} \tag{3.129}$$

and the non-exceedance probability is described as:

$$F_1\left(x_1\right) = 1 - \frac{\mu}{T}. \tag{3.130}$$

The return period is not always associated with the exceedance probability $P(X_1 > x_1)$ of variables. The denominator of Eq. 3.128 can be replaced by any probability that describes the desirable characteristics of an event, considering the coastal storm parameters as continuous random variables. For the estimation of return periods in higher dimensions, the important probabilities (Eqs. 3.41-3.61) are required and the

symbols $\cup$ and $\cap$ are used when the parameters exceed a specific value simultaneously or not, respectively. In literature, the symbols of union $\cup$ and intersection $\cap$ indicate both “OR” and “AND” cases.

The bivariate and the trivariate cases of return periods (Salvadori, 2004; Salvadori and De Michele, 2004; Salvadori et al., 2011), based on Eqs. 3.41-3.44 can be described as follows:

$$T_{(X_1>x_1\cup X_2>x_2)}=\frac{\mu}{1-P\left(X_1\le x_1,X_2\le x_2\right)}=\frac{\mu}{1-C_{12}\left(u_1,u_2\right)} \tag{3.131}$$

$$T_{(X_1>x_1\cap X_2>x_2)}=\frac{\mu}{P\left(X_1>x_1,X_2>x_2\right)}=\frac{\mu}{1-u_1-u_2+C_{12}\left(u_1,u_2\right)} \tag{3.132}$$

$$T_{(X_1>x_1\cup X_2>x_2\cup X_3>x_3)}=\frac{\mu}{1-P\left(X_1\le x_1,X_2\le x_2,X_3\le x_3\right)}=\frac{\mu}{1-C\left(u_1,u_2,u_3\right)} \tag{3.133}$$

$$\begin{aligned}T_{(X_1>x_1\cap X_2>x_2\cap X_3>x_3)}&=\frac{\mu}{P\left(X_1>x_1,X_2>x_2,X_3>x_3\right)}\\&=\frac{\mu}{1-u_1-u_2-u_3+C_{12}\left(u_1,u_2\right)+C_{13}\left(u_1,u_3\right)+C_{23}\left(u_2,u_3\right)-C\left(u_1,u_2,u_3\right)}.\end{aligned} \tag{3.134}$$

Similarly, Eq. 3.128 is extended to four and five dimensions by substituting the associated probabilities (Eqs. 3.45-3.47).

$$T_{(X_1>x_1\cup X_2>x_2\cup X_3>x_3\cup X_4>x_4)}=\frac{\mu}{1-P\left(X_1\le x_1,X_2\le x_2,X_3\le x_3,X_4\le x_4\right)}=\frac{\mu}{1-C\left(u_1,u_2,u_3,u_4\right)} \tag{3.135}$$

$$\begin{aligned}T_{(X_1>x_1\cap X_2>x_2\cap X_3>x_3\cap X_4>x_4)}&=\frac{\mu}{P\left(X_1>x_1,X_2>x_2,X_3>x_3,X_4>x_4\right)}\\&\frac{\mu}{\begin{aligned}&1-u_1-u_2-u_3-u_5+C_{12}\left(u_1,u_2\right)+C_{13}\left(u_1,u_3\right)+C_{23}\left(u_2,u_3\right)\\&+C_{24}\left(u_2,u_4\right)+C_{34}\left(u_3,u_4\right)-C\left(u_1,u_2,u_3\right)-C\left(u_1,u_2,u_4\right)\\&-C\left(u_1,u_3,u_4\right)-C\left(u_2,u_3,u_4\right)+C\left(u_1,u_2,u_3,u_4\right)\end{aligned}}\end{aligned} \tag{3.136}$$

$$T_{(X_1>x_1\cup X_2>x_2\cup X_3>x_3\cup X_4>x_4\cup X_5>x_5)}=\frac{\mu}{1-P\left(X_1\le x_1,X_2\le x_2,X_3\le x_3,X_4\le x_4,X_5\le x_5\right)}=\frac{\mu}{1-C\left(u_1,u_2,u_3,u_4,u_5\right)} \tag{3.137}$$

$$T_{(X_1>x_1\cap X_2>x_2\cap X_3>x_3\cap X_4>x_4\cap X_5>x_5)}=\frac{\mu}{P\left(X_1>x_1,X_2>x_2,X_3>x_3,X_4>x_4,X_5>x_5\right)}$$

$$= \frac{\mu}{\begin{array}{l} 1-u_1-u_2-u_3-u_4-u_5+C\left(u_1,u_2\right)+C\left(u_1,u_3\right)+C\left(u_1,u_4\right)+C\left(u_1,u_5\right) \\ +C\left(u_2,u_3\right)+C\left(u_1,u_4\right)+C\left(u_2,u_5\right)+C\left(u_3,u_4\right)+C\left(u_3,u_5\right)+C\left(u_4,u_5\right) \\ -C\left(u_1,u_2,u_3\right)-C\left(u_1,u_2,u_4\right)-C\left(u_1,u_2,u_5\right)-C\left(u_1,u_3,u_4\right)-C\left(u_1,u_3,u_5\right) \\ -C\left(u_1,u_4,u_5\right)-\left(u_2,u_3,u_4\right)-C\left(u_2,u_3,u_5\right)-C\left(u_2,u_4,u_5\right)-C\left(u_3,u_4,u_5\right) \\ +C\left(u_1,u_2,u_3,u_4\right)+C\left(u_1,u_2,u_3,u_5\right)+C\left(u_1,u_2,u_4,u_5\right)+C\left(u_1,u_3,u_4,u_5\right) \\ +C\left(u_2,u_3,u_4,u_5\right)-C\left(u_1,u_2,u_3,u_4,u_5\right) \end{array}}. \quad (3.138)$$

Indicatively, using the Eqs. 3.51-3.61, the return periods can be defined as follows:

$$T_{\left(X_1>x_1\middle|X_2\le x_2\right)} = \frac{\mu}{1-P\left(X_1\le x_1\middle|X_2\le x_2\right)} = \frac{\mu}{1-\dfrac{C_{12}\left(u_1,u_2\right)}{u_2}} \quad (3.139)$$

$$T_{\left(X_2>x_2\middle|X_1=x_1\right)} = \frac{\mu}{1-P\left(X_2\le x_2\middle|X_1=x_1\right)} = \frac{\mu}{1-\dfrac{\partial C_{12}\left(u_1,u_2\right)}{\partial u_1}} \quad (3.140)$$

$$T_{\left(X_1>x_1\cup X_2>x_2\cup X_3>x_3\cup X_4>x_4\middle|X_5\le x_5\right)} = \frac{\mu}{1-\dfrac{C\left(u_1,u_2,u_3,u_4,u_5\right)}{u_5}} \quad (3.141)$$

$$T_{\left(X_5>x_5\middle|X_1\le x_1,X_2\le x_2,X_3\le x_3,X_4\le x_4\right)} = \\ = \frac{\mu}{1-P\left(X_5\le x_5\middle|X_1\le x_1,X_2\le x_2,X_3\le x_3,X_4\le x_4\right)} \\ = \frac{\mu}{1-\dfrac{C\left(u_1,u_2,u_3,u_4,u_5\right)}{C\left(u_1,u_2,u_3,u_4\right)}}. \quad (3.142)$$

However, working with the vine copula (Fig. 3.6c), the return periods can be efficiently estimated according to the probabilities which are defined at each tree of C-Vine structure (i.e., Eqs. 3.112-3.121), for instance:

$$T_{\left(X_3\le x_3\middle|X_1\le x_1,X_2\le x_2\right)} = \\ = \frac{\mu}{P\left(X_3\le x_3\middle|X_1\le x_1,X_2\le x_2\right)} = \frac{\mu}{\dfrac{C_{23|1}\left(C_{3|1},C_{2|1};\theta_{23}\right)}{C_{2|1}}} \quad (3.143)$$

$$T_{\left(X_4\le x_4\middle|X_1\le x_1,X_2\le x_2,X_3\le x_3\right)} = \\ = \frac{\mu}{P\left(X_4\le x_4\middle|X_1\le x_1,X_2\le x_2,X_3\le x_3\right)} = \frac{\mu}{C_{34|12}\left(C_{4|12},C_{3|12};\theta_{31}\right)}. \quad (3.144)$$

It should be noted that for the estimation of the return periods, the best-selected copulas for the variables X_1, X_2 are needed, plugging in the estimated copula parameters. Similarly, for three or more variables, the multivariate return periods can be estimated following the structure of high-dimensional C-Vines and the corresponding probabilities.

Chapter 4

Results & discussion

This chapter presents and discusses the results of the coastal storms analysis and their modelling through copulas. The findings are essential for the description of coastal storm activity in the Mediterranean Sea but mainly for the application of copulas in their modelling. The dependence of the associated variables, the simulation of coastal storms, and their return periods can be estimated by following the methodology of the previous Chapter.

The identification of coastal storms as well as their analysis are usually limited to a specific location or a region (e.g., a gulf) and rarely involve more locations. In this case study, 30 locations in the Mediterranean Sea are examined, and information about the thresholds, the annual and monthly frequency of occurrence, the descriptive statistics, and the behaviour of important coastal storm parameters are presented. Furthermore, the relation of coastal storm energy with the wave energy flux, the variance of the wave period and the direction, as well as the shape of coastal storms are discussed below.

The copulas are applied at each event for the wave height and the wave period within the event, or at a specific location for two to five variables that describe a coastal storm (i.e., wave height, wave period, duration, calm period and energy). Instead of the conventional bivariate copulas (e.g., Archimedean or Gaussian) which are usually used for the modelling of the wave height and the wave period, the best-selected copulas are investigated in this thesis among 40 copulas. The two best-selected copulas are described while presenting their characteristics and their efficiency to model the tail dependence.

Similarly, a location-based five-dimensional copula is created following the C-Vine structure by investigating the dependence of each pair of variables.

The simulation of coastal storms is accomplished by utilizing the algorithms A, B, and C as described in the previous Section. The C-Vine copulas are used for the simulation of coastal storms (Algorithms A and B) but also are used to estimate the return periods for two to five dimensions, and the results are compared to other multivariate copulas. The findings highly contribute to the research field due to the extended use of copulas. The results are innovative, especially for high dimensions. The latter is identified when the conventional copulas are compared to the C-Vines.

Finally, the findings of this thesis are discussed with regard to their importance for coastal engineering and their application in harbour and coastal structures design.

4.1. Mediterranean coastal storms

4.1.1. Data and study area

An extensive database of wave measurements is analysed to present a coastal storm activity over the Mediterranean Sea through the frequency of storm occurrence and the statistical analysis of their characteristics. The purpose is to gain a deeper understanding of coastal storm severity, their past activity, and their seasonal variation over the years in a changing climate.

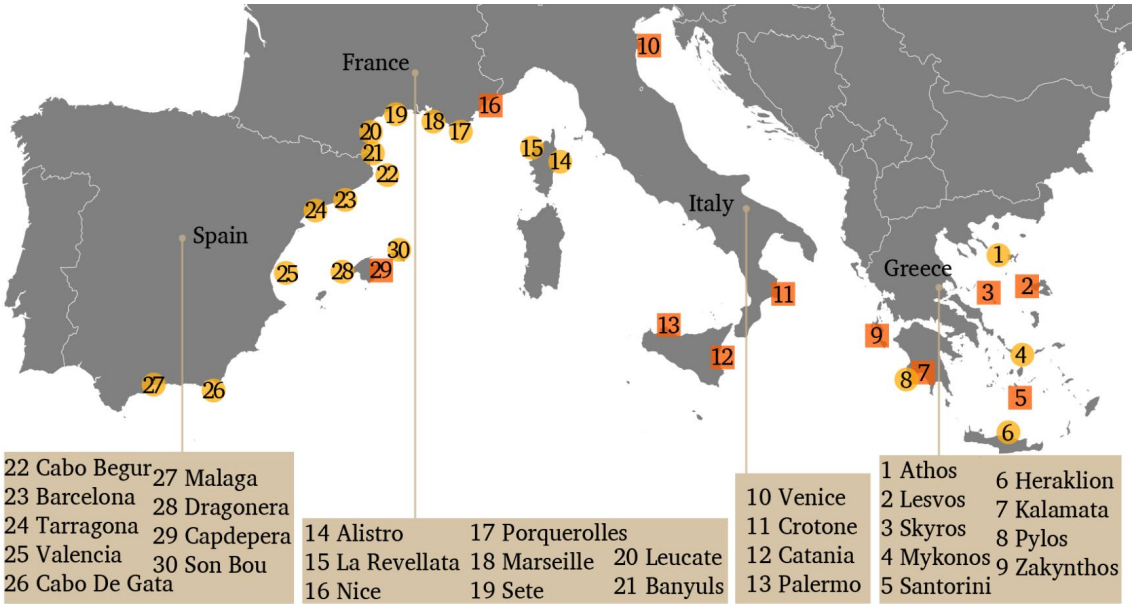

Figure 4.1. Regional description of the buoys' location over the Mediterranean Sea. The squares indicate buoys that are out of order (last check May 13, 2021).

The 30 locations are selected based on the buoys' shortest distance from the coasts (Fig. 4.1) and the description of these stations is presented in Table 4.1, including sampling and regional details. The temporal data coverage - or the period for which data are available - depends on the operation period of buoys, with most of them examined until 30/6/2017. In case more data were available, the examined period was extended up to 31/3/2019 (Fig. 4.2). According to the database of EMODnet, in Italy, only a few buoys are nowadays in operation, and most of the Greek buoys are currently out of order.

The basic input variables in this analysis are the wave height and the wave period. These critical variables have been estimated by the operational centres of data providers, following a spectral analysis or zero-crossing method (OceanSITES, 2015; Copernicus Marine In Situ Tac Data Management Team, 2018). However, the spectral significant wave height and the wave period at the spectral peak, also known as peak period, are preferred, and mentioned below as H and T.

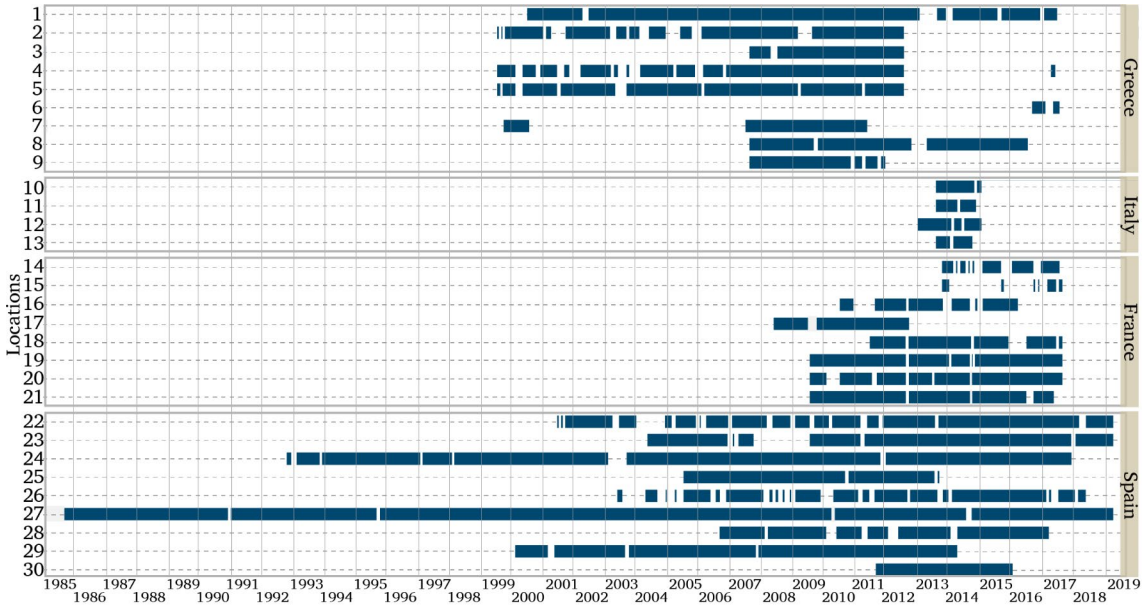

Figure 4.2. Temporal availability and coverage of historical data.

The datasets are carefully scrutinised to eliminate all the errors and missing values. The events with a measurement gap longer than 18 hours are also excluded, considering that the specific buoy might be out of operation for a while. The elapsed time between consecutive measurements, also known as the sampling interval, mainly varies from 0.5 to 3 hours (see Table 4.1). All the estimations are performed in the R language (R Core Team, 2021).

Table 4.1

Coordinates and sampling details of buoys stations for 30 locations in the Mediterranean Sea.

Location		Coordinates [Longitude, Latitude]	Depth [m]	Distance from coast [km]	Covering Period	Duration of record [months]	Sampling Interval [hr]
				Greece			
1	Athos	[24.73° E, 39.97° N]	215	27.7	25/05/2000-31/05/2017	181	3.0
2	Lesvos	[25.80° E, 39.15° N]	120	4.5	29/05/1999-28/07/2012	133	3.0
3	Skyros	[24.46° E, 39.11° N]	83	14.4	28/08/2007-18/07/2012	57	3.0
4	Mykonos	[25.46° E, 37.51° N]	80	5.3	27/05/1999-30/04/2017	132	3.0
5	Santorini	[25.50° E, 36.26° N]	286	9.2	28/05/1999-27/07/2012	141	3.0
6	Heraklion	[25.07° E, 35.43° N]	170	5.1	15/07/2016-31/05/2017	8	3.0
7	Kalamata	[22.09° E, 36.97° N]	290	4.2	17/10/1999-17/05/2011	57	3.0
8	Pylos	[21.60° E, 36.83° N]	3016	7.2	09/11/2007-30/06/2016	92	3.0
9	Zakynthos	[20.60° E, 37.96° N]	297	7.5	08/11/2007-23/01/2012	47	3.0
				Italy			
10	Venice	[12.66° E, 44.97° N]	33	7.3	01/06/2013-01/01/2015	18	0.5
11	Crotone	[17.22° E, 39.02° N]	37	1.3	04/06/2013-10/12/2014	17	0.5
12	Catania	[15.15° E, 37.43° N]	45	5.3	06/01/2013-01/01/2015	14	0.5
13	Palermo	[13.33° E, 38.26° N]	135	6.9	01/06/2013-30/10/2014	8	0.5
				France			
14	Alistro	[9.64° E, 42.26° N]	116	6.7	29/10 2013-01/06/2017	16	0.5
15	La Revellata	[8.65° E, 42.57° N]	194	5.6	30/10 2013-30/06/2017	8	0.5
16	Nice	[7.23° E, 43.64° N]	45	1.7	22/06/2010-07/03/2016	38	0.5
17	Porquerolles	[6.21° E, 42.93° N]	347	5.4	24/04/2008-24/08/2012	44	0.5

Table 4.1 *(continue)*

Coordinates and sampling details of buoys stations for 30 locations in the Mediterranean Sea.

Location	Coordinates [Longitude, Latitude]	Depth [m]	Distance from coast [km]	Covering Period	Duration of record [months]	Sampling Interval [hr]	Location
				France			
18	Marseille	[5.23° E, 43.21° N]	30	8.9	17/04/2011-30/06/2017	61	0.5
19	Sete	[3.78° E, 43.37° N]	34	6.2	06/10/2009-30/06/2017	88	0.5
20	Leucate	[3.12° E, 42.92° N]	43	4.8	06/10/2009-30/06/2017	82	0.5
21	Banyuls	[3.17° E, 42.49° N]	15	3.2	06/10/2009-19/05/2017	83	0.5
				Spain			
22	Cabo Begur	[3.65° E, 41.92° N]	1200	34.6	27/03/2001-31/03/2019	170	1.0
23	Barcelona	[2.20° E, 41.32° N]	68	2.5	08/03/2004-31/03/2019	152	1.0
24	Tarragona	[1.19° E, 41.07° N]	15	0.8	12/11/1992-22/12/2017	283	1.0
25	Valencia	[0.20° W, 39.51° N]	50	9.1	08/06/2005-30/10/2013	97	1.0
26	Cabo De Gata	[2.32° W, 36.57° N]	536	20.1	28/04/2003-23/03/2018	137	1.0
27	Malaga	[4.42° W, 36.69° N]	15	1.5	19/11/1985-31/03/2019	382	1.0-3.0
28	Dragonera	[2.10° E, 39.56° N]	135	17.5	29/11/2006-31/03/2017	136	1.0
29	Capdepera	[3.49° E, 39.65° N]	48	3.1	01/01/2000-01/04/2014	163	1.0
30	Son Bou	[4.06° E, 39.90° N]	5	0.5	5/10/2011-31/01/2016	52	1.0

4.1.2. Coastal storm thresholds

For the analysis of coastal storms, the buoys closest to the coast are considered, discarding the events with a measurement gap of over 18 hours. Then, three thresholds for the significant wave height, the coastal storm duration, and the calm period are applied to identify the storm events as described in Section 3.1.

Significant wave height • H_{thr}

The threshold of significant wave height (H_{thr}) is the most important for the identification of coastal storms. For the definition of H_{thr}, a stability check of generalised Pareto parameters σ^* and ξ can be applied for different thresholds, as used in EVT. For example, in the area of Malaga (Fig. 4.3) the check is accomplished for a range of thresholds between 0.5-2.5 metres. Both parameters are more stable between 1-1.25 metres, according to their variation in this range and their confidence intervals which correspond to the vertical lines inside the circles (Gilleland and Katz, 2016). Hence, a value between 1-1.25 metres is considered the optimal choice for the threshold of significant wave height. This method can be useful for the estimation of threshold (Bernardara et al., 2014; Martzikos et al., 2018) but is time-consuming and it is not recommended when the threshold should be defined many times for different locations. For this reason, in this thesis, the H_{thr} is defined as the 95^{th} percentile of significant wave height for each location, a value that usually coincides with the result of the stability check (Martzikos et al., 2018).

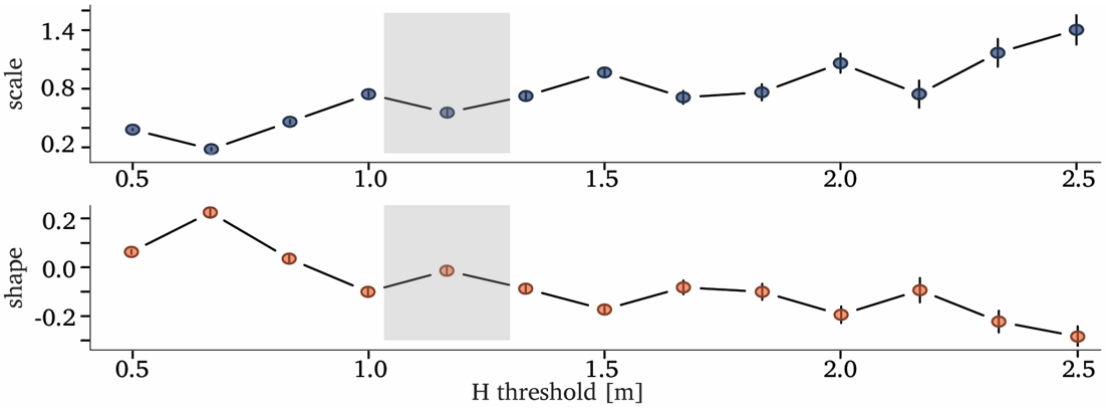

Figure 4.3. The stability check for scale and shape parameters of Generalized Pareto distribution, for the definition of H_{thr} in Malaga.

Duration •D_{thr}

The exceedances over the threshold, after applying the H_{thr}, are grouped and considered as coastal storm events. The boxplots of Figure 4.4(a) illustrate the full range and the distribution of coastal storm duration without significant divergence between countries. The rectangles of boxplots correspond to the interquartile range (75^{th} – 25^{th} percentile), while everything out of this range is considered as an outlier. Inside the rectangle, the dot represents the mean value, and the horizontal line shows the median.

The upper side of the rectangles is almost 20 hours, which means that 75% of events last less than 20 hours. Consequently, the minimum storm duration D_{thr} has no meaning to be set higher than this value. The average duration (internal dot) is almost 10 hours for all the countries, while the median and thus 50% (horizontal line) of events last less than 7.5 hours. The D_{thr} is set at 9 hours for the examined locations so as to be higher than the median but without exceeding the mean value. By applying the D_{thr} all the events with a shorter duration are discarded. The value of 9 hours is also multiple of 3 hours based on the longest sampling interval.

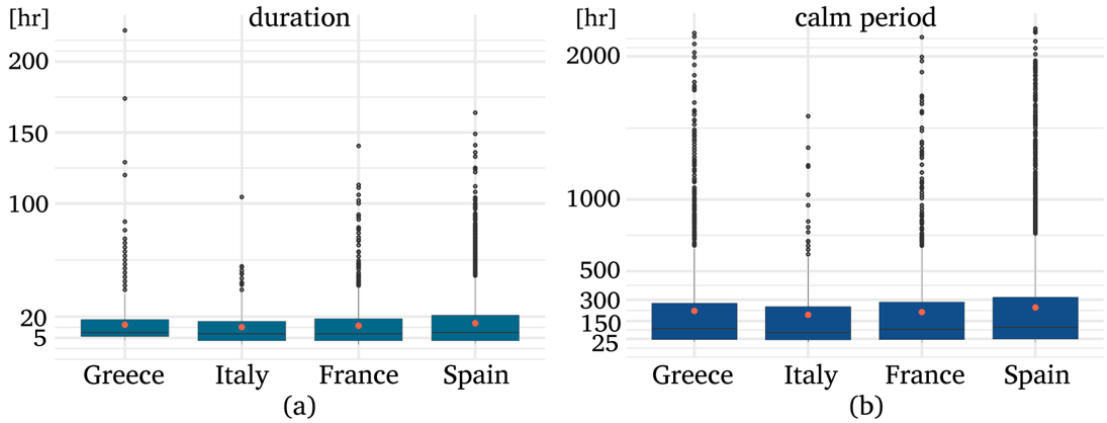

Figure 4.4. Boxplots for the range of the duration of storm events (a) and the calm period between two consecutive storm events (b), when it does not exceed three months (in approximately 2190 hours).

Calm period • I_{thr}

Following the boxplots of Figure 4.4(b), the examined events have an average calm period of almost 200 hours (internal dots), and 50% of them usually occur in less than 87.5 hours from the previous event. The lower side of rectangles shows that 25% of coastal storms are consecutive events that hit the exact location in a row in less than 24 hours.

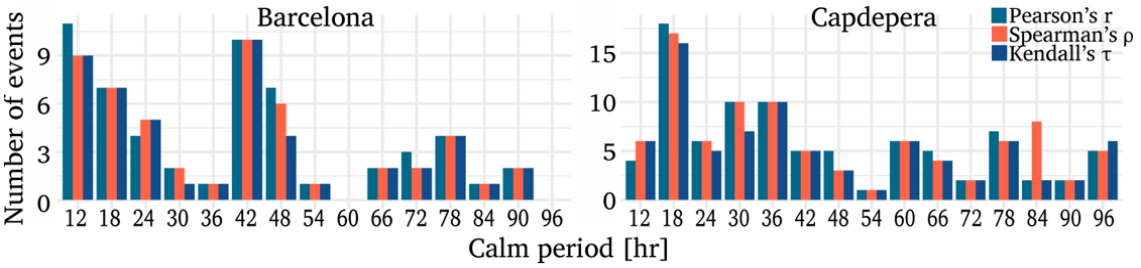

Figure 4.5. The number of coastal storm events in Barcelona and Capdepera, which are not correlated with the next event, having the Spearman's ρ, Kendall's τ, and Pearson's r coefficients close to zero.

The calm period threshold I_{thr} is set as the minimum calm period, with coefficients ρ, τ, and r of H to be close to zero for the most consecutive coastal storms (and similarly for T). For instance, in Barcelona (Fig. 4.5), coastal storms without correlation with the consecutive events (based on H, r, ρ, and τ) are separated mainly by a calm period of 12 or 42 hours and similarly, by 18 hours for Capdepera. Hence, the twelve and eighteenth hourly calm periods are considered the threshold I_{thr} for separating consecutive Barcelona and Capdepera events.

Therefore, the coastal storm identification is conducted through three thresholds, namely: a) the significant wave height, b) the duration, and c) the calm period. As previously indicated, the D_{thr} is generally set at 9 hours for all the examined locations. The H_{thr}, is defined as the 95% of the sample of significant wave height per location and the I_{thr} is established according to the correlation coefficients Spearman's ρ, Kendall's τ, *and* Pearson's r. The thresholds of the significant wave height (H_{thr}) and the calm period (I_{thr}) between two consecutive events are estimated for each location (Table 4.2).

Similar findings are also presented in other studies. For instance, the calm period threshold of 12 hours is in agreement with Lin-Ye et al. (2016) for Barcelona and the north-western Mediterranean Sea. For Marseille, Bernardara et al. (2014) identify the independence threshold at 24 hours, while this thesis results indicate 12 hours as a threshold. For Sete in the Gulf of Lions, Gervais et al. (2012) indicate that storms with $H = 2.7$ metres or higher can cause specific impacts in beach morphology or overtopping. Here, for Sete the H_{thr} is 1.7 metres, the average H of all events is 2.36 metres, and the average of the most extreme events is at 3.33 metres, which means that they concur. The divergences of this thesis from other works could be explained both by the different reference periods and the model data that are used by other researchers.

Table 4.2

The estimated thresholds H_{thr} and I_{thr} for the 30 examined locations.

	Location	H_{thr} [m]	I_{thr} [hr]
	Greece		
1	Athos	2.3	12
2	Lesvos	1.9	12
3	Skyros	2.3	12
4	Mykonos	2.4	12
5	Santorini	2.0	18
6	Heraklion	1.8	18
7	Kalamata	0.9	18
8	Pylos	2.4	12
9	Zakynthos	2.0	18
	Italy		
10	Venice	1.3	18
11	Crotone	1.7	24
12	Catania	1.5	12
13	Palermo	2.2	24
	France		
14	Alistro	1.6	18
15	La Revellata	3.1	24
16	Nice	1.3	12
17	Porquerolles	2.6	12
18	Marseille	2.1	12
19	Sete	1.7	12
20	Leucate	1.7	12
21	Banyuls	1.7	12
	Spain		
22	Cabo Begur	3.4	18
23	Barcelona	1.6	12
24	Tarragona	1.1	12
25	Valencia	1.4	24
26	Cabo De Gata	2.4	12
27	Malaga	1.2	12
28	Dragonera	2.7	12
29	Capdepera	2.5	18
30	Son Bou	1.4	24

4.1.3. Coastal storm characteristics

The identification of coastal storms leads to the study of their characteristics, as described in Section 3.2. Following the proposed methodology (Fig. 3.2), the coastal storm thresholds are defined. Subsequently, the coastal storm events are identified and analysed. The analysis of 30 different locations and their datasets provides valuable information about the variation of important variables (Fig.4.6) and the storm activity over the Mediterranean Sea during the last decades.

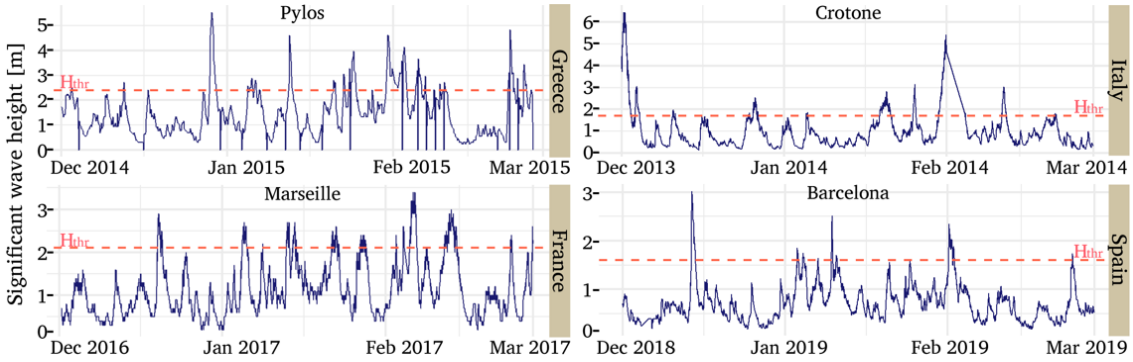

Figure 4.6. Illustration of significant wave height variation and their thresholds for 4 typical locations.

Frequency of occurrence

In summary, 4008 coastal storms are analysed, corresponding to 41-127 storm events per year. Most of them (77-86%) occur during the winter months, especially from October to March (Table 4.3). The average temporal coverage of datasets is shorter than 15 years. To better understand the coastal storm frequency of occurrence, the annual average of coastal storms per location is also estimated, excluding the short-length datasets to avoid underestimation (i.e., Heraklion, Allistro and La Revellata). Subsequently, 10-14 coastal storms, on average, hit the examined coastal areas annually. More specifically, the frequency of occurrence is taken into account for each location, and the annual average is presented in Figure 4.7. Once again, the locations with a short dataset regarding the record duration, such as Heraklion, Venice, Crotone, Catania, Palermo, Alistro and La Revellata, are not included (Fig. 4.7). The percentage frequency of coastal storm occurrence at a monthly level, as presented in Figure 4.8, confirms that coastal storms are more frequent in the winter semester for each location. During a summer month (July, June, August), the coastal storm activity is usually less than 5% of the annual coastal storm activity, while the percentage for a winter month ranges

between 10% to 30%. Furthermore, it is worth mentioning that storm activity is more intense during the summer for most of the Spanish locations.

Table 4.3
The total number of examined coastal storm events in each country and their characteristics.

	Overall	Oct-Mar	Ap-Sep	Annual average				Average temporal coverage [years]
				Overall	Oct-Mar %	Ap-Sep %	Per location/area	
Greece	1103	950	153	98	86	14	12	8.8
Italy	87	69	18	41	78	22	10	1.2
France	633	509	124	87	80	20	13	5.5
Spain	2185	1668	517	127	77	23	14	14.6

The present findings could be used in the future by any researcher who wants to pursue a coastal storm analysis at the examined locations. Both annual and monthly frequency of occurrence are essential for understanding the load of coastal storms to coastal structures. The annual frequency of occurrence of coastal storms, according to Figures 4.7-4.8, is useful for applying extreme value analysis based on the Block Maxima or the r-largest order statistics (Coles, 2001; Dey and Yan, 2015) by selecting the optimal number of maximum values as the number of coastal storms per location per area in Table 4.3 or the Figure 4.7.

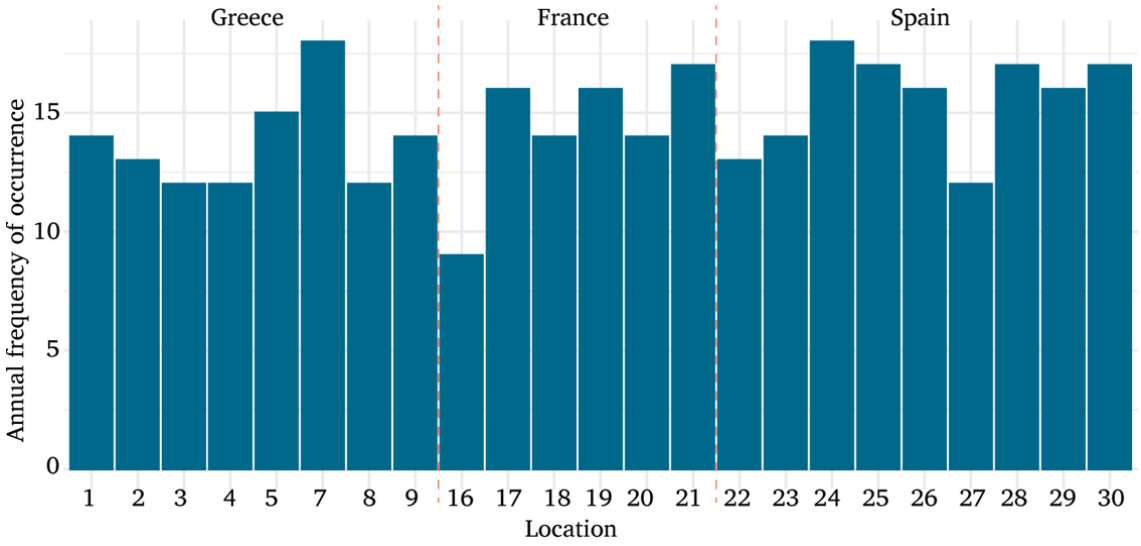

Figure 4.7. The annual average number of coastal storms for each location, (the locations with a short temporal coverage are not included).

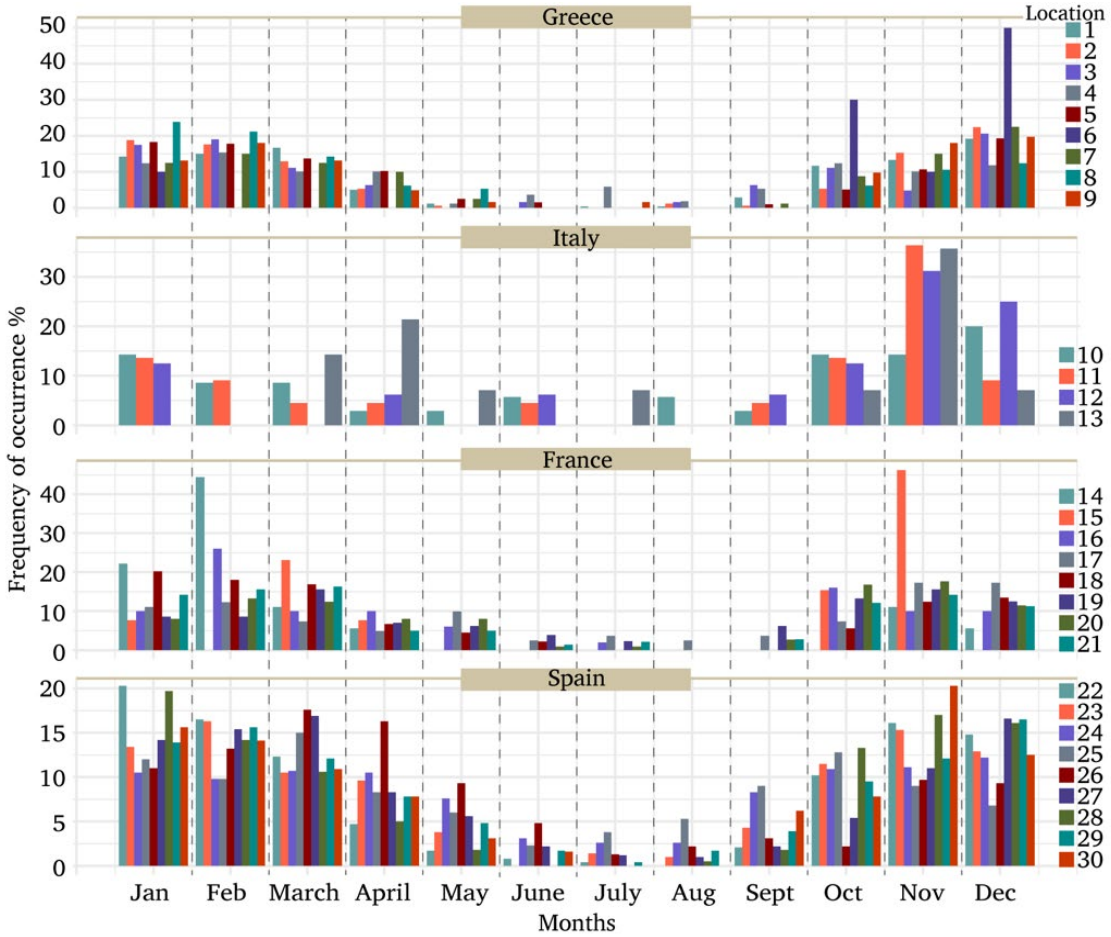

Figure 4.8. The percentage monthly frequency of coastal storm occurrence for each location.

In an attempt to compare the results of this thesis to other similar researches, Bernardara et al. (2014), working with a more extended dataset, detect 10 events per year in Marseille, while in this thesis 14 events are identified. Lionello et al. (2016) mention 18 events annually, describing the climatology of cyclones in the Mediterranean but this approach cannot be directly comparable with the outcome of this thesis, since cyclones are not considered coastal storms. Previous studies have indicated that the most active areas in cyclones in the Mediterranean Sea are the Aegean, the Adriatic, the Gulf of Genoa, the Gulf of Lion, and the Catalan Sea (Lionello et al., 2006; Cavicchia et al., 2014; González-Alemán et al., 2019). This information ties well with the present study's findings, where the highest frequency of coastal storms and the highest values of H and T were identified in representative coastal locations of the aforementioned seas; namely in Athos, Pylos, La Revellata, Porquerolles, Cabo Begur.

Descriptive statistics

The overview of Mediterranean coastal storms analysis is completed by investigating their characteristics as described in Section 3.2 and performing analysis for their descriptive statistics (Table 4.4). The mean (m_H and m_T) and the maximum (max_H and max_T) values of all significant wave heights and wave periods (m_T) are estimated for the coastal storms at each location. The coastal storm energy, the wave energy flux and the coastal storm duration of events are described by their mean values and hereto referred to as m_E, $m_{P,}$ and m_D, respectively. The most extreme events are also examined by considering the average of the highest 5% of all the wave heights ($m_{H5\%}$) and the wave periods ($m_{T5\%}$) that occur at a given location.

According to Table 4.4, the highest significant wave heights occur, as expected, at the most exposed locations, where the fetches are long, such as Cabo Begur in Spain, La Revellata in France, Palermo in Italy and Pylos in Greece. On the other hand, the lowest wave heights appear in shallow waters and sheltered locations, such as Kalamata (Greece), Venice (Italy), Nice (France) and Tarragona (Spain). This analysis is of essential importance for the locations where the buoys are located in shallow waters (i.e., Tarragona, Malaga and Son Bou in Spain) and also, for the nearshore locations (i.e., Crotone and Nice). For buoys close to the coasts, the measured waves preserve their characteristics as reaching the coasts, whereas the opposite is the case for the buoys

in deep waters where many processes (e.g., refraction, shoaling or breaking) induce significant changes to incident waves.

The highest values of T and E also appear in the most exposed locations, as previously mentioned for the case of H and T. For the most extreme events, the analysis reveals that $m_{H5\%}$ and $m_{T5\%}$ are higher than m_H, and m_T respectively (in approximately over 10%), describing the most extreme characteristics of coastal storms at each location. Within the context of investigating the most extreme coastal storms, with the wave height exceeding 90% of the overall dataset, it is observed that the wave period shows a great variation and depends on the location (Fig. 4.9). The majority of coastal storms with the highest wave heights have, simultaneously, wave periods between 6-8 seconds, with an average of over 7 seconds. For locations such as Pylos, Zakynthos, Porquerolles and Capderpera, the large waves usually occur with wave periods over 8 seconds.

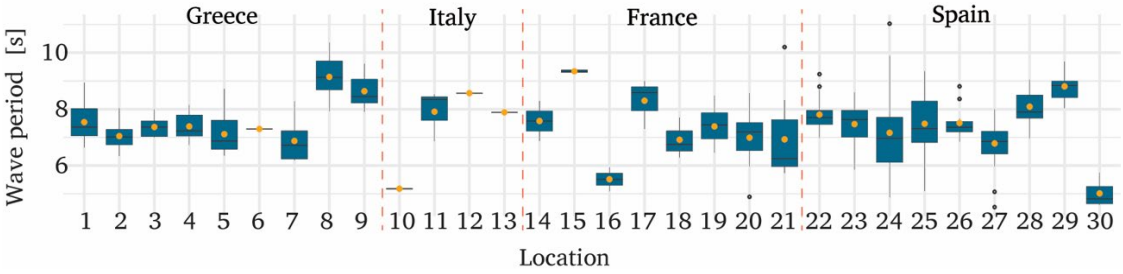

Figure 4.9. The range of coastal storm wave period when their mean wave height exceeds 90%.

The coastal storm energy (E) ranges between 38 and 447 m^2hr and is high when H and D also have high values as expected by its definition. Coastal storms with the highest energy occur in deep waters, i.e., Pylos, Palermo, La Revellata and Cabo Begur. Moreover, it could be stated that coastal storms in Greece have higher energy than those in the other countries since they are in the deepest waters (among the dataset's boundaries), followed by Spain, France, and Italy. Considering the most extreme coastal storms, when the wave height within an event exceeds 90% and lasts over 24 hours, the energy shows a significant variation at any location (Fig. 4.10), while the highest values indicate the presence of coastal storms with high waves or long duration at a specific location. The wave energy flux (P) at each location ranges between 1014.57 and 37867.01 Whr/m, having similar behaviour to the coastal storm energy. Since the coastal storm impacts are not clearly associated with the energy of coastal storms, both

variables are estimated in the context of the coastal storm severity index for the examined locations.

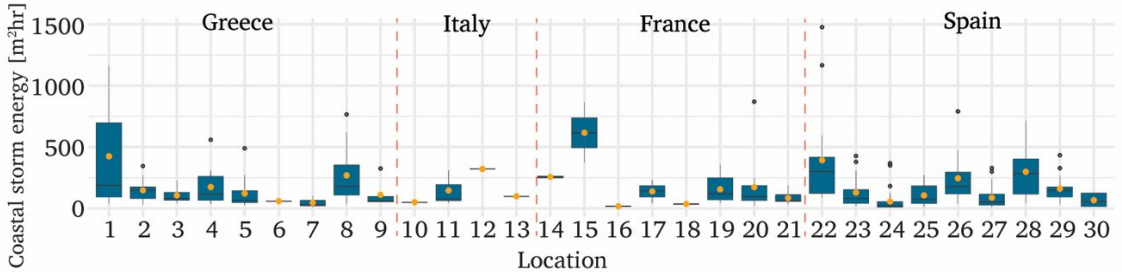

Figure 4.10. The range of coastal storm energy when their mean wave height exceeds 90% and last over 24 hours.

Table 4.4

Basic statistics of the coastal storm characteristics for the examined locations.

	Location	m_H [m]	max_H [m]	m_T [s]	max_T [s]	m_E [m^{2}hr]	m_P [Whr/m]	m_D [hr]	$m_{H5\%}$ [m]	$m_{T5\%}$ [s]
					Greece					
1	Athos	3.01	5.99	7.57	11.01	243.84	19850.37	27.06	4.01	9.05
2	Lesvos	2.43	4.92	7.13	10.56	169.71	14645.21	24.13	4.61	10.08
3	Skyros	3.01	5.45	7.82	10.04	248.04	20495.81	28.10	3.75	8.81
4	Mykonos	3.10	5.76	7.87	11.36	234.35	20860.71	27.38	5.13	9.47
5	Santorini	2.46	4.92	7.37	13.82	143.32	10966.83	24.51	3.08	9.16
6	Heraklion	2.47	4.25	7.33	10.04	191.64	16720.21	31.13	2.77	7.61
7	Kalamata	1.28	3.28	7.37	11.13	38.93	3049.20	24.31	1.76	9.13
8	Pylos	3.10	7.57	8.95	13.71	273.69	25949.15	28.64	4.05	10.21
9	Zakynthos	2.68	9.37	9.49	24.37	219.77	13874.17	28.82	4.62	18.37
					Italy					
10	Venice	1.67	3.77	6.39	10.53	57.91	3956.21	20.23	2.34	8.34
11	Crotone	2.34	6.46	8.26	13.33	178.60	12565.84	29.09	3.41	9.67
12	Catania	2.21	4.96	8.57	12.50	131.63	10365.29	24.03	3.92	10.33
13	Palermo	2.85	5.49	8.99	13.33	152.46	15581.80	18.50	3.73	11.90
					France					
14	Alistro	2.25	5.80	7.45	11.80	128.61	11851.22	23.31	3.45	9.12
15	La Revellata	3.94	7.70	9.65	13.30	374.49	33189.66	22.57	5.32	10.88
16	Nice	1.73	4.00	7.23	13.30	69.23	5042.72	22.45	2.24	10.82
17	Porquerolles	3.06	6.20	8.52	12.10	175.94	14482.73	19.09	3.85	10.07
18	Marseille	2.47	8.60	7.45	25.00	123.21	7947.60	20.57	3.10	8.94
19	Sete	2.36	5.90	7.41	11.80	162.38	10889.63	27.70	3.33	9.34
20	Leucate	2.33	9.10	7.40	28.60	164.50	11851.71	27.74	3.57	9.56
21	Banyuls	2.15	12.80	7.27	25.00	127.29	3901.43	25.77	3.17	9.80
					Spain					
22	Cabo Begur	4.05	7.40	8.06	12.70	446.36	37867.01	26.98	5.11	9.91
23	Barcelona	2.03	5.20	7.56	12.30	118.88	10077.18	27.49	2.83	9.46
24	Tarragona	1.39	3.90	6.97	12.20	52.57	2024.92	25.02	1.81	7.09
25	Valencia	1.80	4.50	7.35	12.50	101.38	7684.43	29.51	2.42	9.57
26	Cabo De Gata	2.94	6.60	7.42	10.60	205.07	16190.26	23.47	3.76	8.77
27	Malaga	1.69	4.70	6.94	15.60	98.79	3720.91	30.37	2.47	6.83
28	Dragonera	3.27	6.30	8.24	12.80	269.30	26876.39	24.97	4.03	9.93
29	Capdepera	3.16	7.00	8.88	12.80	264.94	21296.32	25.88	4.16	10.09
30	Son Bou	1.73	4.98	5.33	8.52	89.94	1014.57	28.98	2.25	6.30

Duration and calm period

The examined coastal storm events have a mean duration between 18 to 31 hours, while the shortest events occur in Palermo, Italy and the longest in Malaga, Spain (Table 3.4). Additional analysis for the duration is accomplished by taking the events which exceed the significant wave height threshold before rejecting some of them due to the minimum duration (D_{thr}) of 9 hours. The boxplots of Figure 4.11(a) show the full range of the storm duration. The average duration is lower than 30 hours, and according to the median, 50% of coastal storms last less than a day.

Moreover, the variation of the median is very small for the Greek and Spanish locations. The upper quartile (75%) is almost the same for the Greek locations that are not in the centre of the Aegean Sea, as well as for Leucate, Sete and Banyuls in France. The highest upper quartiles and the most outliers of duration occur in Spain. In the same context, Lionello et al. (2006) state that the shortest cyclones in the Mediterranean last less than 12 hours and the most severe cyclones have an average duration of 18-24 hours. It could be said that the coastal storm duration has the same characteristics, according to Figure 4.11, and it is a rational outcome since coastal storms originate from cyclones and synoptic systems.

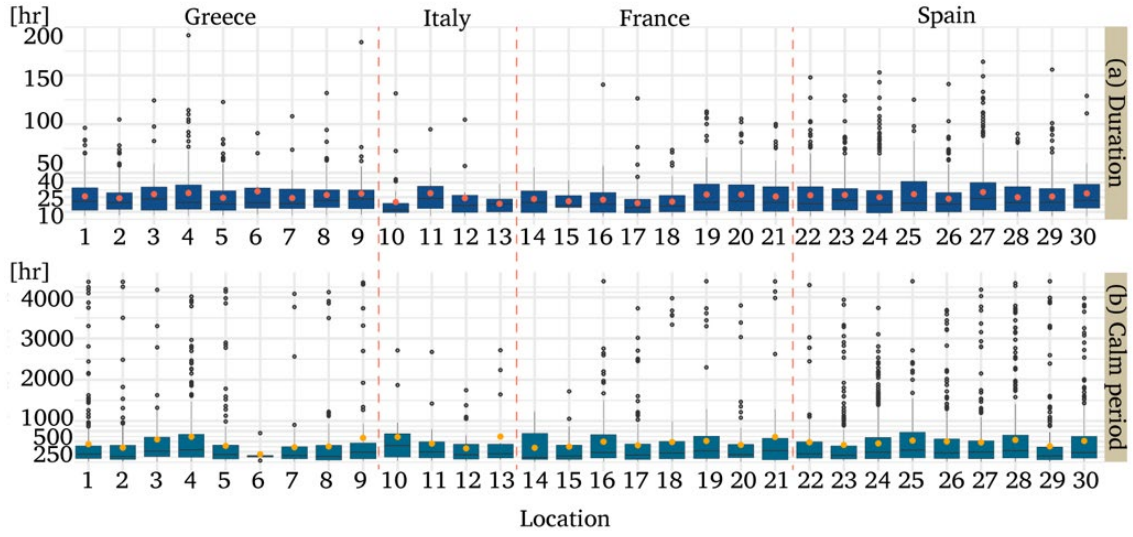

Figure 4.11. Boxplots for the full range of variation of coastal storm duration (a) and the calm period between two consecutive events (b).

The average calm period of coastal storms is shorter than 625 hours, or less than one month, according to Figure 4.11(b). Most events (75%) have a calm period shorter than 750 hours, while 25% of events have a calm period of almost 150 hours, hitting

consecutively the same location in less than a week. In general, the variation of the calm period is higher than the duration. The median is around 190 hours for most of the Greek locations and around 250 hours for Spain. The highest upper quartiles belong to Spain, and the average calm period of 500 hours is the most common for the Spanish locations. The results about the mean storm duration and the calm period are also crucial for the coastal erosion (Callaghan et al., 2008; Corbella and Stretch, 2012a; Dissanayake et al., 2015), the vulnerability of coastal structures and their design (Salvadori et al., 2014; Lira-Loarca et al., 2020). Consecutive storm events and events with long duration are responsible for significant loads in the coastal structures as well as for a short time for beach recovery.

The shape of coastal storm

The detected coastal storms at Malaga are investigated concerning the significant wave height to understand the shape of coastal storms. A great variety in the shape of storms is confirmed in Figure 4.12, which is in agreement with Lira-Loarca et al. (2020).For the sharpness of their shape, further analysis is implemented at different locations. Considering a simplified triangular shape, the base represents the duration of a coastal storm and the peak corresponds to the maximum wave height. Then, the triangular shape of coastal storms is investigated for whether the coastal storms have a) their peak in the centre, or at the half duration ($\pm 5\%$), b) a positive skewness where the peak is on the left, similar to the description of Lin-Ye et al. (2016), and c) a negative skewness, where the peak is on the right. The frequency of occurrence of three categories is presented in Figure 4.13 for locations in Greece and Spain.

The three shape categories are also examined regarding the direction and the wave period within a coastal storm. In Figure 4.14 each dot represents a coastal storm with a specific wave period and wave direction, and the colour corresponds to the three examined categories of triangular shape. The absence of any trend in the results shows that a coastal storm's shape is not related to the direction and the wave period. The range of wave period and the direction within a coastal storm depends on the location and they are not related to the shape of coastal storms, having different behaviour. The coastal storms which are consisted of long waves ($T > 9$ s) have no positive or negative skewness, with their peak left (b) or right (c) from the centre and should neither have a specific direction. The different colours in Figures 4.13 and 4.14 show a few centre-

oriented triangular coastal storms, but this is a rational outcome given that the range of having an isosceles triangle is very short. On the other hand, there is also no dominance of left peak oriented coastal storms, confirming that most Mediterranean coastal storms do not present a sharp slope during the growth of wave height and a milder one during its decay.

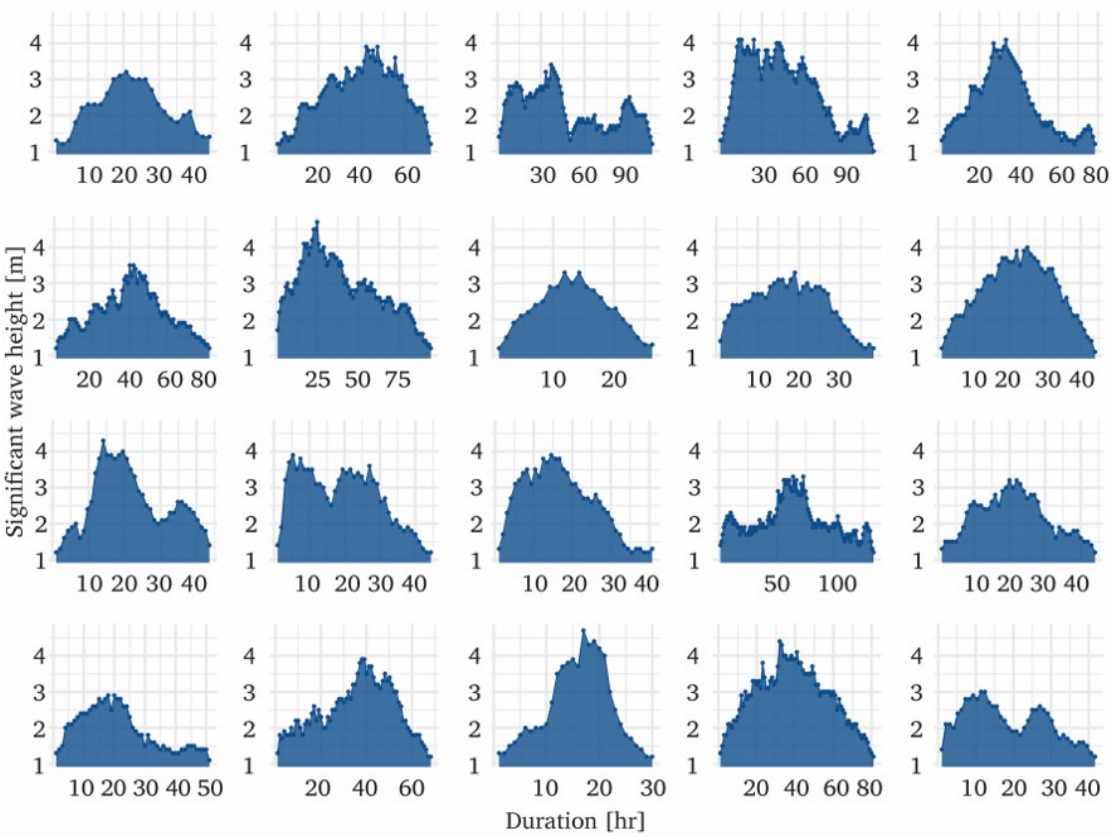

Figure 4.12. Typical shapes of coastal storms according to significant wave height time series at Malaga.

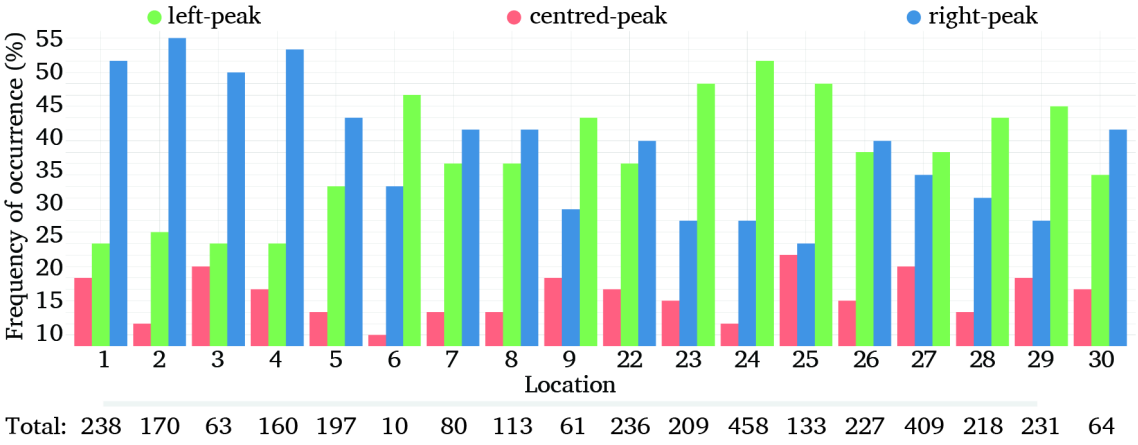

Figure 4.13. Boxplots for the full range of variation of coastal storm duration (a) and the calm period between two consecutive events (b).

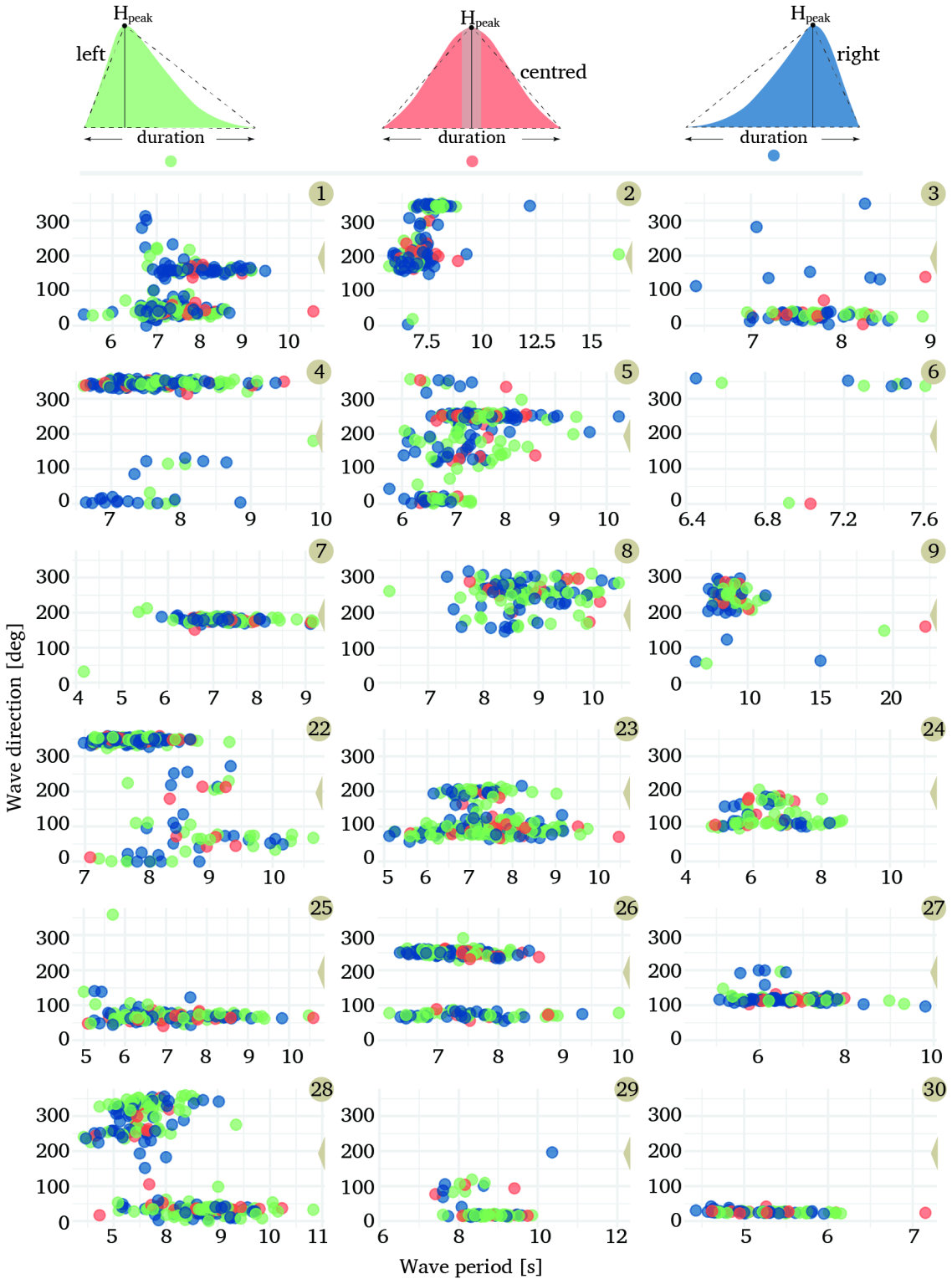

Figure 4.14. The relation of wave period during a coastal storm with the direction and the triangular shape for different locations in the Mediterranean Sea.

4.1.4. Coastal storm parameters

Following the identification of the coastal storms, the coastal storm parameters are considered in order to describe each event by representing their characteristic variables H, T, D, I, E, P, D_{ir}. The coastal storm parameters H_1, T_1, D, I, E, P, D_{ir1} are specific values for each coastal storm and therefore a dataset including them is created at a given location. As mentioned in Section 3.3, the parameters D, I, E, P have already been estimated in the stage of coastal storm identification and the parameter H_1 is defined as the average wave height within a coastal storm. However, a further investigation is needed for the definition of the parameters T_1, D_{ir1} as well as for the parameters E, P regarding the coastal storm severity index.

Wave period and the direction

The wave period and the wave direction are usually stable during a coastal storm. To understand the level of dispersion around the mean (or the circular mean), the coefficient of variation of wave period (CV_T) and the circular standard deviation of wave direction are estimated for each coastal storm (Figs. 4.15 and 4.16).

Regarding the wave period, no significant patterns are detected between locations, but generally, it can be stated that 75% of storm events have the CV_T usually less than 0.15, while for the 25% of them the CV_T is even less than 0.05 (Fig. 4.15). Similarly, the standard deviation of the wave direction (wherever is available) during a coastal storm is very short (Fig. 4.16a). For most locations, most coastal storms (75%) have a standard deviation of the wave direction shorter than 10 degrees, except for some outliers. The latter means that the wave direction does not significantly change during a coastal storm. For instance, the wave direction in Malaga usually ranges between 108° and 131° with a short standard deviation around the mean direction during a coastal storm, as presented in three cases of Figure 4.16(b).

Following Figures 4.15 and 4.16, it is shown that there is no high dispersion for the wave period *(T)* and the direction (D_{ir}) during a coastal storm. The values of T and D_{ir} are normally spread around the mean during a coastal storm for most storm events. Consequently, the mean value of the wave period T_1 and the direction D_{ir1} can efficiently represent these variables during a coastal storm, and thus they are considered as coastal storm parameters.

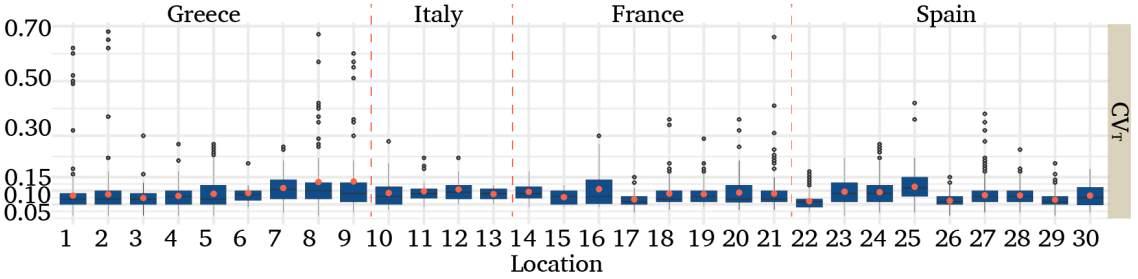

Figure 4.15. Boxplots for the full range of the coefficient of variation for the wave period CV_T during a coastal storm.

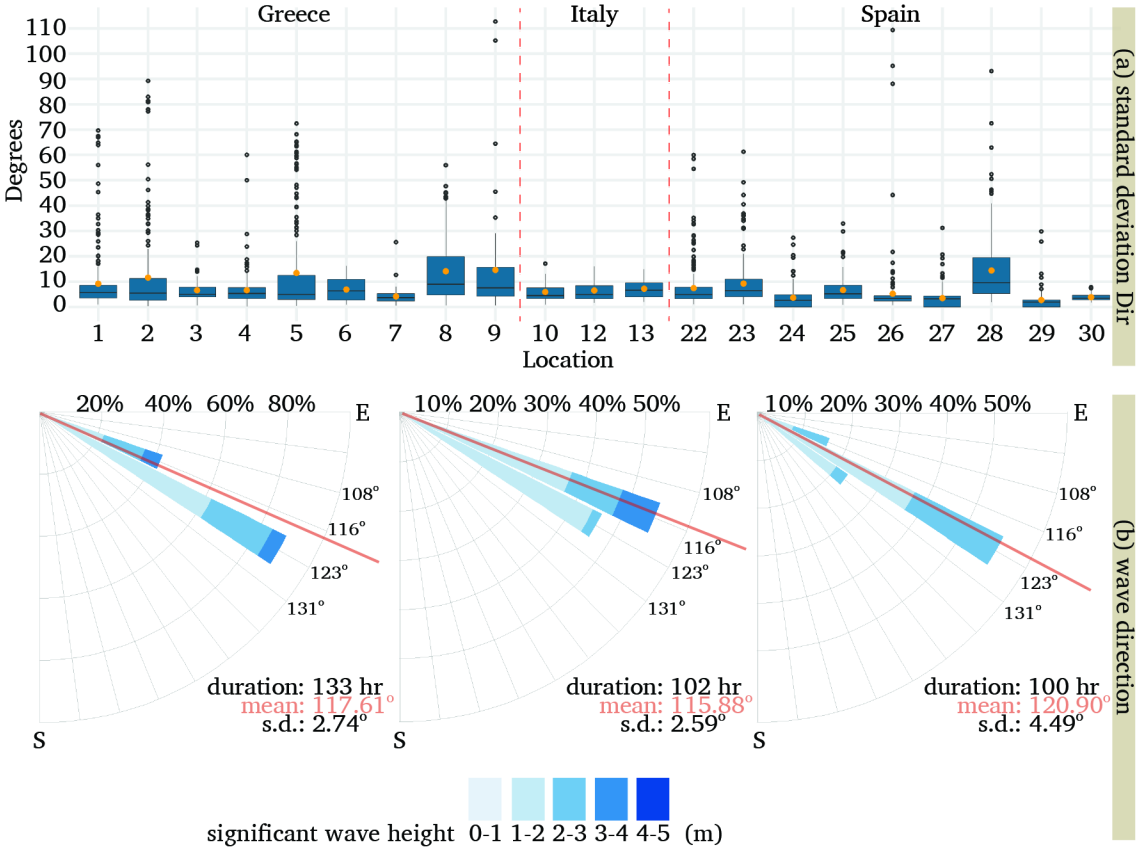

Figure 4.16. Boxplots for the full range of the standard deviation for the wave direction during a coastal storm (a). The wave direction for three coastal storms in Malaga and their characteristics (b).

The coastal storm severity index

The coastal storm severity index is approached through two different equations (Eqs. 3.5-3.6) for coastal storm energy (E) and the wave energy flux (P) during a coastal storm. Their mean values at each location are presented in Table 4.4. The parameters E, P of a coastal storm differ in their definition, but both are used in literature to understand the

storm strength. The coastal storm energy (Eq. 3.5) incorporates the square of H during a coastal storm and its duration. On the other hand, the energy flux (Eq. 3.6) mostly depends on the square of H, the wave period (T) and the water depth. However, their variation has similar behaviour, with the highest values for both occurring at the same locations. An investigation of both approaches is accomplished based on their relation to other variables for understanding if their estimation is affected by long or short-period waves.

The relation of coastal storm energy to the significant wave height and the wave period is presented in Figures 4.17-4.18 for all the detected coastal storms. Each dot in these figures represents a coastal storm with a specific wave height and the colour indicates the three categories of wave height ($T < 8$ s, $8 < T \leq 10$ s, $T \geq 10$ s). The two plots (left and right at each location) confirm the similar behaviour of both types of the coastal storm severity index. The relation between wave height and the wave period during a coastal storm is illustrated in Figures 4.17-4.18. However, the coastal storms characterised by long-period waves, present mostly high energy and wave height values. More specifically, at the same wave height, the highest values of E and P occur simultaneously with long-period waves ($8 \leq T < 10$ s) or swell ($T \geq 10$ s).

Due to the similar behaviour of the two approaches, the coastal storm energy (E) is chosen for the coastal storm severity description, and it is preferred, as also used in literature (Duo et al., 2020), against the (P) for the copulas application.

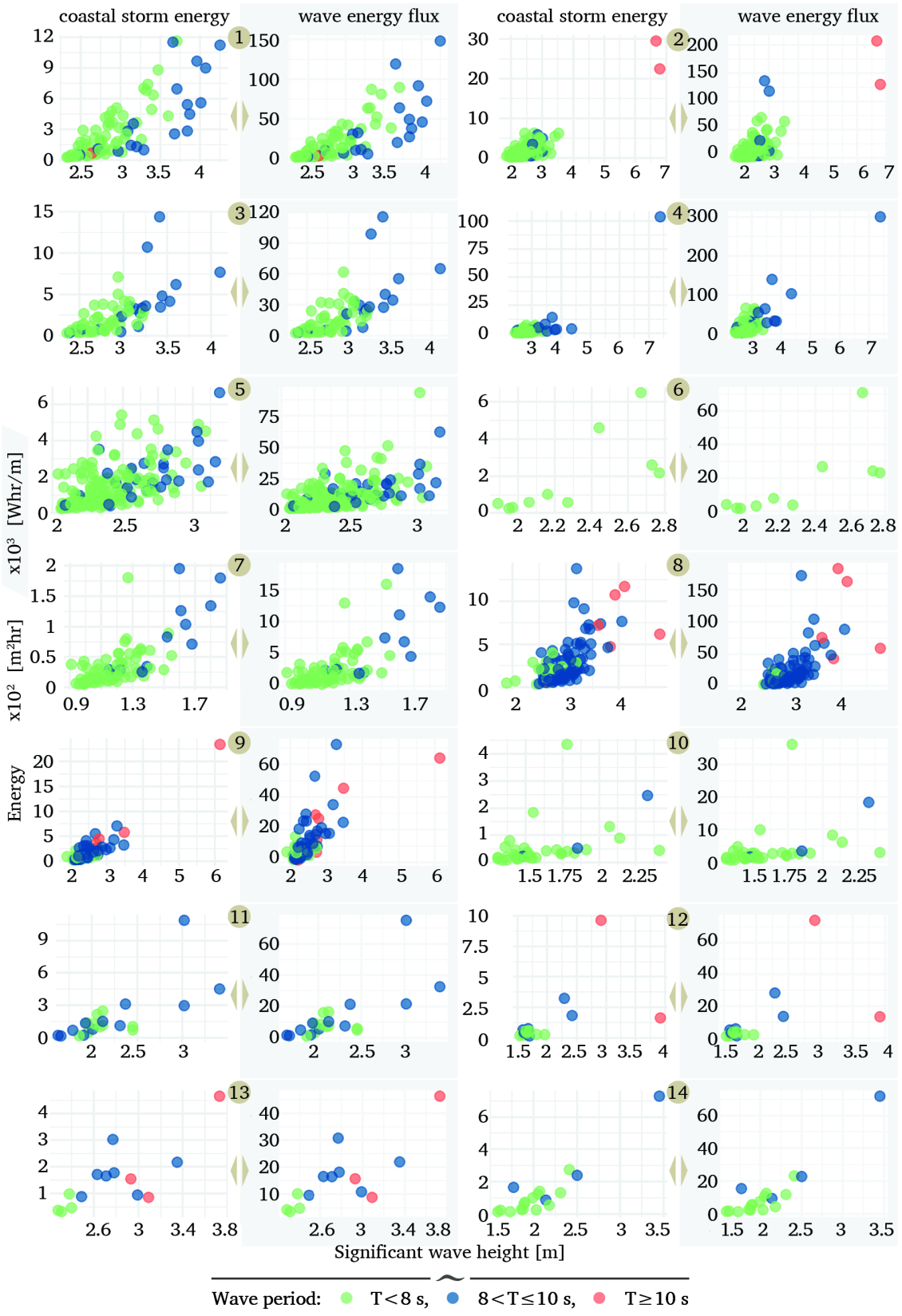

Figure 4.17. The relation between coastal storm energy with the wave energy flux (in grey background) and the significant wave height for a) $T<8$ s, b) $8 \leq T<10$ s, and c) $T \geq 10$ s at locations 1-14 in the Mediterranean Sea.

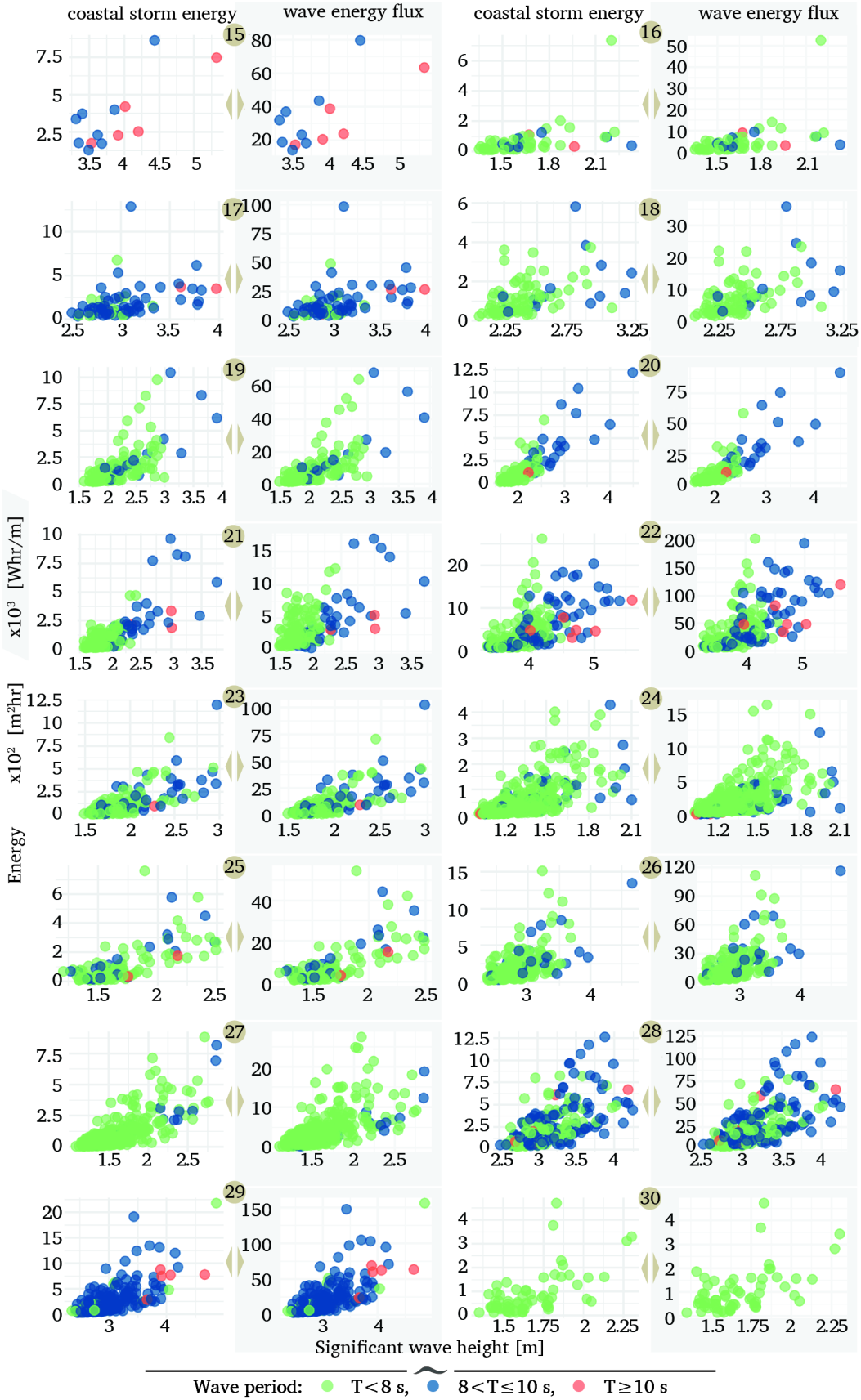

Figure 4.18. The relation between coastal storm energy with the wave energy flux (in grey background) and the significant wave height for a) $T<8$ s, b) $8 \leq T<10$ s, and c) $T \geq 10$ s at locations 15-30 in the Mediterranean Sea.

4.2. Coastal storm modelling through copulas

4.2.1. Event-based copulas for *H* and *T*

The bivariate copulas are used both to describe the dependence of the wave height and the wave period during a coastal storm and to model this relationship. The best copula family for *H* and *T* of coastal storms at a given location is investigated among 40 different copulas (Table 3.4). The copula families and their rotated versions (90°, 180° and 270°) are examined through the "VineCopula" package in R (Nagler et al., 2021). The selection of the best copula family is accomplished mainly by considering the minimum values of both AIC and BIC.

All the samples are checked concerning their random variables to report if *H* and *T* are independent and identically distributed random variables (i.i.d.) before the copulas application (Czado, 2019). The autocorrelation function or ACF (Hyndman and Athanasopoulos, 2021) is estimated for each pair of *H* and *T* within a coastal storm event to check the time series correlation at different time steps (lags). The samples with values of ACF (Fig. 4.19a) outside of confidence intervals (dotted lines in correlogram) are discarded. As expected, the autocorrelation depends on the duration of coastal storms. Actually, 87.5% of coastal storms with a duration of 9-12 hours consist of wave height time series without autocorrelation at any lag. The percentage is significantly reduced when the duration is increased (Fig. 4.19b), and this happens because the longest time series implies longer memory than short time series.

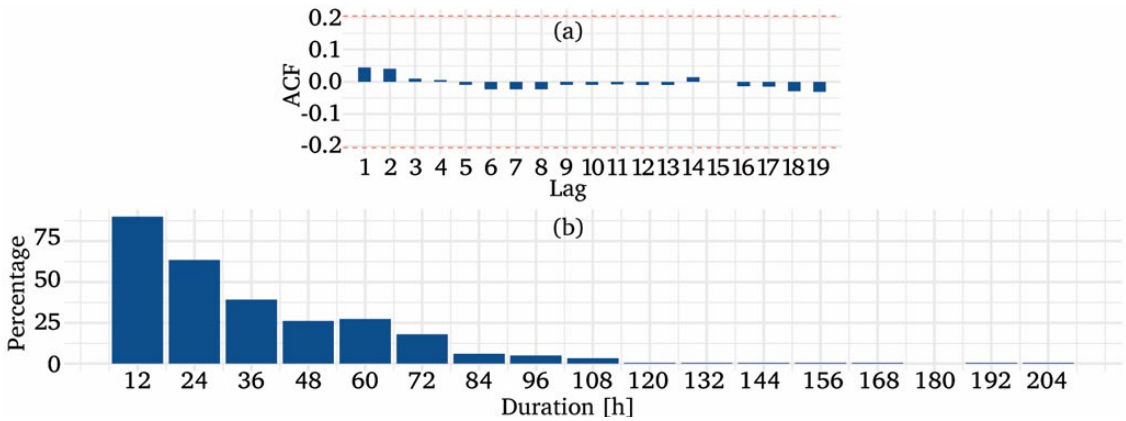

Figure 4.19. A typical correlogram of *H* without autocorrelation at any lag (a). The percentage of coastal storms without autocorrelation regarding the duration (b).

The most prevailing copula families for *H* and *T* during a coastal storm are presented in Figure 4.20. Once excluding the independent cases in the dataset, the Tawn, the Joe

(and their rotated versions) and the Clayton copulas are the most frequent families among the 40 copula families. The Tawn copula belongs to the extreme class of copulas, while its efficiency to model extreme events is confirmed here for coastal storms. The best-selected Tawn copulas have been discussed recently in the literature for applications in hydrology such as drought analysis (Sun et al., 2019; Botai et al., 2020). The Joe and the Clayton copulas belong to the well-known Archimedean class and they were widely used in the past, primarily due to their simplicity (Corbella and Stretch, 2013; Martín Soldevilla et al., 2015; Lin-Ye et al., 2016; Li et al., 2018; Lira-Loarca et al., 2020).

A further investigation is undertaking regarding the coastal storm characteristics (Kendall's τ, H, T, D, and I) to understand why a specific copula family describes better a pair of H and T during a coastal storm. The boxplots of the following Figures 4.21-4.25 describe the range of these parameters. Due to a large number of different families, the information is dense and may mislead the reader. However, a more comparative reading can yield significant conclusions. A more detailed study and interpretation of these boxplots could be helpful to anyone interested in fitting bivariate copulas to the wave height and the wave period of coastal storms.

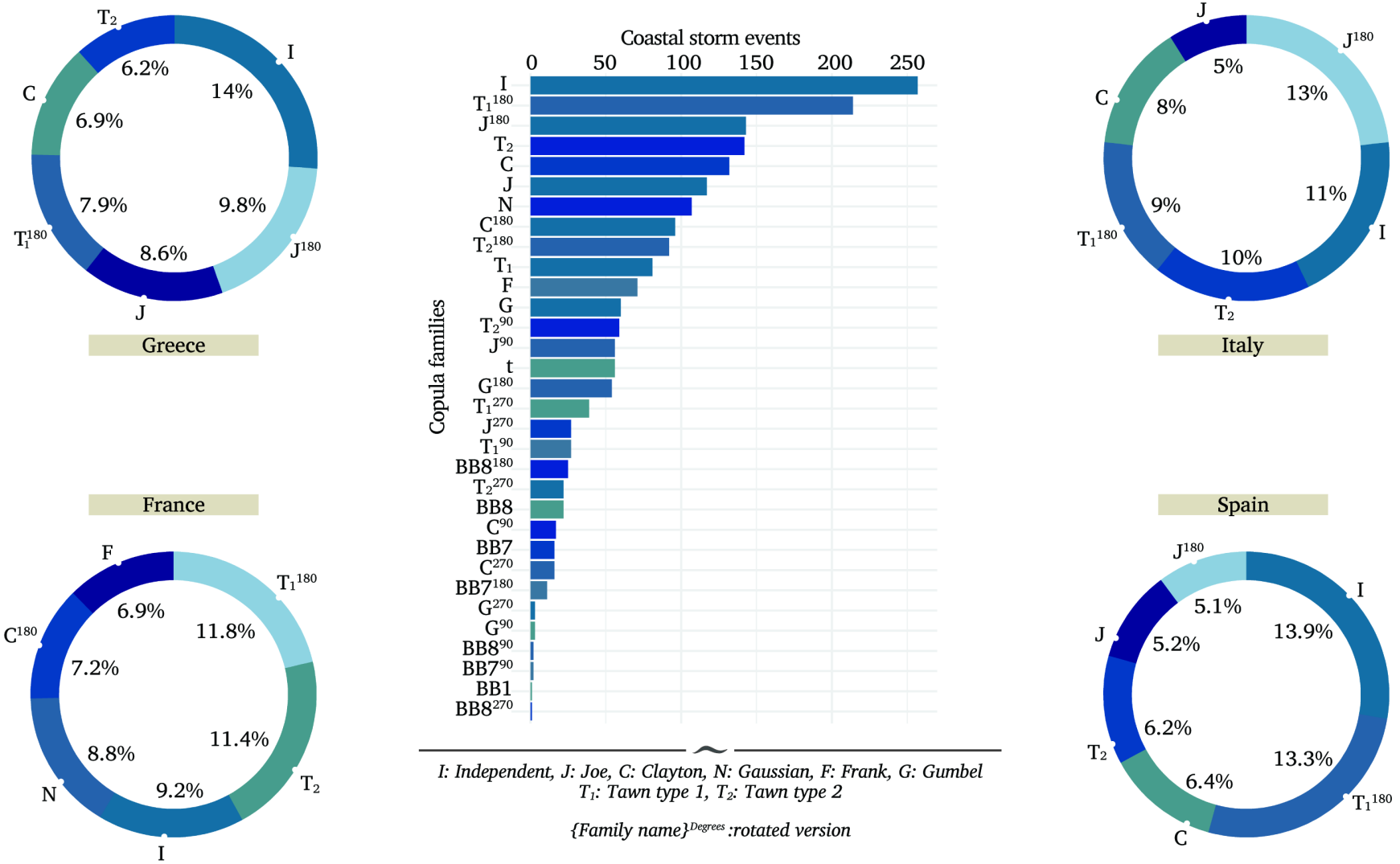

Figure 4.20. The most common copula families for wave height and wave period of coastal storm events in the Mediterranean Sea (in the centre). The six most common copula families for each country (at the corners).

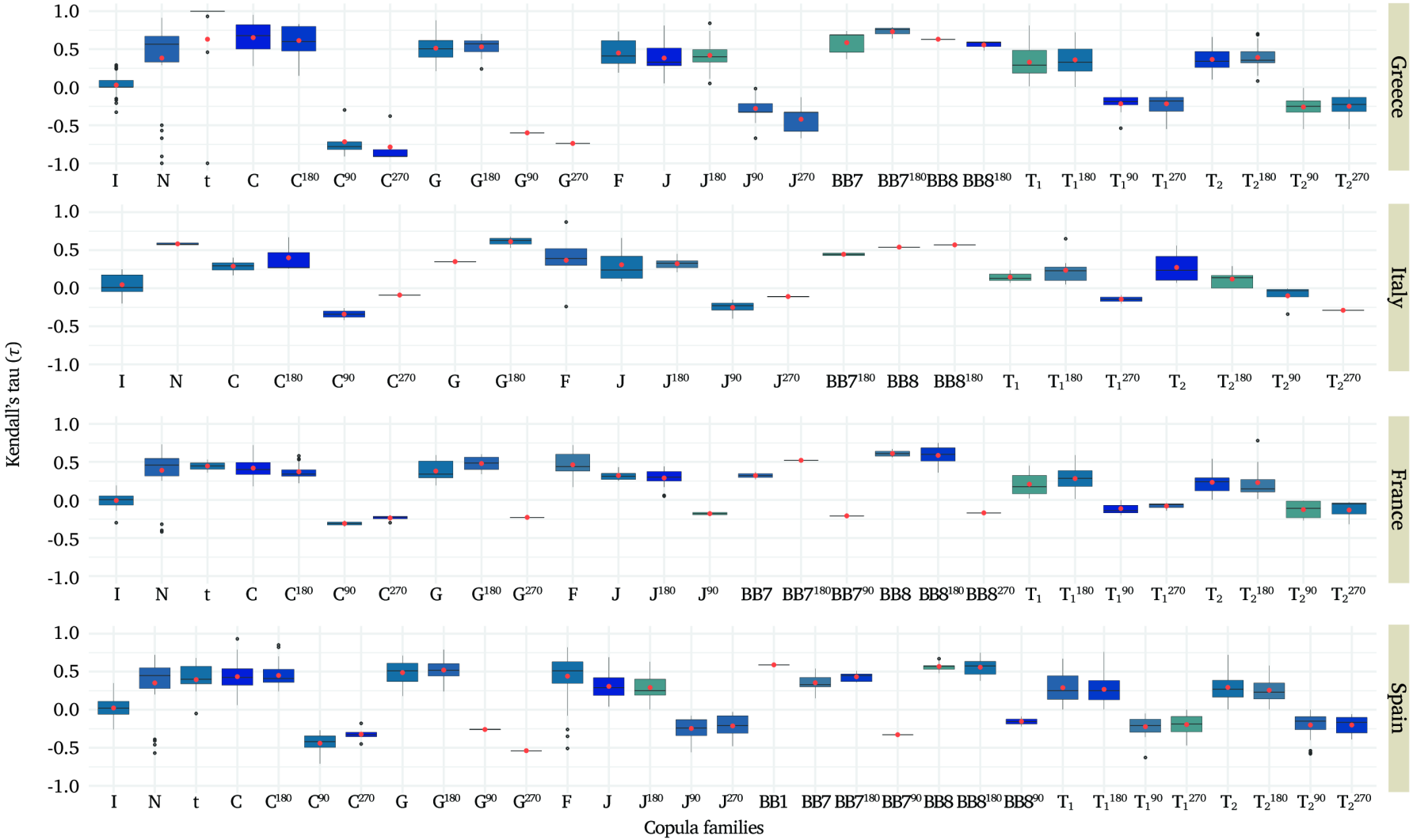

Figure 4.21. Kendall's τ correlation coefficient for H and T of coastal storms which are modelled by different copula families.

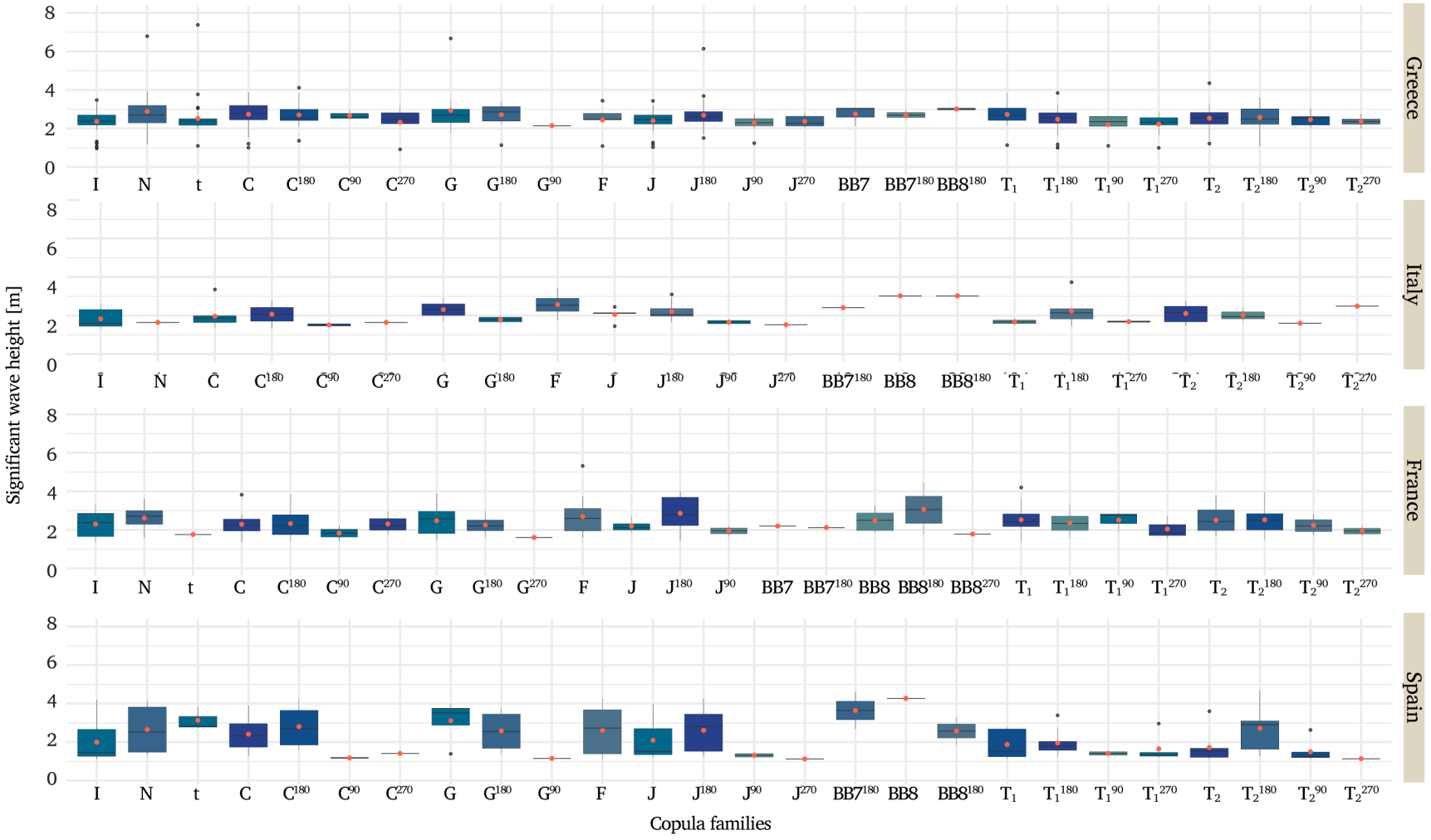

Figure 4.22. The range of significant wave height of coastal storms which are modelled by different copula families.

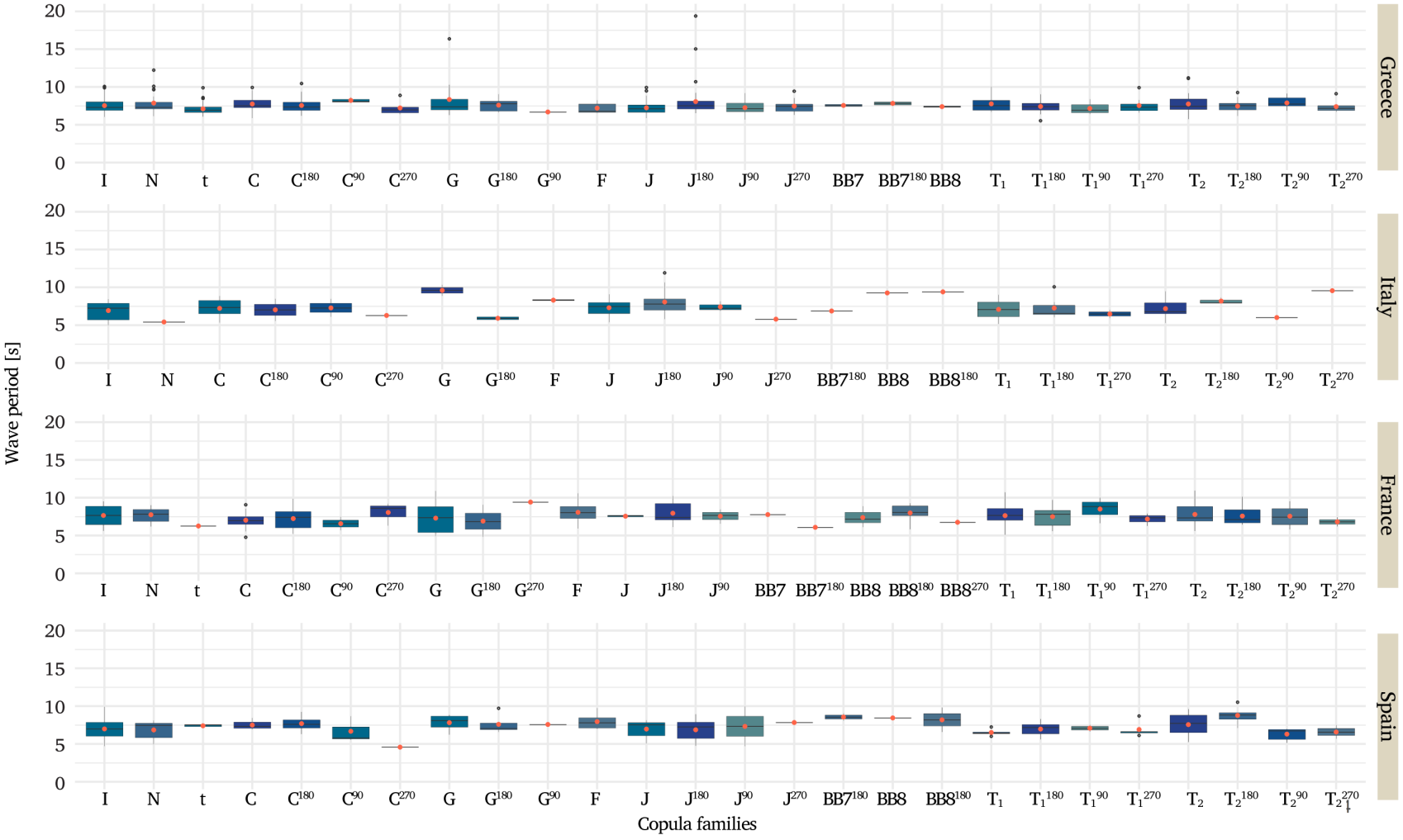

Figure 4.23. The range of wave period of coastal storms which are modelled by different copula families.

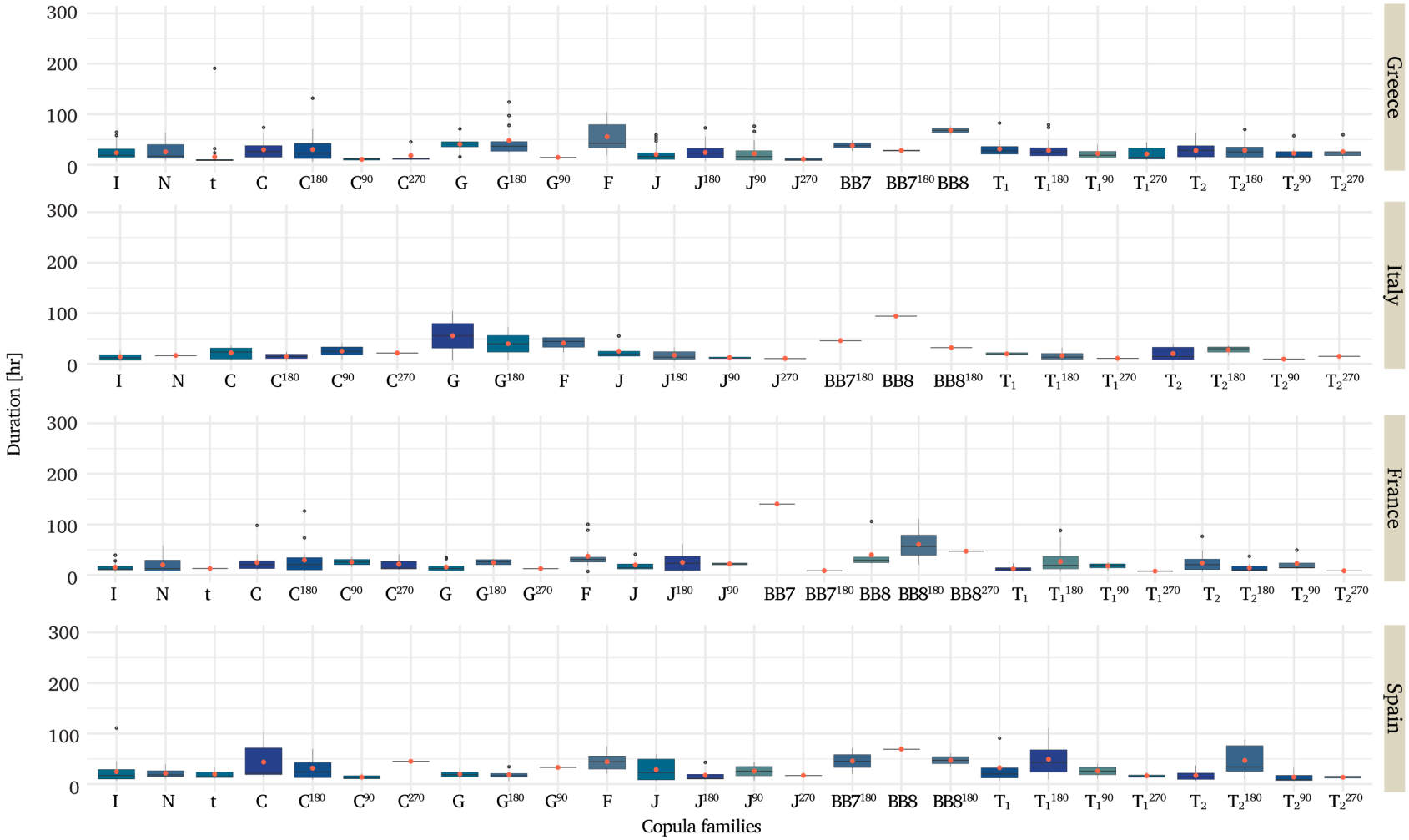

Figure 4.24. The range of duration of coastal storms which are modelled by different copula families.

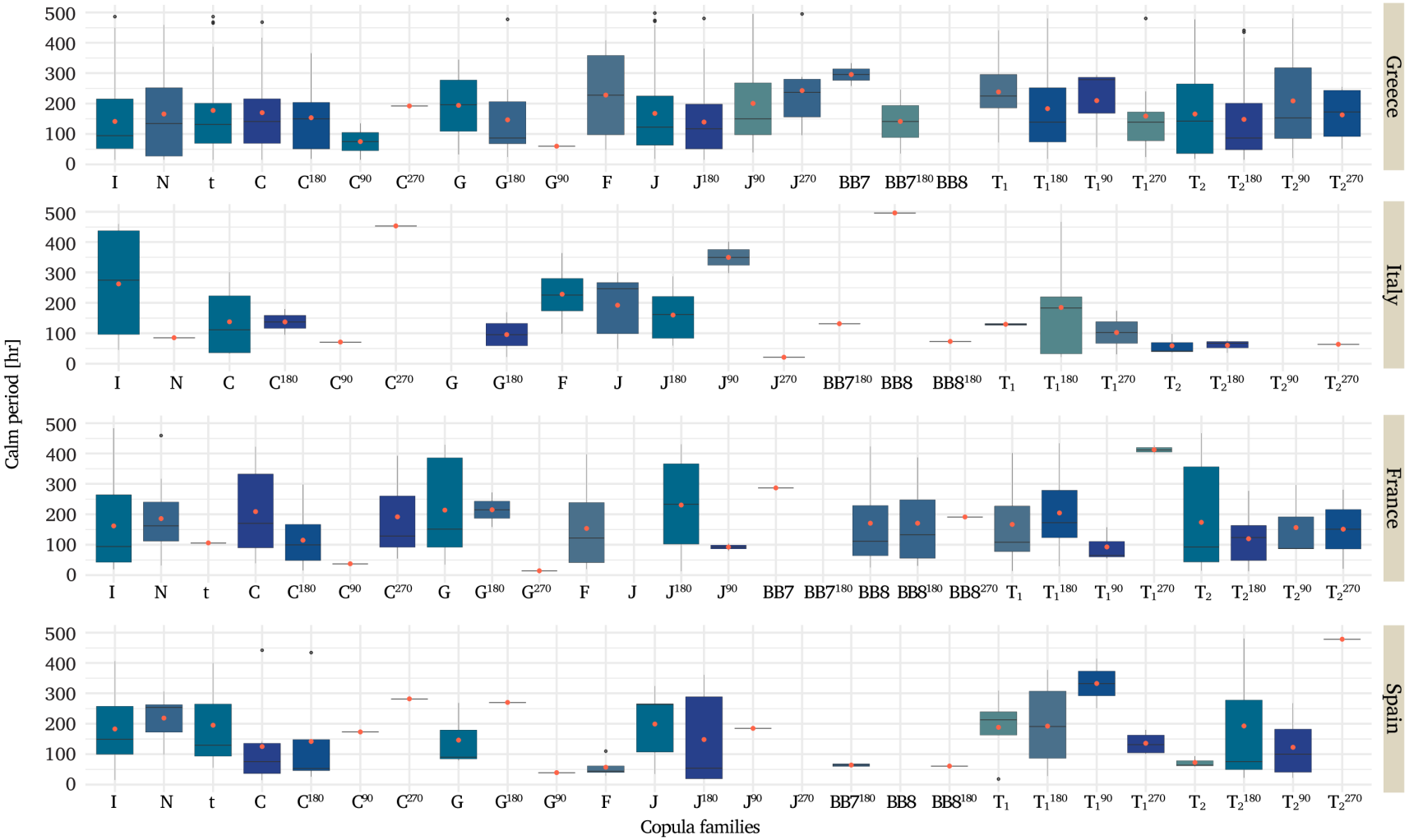

Figure 4.25. The range of calm period of coastal storms which are modelled by different copula families.

The boxplots of Figure 4.21 present the different ranges of Kendall's tau regarding the copula family. As expected, the rotated versions (90 or 270 degrees) present negative correlation values between *H* and *T*, while the correlation is close to zero when the independent copula is chosen. The Tawn copulas (T_1 and T_2) better describe the pairs of *H* and *T* with a correlation of almost 0.25, while the pairs of *H* and *T* have slightly higher values of Kendall's τ when they are modelled by Joe and Clayton copulas. The boxplots of other storm parameters (Figs. 4.22 - 4.25) present shorter variation than Kendall's τ, but it could be said that the Tawn, Joe and Clayton copulas mostly fit with pairs of *H* and *T* with similar and not extreme characteristics. Finally, it cannot be assumed that the best bivariate copula family better describes coastal storms with specific characteristics.

The upper and the lower tail dependence coefficients (Fig. 4.26), as described by Eq. 3.40, are estimated for determining the adequacy of certain copula families to a sample. Most copulas are not able to describe the dependence of tails, either lower (λ_L) or upper (λ_U), hence their values are set to zero (e.g., the Gaussian copula). The Tawn (T_1, T_2), the BB7 and the t copulas fit better to coastal storms with upper tail dependence of *H* and *T* around 0.25, while the Clayton (C^{180}), the Gumbel and the Joe copulas are more accurate for dependence around 0.60. Regarding the lower tail dependence, the Clayton, Gumbel (G^{180}) and Joe (J^{180}) copulas better describe high dependence around 0.60. The pairs of *H* and *T*, which are modelled by BB7 and $BB7^{180}$, present dependence λ_L around 0.40, while the Tawn (T_1^{180}, T_2^{180}) and the t copulas better describe data with lower dependence. In both cases (λ_L, λ_U), the t copulas have the more extensive interquartile range, the Clayton and survival Joe copulas describe the highest values of tails dependence. It is worth mentioned that the best-copula selection is quite difficult when two or more families have similar tail dependence as they fit similar well to the data (Nikoloulopoulos and Karlis, 2008), such as Clayton (C) and survival Joe (J^{180}). Consequently, the investigation of best-selected copula can also be limited to families that provide different behaviour in tail dependence (Nikoloulopoulos et al., 2012; Kadhem and Nikoloulopoulos, 2021).

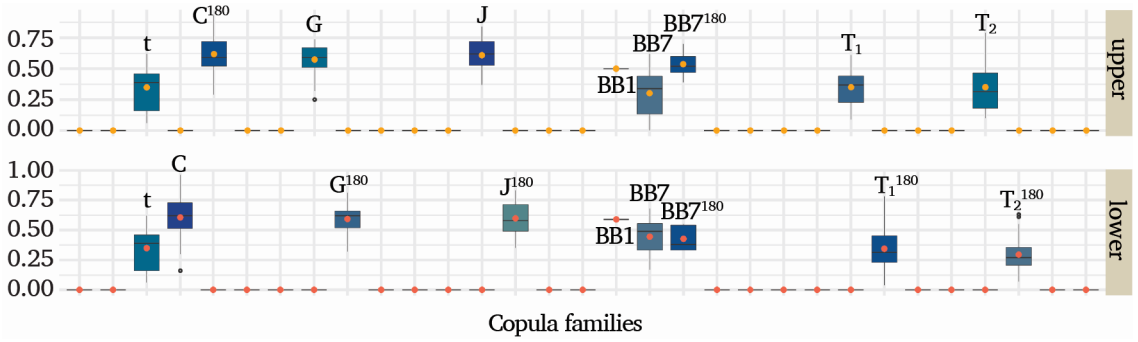

Figure 4.26. The range of upper and lower tail dependence coefficients for different copula families.

Since the best copula is identified, another copula with slightly higher AIC (or BIC) might be also appropriate to describe and model the dependence of *H* and *T*. Subsequently, the second-best copula families are investigated and their characteristics are presented (Table 4.5).

The Clayton copulas (C) are the most frequent second-best copulas. The Gaussian (N) and the Frank copula (F) change their position as the best-selected copula. The Clayton copulas are replaced by the Joe copulas (J) and vice-versa. Clayton copulas can replace the Gumbel copulas (G), while the BB8 copulas have as an alternative the Gumbel or the Clayton ones. The case of Tawn copulas is the most interesting because their versions (T_1, T_2 and rotated) mostly contain the independent copula (I) as the second-best copula. Though it has to be noted that the second-best is not unique for each copula family but the most frequent of the second-best copula as described in Table 4.5 (e.g., 74.9% of Clayton copulas can be replaced by rotated Joe copulas).

The differences of AIC, BIC and the Log-likelihood between the two best-selected copulas are usually too small, as described by the absolute difference of their mean values and the standard deviations. The Tawn copulas are again an exception, while the differences between AIC and BIC present the highest values among the others, which their replacement may explain by independent copulas.

Table 4.5

Characteristics of two best-selected copulas for *H* and *T*.

Best copula			Absolute difference					
			mean			standard deviation		
1st	2nd	Occurrence %	AIC	BIC	Loglik.	AIC	BIC	Loglik.
N	F	29.20	0.70	0.93	0.37	0.63	1.02	0.30
t	N	62.70	1.45	2.02	1.63	5.63	5.33	2.86
C	J^{180}	74.90	0.25	0.38	0.17	0.29	0.64	0.23
C^{180}	J	73.20	0.25	0.38	0.17	0.32	0.64	0.24
C^{90}	J^{270}	71.40	0.17	0.30	0.17	0.17	0.50	0.28
C^{270}	J^{90}	86.20	0.22	0.31	0.15	0.24	0.59	0.22
G	C^{180}	38.30	0.38	0.85	0.38	0.34	0.95	0.34
G^{180}	C	40.00	0.48	0.97	0.34	0.45	1.07	0.32
G^{90}	C^{270}	40.00	0.28	0.32	0.34	0.27	0.25	0.41
G^{270}	C^{90}	66.70	0.29	0.30	0.26	0.25	0.24	0.31
F	N	56.80	1.48	2.19	0.62	1.73	2.31	0.74
J	C^{180}	83.60	0.27	0.35	0.20	0.37	0.56	0.30
J^{180}	C	87.80	0.32	0.44	0.21	0.36	0.66	0.27
J^{90}	C^{270}	85.70	0.29	0.33	0.27	0.37	0.41	0.36
J^{270}	C^{90}	83.30	0.22	0.27	0.27	0.30	0.37	0.41
BB1	BB7	100.00	0.41	0.41	0.20	-	-	-
BB7	BB1	48.30	0.52	0.57	0.67	0.82	0.75	0.67
$BB7^{180}$	G	33.30	0.56	1.08	1.00	0.54	0.66	0.55
$BB7^{90}$	$BB1^{270}$	50.00	0.07	0.08	0.03	0.10	0.09	0.05
BB8	G	41.50	3.83	2.89	2.74	4.96	4.10	2.57
$BB8^{180}$	G^{180}	47.20	2.84	2.13	2.20	2.90	2.30	1.48
$BB8^{90}$	C^{270}	50.00	0.58	1.36	1.04	0.77	1.19	0.76
$BB8^{270}$	C^{90}	100.00	0.71	1.76	1.36	-	-	-
T_1	I	30.50	2.98	2.60	2.57	3.05	2.86	1.63
T_1^{180}	I	23.30	4.38	3.69	3.20	5.00	4.54	2.57
T_1^{90}	I	44.70	2.74	2.31	2.52	2.27	2.08	1.38
T_1^{270}	I	39.50	3.28	2.69	2.76	2.99	2.76	1.68
T_2	I	21.40	3.34	2.84	2.65	3.43	3.12	1.82
T_2^{180}	T_1	24.00	3.37	2.91	2.56	4.06	3.92	2.18
T_2^{90}	I	43.60	2.98	2.33	2.74	2.41	2.07	1.43
T_2^{270}	I	42.90	3.01	2.80	2.75	2.78	2.61	1.35

4.2.2. Location-based five-dimensional copulas

The multivariate modelling of coastal storms is accomplished through the application of multivariate copulas at a given location. For this application, the case study of Malaga is selected. This dataset is the longest among the datasets of other locations (Figure 4.2), the buoy is located in shallow waters and very close to the coast, the threshold of significant wave height (H_{thr}) is 1.2 metres, and the calm period threshold (I_{thr}) is 12 hours.

The most important coastal storm parameters (H_1, T_1, D, I, E) are examined for 409 coastal storms of Malaga (Table 4.6). The correlation coefficients are also considered to investigate the correlation of variables in pairs (Fig. 4.27). As expected, the highest correlation is observed in pairs of *H-E* and *D-E*.

Table 4.6

Sample of coastal storm events in Malaga.

Start	End	H_1 [m]	T_1 [s]	D [h]	I [h]	E [m^{2}h]
12/14/1985 15:00	12/15/1985 0:00	1.48	6.65	11.25	1788	20.85
2/27/1986 12:00	3/1/1986 3:00	1.42	7.54	39.00	291	79.19
3/13/1986 6:00	3/13/1986 12:00	1.20	4.53	7.50	1182	9.65
5/1/1986 18:00	5/2/1986 6:00	1.30	7.18	14.00	669	22.07
5/30/1986 3:00	6/2/1986 3:00	1.77	7.89	72.55	4407	239.87
12/2/1986 18:00	12/5/1986 3:00	1.50	6.68	58.50	732	133.03
1/4/1987 15:00	1/4/1987 21:00	1.47	6.10	8.70	378	15.25
1/20/1987 15:00	1/22/1987 9:00	1.51	6.19	42.82	42	97.97
1/24/1987 3:00	1/25/1987 15:00	1.20	5.97	36.00	1092	50.57
3/12/1987 3:00	3/14/1987 3:00	1.46	6.25	52.82	30	109.86
…	…	…	…	…	…	…

The marginal distribution functions and the probability integral transform are used to convert the data from the real domain to uniform random variables. In this way, the data are standardised (Fig. 4.28). Subsequently, the variables are examined for their dependence through the chi and K-plots (Fig. 4.29). The pairs of H_1, E, and D, E have positive dependence since they follow the curve line ($y=-lnx$) in K-plots, and they are outside of the confidence intervals (dotted lines) of chi-plots. On the contrary, all the pairs that include the calm period (I) are independent, while they approach the diagonal line ($y=x$) in K-plot, and they are inside the confidence intervals of chi-plots.

The five-dimensional copula is constructed with the pair copula method and especially with the method of C-Vines. The coastal storm energy (*E*) is the first variable of the C-Vine structure, as the most dependent variable among the others. Starting with *E*, the other bivariate copulas of the first tree (T_1) are constructed. Then the bivariate copulas are combined to the three-dimensional copulas of the second tree (T_2) and so forth, following the methodology of Figure 3.7. At each stage, the best-selected copula family and the associated copula parameters are investigated. Here, for the case study of Malaga, the proposed C-Vine structure is presented in Figure 3.6, with all the details and the parameters at each tree to be described in Table 4.7 (Nagler et al., 2021).

The proposed C-Vine structure is not unique. Minor changes regarding the selection of best copula families or in the order of coastal storm parameters may create an equally efficient model. Further investigation shows that the proposed structure suits the most examined locations in the Mediterranean Sea. Besides, the pair copula method of C-Vines is not the only method to construct a five-dimensional copula. Most copula families can be extended to higher dimensions, but in this way, the dependence of coastal storm parameters and their combinations cannot be investigated as described in C-Vines.

Table 4.7
Characteristics of proposed C-vine copula.

Tree	Edge	Copula	1st Parameter	2nd Parameter	τ	Tail dependence	
						λ_U	λ_L
1	5,2	T_2	01.84	0.55	0.30	0.38	-
1	5,3	N	00.95	-	0.80	-	-
1	5,1	G	02.17	-	0.54	0.62	-
1	5,4	F	-00.99	-	-0.11	-	-
2	1,2|5	C	00.29	-	0.13	-	0.09
2	1,3|5	F	19.03	-	-0.81	-	-
2	1,4|5	F	-00.65	-	-0.07	-	-
3	4,2|1,5	T_2	01.21	0.28	0.08	0.11	-
3	4,3|1,5	F	-00.64	-	-0.07	-	-
4	2,3|4,1,5	T_2^{90}	-01.67	0.03	-0.03	-	-
1: H_1 • 2: T_1 • 3: *D* • 4: *I* • 5: *E*							

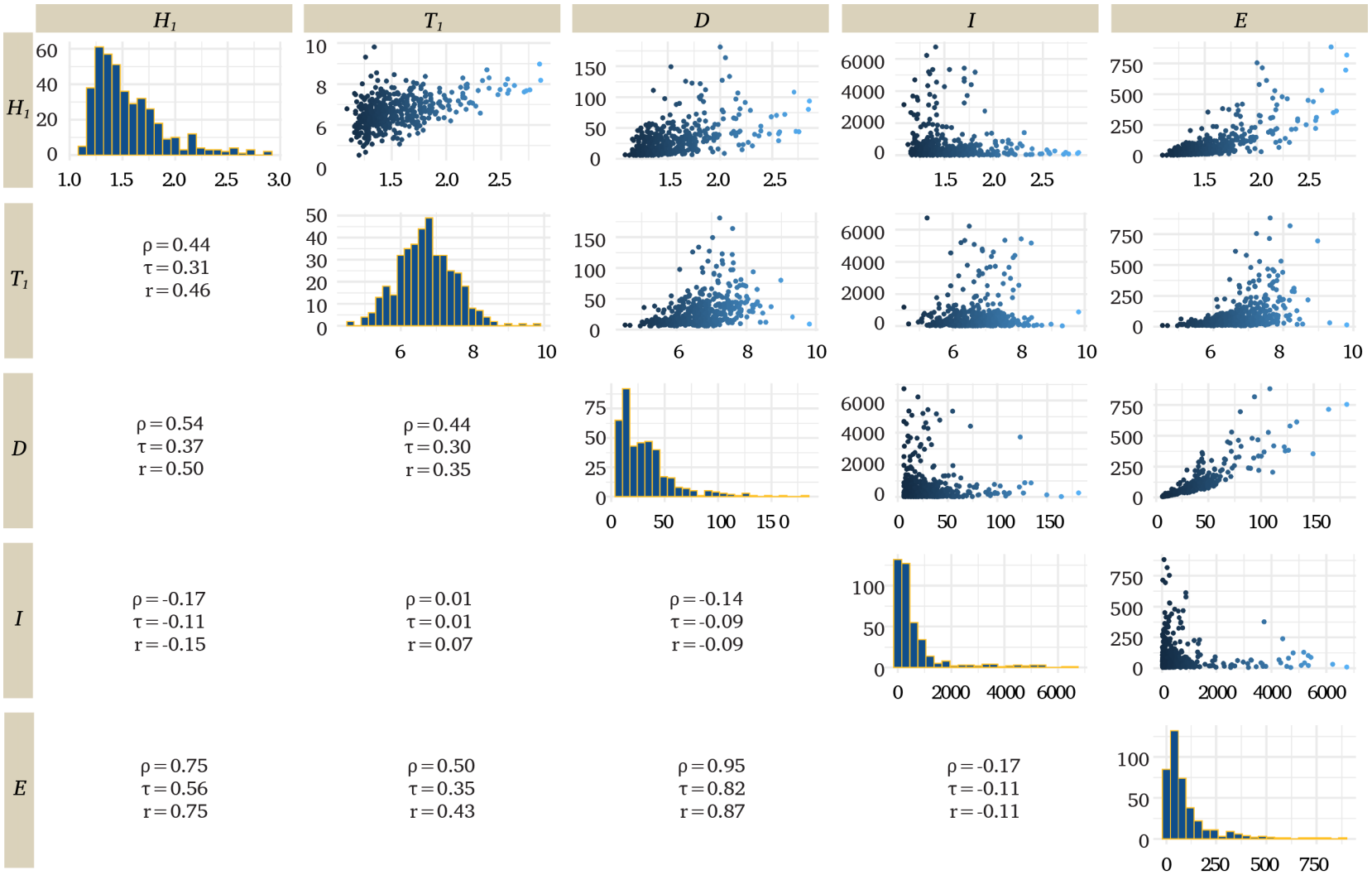

Figure 4.27. Scatterplots of examined variables in real domain (upper), their frequency histograms (diagonal), and the correlation coefficients of Spearman (ρ), Kendall (τ), and Pearson (r) (lower).

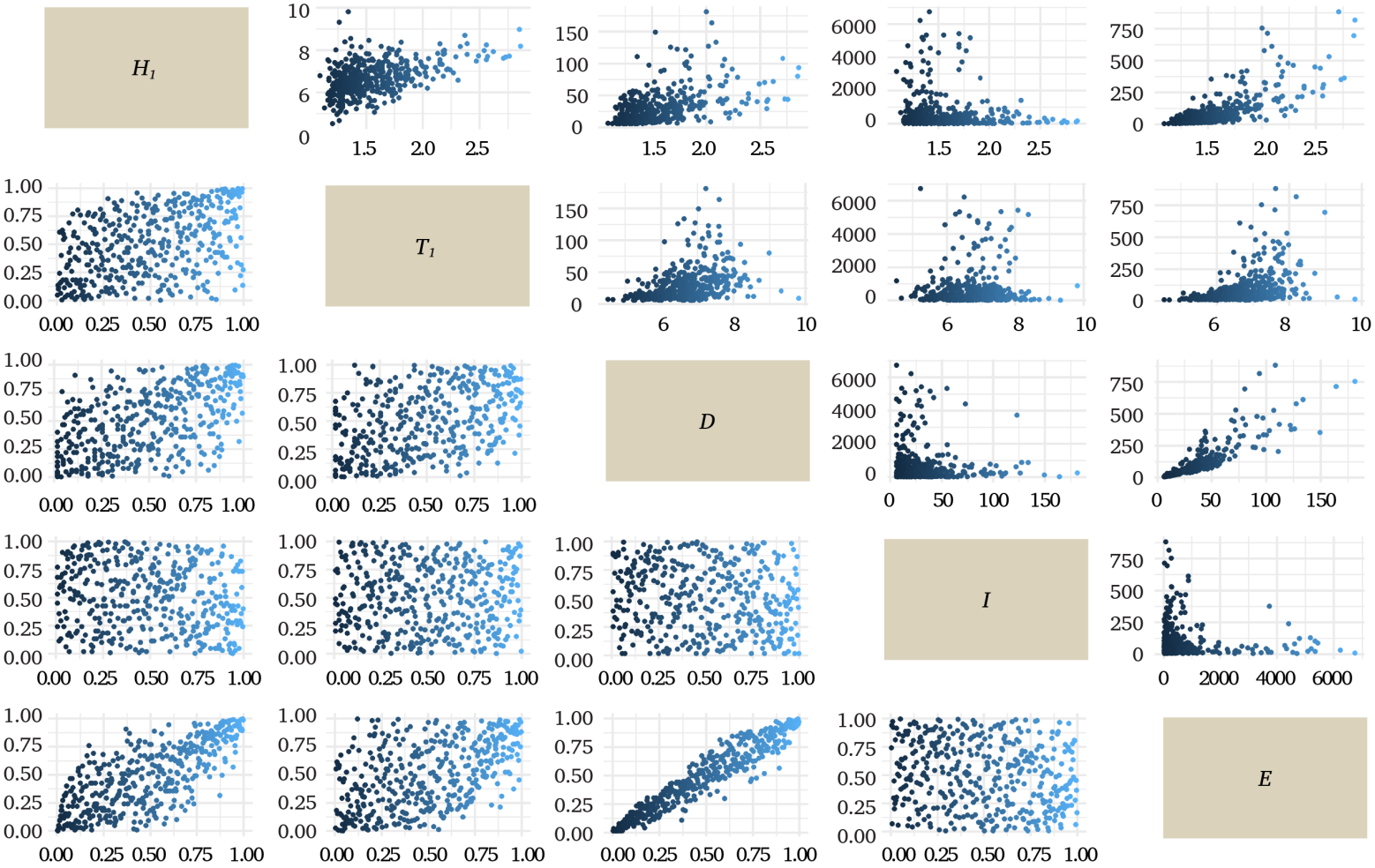

Figure 4.28. Scatterplots of examined variables in real domain (upper) and in domain U[0,1] after their conversion (lower).

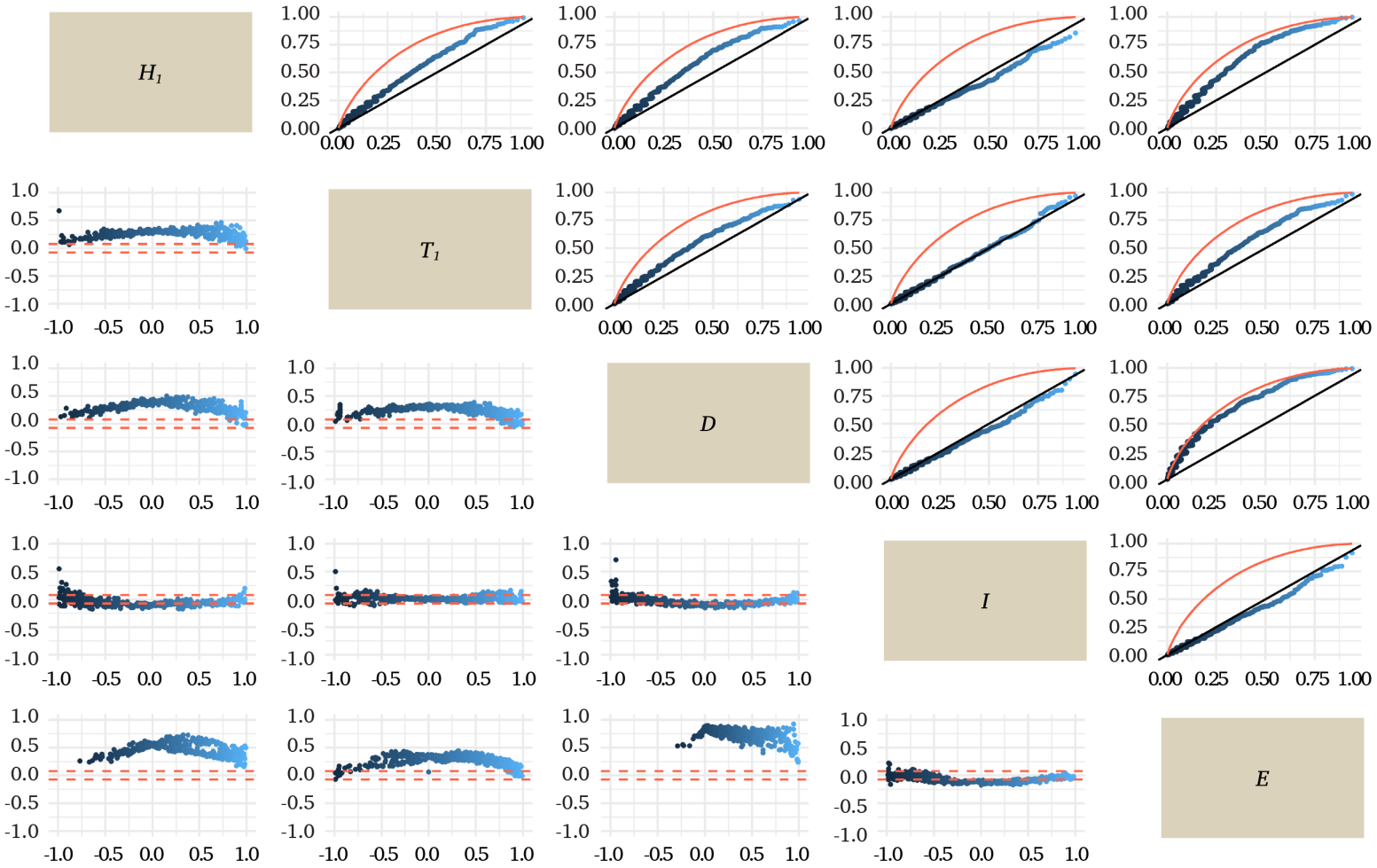

Figure 4.29. The K-plots (upper) and the chi-plots (lower) for the dependence check of the examined variables.

4.2.3. Coastal storm simulation example

The simulation of coastal storms can be produced by combining the coastal storm parameters in pairs through copulas. The simulation can help reproduce the coastal storm activity at a specific location and enables the construction of synthetic storms when the data are insufficient. The methodology of De Michele et al. (2007) for sea storm simulation is extended from four to five variables and compared to the algorithms of Stöber and Czado (2017) and Aas et al. (2009), that are usually applied in the field of economics.

A random dataset of five coastal storm parameters H_1, T_1, D, I, E variables in univariate domain U[0,1] is used as input, and the validation is performed through the dataset of Malaga's coastal storms. Following the simulation algorithms A, B, C and the methodology of C-Vine copulas (Table 4.7), a new dataset of simulated coastal storms is produced, with five variables and a length of 409 coastal storms. A comparison of standardised observations and simulations of coastal storms is accomplished a) graphically by their scatterplots (Figure 4.30a) and b) through the correlation coefficients of Kendall's τ (Figure 4.30b). The Algorithms A, B based on the work of Aas et al. (2009) and Stöber and Czado (2017) produce the same results (upper-triangular); hence they are together presented below. A careful study of scatterplots indicates different simulations. The Algorithm C that is based on the methodology of De Michele et al. (2007), provides simulations (lower-triangular) that are not in good agreement with observations (i.e., real coastal storms), especially for the pairs (H_1-E, T_1-E, D-E, I-E). However, the simulated coastal storms of the other two methods approach the observations satisfactorily. The better results of Algorithms A and B are also confirmed by Kendall's τ, which are close enough for both observations and simulations contrary to Algorithm C, which presents divergences among observations and simulations of coastal storms.

A thorough investigation of the best-selected copulas and the *h-functions* at each step in these algorithms can improve further their results. However, both the complexity and the requirement for the most bivariate copulas in Algorithm C lead to inadequate five-dimensional simulations of coastal storms. On the other hand, the simplest algorithms A and B can be used for the coastal storm simulations with similar results.

Similar works of simulation can be found in De Michele et al. (2007), Corbella and Stretch (2013), Li et al. (2014, 2018), and Orcel et al. (2021). Their results are site-specific; hence it is not easy to be compared. These works are usually based on three or four variables, and they are limited to one specific copula (e.g., Archimedean or Gaussian). This may simplify the calculations, but the accuracy is usually decreased when they are extended to higher dimensions. Besides, it is not easy to ensure that a specific copula can model all the dependency structures among variables. In this direction, a mixture of copulas is proposed as more promising (Li et al., 2018) and generally the Vine copulas, also known as PCC, are considered better than other methods (Jäger and Nápoles, 2017; Orcel et al., 2021). This efficiency of C-Vine copulas has also been discussed in Joe et al. (2010) by describing their flexibility in modelling the tail dependencies. Up to now, the Vine copulas have been used successfully for simulations of wave height and wave period time series (Jäger and Nápoles, 2017), for storm surges which are induced by tropical cyclones (Zhang and Wang, 2021), and for the modelling of flood characteristics (Tosunoglu et al., 2020).

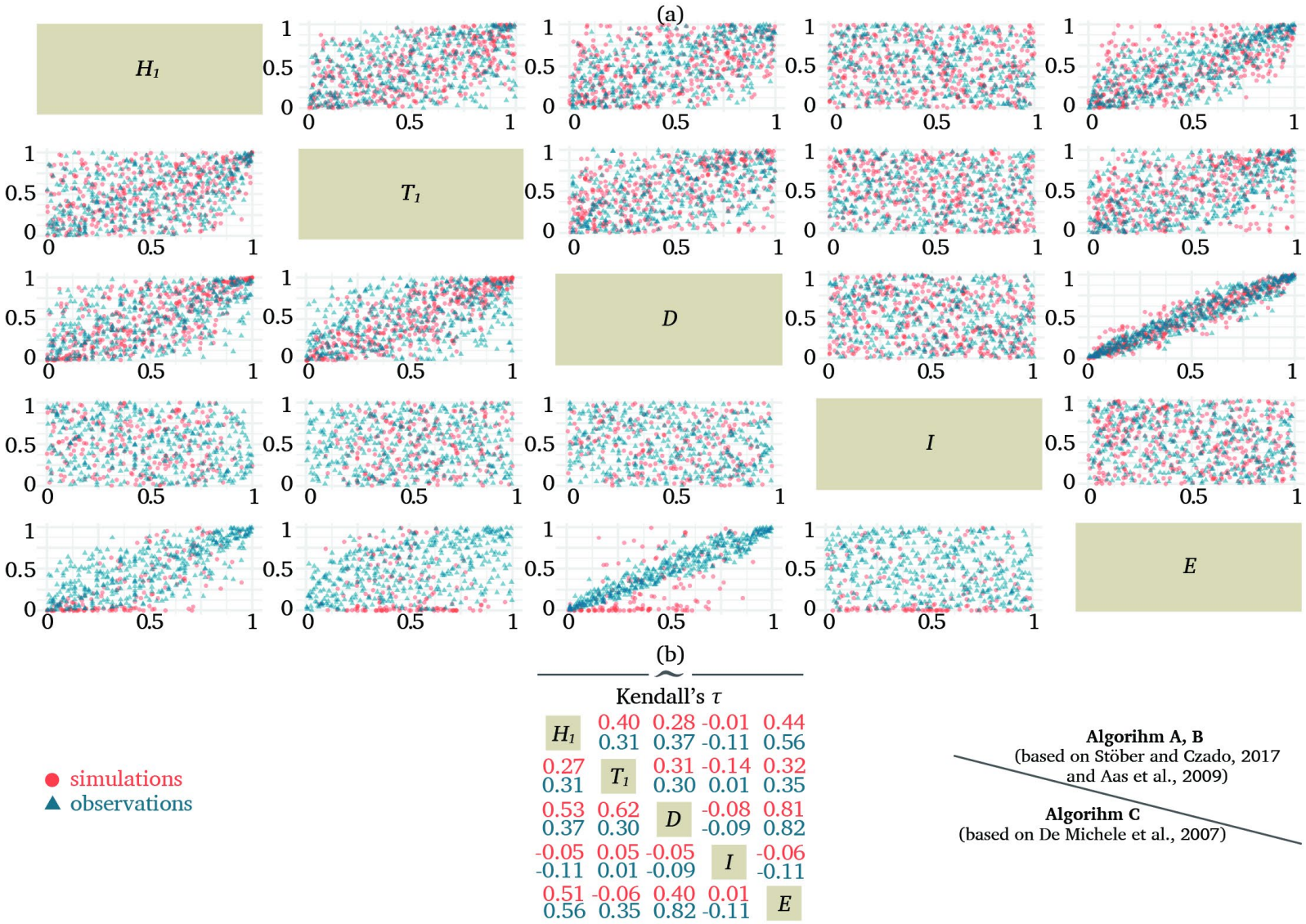

Figure4.30. (a) Comparison of standardised observations and copulas simulations of coastal storms following the Algorithms A, B (upper) and Algorithm C (lower). (b) Comparison of three algorithms according to Kendall's τ.

4.2.4. Coastal storm return periods

The return period describes how often a coastal storm with specific characteristics may occur. For these estimations, the joint probability of five important coastal storm parameters H_1, T_1, D, I, E, or a combination of them, is needed making the use of copulas is inevitable. The multivariate copulas of different families and the proposed C-Vine structure (section 4.2.2) are compared for this application.

The return periods of the most extreme coastal storms are investigated following the theory of section 3.4.5. The application is performed to the dataset of Malaga's coastal storms, but the same methodology can be applied to any location. Considering the overall description of the storm activity, according to Figures 4.9 - 4.10 and Table 4.4, the return periods are estimated for the highest values of storm parameters (over 90^{th} percentiles) as described in Table 4.8. The short calm period (I) implies the short time for post-storm recovery of the coast and is indicative of significant impacts. Hence, I has the opposite interpretation among the parameters, and thus the lowest values up to the 10^{th} percentile are considered as the most extreme.

Table 4.8
The highest values of important coastal storm parameters.

Percentiles	H_1 [m]	T_1 [s]	D [h]	E [m^{2}hr]	I [h]	Percentiles
90^{th}	2.02	7.71	61.23	232.92	37.80	10^{th}
93^{th}	2.15	7.84	72.24	316.11	27.24	7^{th}
95^{th}	2.22	7.99	89.20	367.03	21.00	5^{th}
97^{th}	2.39	8.18	102.21	449.00	18.00	3^{th}
98^{th}	2.56	8.31	111.84	520.99	17.00	2^{th}
99^{th}	2.70	8.54	127.38	688.75	13.08	1^{th}

Bivariate return periods

The bivariate return periods of coastal storms are estimated for all the pairs of parameters H_1, T_1, D, I, E using Eqs. 3.131-3.132, where the μ represents the average coastal storm events in a year. The best-selected copula does not significantly affect the calculation of the return period. Therefore, no large discrepancies are observed between the selected bivariate copulas and especially when the parameters as physical quantities are related to each other (e.g., wave height and wave period). In addition, the best-

selected copula never presents extreme values of the return period in relation to the other two copulas and usually gives similar results to the second-best copula. The minor deviations of bivariate copulas are insignificant for coastal engineering applications.

For the significant wave height (H_1) and the wave period (T_1), the Tawn (T_2), the Gumbel (G), and the BB1 copulas are the best three copulas (Table 4.9). For comparison, the return periods of coastal storms are estimated (Fig. 4.31), when the H ranges over the highest values (90^{th}-99^{th}), and the T_1 is over the 8.54 seconds (99^{th}). The return period of a coastal storm with the mean significant wave height over 2.7 metres and the mean wave period over 8.54 seconds is almost 17 years for three copulas. Consequently, a coastal storm with these characteristics can occur in Malaga once in 17 years.

Table 4.9

The best three bivariate copulas for H_1 and T_1 and their characteristics.

Copula	1st parameter	2nd parameter	τ	AIC	BIC	Loglik.
1. T_2	1.82	0.49	0.28	-110.13	-102.10	57.07
2. G	1.41	0.00	0.29	-95.73	-91.72	48.87
3. BB1	0.12	1.35	0.30	-95.41	-87.38	49.71

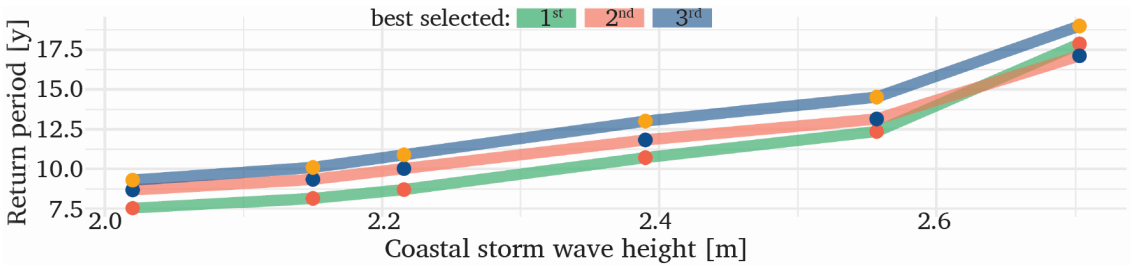

Figure 4.31. Comparison of return periods when the H_1 ranges over the highest values (90-99^{th}) and the T_1 is over the 8.54 seconds (99^{th}).

The return periods for all the pairs of their highest values are estimated below by taking the best-selected copula. According to Table 4.10, the most extreme coastal storms (i.e., with high values of H_1 and T_1) are quite often and may occur at least once in a decade or once in 20 years for the most extremes. These results are confirmed by the dataset, where coastal storms with high values of H_1 and T_1 are very common, as described in Figure 4.9.

Table 4.10

The bivariate return period of coastal storms for any combination of H_1 and T_1.

	AND case		H_1 [m]					
			90^{th}	93^{th}	95^{th}	97^{th}	98^{th}	99^{th}
			2.02	2.15	2.22	2.39	2.56	2.70
T_1[s]	90^{th}	7.71	1.98	2.68	3.30	5.42	7.06	12.32
	93^{th}	7.84	2.31	3.02	3.65	5.82	7.52	12.93
	95^{th}	7.99	2.68	3.38	4.02	6.21	7.93	13.44
	97^{th}	8.18	3.79	4.47	5.08	7.26	8.99	14.61
	98^{th}	8.31	4.67	5.33	5.93	8.06	9.78	15.40
	99^{th}	8.54	7.53	8.15	8.71	10.72	12.36	17.87

For the wave height (H_1) and the duration (D_1) of a coastal storm, the best three copulas are the Gaussian (N), the Students' t, and the BB8 copulas (Table 4.11). The three copulas are used for the return period's estimation of a coastal storm when the H_1 exceeds the 90^{th}-99^{th} percentile and the D is over 127.38 hours. Figure 4.32 shows the same efficiency of the best two models (N and t). However, the third best-selected copula has considerable divergence from the other copulas and overestimates the return period.

Table 4.11

The best three bivariate copulas for H_1 and D and their characteristics.

Copula	1st parameter	2nd parameter	τ	AIC	BIC	Loglik.
1. N	0.55	0	0.37	-138.83	-134.82	70.42
2. t	0.55	30	0.37	-134.54	-126.52	69.27
3. BB8	4.55	0.62	0.37	-133.48	-125.45	68.74

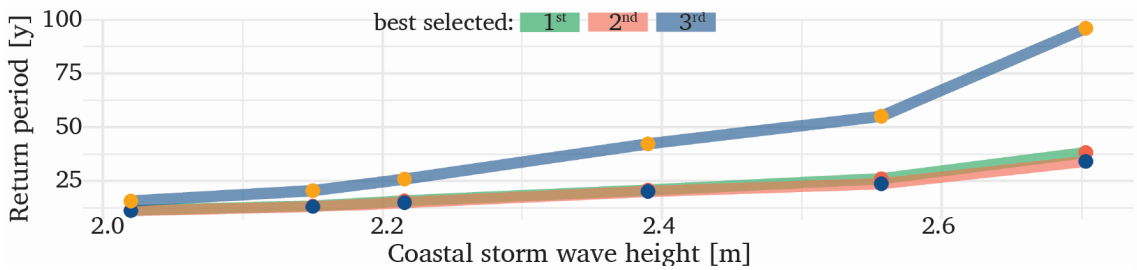

Figure 4.32. Comparison of return periods when the H_1 ranges over the highest values (90^{th}-99^{th}) and the D is over the 127.38 hours (99^{th}).

The Gaussian copula (N) is used for the estimation of coastal storms' return period for all the percentiles of wave height (H_1) and the duration (D). The joint occurrence of

high waves and long duration occurs less often than H_1 and T_1 combinations (Table 4.12). With the wave height exceeding 2.7 metres and the duration to be over 127.38 hours, the most extreme event probably occurs once in 38 years.

Table 4.12

The bivariate return period of coastal storms for any combination of H_1 and D.

			H_1 [m]					
			90^{th}	93^{th}	95^{th}	97^{th}	98^{th}	99^{th}
			2.02	2.15	2.22	2.39	2.56	2.70
D [h]	90^{th}	61.23	2.23	2.84	3.61	5.22	7.00	11.39
	93^{th}	72.24	2.87	3.61	4.52	6.42	8.51	13.57
	95^{th}	89.20	3.55	4.42	5.48	7.67	10.06	15.81
	97^{th}	102.21	5.49	6.68	8.13	11.10	14.29	21.83
	98^{th}	111.84	6.92	8.34	10.06	13.56	17.30	26.06
	99^{th}	127.38	11.26	13.33	15.81	20.81	26.06	38.22

For the wave period (T_1) and the duration (D) of a coastal storm, the best three copulas are the Frank (F), the survival BB8, and the Gaussian (N) copulas (Table 4.13). The return periods of a coastal storm, with T_1 exceeding the 90^{th}-99^{th} percentile and the D is over 127.38 hours, are estimated. Figure 4.33 presents the same efficiency of first and second best-selected copulas. On the contrary, the third copula underestimates the return periods for all the pairs of T_1-D.

Table 4.13

The best three bivariate copulas for T_1 and D and their characteristics.

Copula	1st parameter	2nd parameter	τ	AIC	BIC	Loglik.
1. Frank	2.88	0.00	0.30	-83.75	-79.73	42.87
2. $BB8^{180}$	5.04	0.48	0.30	-83.00	-74.97	43.50
3. N	0.44	0.00	0.29	-80.78	-76.76	41.39

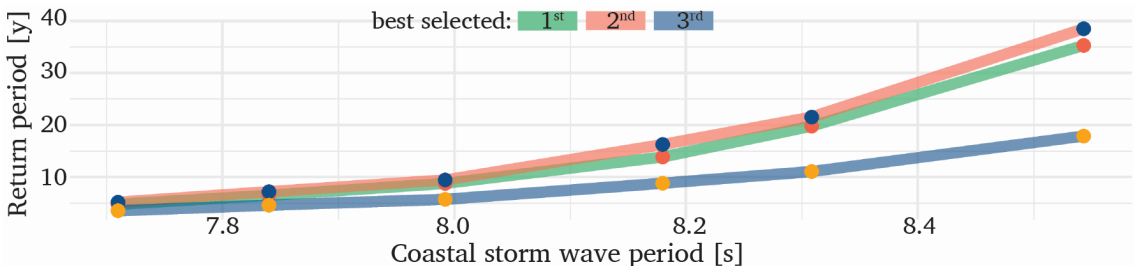

Figure 4.33. Comparison of return periods when the T_1 ranges over the highest values (90^{th}-99^{th}) and the D is over the 127.38 hours (99^{th}).

The coastal storms' return period in different combinations of T_1 and D is estimated by using Frank copula (Table 4.14). The results show that coastal storms with the joint occurrence of high wave periods and long duration occur rarely. Almost the half return periods are over 25 years, and both highest values of T_1 and D occur once in 177 years.

Table 4.14

The bivariate return period of coastal storms for any combination of T_1 and D.

			T_1 [s]					
			90^{th}	93^{th}	95^{th}	97^{th}	98^{th}	99^{th}
			7.71	7.84	7.99	8.18	8.31	8.54
D[h]	90^{th}	61.23	3.33	4.56	6.17	9.76	13.96	24.86
	93^{th}	72.24	4.77	6.52	8.8	13.89	19.83	35.29
	95^{th}	89.20	6.04	8.24	11.11	17.52	25.01	44.48
	97^{th}	102.21	10.33	14.06	18.93	29.81	42.51	75.54
	98^{th}	111.84	13.66	18.59	25.01	39.37	56.12	99.71
	99^{th}	127.38	24.33	33.08	44.48	69.96	99.71	177.07

For the return periods of coastal storms, the best three copulas are chosen regarding their calm period (I) and their energy (E). The Frank (F), the Gaussian (N) and the survival BB8 copulas (Table 4.15) are used for the return period's estimation of a coastal storm when the I does not exceed the $1\text{-}10^{th}$ percentiles, and the E is over the 232.92 m^2h (90^{th}). The efficiency of the three copulas (Fig. 4.34) is very similar.

Table 4.15

The best three bivariate copulas for *I* and *E* and their characteristics.

Copula	1st parameter	2nd parameter	τ	AIC	BIC	Loglik.
1. Frank	0.99	0.00	0.11	-9.14	-5.13	5.57
2. N	0.16	0.00	0.10	-7.80	-3.79	4.90
3. BB8[180]	3.09	0.36	0.11	-7.31	0.72	5.65

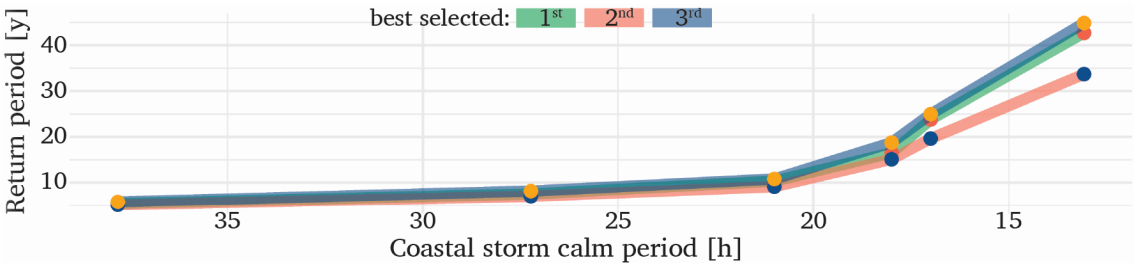

Figure 4.34. Comparison of return periods when the *I* does not exceed the lowest values (*1-10th*) and the *E* is over the 232.92 m^{2}h (*90th*).

Taking the best-selected Frank copula, the return period of coastal storms is estimated for any combination of *I* and *E* (Table 4.16). The joint occurrence of both parameters within a coastal storm is not usual. Almost the 50% of estimated return periods in Table 4.16 are over 30 years, which means that coastal storm with high energy is rarely followed by a short calm period.

Table 4.16

The bivariate return period of coastal storms for any combination of *I* and *E*.

			I [h]					
			10th	*7th*	*5th*	*3th*	*2th*	*1th*
			37.80	27.24	21.00	18.00	17.00	13.08
E[m^{2}h]	*90th*	232.92	5.41	7.55	10.34	16.57	23.83	42.73
	93th	316.11	7.55	10.54	14.43	23.11	33.23	59.56
	95th	367.03	10.85	15.13	20.71	33.16	47.69	85.46
	97th	449.00	17.93	25.01	34.22	54.77	78.75	141.10
	98th	520.99	26.79	37.35	51.10	81.78	117.58	210.65
	99th	688.75	42.73	59.56	81.49	130.40	187.47	335.85

Trivariate return periods

For three variables, the trivariate copulas can be constructed through C-Vine as described in Figure 3.6(a), following the methodology of Figure 3.7, or by applying a specific copula family in three dimensions based on Eqs. 3.133-3.134.

For the estimation of the return periods, the C-Vine copula can be defined through the following structure (Table 4.17), and a comparison is accomplished by applying the t copula from the Elliptical class and the Gumbel copula, which belongs both to the Archimedean and Extreme class. The return period $T_{(H_1>2.39 \cap T_1>8.18 \cap D>102.21)}$ is almost 40 years, based on the C-Vine, and much shorter than those of the Gumbel or the t copulas (Table 4.18). The results of C-Vine are more reasonable, contrary to the results of the other two copulas, for which their return periods are short and they do not agree with the real data. On the other hand, the OR case $T_{(H_1>2.39 \cup T_1>8.18 \cup D>102.21)}$ presents small values for all the copulas, which means that a coastal storm with at least one parameter to exceed a specific value occurs almost once per year.

Table 4.17

Characteristics of the proposed C-Vine structure for H_1, T_1, and D.

Tree	edge	copula	1st Parameter	2nd Parameter	τ
1	1,2	T_2	1.82	0.49	0.28
	3,1	N	0.55	0.00	0.37
2	3,2|1	C	0.44	0.00	0.18

Table 4.18

The return period (in years) of coastal storms when $H_1 > 2.39$ m, $T_1 > 8.18$ s, $D > 102.21$ h.

	C-Vine	Gumbel	t
AND case	40.22	8.19	16.68
OR case	1.08	1.26	1.17

Similarly, for the return periods based on the variables of the wave period (T_1), the calm period (I), and the energy (E) during a coastal storm, the C-Vine (Table 4.19) compared to Gumbel and t copulas. The return period $T_{(T_1>7.99 \cap I<21 \cap E>367.03)}$ is 57.64 years based on the C-Vine, but the other two copulas have shorter periods (Table 4.20). Hence, the Gumbel and t copulas results cannot be accepted, given that they are not confirmed

by Malaga's dataset covering 30 years. The OR case $T_{(T_1>7.99 \cup I<21 \cup E>367.03)}$ is under one year for all the cases.

Table 4.19

Characteristics of the proposed C-Vine structure for T_1, I, and E.

Tree	edge	copula	1st Parameter	2nd Parameter	τ
1	5,2	T_2	1.84	0.55	0.30
	5,4	F	0.99	0.00	0.11
2	4,2|5	T_1^{90}	-1.21	0.27	-0.08

Table 4.20

The return period (in years) of coastal storms when $T_1>7.99$ s, $E>$ 367.03 m^{2}h and $I<21$ h.

	C-Vine	Gumbel	t
AND case	57.64	23.73	22.98
OR case	0.62	0.65	0.64

Four-dimensional return periods

The C-Vine of four variables is presented in Table 4.21, and the return periods are compared using the t and the Gaussian copula. The estimation of the return period for both AND and OR case is accomplished based on Eqs. 3.135-3.136. The results (Table 4.22) show the C-Vine to be more efficient, having a return period $T_{(H_1>2.15 \cap T_1>7.84 \cap D>72.24 \cap I<27.24)}$ of over 35 years. The other two copulas underestimate the return period. For t and Gaussian copulas, the joint occurrences of variables within a coastal storm may happen almost once per 26 or 16 years, respectively, but this dataset does not confirm it. The return period $T_{(H_1>2.15 \cup T_1>7.84 \cup D>72.24 \cup I<27.24)}$ is shorter than 0.4 years, with small divergences among the three copulas.

Table 4.21

Characteristics of the proposed C-Vine structure for H_1, T_1, I, and E.

tree	edge	copula	1st Parameter	2nd Parameter	τ
1	1,3	N	0.55	0.00	0.37
	1,2	T_2	1.82	0.49	0.28
	4,1	F	1.02	0.00	0.11
	2,3|1	C	0.44	0.00	0.18
	4,2|1	T_1^{90}	-1.23	0.27	-0.08
2	4,3|2,1	N	0.07	0.00	0.05

Table 4.22

The return period (in years) of coastal storms when $H_1 > 2.15$ m, $T_1 > 7.84$ s, $D > 72.24$ h, $I < 27.24$ h.

	C-Vine	t	Gaussian
AND case	35.97	25.63	15.54
OR case	0.37	0.39	0.35

Five-dimensional return periods

Finally, the return periods of coastal storms with all parameters exceeding (or not, for the calm period) the specific values are estimated through Eqs. 3.137 and 3.138. The C-Vine copula of Table 4.7 is applied for these estimations and is compared with t and Gaussian copulas (Table 4.23). The results have similar behaviour with fewer dimensions. Finally, the return period $T_{(H_1>2.39 \cap T_1>8.18 \cap D>102.21 \cap I<18 \cap E>449)}$ is almost 58 years based on the C-Vine copula, whereas it is overestimated by t copulas (76.25 years) and the Gaussian one underestimates it. On the other hand, the OR case of the return period is almost the same for all the copulas. This outcome indicates that the copulas are equally effective when the return period depends on simple calculations (e.g., OR case), and the C-Vine copulas present more realistic results when the return period's estimation depends on many copulas (e.g. AND case). The significant deviation of results for more than three coastal storm parameters indicates that the use of copulas leads to wrong decisions if not used properly. A model averaging method could be used to have a better approximation of the return period in practice. The average return period as estimated by different copulas may be considered in any case to decrease the uncertainty of different copulas.

Table 4.23

The return period (in years) of coastal storms when $H_1 > 2.39$ m, $T_1 > 8.18$ s, $D > 102.21$ h, $I < 18$ h, $E > 449$ m^{2}h.

	C-Vine	t	Gaussian
AND case	57.99	76.25	7.65
OR case	0.82	0.88	0.76

4.3. Application of coastal storms in harbour and coastal structures design

The coastal storm analysis is based on the wave climate variables and primarily on the analysis of historical events at a given location. The historical coastal storms and their characteristics provide essential information for understanding such phenomena, their definition, as well as their identification. The frequency of occurrence, the descriptive statistics, the shape, the simulation through copulas and the return periods of coastal storms are fundamental for harbour's and coastal structures' design since they actively support a technical study in coastal engineering.

A coastal storm with high wave heights and short duration can be similarly destructive to another event with a long wave period and long duration. Their impacts are becoming increasingly significant when the calm period is very short, and they are negligible when the storm direction is not critical to the infrastructure or the coast. Coastal storms depend on many variables, and hence a multivariate analysis of such events is necessary. Such analyses of coastal storms should include the frequency of occurrence, the descriptive statistics of their characteristics such as the wave height, the wave period, the wave direction, the duration, the calm period, and the energy. These characteristics are fundamental for a study in coastal engineering, providing a general overview of local wave climate.

The average characteristics but also the most extremes due to coastal storms can be used for determining the design wave height and the design storm conditions (Altomare et al., 2015), improving the conventional design methods of (Rao and Mandal, 2005; Benassai et al., 2009; Basco and Mahmoudpour, 2012; Burmeister et al., 2015; Basco, 2016). The study of coastal storms can also be used for the design of more specific coastal structures (e.g., storm walls-barriers) in order to protect further the coastal communities during a coastal storm (Mooyaart and Jonkman, 2017; Van Doorslaer et al., 2017).

The coastal storm simulation is essential for studying coastal storms when data are not available or for studying more severe events than historical ones. The shape of coastal storm contributes to the simulation since it is used in the construction of synthetic coastal storms having similar or most extreme characteristics compared to historical events (Martín-Hidalgo et al., 2014; Boccotti, 2015; Martín Soldevilla et al.,

2015; Laface and Arena, 2016; Duo et al., 2020; Marzeddu et al., 2020). The copulas are also accomplished for the simulation of coastal storms. By describing the dependencies of associated variables, copulas can model them and generate simulated data (De Michele et al., 2007).

The simulated coastal storms, as well as the historical events, can be used for the investigation of the performance design of coastal structures under extreme conditions. Therefore, the failure probability of coastal structures (Takahashi et al., 2014; Hatzikyriakou and Lin, 2017) and their reliability (Lira-Loarca et al., 2020) is investigated during severe coastal storms. Furthermore, the simulated and observed coastal storms can force numerical models such as MIKE21 or XBeach for studying the wave and coastal processes. These numerical models can also be applied to investigate the shoreline response due to coastal storms (e.g., abruptly loss of sediment), as well as the effects on harbour operation and their tranquillity due to overtopping, diffraction, reflection.

The frequency of occurrence is helpful for understanding how often severe coastal storms will load the structures. Similarly, the estimation of the return period is also crucial for the reoccurrence of a coastal storm. The return periods are a prerequisite for the risk management of infrastructure; hence they have applications to the design of breakwater (Salvadori et al., 2014, 2015), for the design of coastal structures in general (Li et al., 2020; Orcel et al., 2021), and for studying coastal erosion (Corbella and Stretch, 2012b).

Recently, the copula theory has been established in extreme hydrometeorological events' research, especially for the multivariate analysis of extra-tropical and tropical cyclones. For instance, the Coastal Hazards System (Nadal-Caraballo et al., 2020) of the U.S. Army Corps of Engineers (USACE) is an ambitious program based on multivariate analysis and copulas to quantify the hazard due to storms along the U.S. coastline. Similarly, recent works are of great interest since they combine both storm analysis and copula theory in coastal engineering applications relative to the risk modelling (Bushra et al., 2019), their vulnerability analysis (Li et al., 2020), and their simulation (Wei et al., 2021).

The coastal storm analysis highlights the importance of a multivariate approach for such extreme events through the copula theory. The copulas' approach for coastal storms

is at an early stage at the regulations, but the multivariate analysis is increasingly gaining ground against the conventional design theories.

The Eurocode EN 1990 (2002) sets the basis of structural design according to European standards and a new version is forthcoming, including inter alias the design of coastal structures. The multivariate analysis in these regulations is considered a combination of actions (similar to coastal storm parameters) that may affect the structures when they occur at the same time. This combination of actions and the joint occurrence of important variables (e.g., wave wind, currents) is used for estimating return periods, the failure probability, and the reliability of structures. Many other regulations also use the combination of actions for the design of coastal structures (e.g., BS 6349, 2013; ISO 21650, 2007; NORSOK N-003, 2017). The regulations propose a more simplified method than the proposed copula theory of this thesis. The copulas are not yet mentioned in standards, but they can be incorporated into them and offer improved assistance in the near future. In any case, these standards highlight and confirm the importance of multivariate analysis that should be considered for the structures' design.

Chapter 5

Conclusions

"Il est impossible que l'improbable n'arrive jamais"

Emil Gumbel

Coastal storms are meteorologically-induced disturbed sea states that affect both the coastal morphology and infrastructure. They can cause serious problems such as coastal flooding, coastal erosion, and damages to ports and coastal structures. Motivated by the extreme nature of coastal storms and their severe impacts on coastal communities, this thesis focuses on analysing coastal storms and aims to better approach their modelling using copula functions.

Agreeing with Mazas (2019) regarding the subjectivity of any extreme event analysis and the need for a holistic approach with general recommendations for the analysis, this thesis elaborates on coastal storms and attempts to properly understand this physical phenomenon. According to the literature review described in Section 2.1, the analysis of coastal storms can be accomplished by investigating the following aspects:

- Definition of coastal storms.
- Storminess, studying the synoptic systems, storm surges, time series analysis, as well as storm energy.
- Thresholds, regarding the wave height, the duration, and the calm period.
- Impacts of coastal storms.
- Classification of coastal storms.
- Societal aspects of coastal storms.

This thesis focuses on the first three aspects, describing the definition and the thresholds for the identification of coastal storms, the coastal storm characteristics, as well as their modelling through copulas.

Relative to the research objectives set in advance regarding coastal storms' definition, important variables and identification thresholds, this thesis reports that the coastal storm definition depends on the local coastal environment, and it is usually unique for each location. Therefore, the proper identification of coastal storms should be based on the investigation of the wave height, duration, and calm period for each location and their thresholds. Once coastal storms are identified, they can be described by representatives of the following variables: the wave height, the wave period, and the direction within an event, as well as the storm's duration, calm period, and energy.

In the context of this thesis, the copula theory is investigated as a potential approach for coastal storm modelling. This theory is indeed considered widespread during the last decades for modelling multivariate extreme events such as coastal storms. The copulas enable a better description of associated parameters' dependencies. The copula theory is applied on three different cases: a) for modelling one particular storm event (two dimensions; i.e., wave height and wave period), b) for simulating coastal storms at each location (requiring five dimensions), and c) for estimating the storms' return periods (two to five dimensions).

However, current research is mainly limited to the bivariate case and the use of certain copula families. On the contrary, this thesis achieves to identify the optimal copula among 40 families for each of the examined coastal storms (2-5 variables). In the case of two dimensions, the range of coastal storm parameters is also estimated for the specific copula that modelled each event. In addition, the second-best copula is investigated.

While trying to simulate coastal storm events in five dimensions so as to better describe the phenomenon, the extension of the De Michele et al. (2007) methodology was performed. A new algorithm (Algorithm C) was developed and proposed for sea storm simulation using the PCC and it was compared to two other algorithms (A and B) stemming from the economic field (Stöber and Czado, 2017; Aas et al., 2009) to indicate their effectiveness in five dimensions. In addition, C-Vines copulas are also applied for

coastal storm simulation, especially in algorithms A and B, as well as for estimation of the return periods in an attempt to answer the relevant research questions of this thesis.

Overall, the main conclusions of copulas applications can be summarised as follows:

- The Tawn and Joe copulas are often considered the best families for modelling H and T during a coastal storm. Datasets with light tails are described better by Tawn copulas and Joe copulas suit to the heaviest tails. Concerning the second-best copulas, some families are similarly effective in modelling H and T, such as the Joe copulas with Clayton.
- The five-dimensional C-Vine copula is constructed following the PCC method for the pairs of important parameters. The simulation Algorithm C (based on De Michele et al., 2007) leads to inadequate simulations of coastal storms. On the other hand, the algorithms A and B (based on Stöber and Czado, 2017 and Aas et al., 2009) can efficiently simulate coastal storms.
- Many copula families can estimate the bivariate return periods of coastal storms with slight divergences in their results. For higher dimensions, the C-Vine copulas provide more realistic return periods against the multivariate conventional copulas. The investigation of copula families and the best methodology for coastal storm return periods is required in any case.
- More specifically, particular attention should be paid to the use of Tawn copulas for the modelling of H and T instead of the well-known Archimedean copulas that are usually preferred, especially when there are light tails. Both Joe and Clayton copulas should be chosen when heavy tails exist in the examined dataset. The methodology of five-dimensional C-Vines that is proposed for Malaga's coastal storms can be applied to any location since there are no differences in the interrelation of important parameters over the Mediterranean Sea. Algorithms A and B present similar results and prevail over Algorithm C in coastal storms simulation. It can also be stated that the C-Vine copulas (for three to five dimensions) are more effective on the return periods estimation contrary to other copulas, which usually over or under-estimate them.

The proposed methodology is validated by studying real coastal storms, conducted using wave data from buoys measurements in 30 locations over the Mediterranean Sea. The analysis of coastal storms is based on historical events and enables many features of coastal storms to be investigated. From this analysis, 4008 coastal storms are detected in Greece, Italy, France, and Spain. A general overview of Mediterranean coastal storms activity is presented by describing their characteristics through the frequency of occurrence, the descriptive statistics, as well as their shape. The outcomes are of great importance given that they are raised by raw data from many locations, whereas other works usually focus only on one location or on model data. The characteristics of Mediterranean coastal storms can also be applied to the harbour and coastal structures design as described in Section 4.3.

Regarding the Mediterranean coastal storms, some additional minor conclusions can be drawn:

- 10 - 14 coastal storm events occur annually in the Mediterranean Sea at each country examined in this thesis.
- Most coastal storms (over 80%) are developed between October to March, as expected, while the Spanish locations face an intense coastal storm activity during the summer months.
- The highest wave heights, the longest periods, and the high energy occur, as expected, at the most exposed locations in deep waters.
- The average duration of coastal storms is shortest than 30 hours, and almost 50% of them last less than 24 hours.
- Regarding the calm period, 25% of coastal storms hit twice a certain location in less than a week.
- The wave period and direction have a slight variation during a coastal storm. The coefficient of variation for the wave period is usually less than 0.15, for over 75% of the events. Similarly, the standard deviation of wave direction is usually less than 20 degrees during a coastal storm for most coastal storms (75%). The latter means that the average wave direction and wave period can efficiently describe both variables within a coastal storm.
- The energy flux and the coastal storm energy have similar behaviour, with no indication for which of the two best describes the coastal storm severity

index. Furthermore, coastal storms with high wave periods also have high values of coastal storm energy and wave energy flux at the same wave height.

- Mediterranean coastal storms can be represented by multiple triangular shapes, with no significant effect of the triangle's shape (e.g., isosceles or scalene) on their representation. Furthermore, the triangular shape does not depend on the wave direction or the wave period.
- In contrast to some related works, this thesis concluded that the triangular representation of Mediterranean coastal storms presents a positive skewness in their shape. Therefore, it is not a priori known that they reach their peak at the beginning of their duration.

The results of this thesis are primarily useful for efficiently simulating the coastal storms and for estimating the return periods of extreme coastal storms. The thesis' contribution to the field of coastal engineering is to improve both reliability and design of existing or future coastal structures by applying state-of-the-art methodologies of copulas for coastal storms simulation and their return periods. Additionally, this work provides information about coastal storms activity in the Mediterranean Sea and also stands as a guiding framework for analysing coastal storms.

Thesis limitations

The limitations of this thesis are mainly related to the data of the Mediterranean Sea case study. The analysed datasets, although extensive, are not sufficient to show the effect of climate change on the severity and frequency of occurrence of coastal storms in the Mediterranean Sea. The temporal data coverage is very short and different for a few locations, and the sampling interval of buoys measurements ranges between 0.5 and 3 hours. These datasets' differences are restrictive on providing a more general overview of coastal storm activity in this region.

Regarding the copulas application for coastal storm analysis, the C-Vines are more accurate compared to other commonly used copulas, but their application requires manual handling of many calculations, and thus they are time-consuming.

Future research

The analysis of coastal storms and their modelling through copulas can be further improved. Some suggestions for future research are summarized below:

- A more extensive database with the shortest possible recording interval can be used to improve the selection of coastal storm thresholds as well as their identification. The effect of the recording interval can also be investigated, which ranges between 0.5 to 3 hours, for both duration and calm period of coastal storms.
- The proposed methodology can be further improved by incorporating information on coastal storm impacts on coasts. The satellite data, the information about synoptic systems, and other parameters such as atmospheric pressure could be included for a more detailed coastal storm analysis.
- A denser network of buoys and increased data availability are also needed to identify the storm activity for more locations and assess the interrelation of parameters.
- The analysis of this thesis and its findings are useful for the development of synthetic storms and the estimation of important return periods at any examined location. The synthetic storms can be used for future projections and the return periods should be taken into account for the design of harbours and coastal structures.
- It will also be interesting to apply the proposed methodology for modelling coastal storms in more locations so that a better comparison of the simulations and the return periods can be made.
- Future researches can also extend the application of Vine copulas incorporating spatial information of data by using spatial Vine copulas as well as to focus on the time-series dependence and use the Vine copulas to model multivariate time-series. Regular vine copulas (R-Vines) could also be applied, especially for a higher dimension, given that C-Vine copulas might be restrictive as a limited case of R-Vines.

The multidimensional nature of coastal storms and the plethora of impacts on the coastal zone and the coastal communities require an integrated analysis that considers as many storm aspects as possible. The only way to contribute to this challenging problem is by firstly focusing on historical coastal storms and subsequently on their multivariate analysis. In this direction, the copula theory is very promising and deserves the attention of the research community.

Appendix

The analysis and visualisations of this thesis are performed in R Programming Language (R Core Team, 2021) and especially using the following packages: “abind” (Plate and Heiberger, 2016),“actuar” (Dutang et al., 2008), “cowplot” (Wilke,2020), “clifro” (Seers and Shears,2015), “CircStats” (Lund and Agostinelli 2018), “devtools” (Wickham et al., 2020), “DescTools” (Signorell et al.,2021), “dplyr” (Wickham et al., 2021), “extRemes” (Gilleland and Katz, 2016), “extrafont” (Chang, 2014), “EQL” (Thaler, 2009, “epiDisplay” (Chongsuvivatwong, 2018), “evd” (Stephenson, 2002), “forecast” (Hyndman et al.,2021), “factoextra” (Kassambara and Mundt, 2020), “fitdistrplus” (Delignette-Muller and Dutang, 2015), “ggplot2” (Wickham, 2016), “ggthemes” (Arnold et al., 2021), “ggpubr” (Kassambara, 2020), “GGally” (Schloerke et al., 2021), “gridExtra” (Auguie, 2017), “gmodels” (Warnes et al., 2018), “ggExtra” (Attali and Baker, 2019), “GoFKernel” (Pavia, 2015), “Kdensity” (Moss and Tveten, 2020), “Lubridate” (Grolemund and Wickham, 2011), “logspline” (Kooperberg, 2020), “latticeExtra” (Sarkar and Andrews, 2019), “magrittr” (Bache and Wickham, 2020), “moments” (Komsta and Novomestky, 2015), “NbClust” (Charrad et al.,2014), “ncdf4” (Pierce, 2019), “nnet” (Venables and Ripley, 2002), “network” (Butts, 2020), “openair” (Carslaw and Ropkins, 2012), “pracma” (Borchers, 2021), “psych” (Revelle, 2020), “plotrix” (Lemon, 2006), “plotly” (Sievert, 2020), “patchwork” (Pedersen, 2020), “remotes” (Hester et al., 2020), “Rttf2pt1” (Chang et al., 2020), “rVineCopLib” (Nagler and Vatte, 2021), “readr” (Wickham and Hester, 2020), “reshape2” (Wickham, 2007), “rafalib” (Irizarry and Love, 2015), “RColorBrewer” (Neuwirth, 2014), “summarytools” (Comtois, 2021), “sjstats” (Lüdecke, 2021), “tidyr” (Wickham, 2021), “tibble” (Müller

and Wickham, 2021), “tidyverse” (Wickham et al., 2019), “VineCopula” (Nagler et al., 2020), “VC2copula” (Nagler, 2020), “xlsx” (Dragulescu and Arendt, 2020).

References

Aagaard, T., Kroon, A., 2017. Sediment Transport Under Storm Conditions on Sandy Beaches, in: Coastal Storms. John Wiley & Sons, Ltd, Chichester, UK, pp. 45–63. https://doi.org/10.1002/9781118937099.ch3

Aas, K., Czado, C., Frigessi, A., Bakken, H., 2009. Pair-copula constructions of multiple dependence. Insur. Math. Econ. 44, 182–198. https://doi.org/10.1016/j.insmatheco.2007.02.001

AghaKouchak, A., Bárdossy, A., Habib, E., 2010. Conditional simulation of remotely sensed rainfall data using a non-Gaussian v-transformed copula. Adv. Water Resour. 33, 624–634. https://doi.org/10.1016/j.advwatres.2010.02.010

Ahrens, D., Henson, R., 2016. Meteorology Today: An Introduction to Weather, Climate, and the Environment, 11th ed. Cengage Learning.

Allis, M.J., Stephens, S., Ramsay, D., Gorman, R., Bell, R., 2015. The coastal calculator: A user-friendly tool for estimating coastal storm-driven water-levels, in: Australian Coasts and Ports 2015 Conference. pp. 1–7.

Almeida, L.P., Ferreira, Ó., Vousdoukas, M.I., Dodet, G., 2011. Historical variation and trends in storminess along the Portuguese South Coast. Nat. Hazards Earth Syst. Sci. 11, 2407–2417. https://doi.org/10.5194/nhess-11-2407-2011

Almeida, L.P., Vousdoukas, M.V., Ferreira, Ó., Rodrigues, B.A., Matias, A., 2012. Thresholds for storm impacts on an exposed sandy coastal area in southern Portugal. Geomorphology 143–144, 3–12. https://doi.org/10.1016/j.geomorph.2011.04.047

Altomare, C., Crespo, A.J.C., Domínguez, J.M., Gómez-Gesteira, M., Suzuki, T., Verwaest, T., 2015. Applicability of Smoothed Particle Hydrodynamics for estimation of sea wave impact on coastal structures. Coast. Eng. 96, 1–12. https://doi.org/10.1016/j.coastaleng.2014.11.001

AMS, 2019. American Meteorological Society -Storm. Gloss. Meteorol.

Androulidakis, Y.S., Kombiadou, K.D., Makris, C. V., Baltikas, V.N., Krestenitis, Y.N., 2015. Storm surges in the Mediterranean Sea: Variability and trends under future climatic conditions. Dyn. Atmos. Ocean. 71, 56–82. https://doi.org/10.1016/j.dynatmoce.2015.06.001

Armaroli, C., Ciavola, P., Perini, L., Calabrese, L., Lorito, S., Valentini, A., Masina, M., 2012. Critical storm thresholds for significant morphological changes and damage along the Emilia-Romagna coastline, Italy. Geomorphology 143–144, 34–51. https://doi.org/10.1016/j.geomorph.2011.09.006

Armaroli, C., Duo, E., 2018. Validation of the coastal storm risk assessment framework along the Emilia-Romagna coast. Coast. Eng. 134, 159–167. https://doi.org/10.1016/j.coastaleng.2017.08.014

Armitage, A.R., Weaver, C.A., Kominoski, J.S., Pennings, S.C., 2020. Resistance to Hurricane Effects Varies Among Wetland Vegetation Types in the Marsh–Mangrove Ecotone. Estuaries and Coasts 43, 960–970. https://doi.org/10.1007/s12237-019-00577-3

Arns, A., Wahl, T., Haigh, I.D., Jensen, J., Pattiaratchi, C., 2013. Estimating extreme water level probabilities: A comparison of the direct methods and recommendations for best practise. Coast. Eng. 81, 51–66. https://doi.org/10.1016/j.coastaleng.2013.07.003

Australian Bureau of Meteorology, 2020. What is a tropical cyclone? [WWW Document]. URL http://www.bom.gov.au/cyclone/tropical-cyclone-knowledge-centre/understanding/tc-info/

Balomenos, G.P., Padgett, J.E., 2018. Vulnerability Assessment of Port Structures Subjected to Storm Surge and Waves, in: Structures Congress 2018: Buildings and Disaster Management - Selected Papers from the Structures Congress 2018. pp. 345–358. https://doi.org/10.1061/9780784481325.036

Bárdossy, A., Pegram, G.G.S., 2009. Copula based multisite model for daily precipitation simulation. Hydrol. Earth Syst. Sci. 13, 2299–2314. https://doi.org/10.5194/hess-13-2299-2009

Baring, R.J., Fairweather, P.G., Lester, R.E., 2014. Storm versus calm: Variation in fauna associated with drifting macrophytes in sandy beach surf zones. J. Exp. Mar. Bio. Ecol. 461, 397–406. https://doi.org/10.1016/j.jembe.2014.09.011

Barnard, P.L., van Ormondt, M., Erikson, L.H., Eshleman, J., Hapke, C., Ruggiero, P., Adams, P.N., Foxgrover, A.C., 2014. Development of the Coastal Storm Modeling System (CoSMoS) for predicting the impact of storms on high-energy, active-margin coasts. Nat. Hazards 74, 1095–1125. https://doi.org/10.1007/s11069-014-1236-y

Basco, D.R., 2016. Storm Hazard Mitigation Structures, in: Springer Handbook of Ocean Engineering. Springer International Publishing, Cham, pp. 653–684. https://doi.org/10.1007/978-3-319-16649-0_30

Basco, D.R., Mahmoudpour, N., 2018. On the Hydrodynamic Strength of a Coastal Storm, in: Handbook of Coastal and Ocean Engineering. WORLD SCIENTIFIC, pp. 1423–1452. https://doi.org/10.1142/9789813204027_0050

Basco, D.R., Mahmoudpour, N., 2014. Toward a hydrodynamic definition of the strength of a coastal storm: The coastal storm impulse (COSI) parameter, in: From Sea to Shore – Meeting the Challenges of the Sea. pp. 1043–1049. https://doi.org/10.1680/fsts.59757.1043

Basco, D.R., Mahmoudpour, N., 2012. The Modified Coastal Storm Impulse (Cosi) Parameter and Quantification of Fragility Curves for Coastal Design. Coast. Eng. Proc. 1, 66. https://doi.org/10.9753/icce.v33.management.66

Basco, D.R., Walker, R.A., 2010. Application of the Coastal Storm Impulse (COSI) parameter to predict coastal erosion, in: Proceedings of the Coastal Engineering Conference.

Bathi, J., Das, H., 2016. Vulnerability of Coastal Communities from Storm Surge and Flood Disasters. Int. J. Environ. Res. Public Health 13, 239. https://doi.org/10.3390/ijerph13020239

Bazzichetto, M., Sperandii, M.G., Malavasi, M., Carranza, M.L., Acosta, A.T.R., 2020. Disentangling the effect of coastal erosion and accretion on plant communities of Mediterranean dune ecosystems. Estuar. Coast. Shelf Sci. 241, 106758. https://doi.org/10.1016/j.ecss.2020.106758

Beavers, R.L., Babson, A.L., Schupp, C.A. (Eds.), 2016. Coastal Adaptation Strategies Handbook. National Park Service, Washington, DC.

Becker, A., Ng, A.K.Y., McEvoy, D., Mullett, J., 2018. Implications of climate change for shipping: Ports and supply chains. Wiley Interdiscip. Rev. Clim. Chang. 9, e508. https://doi.org/10.1002/wcc.508

Bedford, Cooke, 2001. Probability Density Decomposition for Conditionally Dependent Random Variables Modeled by Vines. Ann. Math. Artif. Intell. 32, 245–268. https://doi.org/10.1023/A:1016725902970

Bedford, T., Cooke, R.M., 2002. Vines--a new graphical model for dependent random variables. Ann. Stat. 30, 1031–1068. https://doi.org/10.1214/aos/1031689016

Beer, T., 2013. Beaufort Wind Scale, in: Encyclopedia of Earth Sciences Series. pp. 42–45. https://doi.org/10.1007/978-1-4020-4399-4_24

Beirlant, J., Goegebeur, Y., Teugels, J., Segers, J., 2004. Statistics of Extremes, Wiley Series in Probability and Statistics. John Wiley & Sons, Ltd, Chichester, UK. https://doi.org/10.1002/0470012382

Benassai, G., Celentano, P., Sessa, F., 2009. Coastal storm damage reduction program in Salerno Province after the winter 2008 storms, in: WIT Transactions on Ecology and the Environment. pp. 119–128. https://doi.org/10.2495/CP090111

Bender, C.J., Miller, W., Naimaster, A., Mahoney, T., 2012. Wave modeling with SWAN + ADCIRC for the south carolina coastal storm surge study, in: Proceedings of the Coastal Engineering Conference.

Bengtsson, L., Hodges, K.I., Roeckner, E., 2006. Storm Tracks and Climate Change. J. Clim. 19, 3518–3543. https://doi.org/10.1175/JCLI3815.1

Bernardara, P., Mazas, F., Kergadallan, X., Hamm, L., 2014. A two-step framework for over-threshold modelling of environmental extremes. Nat. Hazards Earth Syst. Sci. 14, 635–647. https://doi.org/10.5194/nhess-14-635-2014

Bertin, X., Bruneau, N., Breilh, J.-F., Fortunato, A.B., Karpytchev, M., 2012. Importance of wave age and resonance in storm surges: The case Xynthia, Bay of Biscay. Ocean Model. 42, 16–30. https://doi.org/10.1016/j.ocemod.2011.11.001

Bertin, X., Olabarrieta, M., McCall, R., 2017. Hydrodynamics Under Storm Conditions, in: Coastal Storms. John Wiley & Sons, Ltd, Chichester, UK, pp. 23–43. https://doi.org/10.1002/9781118937099.ch2

Besio, G., Briganti, R., Romano, A., Mentaschi, L., De Girolamo, P., 2017. Time clustering of wave storms in the Mediterranean Sea. Nat. Hazards Earth Syst. Sci. 17, 505–514. https://doi.org/10.5194/nhess-17-505-2017

Bezak, N., Brilly, M., Šraj, M., 2014. Comparison between the peaks-over-threshold method and the annual maximum method for flood frequency analysis. Hydrol. Sci. J. 59, 959–977. https://doi.org/10.1080/02626667.2013.831174

Bhatia, K., Vecchi, G., Murakami, H., Underwood, S., Kossin, J., 2018. Projected Response of Tropical Cyclone Intensity and Intensification in a Global Climate Model. J. Clim. 31, 8281–8303. https://doi.org/10.1175/JCLI-D-17-0898.1

Bhatia, K.T., Vecchi, G.A., Knutson, T.R., Murakami, H., Kossin, J., Dixon, K.W., Whitlock, C.E., 2019. Recent increases in tropical cyclone intensification rates. Nat. Commun. 10, 635. https://doi.org/10.1038/s41467-019-08471-z

Bilkovic, D.M., Mitchell, M.M., Peyre, M.K. La, Toft, J.D., 2017. Living Shorelines The Science and Management of Nature-Based Coastal Protection. CRC Press.

Binder, S.B., Baker, C.K., Barile, J.P., 2015. Rebuild or Relocate? Resilience and Postdisaster Decision-Making After Hurricane Sandy. Am. J. Community Psychol. 56, 180–196. https://doi.org/10.1007/s10464-015-9727-x

Boccotti, P., 2015. Wave Mechanics and Wave Loads on Marine Structures, Wave Mechanics and Wave Loads on Marine Structures. Elsevier. https://doi.org/10.1016/C2013-0-13663-X

Boccotti, P., 2000. Chapter 6 The Wave Climate, in: Elsevier Oceanography Series. Elsevier Science, pp. 183–206. https://doi.org/10.1016/S0422-9894(00)80032-X

Boldingh Debernard, J., Petter Roed, L., 2008. Future wind, wave and storm surge climate in the

Northern Seas: a revisit. Tellus A 60, 427–438. https://doi.org/10.1111/j.1600-0870.2008.00312.x

Booth, J.F., Rieder, H.E., Kushnir, Y., 2016. Comparing hurricane and extratropical storm surge for the Mid-Atlantic and Northeast Coast of the United States for 1979–2013. Environ. Res. Lett. 11, 094004. https://doi.org/10.1088/1748-9326/11/9/094004

Botai, C.M., Botai, J.O., Adeola, A.M., de Wit, J.P., Ncongwane, K.P., Zwane, N.N., 2020. Drought Risk Analysis in the Eastern Cape Province of South Africa: The Copula Lens. Water 12, 1938. https://doi.org/10.3390/w12071938

Breilh, J.-F., Bertin, X., Chaumillon, É., Giloy, N., Sauzeau, T., 2014. How frequent is storm-induced flooding in the central part of the Bay of Biscay? Glob. Planet. Change 122, 161–175. https://doi.org/10.1016/j.gloplacha.2014.08.013

Brown, D., 2013. Climate Change Ethics, Climate Change Ethics: Navigating the Perfect Moral Storm. Routledge. https://doi.org/10.4324/9780203103234

BS 6349, 2013. Maritime works. https://doi.org/https://doi.org/10.3403/BS6349

Burmeister, N., James, D., Victory, S., 2015. Effects of storm event on coastal structures in Port Phillip, Victoria, Australia, in: Australian Coasts and Ports 2015 Conference. pp. 121–127.

Burton, C.G., 2010. Social Vulnerability and Hurricane Impact Modeling. Nat. Hazards Rev. 11, 58–68. https://doi.org/10.1061/(ASCE)1527-6988(2010)11:2(58)

Burzel, A., Dassanayake, D., Naulin, M., Kortenhaus, A. Oumeraci, H., Wahl, T., Mudersbach, C., Jensen, J., Gönnert, G., Sossidi, K., Ujeyl, G., Pasche, E., 2010. Integrated flood risk analysis for extreme storm surges (XtremRisk), in: 32nd International Conference on Coastal Engineering, ICCE 2010. p. 13.

Bushra, N., Trepanier, J.C., Rohli, R. V., 2019. Joint probability risk modelling of storm surge and cyclone wind along the coast of Bay of Bengal using a statistical copula. Int. J. Climatol. 39, 4206–4217. https://doi.org/10.1002/joc.6068

Caires, S., Sterl, A., 2005. 100-Year Return Value Estimates for Ocean Wind Speed and Significant Wave Height from the ERA-40 Data. J. Clim. 18, 1032–1048. https://doi.org/10.1175/JCLI-3312.1

Calafat, F.M., Marcos, M., 2020. Probabilistic reanalysis of storm surge extremes in Europe. Proc. Natl. Acad. Sci. 117, 1877–1883. https://doi.org/10.1073/pnas.1913049117

Callaghan, D.P., Nielsen, P., Short, A., Ranasinghe, R., 2008. Statistical simulation of wave climate and extreme beach erosion. Coast. Eng. 55, 375–390. https://doi.org/10.1016/j.coastaleng.2007.12.003

Capstick, S., Whitmarsh, L., Poortinga, W., Pidgeon, N., Upham, P., 2015. International trends in public perceptions of climate change over the past quarter century. Wiley Interdiscip. Rev. Clim. Chang. 6, 35–61. https://doi.org/10.1002/wcc.321

Cascajo, R., García, E., Quiles, E., Correcher, A., Morant, F., 2019. Integration of Marine Wave Energy Converters into Seaports: A Case Study in the Port of Valencia. Energies 12, 787. https://doi.org/10.3390/en12050787

Cavicchia, L., von Storch, H., 2012. The simulation of medicanes in a high-resolution regional climate model. Clim. Dyn. 39, 2273–2290. https://doi.org/10.1007/s00382-011-1220-0

Cavicchia, L., von Storch, H., Gualdi, S., 2014. Mediterranean Tropical-Like Cyclones in Present and Future Climate. J. Clim. 27, 7493–7501. https://doi.org/10.1175/JCLI-D-14-00339.1

Chadenas, C., Creach, A., Mercier, D., 2014. The impact of storm Xynthia in 2010 on coastal flood prevention policy in France. J. Coast. Conserv. 18, 529–538. https://doi.org/10.1007/s11852-013-0299-3

Chan, C., 2019. Extra-tropical Cyclone vs Tropical Cyclone [WWW Document]. URL http://www.hko.gov.hk/education/edu01met/01met_tropical_cyclones/ele_typhoon3_e.htm

Chang, J., Li, Y., Wang, Y., Yuan, M., 2016. Copula-based drought risk assessment combined with an integrated index in the Wei River Basin, China. J. Hydrol. 540, 824–834. https://doi.org/10.1016/j.jhydrol.2016.06.064

Chavez, M., Ghil, M., Urrutia-Fucugauchi, J. (Eds.), 2015. Extreme Events, Geophysical Monograph Series. John Wiley & Sons, Inc, Hoboken, NJ. https://doi.org/10.1002/9781119157052

Chen, L., Guo, S., 2019. Copulas and Its Application in Hydrology and Water Resources, Springer Water. Springer Singapore, Singapore. https://doi.org/10.1007/978-981-13-0574-0

Chen, T.-C., Tsay, J.-D., Yen, M.-C., Cayanan, E.O., 2010. Formation of the Philippine Twin Tropical Cyclones during the 2008 Summer Monsoon Onset. Weather Forecast. 25, 1317–1341. https://doi.org/10.1175/2010WAF2222395.1

Cheng, L., AghaKouchak, A., Gilleland, E., Katz, R.W., 2014. Non-stationary extreme value analysis in a changing climate. Clim. Change 127, 353–369. https://doi.org/10.1007/s10584-014-1254-5

Cherubini, U., Gobbi, F., Mulinacci, S., 2016. Convolution Copula Econometrics, SpringerBriefs in Statistics. Springer International Publishing, Cham. https://doi.org/10.1007/978-3-319-48015-2

Cherubini, U., Luciano, E., Vecchiato, W., 2004. Copula Methods in Finance. John Wiley & Sons Ltd, Oxford, UK. https://doi.org/10.1002/9781118673331

Christie, E.K., Spencer, T., Owen, D., McIvor, A.L., Möller, I., Viavattene, C., 2018. Regional coastal flood risk assessment for a tidally dominant, natural coastal setting: North Norfolk, southern North Sea. Coast. Eng. 134, 177–190. https://doi.org/10.1016/j.coastaleng.2017.05.003

Ciavola, P., Coco, G. (Eds.), 2017. Coastal Storms. John Wiley & Sons, Ltd, Chichester, UK. https://doi.org/10.1002/9781118937099

Ciavola, P., Ferreira, O., Dongeren, A. Van, Vries, J.V.T. de, Armaroli, C., Harley, M., 2014. Prediction of Storm Impacts on Beach and Dune Systems, in: Hydrometeorological Hazards. John Wiley & Sons, Ltd, Chichester, UK, pp. 227–252. https://doi.org/10.1002/9781118629567.ch3d

Ciavola, P., Ferreira, O., Haerens, P., Van Koningsveld, M., Armaroli, C., 2011a. Storm impacts along European coastlines. Part 2: lessons learned from the MICORE project. Environ. Sci. Policy 14, 924–933. https://doi.org/10.1016/j.envsci.2011.05.009

Ciavola, P., Ferreira, O., Haerens, P., Van Koningsveld, M., Armaroli, C., Lequeux, Q., 2011b. Storm impacts along European coastlines. Part 1: The joint effort of the MICORE and ConHaz Projects. Environ. Sci. Policy 14, 912–923. https://doi.org/10.1016/j.envsci.2011.05.011

Ciavola, P., Stive, M.J.F., 2012. Thresholds for storm impacts along European coastlines: Introduction. Geomorphology 143–144, 1–2. https://doi.org/10.1016/j.geomorph.2011.10.002

Cinner, J.E., Adger, W.N., Allison, E.H., Barnes, M.L., Brown, K., Cohen, P.J., Gelcich, S., Hicks, C.C., Hughes, T.P., Lau, J., Marshall, N.A., Morrison, T.H., 2018. Building adaptive capacity to climate change in tropical coastal communities. Nat. Clim. Chang. 8, 117–123. https://doi.org/10.1038/s41558-017-0065-x

Clements, B.W., Casani, J.A.P., 2016. Hurricanes, Typhoons, and Tropical Cyclones, in: Disasters and Public Health: Planning and Response: Second Edition. pp. 331–355. https://doi.org/10.1016/B978012801980100014-3

Coco, G., Senechal, N., Rejas, A., Bryan, K.R., Capo, S., Parisot, J.P., Brown, J.A., MacMahan, J.H.M., 2014. Beach response to a sequence of extreme storms. Geomorphology 204, 493–501. https://doi.org/10.1016/j.geomorph.2013.08.028

Coles, S., 2001. An Introduction to Statistical Modeling of Extreme Values, Springer Series in Statistics. Springer London, London. https://doi.org/10.1007/978-1-4471-3675-0

Cooper, J.A.G., Jackson, D.W.T., Navas, F., McKenna, J., Malvarez, G., 2004. Identifying storm impacts on an embayed, high-energy coastline: examples from western Ireland. Mar. Geol. 210, 261–280. https://doi.org/10.1016/j.margeo.2004.05.012

Copernicus Marine In Situ Tac Data Management Team, 2018. Copernicus Marine in situ TAC - physical parameters list. https://doi.org/https://doi.org/10.13155/53381

Corbella, S., Pringle, J., Stretch, D., 2015. Assimilation of ocean wave spectra and atmospheric circulation patterns to improve wave modelling. Coast. Eng. 100, 1–10. https://doi.org/10.1016/j.coastaleng.2015.03.003

Corbella, S., Stretch, D., 2013. Simulating a multivariate sea storm using Archimedean copulas. Coast. Eng. 76, 68–78. https://doi.org/10.1016/j.coastaleng.2013.01.011

Corbella, S., Stretch, D., 2012a. Predicting coastal erosion trends using non-stationary statistics and process-based models. Coast. Eng. https://doi.org/10.1016/j.coastaleng.2012.06.004

Corbella, S., Stretch, D., 2012b. Multivariate return periods of sea storms for coastal erosion risk assessment. Nat. Hazards Earth Syst. Sci. 12, 2699–2708. https://doi.org/10.5194/nhess-12-2699-2012

Corbella, S., Stretch, D., 2012c. Shoreline recovery from storms on the east coast of Southern Africa. Nat. Hazards Earth Syst. Sci. 12, 11–22. https://doi.org/10.5194/nhess-12-11-2012

Costas, S., Ferreira, O., Martinez, G., 2015. Why do we decide to live with risk at the coast? Ocean Coast. Manag. 118, 1–11. https://doi.org/10.1016/j.ocecoaman.2015.05.015

Cuite, C.L., Shwom, R.L., Hallman, W.K., Morss, R.E., Demuth, J.L., 2017. Improving Coastal Storm Evacuation Messages. Weather. Clim. Soc. 9, 155–170. https://doi.org/10.1175/WCAS-D-16-0076.1

Curtis, S., 2013. In the Eye of the Storm: A Participatory Course on Coastal Storms. J. Geog. 112, 133–142. https://doi.org/10.1080/00221341.2012.707226

Czado, C., 2019. Analyzing Dependent Data with Vine Copulas, Lecture Notes in Statistics. Springer International Publishing, Cham. https://doi.org/10.1007/978-3-030-13785-4

Davies, G., Callaghan, D.P., Gravois, U., Jiang, W., Hanslow, D., Nichol, S., Baldock, T., 2017. Improved treatment of non-stationary conditions and uncertainties in probabilistic models of storm wave climate. Coast. Eng. 127, 1–19. https://doi.org/10.1016/j.coastaleng.2017.06.005

Davis, R.E., Demme, G., Dolan, R., 1993. Synoptic climatology of atlantic coast North-Easters. Int. J. Climatol. 13, 171–189. https://doi.org/10.1002/joc.3370130204

De la Torre, Y., Balouin, Y., Heurtefeux, H., Lanzellotti, P., Guérinel, B., 2013. The « storm network » as a participative network for monitoring the impacts of coastal storms along the littoral zone of the Gulf of Lions, France. J. Coast. Res. 65, 927–932. https://doi.org/10.2112/SI65-157.1

De Michele, C., Salvadori, G., 2003. A Generalized Pareto intensity-duration model of storm rainfall exploiting 2-Copulas. J. Geophys. Res. 108, 4067. https://doi.org/10.1029/2002JD002534

De Michele, C., Salvadori, G., Passoni, G., Vezzoli, R., 2007. A multivariate model of sea storms using copulas. Coast. Eng. 54, 734–751. https://doi.org/10.1016/j.coastaleng.2007.05.007

De Michele, C., Salvadori, G., Vezzoli, R., Pecora, S., 2013. Multivariate assessment of droughts: Frequency analysis and dynamic return period. Water Resour. Res. 49, 6985–6994. https://doi.org/10.1002/wrcr.20551

Dee, D.P., Uppala, S.M., Simmons, A.J., Berrisford, P., Poli, P., Kobayashi, S., Andrae, U., Balmaseda, M.A., Balsamo, G., Bauer, P., Bechtold, P., Beljaars, A.C.M., van de Berg, L., Bidlot, J., Bormann, N., Delsol, C., Dragani, R., Fuentes, M., Geer, A.J., Haimberger, L., Healy, S.B., Hersbach, H., Hólm, E. V., Isaksen, L., Kållberg, P., Köhler, M., Matricardi, M., McNally, A.P., Monge-Sanz, B.M., Morcrette, J.-J., Park, B.-K., Peubey, C., de Rosnay, P., Tavolato, C., Thépaut, J.-N., Vitart, F., 2011. The ERA-Interim reanalysis: configuration and performance of the data assimilation system. Q. J. R. Meteorol. Soc. 137, 553–597. https://doi.org/10.1002/qj.828

Del Río, L., Plomaritis, T.A., Benavente, J., Valladares, M., Ribera, P., 2012. Establishing storm thresholds for the Spanish Gulf of Cádiz coast. Geomorphology 143–144, 13–23. https://doi.org/10.1016/j.geomorph.2011.04.048

den Heijer, C., Baart, F., van Koningsveld, M., 2012. Assessment of dune failure along the Dutch coast using a fully probabilistic approach. Geomorphology 143–144, 95–103. https://doi.org/10.1016/j.geomorph.2011.09.010

Devis-Morales, A., Montoya-Sánchez, R.A., Bernal, G., Osorio, A.F., 2017. Assessment of extreme wind and waves in the Colombian Caribbean Sea for offshore applications. Appl. Ocean Res. 69, 10–26. https://doi.org/10.1016/j.apor.2017.09.012

Dey, D., Yan, J., 2015. Extreme Value Modeling and Risk Analysis. Chapman and Hall/CRC. https://doi.org/10.1201/b19721

Ding, Y., 2017. Sea-Level Rise and Hazardous Storms: Impact Assessment on Coasts and Estuaries, in: Chen, W.-Y., Suzuki, T., Lackner, M. (Eds.), Handbook of Climate Change Mitigation and Adaptation. Springer International Publishing, Cham, pp. 621–656. https://doi.org/10.1007/978-3-319-14409-2

Dissanayake, P., Brown, J., Wisse, P., Karunarathna, H., 2015. Effects of storm clustering on beach/dune evolution. Mar. Geol. 370, 63–75. https://doi.org/10.1016/j.margeo.2015.10.010

Dißmann, J., Brechmann, E.C., Czado, C., Kurowicka, D., 2013. Selecting and estimating regular vine copulae and application to financial returns. Comput. Stat. Data Anal. 59, 52–69. https://doi.org/10.1016/j.csda.2012.08.010

Do, T.Q., van de Lindt, J.W., Cox, D.T., 2016. Performance-based design methodology for inundated elevated coastal structures subjected to wave load. Eng. Struct. 117, 250–262. https://doi.org/10.1016/j.engstruct.2016.02.046

Dolan, R; Lins, H; Hayden, B., 1988. Mid-Atlantic Coastal Storms. 1Journal Coast. Res. 4, 417–433.

Dolan, R., Davis, R., 1994. Coastal Storm Hazards. J. Coast. Res. 103–114.

Dolan, R., Davis, R., 1992. An Intensity Scale for Atlantic Coast Northeast Storms. J. Coast. Res.

8, 840–853.

Dong, S., Wang, N., Lu, H., Tang, L., 2015. Bivariate distributions of group height and length for ocean waves using Copula methods. Coast. Eng. 96, 49–61. https://doi.org/10.1016/j.coastaleng.2014.11.005

Donnelly, J.P., Butler, J., Roll, S., Wengren, M., Webb, T., 2004. A backbarrier overwash record of intense storms from Brigantine, New Jersey. Mar. Geol. 210, 107–121. https://doi.org/10.1016/j.margeo.2004.05.005

Dorsch, W., Newland, T., Tassone, D., Tymons, S., Walker, D., 2008. A Statistical Approach to Modelling the Temporal Patterns of Ocean Storms. J. Coast. Res. 246, 1430–1438. https://doi.org/10.2112/07-0847.1

Duo, E., Sanuy, M., Jiménez, J.A., Ciavola, P., 2020. How good are symmetric triangular synthetic storms to represent real events for coastal hazard modelling. Coast. Eng. 159, 103728. https://doi.org/10.1016/j.coastaleng.2020.103728

Durante, F., Sempi, C., 2015. Principles of Copula Theory. Chapman and Hall/CRC. https://doi.org/10.1201/b18674

Duvat, V.K.E., Magnan, A.K., Etienne, S., Salmon, C., Pignon-Mussaud, C., 2016. Assessing the impacts of and resilience to Tropical Cyclone Bejisa, Reunion Island (Indian Ocean). Nat. Hazards 83, 601–640. https://doi.org/10.1007/s11069-016-2338-5

Eastoe, E., Koukoulas, S., Jonathan, P., 2013. Statistical measures of extremal dependence illustrated using measured sea surface elevations from a neighbourhood of coastal locations. Ocean Eng. 62, 68–77. https://doi.org/10.1016/j.oceaneng.2013.01.002

Emanuel, K., 2017. Will Global Warming Make Hurricane Forecasting More Difficult? Bull. Am. Meteorol. Soc. 98, 495–501. https://doi.org/10.1175/BAMS-D-16-0134.1

Emanuel, K., 2005a. Divine Wind: The History and Science of Hurricanes. Oxford University Press, New York.

Emanuel, K., 2005b. Genesis and maintenance of “Mediterranean hurricanes.” Adv. Geosci. 2, 217–220. https://doi.org/10.5194/adgeo-2-217-2005

Embrechts, P., 2009. Copulas: A Personal View. J. Risk Insur. 76, 639–650. https://doi.org/10.1111/j.1539-6975.2009.01310.x

Erikson, L.H., Espejo, A., Barnard, P.L., Serafin, K.A., Hegermiller, C.A., O’Neill, A., Ruggiero, P., Limber, P.W., Mendez, F.J., 2018. Identification of storm events and contiguous coastal sections for deterministic modeling of extreme coastal flood events in response to climate change. Coast. Eng. 140, 316–330. https://doi.org/10.1016/j.coastaleng.2018.08.003

Ernst, J.A., Matson, M., 1983. A Mediterranean Tropical Storm? Weather 38, 332–337. https://doi.org/10.1002/j.1477-8696.1983.tb04818.x

Esteban, M., Takagi, H., Shibayama, T., 2016. Adaptation to an increase in typhoon intensity and

sea level rise by Japanese ports, in: Ng, A.K.Y., Becker, A., Cahoon, S., Chen, S.-L., Earl, P., Yang, Z. (Eds.), Climate Change and Adaptation Planning for Ports. Routledge, pp. 117–132.

Esteves, L.S., Brown, J.M., Williams, J.J., Lymbery, G., 2012. Quantifying thresholds for significant dune erosion along the Sefton Coast, Northwest England. Geomorphology 143–144, 52–61. https://doi.org/10.1016/j.geomorph.2011.02.029

Fan, S., Swift, D.J.P., Traykovski, P., Bentley, S., Borgeld, J.C., Reed, C.W., Niedoroda, A.W., 2004. River flooding, storm resuspension, and event stratigraphy on the northern California shelf: observations compared with simulations. Mar. Geol. 210, 17–41. https://doi.org/10.1016/j.margeo.2004.05.024

Ferguson, T.S., Genest, C., Hallin, M., 2000. Kendall's tau for serial dependence. Can. J. Stat. 28, 587–604. https://doi.org/10.2307/3315967

Ferreira, J.A., Guedes Soares, C., 2002. Modelling bivariate distributions of significant wave height and mean wave period. Appl. Ocean Res. 24, 31–45. https://doi.org/10.1016/S0141-1187(02)00006-8

Ferreira, J.A., Guedes Soares, C., 1998. An Application of the Peaks Over Threshold Method to Predict Extremes of Significant Wave Height. J. Offshore Mech. Arct. Eng. 120, 165. https://doi.org/10.1115/1.2829537

Ferreira, Ó., 2006. The role of storm groups in the erosion of sandy coasts. Earth Surf. Process. Landforms 31, 1058–1060. https://doi.org/10.1002/esp.1378

Ferreira, Ó., 2005. Storm Groups versus Extreme Single Storms: Predicted Erosion and Management Consequences. J. Coast. Res. 221–227.

Ferreira, Ó., Ciavola, P., Armaroli, C., Balouin, Y., Benavente, J., Del Río, L., Deserti, M., Esteves, L.S., Furmanczyk, K., Haerens, P., Matias, A., Perini, L., Taborda, R., Terefenko, P., Trifonova, E., Trouw, K., Valchev, N., Van Dongeren, A., Van Koningsveld, M., Williams, J.J., 2009. Coastal storm risk assessment in Europe: Examples from 9 study sites. J. Coast. Res. 1632–1636.

Ferreira, Ó., Plomaritis, T.A., Costas, S., 2017. Process-based indicators to assess storm induced coastal hazards. Earth-Science Rev. 173, 159–167. https://doi.org/10.1016/j.earscirev.2017.07.010

Flowerdew, J., Horsburgh, K., Wilson, C., Mylne, K., 2010. Development and evaluation of an ensemble forecasting system for coastal storm surges. Q. J. R. Meteorol. Soc. 136, 1444–1456. https://doi.org/10.1002/qj.648

Forbes, D.L., Parkes, G.S., Manson, G.K., Ketch, L.A., 2004. Storms and shoreline retreat in the southern Gulf of St. Lawrence. Mar. Geol. 210, 169–204. https://doi.org/10.1016/j.margeo.2004.05.009

Fouqueray, T., Trommetter, M., Frascaria-Lacoste, N., 2018. Managed retreat of settlements and infrastructures: ecological restoration as an opportunity to overcome maladaptive coastal development in France. Restor. Ecol. 26, 806–812. https://doi.org/10.1111/rec.12836

Frees, E.W., Valdez, E.A., 1998. Understanding Relationships Using Copulas. North Am. Actuar. J. 2, 1–25. https://doi.org/10.1080/10920277.1998.10595667

Freitas, E. da S., Coelho, V.H.R., Xuan, Y., Melo, D. de C.D., Gadelha, A.N., Santos, E.A., Galvão, C. de O., Ramos Filho, G.M., Barbosa, L.R., Huffman, G.J., Petersen, W.A., Almeida, C. das N., 2020. The performance of the IMERG satellite-based product in identifying sub-daily rainfall events and their properties. J. Hydrol. 589, 125128. https://doi.org/10.1016/j.jhydrol.2020.125128

Furmańczyk, K.K., Dudzińska-Nowak, J., Furmańczyk, K.A., Paplińska-Swerpel, B., Brzezowska, N., 2012. Critical storm thresholds for the generation of significant dune erosion at Dziwnow Spit, Poland. Geomorphology 143–144, 62–68. https://doi.org/10.1016/j.geomorph.2011.09.007

Galiatsatou, P., Makris, C., Prinos, P., Kokkinos, D., 2019. Nonstationary joint probability analysis of extreme marine variables to assess design water levels at the shoreline in a changing climate. Nat. Hazards 98, 1051–1089. https://doi.org/10.1007/s11069-019-03645-w

Galiatsatou, P., Prinos, P., 2016. Joint probability analysis of extreme wave heights and storm surges in the Aegean Sea in a changing climate. E3S Web Conf. 7, 02002. https://doi.org/10.1051/e3sconf/20160702002

Gall, R., Franklin, J., Marks, F., Rappaport, E.N., Toepfer, F., 2013. The Hurricane Forecast Improvement Project. Bull. Am. Meteorol. Soc. 94, 329–343. https://doi.org/10.1175/BAMS-D-12-00071.1

Garnier, E., Ciavola, P., Spencer, T., Ferreira, O., Armaroli, C., McIvor, A., 2018. Historical analysis of storm events: Case studies in France, England, Portugal and Italy. Coast. Eng. 134, 10–23. https://doi.org/10.1016/j.coastaleng.2017.06.014

Genest, C., Favre, A.-C., 2007. Everything You Always Wanted to Know about Copula Modeling but Were Afraid to Ask. J. Hydrol. Eng. 12, 347–368. https://doi.org/10.1061/(ASCE)1084-0699(2007)12:4(347)

Genest, C., Rémillard, B., Beaudoin, D., 2009. Goodness-of-fit tests for copulas: A review and a power study. Insur. Math. Econ. 44, 199–213. https://doi.org/10.1016/j.insmatheco.2007.10.005

Gervais, M., Balouin, Y., Belon, R., 2012. Morphological response and coastal dynamics associated with major storm events along the Gulf of Lions Coastline, France. Geomorphology 143–144, 69–80. https://doi.org/10.1016/j.geomorph.2011.07.035

Gilleland, E., Katz, R.W., 2016. extRemes 2.0: An Extreme Value Analysis Package in R. J. Stat. Softw. 72. https://doi.org/10.18637/jss.v072.i08

Glavovic, B.C., Smith, G.P. (Eds.), 2014. Adapting to Climate Change. Springer Netherlands, Dordrecht. https://doi.org/10.1007/978-94-017-8631-7

Godoi, V.A., Bryan, K.R., Gorman, R.M., 2018. Storm wave clustering around New Zealand and its connection to climatic patterns. Int. J. Climatol. 38, e401–e417. https://doi.org/10.1002/joc.5380

Godschalk, D.R.., Brower, D.J.., Beatley, T., 1989. Catastrophic Coastal Storms: Hazard Mitigation and Development Management. Duke University Press, Durham.

Gomes, M.P., Pinho, J.L., Antunes do Carmo, J.S., Santos, L., 2015. Hazard assessment of storm events for The Battery, New York. Ocean Coast. Manag. 118, 22–31. https://doi.org/10.1016/j.ocecoaman.2015.11.006

González-Alemán, J.J., Pascale, S., Gutierrez-Fernandez, J., Murakami, H., Gaertner, M.A., Vecchi, G.A., 2019. Potential Increase in Hazard From Mediterranean Hurricane Activity With Global Warming. Geophys. Res. Lett. https://doi.org/10.1029/2018GL081253

Gracia, A., Rangel-Buitrago, N., Oakley, J.A., Williams, A.T., 2018. Use of ecosystems in coastal erosion management. Ocean Coast. Manag. 156, 277–289. https://doi.org/10.1016/j.ocecoaman.2017.07.009

Grimaldi, S., Serinaldi, F., 2006. Asymmetric copula in multivariate flood frequency analysis. Adv. Water Resour. 29, 1155–1167. https://doi.org/10.1016/j.advwatres.2005.09.005

Haerens, P., Ciavola, P., Ferreira, Ó., Van Dongeren, A., Van Koningsveld, M., Bolle, A., 2012. Online Operational Early Warning System Prototypes to Forecast Coastal Storm Impacts (CEWS). Coast. Eng. Proc. 1, 45. https://doi.org/10.9753/icce.v33.management.45

Hallegatte, S., Green, C., Nicholls, R.J., Corfee-Morlot, J., 2013. Future flood losses in major coastal cities. Nat. Clim. Chang. 3, 802–806. https://doi.org/10.1038/nclimate1979

Hallegatte, S., Ranger, N., Mestre, O., Dumas, P., Corfee-Morlot, J., Herweijer, C., Wood, R.M., 2011. Assessing climate change impacts, sea level rise and storm surge risk in port cities: a case study on Copenhagen. Clim. Change 104, 113–137. https://doi.org/10.1007/s10584-010-9978-3

Hanley, M.E., Bouma, T.J., Mossman, H.L., 2020. The gathering storm: optimizing management of coastal ecosystems in the face of a climate-driven threat. Ann. Bot. 125, 197–212. https://doi.org/10.1093/aob/mcz204

Hard, R., 2004. The routledge handbook of greek mythology. Routledge.

Harley, M., 2017. Coastal Storm Definition, in: Coco, G., Ciavola, P. (Eds.), Coastal Storms. John Wiley & Sons, Ltd, Chichester, UK, pp. 1–21. https://doi.org/10.1002/9781118937099.ch1

Harley, M.D., Kinsela, M.A., Sánchez-García, E., Vos, K., 2019. Shoreline change mapping using

crowd-sourced smartphone images. Coast. Eng. 150, 175–189. https://doi.org/10.1016/j.coastaleng.2019.04.003

Harley, M.D., Turner, I.L., Kinsela, M.A., Middleton, J.H., Mumford, P.J., Splinter, K.D., Phillips, M.S., Simmons, J.A., Hanslow, D.J., Short, A.D., 2017. Extreme coastal erosion enhanced by anomalous extratropical storm wave direction. Sci. Rep. 7, 6033. https://doi.org/10.1038/s41598-017-05792-1

Hartt, M.D., 2014. An innovative technique for modelling impacts of coastal storm damage. Reg. Stud. Reg. Sci. 1, 240–247. https://doi.org/10.1080/21681376.2014.962595

Hartter, J., Hamilton, L.C., Boag, A.E., Stevens, F.R., Ducey, M.J., Christoffersen, N.D., Oester, P.T., Palace, M.W., 2018. Does it matter if people think climate change is human caused? Clim. Serv. 10, 53–62. https://doi.org/10.1016/j.cliser.2017.06.014

Hasse, L., 2015. Basic Atmospheric Structure and Concepts | Beaufort Wind Scale, in: Encyclopedia of Atmospheric Sciences. Elsevier, pp. 1–6. https://doi.org/10.1016/B978-0-12-382225-3.00466-7

Hatzikyriakou, A., Lin, N., 2017. Impact of performance interdependencies on structural vulnerability: A systems perspective of storm surge risk to coastal residential communities. Reliab. Eng. Syst. Saf. 158, 106–116. https://doi.org/10.1016/j.ress.2016.10.011

Helman, P., Tomlinson, R., 2008. Coastal storms and climate change over the last two centuries, east coast, Australia, in: Solutions to Coastal Disasters Congress 2008 - Proceedings of the Solutions to Coastal Disasters Congress 2008. pp. 139–146. https://doi.org/10.1061/40968(312)13

Hill, H.W., Kelley, J.T., Belknap, D.F., Dickson, S.M., 2004. The effects of storms and storm-generated currents on sand beaches in Southern Maine, USA. Mar. Geol. 210, 149–168. https://doi.org/10.1016/j.margeo.2004.05.008

Hissel, F., Morel, G., Pescaroli, G., Graaff, H., Felts, D., Pietrantoni, L., 2014. Early warning and mass evacuation in coastal cities. Coast. Eng. 87, 193–204. https://doi.org/10.1016/j.coastaleng.2013.11.015

Hobæk Haff, I., 2013. Parameter estimation for pair-copula constructions. Bernoulli 19. https://doi.org/10.3150/12-BEJ413

Hobæk Haff, I., 2012. Comparison of estimators for pair-copula constructions. J. Multivar. Anal. 110, 91–105. https://doi.org/10.1016/j.jmva.2011.08.013

Hoegh-Guldberg, O., Jacob, D., Taylor, M., Bindi, M., Brown, S., Camilloni, I., Diedhiou, A., Djalante, R., Ebi, K.L., Engelbrecht, F., Guiot, J., Hijioka, Y., Mehrotra, S., Payne, A., Seneviratne, S.I., Thomas, A., Warren, R., Zhou, G., 2018. Impacts of 1.5ºC Global Warming on Natural and Human Systems., in: Masson-Delmotte, V., Zhai, P., Pörtner, H.-O., Roberts, D., Skea, J., Shukla, P.R., Pirani, A., Moufouma-Okia, W., Péan, C., Pidcock, R., Connors,

S., Matthews, J.B.R., Chen, Y., Zhou, X., Gomis, M.I., Lonnoy, E., Maycock, T., Tignor, M., Waterfield, T. (Eds.), Global Warming of 1.5°C. An IPCC Special Report on the Impacts of Global Warming of 1.5°C above Pre-Industrial Levels and Related Global Greenhouse Gas Emission Pathways, in the Context of Strengthening the Global Response to the Threat of Climate Change,. IPCC.

Hofert, M., Kojadinovic, I., Mächler, M., Yan, J., 2018. Elements of Copula Modeling with R, Use R! Springer International Publishing, Cham. https://doi.org/10.1007/978-3-319-89635-9

Hollander, M., Wolfe, D., Chicken, E., 2015. Nonparametric Statistical Methods, Wiley Series in Probability and Statistics. Wiley, New York. https://doi.org/10.1002/9781119196037

Hondula, D.M., Dolan, R., 2010. Predicting severe winter coastal storm damage. Environ. Res. Lett. 5, 034004. https://doi.org/10.1088/1748-9326/5/3/034004

Hong Kong Observatory, 2009. The New 3-tier Typhoon Classification [WWW Document]. URL https://www.hko.gov.hk/en/aviat/outreach/product/20th/TCclass.htm

Hopsch, S.B., Thorncroft, C.D., Tyle, K.R., 2010. Analysis of African Easterly Wave Structures and Their Role in Influencing Tropical Cyclogenesis. Mon. Weather Rev. 138, 1399–1419. https://doi.org/10.1175/2009MWR2760.1

Hornsey, M.J., Harris, E.A., Bain, P.G., Fielding, K.S., 2016. Meta-analyses of the determinants and outcomes of belief in climate change. Nat. Clim. Chang. 6, 622–626. https://doi.org/10.1038/nclimate2943

Horton, R., Little, C., Gornitz, V., Bader, D., Oppenheimer, M., 2015. New York City Panel on Climate Change 2015 Report Chapter 2: Sea Level Rise and Coastal Storms. Ann. N. Y. Acad. Sci. 1336, 36–44. https://doi.org/10.1111/nyas.12593

Horton, R., Rosenzweig, C., Solecki, W., Bader, D., Sohl, L., 2016. Climate science for decision-making in the New York metropolitan region, in: Climate in Context. John Wiley & Sons, Ltd, Chichester, UK, pp. 51–72. https://doi.org/10.1002/9781118474785.ch3

Huguet, J.-R., Bertin, X., Arnaud, G., 2018. Managed realignment to mitigate storm-induced flooding: A case study in La Faute-sur-mer, France. Coast. Eng. 134, 168–176. https://doi.org/10.1016/j.coastaleng.2017.08.010

Hyndman, R.J., Athanasopoulos, G., 2021. Forecasting: principles and practice, 3rd edition, 3rd ed. OTexts, Melbourne, Australia.

IPCC, 2019. Special Report on the Ocean and Cryosphere in a Changing Climate [WWW Document]. URL https://www.ipcc.ch/srocc/

IPCC, 2018. Global Warming of 1.5 ºC [WWW Document]. URL https://www.ipcc.ch/sr15/

Irish, J.L., Resio, D.T., Ratcliff, J.J., 2008. The Influence of Storm Size on Hurricane Surge. J. Phys. Oceanogr. 38, 2003–2013. https://doi.org/10.1175/2008JPO3727.1

ISO 21650, 2007. Actions from waves and currents on coastal structures. Switzerland.

Izaguirre, C., Méndez, F.J., Espejo, A., Losada, I.J., Reguero, B.G., 2013. Extreme wave climate changes in Central-South America. Clim. Change 119, 277–290. https://doi.org/10.1007/s10584-013-0712-9

Jäger, W.S., Nagler, T., Czado, C., McCall, R.T., 2019. A statistical simulation method for joint time series of non-stationary hourly wave parameters. Coast. Eng. 146, 14–31. https://doi.org/10.1016/j.coastaleng.2018.11.003

Jäger, W.S., Nápoles, O.M., 2017. A Vine-Copula Model for Time Series of Significant Wave Heights and Mean Zero-Crossing Periods in the North Sea. ASCE-ASME J. Risk Uncertain. Eng. Syst. Part A Civ. Eng. 3, 04017014. https://doi.org/10.1061/AJRUA6.0000917

Jammalamadaka, S.R., SenGupta, A., 2001. Topics in Circular Statistics, Series on Multivariate Analysis. WORLD SCIENTIFIC. https://doi.org/10.1142/4031

Jaranovic, B., Trindade, J., Ribeiro, J., Silva, A., 2017. Using a coastal storm hazard index to assess storm impacts in lisbon. Int. J. Saf. Secur. Eng. 7, 221–233. https://doi.org/10.2495/SAFE-V7-N2-221-233

Jarušková, D., Hanek, M., 2006. Peaks over threshold method in comparison with block-maxima method for estimating return levels of several northern Moravia precipitation and discharges series. J. Hydrol. Hydromech., 54, 309–319.

Jean, M.-È., Duchesne, S., Pelletier, G., Pleau, M., 2018. Selection of rainfall information as input data for the design of combined sewer overflow solutions. J. Hydrol. 565, 559–569. https://doi.org/10.1016/j.jhydrol.2018.08.064

Jiménez, J.A., Sancho-García, A., Bosom, E., Valdemoro, H.I., Guillén, J., 2012. Storm-induced damages along the Catalan coast (NW Mediterranean) during the period 1958–2008. Geomorphology 143–144, 24–33. https://doi.org/10.1016/j.geomorph.2011.07.034

Joe, H., 2017. Parametric copula families for statistical models, in: Flores, M.Ú., Artero, E. de A., Durante, F., Fernández-Sánchez, J. (Eds.), Copulas and Dependence Models with Applications. pp. 119–134. https://doi.org/10.1007/978-3-319-64221-5

Joe, H., 2014. Dependence Modeling with Copulas. Chapman and Hall/CRC. https://doi.org/10.1201/b17116

Joe, H., 1997. Multivariate Models and Multivariate Dependence Concepts. Chapman & Hall.

Joe, H., 1996. Families of m-Variate Distributions with Given Margins and m(m-1)/2 Bivariate Dependence Parameters, in: Distributions with Fixed Marginals and Related Topics. pp. 120–141.

Joe, H., Li, H., Nikoloulopoulos, A.K., 2010. Tail dependence functions and vine copulas. J. Multivar. Anal. 101, 252–270. https://doi.org/10.1016/j.jmva.2009.08.002

Jones, J.M., Henry, K., Wood, N., Ng, P., Jamieson, M., 2017. HERA: A dynamic web application for visualizing community exposure to flood hazards based on storm and sea level rise

scenarios. Comput. Geosci. 109, 124–133. https://doi.org/10.1016/j.cageo.2017.08.012

Kadhem, S.H., Nikoloulopoulos, A.K., 2021. Factor copula models for mixed data. Br. J. Math. Stat. Psychol. bmsp.12231. https://doi.org/10.1111/bmsp.12231

Kao, S.-C., Govindaraju, R.S., 2010. A copula-based joint deficit index for droughts. J. Hydrol. 380, 121–134. https://doi.org/10.1016/j.jhydrol.2009.10.029

Karavokiros, G., Lykou, A., Koutiva, I., Batica, J., Kostaridis, A., Alves, A., Makropoulos, C., 2016. Providing Evidence-Based, Intelligent Support for Flood Resilient Planning and Policy: The PEARL Knowledge Base. Water 8, 392. https://doi.org/10.3390/w8090392

Karunarathna, H., Pender, D., Ranasinghe, R., Short, A.D., Reeve, D.E., 2014. The effects of storm clustering on beach profile variability. Mar. Geol. 348, 103–112. https://doi.org/10.1016/j.margeo.2013.12.007

Kates, R.W., Colten, C.E., Laska, S., Leatherman, S.P., 2006. Reconstruction of New Orleans after Hurricane Katrina: A research perspective. Proc. Natl. Acad. Sci. 103, 14653–14660. https://doi.org/10.1073/pnas.0605726103

Katz, R.W., 2010. Statistics of extremes in climate change. Clim. Change 100, 71–76. https://doi.org/10.1007/s10584-010-9834-5

Kereszturi, M., Tawn, J., Jonathan, P., 2016. Assessing extremal dependence of North Sea storm severity. Ocean Eng. 118, 242–259. https://doi.org/10.1016/j.oceaneng.2016.04.013

Kim, H.-J., Suh, S.-W., 2016. Probabilistic Coastal Storm Surge Analyses using Synthesized Tracks Based on Historical Typhoon Parameters. J. Coast. Res. 75, 1132–1136. https://doi.org/10.2112/SI75-227.1

Kirezci, E., Young, I.R., Ranasinghe, R., Muis, S., Nicholls, R.J., Lincke, D., Hinkel, J., 2020. Projections of global-scale extreme sea levels and resulting episodic coastal flooding over the 21st Century. Sci. Rep. 10, 11629. https://doi.org/10.1038/s41598-020-67736-6

Kistler, R., Collins, W., Saha, S., White, G., Woollen, J., Kalnay, E., Chelliah, M., Ebisuzaki, W., Kanamitsu, M., Kousky, V., van den Dool, H., Jenne, R., Fiorino, M., 2001. The NCEP–NCAR 50–Year Reanalysis: Monthly Means CD–ROM and Documentation. Bull. Am. Meteorol. Soc. 82, 247–267. https://doi.org/10.1175/1520-0477(2001)082<0247:TNNYRM>2.3.CO;2

Klemas, V. V., 2009. The Role of Remote Sensing in Predicting and Determining Coastal Storm Impacts. J. Coast. Res. 256, 1264–1275. https://doi.org/10.2112/08-1146.1

Knutson, T.R., Sirutis, J.J., Zhao, M., Tuleya, R.E., Bender, M., Vecchi, G.A., Villarini, G., Chavas, D., 2015. Global Projections of Intense Tropical Cyclone Activity for the Late Twenty-First Century from Dynamical Downscaling of CMIP5/RCP4.5 Scenarios. J. Clim. 28, 7203–7224. https://doi.org/10.1175/JCLI-D-15-0129.1

Komar, P.D., Allan, J.C., 2008. Increasing Hurricane-Generated Wave Heights along the U.S. East Coast and Their Climate Controls. J. Coast. Res. 242, 479–488.

https://doi.org/10.2112/07-0894.1

Koutroumbas, S., Theodoridis, K., 2009. Pattern Recognition. Elsevier. https://doi.org/10.1016/B978-1-59749-272-0.X0001-2

Kremer, H., Nicholls, R., Ratter, B.M.W., Weisse, R., 2013. Preface: Interdisciplinary Research and Perspectives on Current and Future Storm Surges. Nat. Hazards 66, 1293–1294. https://doi.org/10.1007/s11069-013-0613-2

Kurowicka, D., Joe, H., 2010. Dependence Modeling. WORLD SCIENTIFIC. https://doi.org/10.1142/7699

Laface, V., Arena, F., 2016. A new equivalent exponential storm model for long-term statistics of ocean waves. Coast. Eng. 116, 133–151. https://doi.org/10.1016/j.coastaleng.2016.06.011

Lane, D.E., Clarke, C.M., Clarke, J.D., Mycoo, M., Gobin, J., 2015. Managing Adaptation to Changing Climate in Coastal Zones, Coastal Zones: Solutions for the 21st Century. https://doi.org/10.1016/B978-0-12-802748-6.00009-7

Latif, S., Mustafa, F., 2020. Copula-based multivariate flood probability construction: a review. Arab. J. Geosci. 13, 132. https://doi.org/10.1007/s12517-020-5077-6

Leal Filho, W. (Ed.), 2018. Climate Change Impacts and Adaptation Strategies for Coastal Communities, Climate Change Management. Springer International Publishing, Cham. https://doi.org/10.1007/978-3-319-70703-7

Lee, G., Nicholls, R.J., Birkemeier, W.A., 1998. Storm-driven variability of the beach-nearshore profile at Duck, North Carolina, USA, 1981–1991. Mar. Geol. 148, 163–177. https://doi.org/10.1016/S0025-3227(98)00010-3

Li, F., van Gelder, P.H.A.J.M., Ranasinghe, R., Callaghan, D.P., Jongejan, R.B., 2014. Probabilistic modelling of extreme storms along the Dutch coast. Coast. Eng. 86, 1–13. https://doi.org/10.1016/j.coastaleng.2013.12.009

Li, F., Zhou, J., Liu, C., 2018. Statistical modelling of extreme storms using copulas: A comparison study. Coast. Eng. 142, 52–61. https://doi.org/10.1016/j.coastaleng.2018.09.007

Li, Y., Dong, Y., Zhu, D., 2020. Copula-Based Vulnerability Analysis of Civil Infrastructure Subjected to Hurricanes. Front. Built Environ. 6. https://doi.org/10.3389/fbuil.2020.571911

Li, Y., Liu, G., 2020. Risk Analysis of Marine Environmental Elements Based on Kendall Return Period. J. Mar. Sci. Eng. 8, 393. https://doi.org/10.3390/jmse8060393

Lin-Ye, J., García-León, M., Gràcia, V., Ortego, M., Lionello, P., Conte, D., Pérez-Gómez, B., Sánchez-Arcilla, A., 2020. Modeling of Future Extreme Storm Surges at the NW Mediterranean Coast (Spain). Water 12, 472. https://doi.org/10.3390/w12020472

Lin-Ye, J., García-León, M., Gràcia, V., Ortego, M., Stanica, A., Sánchez-Arcilla, A., 2018. Multivariate Hybrid Modelling of Future Wave-Storms at the Northwestern Black Sea.

Water 10, 221. https://doi.org/10.3390/w10020221

Lin-Ye, J., Garcia-Leon, M., Gracia, V., Sanchez-Arcilla, A., 2016. A multivariate statistical model of extreme events: An application to the Catalan coast. Coast. Eng. 117, 138–156. https://doi.org/10.1016/j.coastaleng.2016.08.002

Lionello, P., Bhend, J., Buzzi, A., Della-Marta, P.M., Krichak, S.O., Jansà, A., Maheras, P., Sanna, A., Trigo, I.F., Trigo, R., 2006. Chapter 6 Cyclones in the Mediterranean region: Climatology and effects on the environment. pp. 325–372. https://doi.org/10.1016/S1571-9197(06)80009-1

Lionello, P., Cogo, S., Galati, M.B., Sanna, A., 2008. The Mediterranean surface wave climate inferred from future scenario simulations. Glob. Planet. Change 63, 152–162. https://doi.org/10.1016/j.gloplacha.2008.03.004

Lionello, P., Galati, M.B., Elvini, E., 2012. Extreme storm surge and wind wave climate scenario simulations at the Venetian littoral. Phys. Chem. Earth, Parts A/B/C 40–41, 86–92. https://doi.org/10.1016/j.pce.2010.04.001

Lionello, P., Trigo, I.F., Gil, V., Liberato, M.L.R., Nissen, K.M., Pinto, J.G., Raible, C.C., Reale, M., Tanzarella, A., Trigo, R.M., Ulbrich, S., Ulbrich, U., 2016. Objective climatology of cyclones in the Mediterranean region: a consensus view among methods with different system identification and tracking criteria. Tellus A Dyn. Meteorol. Oceanogr. 68, 29391. https://doi.org/10.3402/tellusa.v68.29391

Lira-Loarca, A., Cobos, M., Losada, M.Á., Baquerizo, A., 2020. Storm characterization and simulation for damage evolution models of maritime structures. Coast. Eng. 156, 103620. https://doi.org/10.1016/j.coastaleng.2019.103620

Liu, P., Li, L., Guo, S., Xiong, L., Zhang, W., Zhang, J., Xu, C.-Y., 2015. Optimal design of seasonal flood limited water levels and its application for the Three Gorges Reservoir. J. Hydrol. 527, 1045–1053. https://doi.org/10.1016/j.jhydrol.2015.05.055

Longshore, D., 2008. Encyclopedia of Hurricanes, Typhoons, and Cyclones.

Longuet-Higgins, M.S., 1983. On the joint distribution of wave periods and amplitudes in a random wave field. Proc. R. Soc. London. A. Math. Phys. Sci. 389, 241–258. https://doi.org/10.1098/rspa.1983.0107

Lowe, J.., Gregory, J.., 2005. The effects of climate change on storm surges around the United Kingdom. Philos. Trans. R. Soc. A Math. Phys. Eng. Sci. 363, 1313–1328. https://doi.org/10.1098/rsta.2005.1570

Lozano, I., Devoy, R.J.N., May, W., Andersen, U., 2004. Storminess and vulnerability along the Atlantic coastlines of Europe: analysis of storm records and of a greenhouse gases induced climate scenario. Mar. Geol. 210, 205–225. https://doi.org/10.1016/j.margeo.2004.05.026

Ludlum, D.M., 1963. Early American hurricanes, 1492-1870. American Meteorological Society,

Boston.

Lukens, K.E., Berbery, E.H., Hodges, K.I., 2018. The Imprint of Strong-Storm Tracks on Winter Weather in North America. J. Clim. 31, 2057–2074. https://doi.org/10.1175/JCLI-D-17-0420.1

Machado, A.A., Calliari, L.J., 2016. Synoptic Systems Generators of Extreme Wind in Southern Brazil: Atmospheric Conditions and Consequences in the Coastal Zone. J. Coast. Res. 75, 1182–1186. https://doi.org/10.2112/SI75-237.1

Madsen, H., Jakobsen, F., 2004. Cyclone induced storm surge and flood forecasting in the northern Bay of Bengal. Coast. Eng. 51, 277–296. https://doi.org/10.1016/j.coastaleng.2004.03.001

Mai, J.-F., Scherer, M., 2017. Simulating Copulas, Series in Quantitative Finance. WORLD SCIENTIFIC. https://doi.org/10.1142/10265

Mai, J.-F., Scherer, M., 2014. Financial Engineering with Copulas Explained. Palgrave Macmillan UK, London. https://doi.org/10.1057/9781137346315

Mannshardt, E., Gilleland, E., 2013. Extremes of Severe Storm Environments under a Changing Climate. Am. J. Clim. Chang. 02, 47–61. https://doi.org/10.4236/ajcc.2013.23A005

Marcos, M., Jordà, G., Gomis, D., Pérez, B., 2011. Changes in storm surges in southern Europe from a regional model under climate change scenarios. Glob. Planet. Change 77, 116–128. https://doi.org/10.1016/j.gloplacha.2011.04.002

Martín-Hidalgo, M., Martín-Soldevilla, M.J., Negro, V., Aberturas, P., López-Gutiérrez, J.S., 2014. Storm evolution characterization for analysing stone armour damage progression. Coast. Eng. 85, 1–11. https://doi.org/10.1016/j.coastaleng.2013.11.008

Martín Soldevilla, M.J., Martín-Hidalgo, M., Negro, V., López-Gutiérrez, J.S., Aberturas, P., 2015. Improvement of theoretical storm characterization for different climate conditions. Coast. Eng. 96, 71–80. https://doi.org/10.1016/j.coastaleng.2014.11.004

Martzikos, N., Afentoulis, V., Tsoukala, V., 2018. Storm clustering and classification for the port of Rethymno in Greece, Water Utility Journal.

Martzikos, Prinos, P., Memos, C.D., Tsoukala, V.K., 2021a. Statistical analysis of Mediterranean coastal storms. Oceanologia 63, 133–148. https://doi.org/10.1016/j.oceano.2020.11.001

Martzikos, Prinos, P.E., Memos, C.D., Tsoukala, V.K., 2021b. Key research issues of coastal storm analysis. Ocean Coast. Manag. 199. https://doi.org/10.1016/j.ocecoaman.2020.105389

Marzeddu, A., Oliveira, T.C.A., Sánchez-Arcilla, A., Gironella, X., 2020. Effect of wave storm representation on damage measurements of breakwaters. Ocean Eng. 200, 107082. https://doi.org/10.1016/j.oceaneng.2020.107082

Masina, M., Lamberti, A., Archetti, R., 2015. Coastal flooding: A copula based approach for estimating the joint probability of water levels and waves. Coast. Eng. 97, 37–52.

https://doi.org/10.1016/j.coastaleng.2014.12.010

Maslo, B., Leu, K., Pover, T., Weston, M.A., Gilby, B.L., Schlacher, T.A., 2019. Optimizing conservation benefits for threatened beach fauna following severe natural disturbances. Sci. Total Environ. 649, 661–671. https://doi.org/10.1016/j.scitotenv.2018.08.319

Masselink, G., Austin, M., Scott, T., Poate, T., Russell, P., 2014. Role of wave forcing, storms and NAO in outer bar dynamics on a high-energy, macro-tidal beach. Geomorphology 226, 76–93. https://doi.org/10.1016/j.geomorph.2014.07.025

Massey, T.C., Wamsley, T.V., Cialone, M.A., 2011. Coastal storm modeling - System integration, in: Solutions to Coastal Disasters 2011 - Proceedings of the 2011 Solutions to Coastal Disasters Conference. pp. 99–108. https://doi.org/10.1061/41185(417)10

Mather, J.R., 2005. Beaufort Wind Scale, in: Encyclopedia of World Climatology. Springer Netherlands, pp. 156–157. https://doi.org/10.1007/1-4020-3266-8_28

Mather, J.R., Adams, H., Yoshioka, G.A., 1964. Coastal Storms of the Eastern United States. J. Appl. Meteorol. 3, 693–706. https://doi.org/10.1175/1520-0450(1964)003<0693:CSOTEU>2.0.CO;2

Mattocks, C., Forbes, C., 2008. A real-time, event-triggered storm surge forecasting system for the state of North Carolina. Ocean Model. 25, 95–119. https://doi.org/10.1016/j.ocemod.2008.06.008

Mazas, F., 2019. Extreme events: a framework for assessing natural hazards. Nat. Hazards. https://doi.org/10.1007/s11069-019-03581-9

Mazas, F., Hamm, L., 2017. An event-based approach for extreme joint probabilities of waves and sea levels. Coast. Eng. 122, 44–59. https://doi.org/10.1016/j.coastaleng.2017.02.003

Mazas, F., Hamm, L., 2011. A multi-distribution approach to POT methods for determining extreme wave heights. Coast. Eng. 58, 385–394. https://doi.org/10.1016/j.coastaleng.2010.12.003

McCullough, M.C., Kareem, A., Donahue, A.S., Westerink, J.J., 2013. Structural damage under multiple hazards in coastal environments. J. Disaster Res. 8, 1042–1051.

McIlveen, R., 2010. Fundamentals of Weather and Climate. Oxford University Press; 2nd edition, USA.

McInnes, K.L., Hubbert, G.D., Macadam, I., O'Grady, J.G., 2007. Assessing the Impact of Climate Change on Storm Surges in Southern Australia. Modsim 2007 Int. Congr. Model. Simul. Land, Water Environ. Manag. Integr. Syst. Sustain.

McNeil, A.J., Frey, R., Embrechts, P., 2005. Quantitative risk management: Concepts, techniques, and tools. Princeton University Press.

Mega, V.P., 2016. Conscious Coastal Cities. Springer International Publishing, Cham. https://doi.org/10.1007/978-3-319-20218-1

Memos, C.D., 1994. On the theory of the joint probability of heights and periods of sea waves. Coast. Eng. 22, 201–215. https://doi.org/10.1016/0378-3839(94)90036-1

Méndez, F.J., Menéndez, M., Luceño, A., Losada, I.J., 2006. Estimation of the long-term variability of extreme significant wave height using a time-dependent Peak Over Threshold (POT) model. J. Geophys. Res. 111, C07024. https://doi.org/10.1029/2005JC003344

Méndez, F.J., Menéndez, M., Luceño, A., Medina, R., Graham, N.E., 2008. Seasonality and duration in extreme value distributions of significant wave height. Ocean Eng. 35, 131–138. https://doi.org/10.1016/j.oceaneng.2007.07.012

Mendoza, E.T., Jimenez, J.A., Mateo, J., 2011. A coastal storms intensity scale for the Catalan sea (NW Mediterranean). Nat. Hazards Earth Syst. Sci. 11, 2453–2462. https://doi.org/10.5194/nhess-11-2453-2011

Mendoza, E.T., Trejo-Rangel, M.A., Salles, P., Appendini, C.M., Lopez-Gonzalez, J., Torres-Freyermuth, A., 2013. Storm characterization and coastal hazards in the Yucatan Peninsula. J. Coast. Res. 65, 790–795. https://doi.org/10.2112/SI65-134.1

Menéndez, M., Méndez, F.J., Izaguirre, C., Luceño, A., Losada, I.J., 2009. The influence of seasonality on estimating return values of significant wave height. Coast. Eng. 56, 211–219. https://doi.org/10.1016/j.coastaleng.2008.07.004

Mesbahzadeh, T., Mirakbari, M., Mohseni Saravi, M., Soleimani Sardoo, F., Miglietta, M.M., 2020. Meteorological drought analysis using copula theory and drought indicators under climate change scenarios (RCP). Meteorol. Appl. 27. https://doi.org/10.1002/met.1856

Met Office, 2018. Tropical Cyclone facts [WWW Document]. URL https://www.metoffice.gov.uk/weather/tropicalcyclone/facts

Michener, W.K., Blood, E.R., Bildstein, K.L., Brinson, M.M., Gardner, L.R., 1997. Climate Change, Hurricanes and Tropical Storms, and Rising Sea Level in Coastal Wetlands. Ecol. Appl. 7, 770. https://doi.org/10.2307/2269434

Mohd Anuar, N., Hashim, A.M., Awang, N.A., Abd Hamid, M.R., 2018. Historical storm surges: Consequences on coastal resources and shoreline protection in the east coast of peninsular Malaysia, in: 7th IAHR International Symposium on Hydraulic Structures, ISHS 2018. pp. 434–443. https://doi.org/10.15142/T33H1T

Mölders, N., Kramm, G., 2014. Lectures in Meteorology. Springer.

Molina, R., Manno, G., Lo Re, C., Anfuso, G., Ciraolo, G., 2019. Storm Energy Flux Characterization along the Mediterranean Coast of Andalusia (Spain). Water 11, 509. https://doi.org/10.3390/w11030509

Mooyaart, L.F., Jonkman, S.N., 2017. Overview and Design Considerations of Storm Surge Barriers. J. Waterw. Port, Coastal, Ocean Eng. 143, 06017001. https://doi.org/10.1061/(ASCE)WW.1943-5460.0000383

Muis, S., Verlaan, M., Winsemius, H.C., Aerts, J.C.J.H., Ward, P.J., 2016. A global reanalysis of storm surges and extreme sea levels. Nat. Commun. 7, 11969. https://doi.org/10.1038/ncomms11969

Musereau, J., Regnauld, H., 2014. Storms impact on morphodynamics of human controlled coastal features in western France: the prevailing role of local management practices. J. Coast. Conserv. 18, 539–550. https://doi.org/10.1007/s11852-014-0311-6

Nadal-Caraballo, N.C., Campbell, M.O., Gonzalez, V.M., Torres, M.J., Melby, J.A., Taflanidis, A.A., 2020. Coastal Hazards System: A Probabilistic Coastal Hazard Analysis Framework. J. Coast. Res. 95, 1211. https://doi.org/10.2112/SI95-235.1

Nagler, T., Schepsmeier, U., Stoeber, J., Brechmann, E.C., Graeler, B., Erhardt, T., 2021. VineCopula: Statistical Inference of Vine Copulas.

Naimaster, A., Bender, C., Miller, W., 2013. Advanced estimation of coastal storm surge: Application of swan + adcirc in georgia/northeast florida storm surge study, in: Advances in Hurricane Engineering: Learning from Our Past - Proceedings of the 2012 ATC and SEI Conference on Advances in Hurricane Engineering. pp. 607–617.

National Research Council, 2014. Reducing coastal risk on the east and Gulf Coasts, Reducing Coastal Risk on the East and Gulf Coasts. The National Academies Press, Washington, DC. https://doi.org/10.17226/18811

Needham, H.F., Keim, B.D., 2011. A storm surge database for the US Gulf Coast. Int. J. Climatol. 32, n/a-n/a. https://doi.org/10.1002/joc.2425

Nelsen, R., 2006. An Introduction to Copulas, Springer Series in Statistics. Springer New York, New York, NY. https://doi.org/10.1007/0-387-28678-0

NHC, 2019. Saffir-Simpson Hurricane Wind Scale [WWW Document]. URL https://www.nhc.noaa.gov/aboutsshws.php (accessed 12.19.19).

Nicholls, R.J., Wong, P.P., Burkett, V.R., Codignotto, J.O., Hay, J.E., McLean, R.F., Ragoonaden, S. Woodroffe, C.D., 2007. Coastal systems and low-lying areas, in: Parry, M., Canziani, O., Palutikof, J., van der Linden, P., Hanson, C. (Eds.), Climate Change 2007: Impacts, Adaptation and Vulnerability, Contribution of Working Group II to the Fourth Assessment Report of the Intergovernmental Panel on Climate Change. Cambridge University Press, Cambridge, UK, pp. 315–356.

Nikoloulopoulos, A.K., Joe, H., Li, H., 2012. Vine copulas with asymmetric tail dependence and applications to financial return data. Comput. Stat. Data Anal. 56, 3659–3673. https://doi.org/10.1016/j.csda.2010.07.016

Nikoloulopoulos, A.K., Karlis, D., 2008. Copula model evaluation based on parametric bootstrap. Comput. Stat. Data Anal. 52, 3342–3353. https://doi.org/10.1016/j.csda.2007.10.028

NOAA, 2019a. Tropical Cyclone [WWW Document]. Glossary. URL

https://w1.weather.gov/glossary/index.php?word=tropical+cyclone

NOAA, 2019b. Storm Surge Overview [WWW Document]. Natl. Hurric. Cent. URL https://www.nhc.noaa.gov/surge/

NOAA, 2013. Know the dangers of nor'easters [WWW Document]. URL https://web.archive.org/web/20160214123432/http:/www.noaa.gov/features/03_protecting/noreasters.html

NOAA, 2010. Adapting to Climate Change: A Planning Guide for State Coastal Managers. NOAA Office of Ocean and Coastal Resource Management.

NORSOK N-003, 2017. Actions and actions effects.

OceanSITES, 2015. OceanSITES Data Format Reference Manual.

Oppenheimer, M., Glavovic, B.C., Hinkel, J., Wal, R. van de, Magnan, A.K., Abd-Elgawad, A., Cai, R., Cifuentes-Jara, M., DeConto, R.M., Ghosh, T., Hay, J., Isla, F., Marzeion, B., Meyssignac, B., Sebesvari, Z., 2019. Sea Level Rise and Implications for Low-Lying Islands, Coasts and Communities, in: Pörtner, H.-O., Roberts, D.C., Masson-Delmotte, V., Zhai, P., Tignor, M., Poloczanska, E., Mintenbeck, K., Alegría, A., Nicolai, M., Okem, A., Petzold, J., Rama, B., Weyer, N.M. (Eds.), IPCC Special Report on the Ocean and Cryosphere in a Changing Climate. IPCC.

Orcel, O., Sergent, P., Ropert, F., 2021. Trivariate copula to design coastal structures. Nat. Hazards Earth Syst. Sci. 21, 239–260. https://doi.org/10.5194/nhess-21-239-2021

Oumeraci, H., Kortenhaus, A., Burzel, A., Naulin, M., Dassanayake, D.R., Jensen, J., Wahl, T., Mudersbach, C., Gönnert, G., Gerkensmeier, B., Fröhle, P., Ujeyl, G., 2015. XtremRisK — Integrated Flood Risk Analysis for Extreme Storm Surges at Open Coasts and in Estuaries: Methodology, Key Results and Lessons Learned. Coast. Eng. J. 57, 1540001-1-1540001–23. https://doi.org/10.1142/S057856341540001X

Pappadà, R., Durante, F., Salvadori, G., De Michele, C., 2018. Clustering of concurrent flood risks via Hazard Scenarios. Spat. Stat. 23, 124–142. https://doi.org/10.1016/j.spasta.2017.12.002

Park, M.-S., Kim, H.-S., Ho, C.-H., Elsberry, R.L., Lee, M.-I., 2015. Tropical Cyclone Mekkhala's (2008) Formation over the South China Sea: Mesoscale, Synoptic-Scale, and Large-Scale Contributions. Mon. Weather Rev. 143, 88–110. https://doi.org/10.1175/MWR-D-14-00119.1

Paton, D., Johnston, D., Rossiter, K., Buergelt, P.T., Richards, A., Anderson, S., 2017. Community understanding of tsunami risk and warnings in Australia. Aust. J. Emerg. Manag. 32, 54–59.

Patrick, C.J., Yeager, L., Armitage, A.R., Carvallo, F., Congdon, V.M., Dunton, K.H., Fisher, M., Hardison, A.K., Hogan, J.D., Hosen, J., Hu, X., Kiel Reese, B., Kinard, S., Kominoski, J.S.,

Lin, X., Liu, Z., Montagna, P.A., Pennings, S.C., Walker, L., Weaver, C.A., Wetz, M., 2020. A System Level Analysis of Coastal Ecosystem Responses to Hurricane Impacts. Estuaries and Coasts 43, 943–959. https://doi.org/10.1007/s12237-019-00690-3

Petterson, J.S., Stanley, L.D., Glazier, E., Philipp, J., 2006. A preliminary assessment of social and economic impacts associated with Hurricane Katrina. Am. Anthropol. 108, 643–670. https://doi.org/10.1525/aa.2006.108.4.643

Phan, L.T., Simiu, E., 2011. Estimation of risk for design of structures exposed to combined effects of hurricane wind speed and storm surge hazards, in: Applications of Statistics and Probability in Civil Engineering -Proceedings of the 11th International Conference on Applications of Statistics and Probability in Civil Engineering. pp. 1967–1974.

Picou, J.S., Marshall, B.K., 2007. Social Impacts of Hurricane Katrina on Displaced K–12 Students and Educational Institutions in Coastal Alabama Counties: Some Preliminary Observations. Sociol. Spectr. 27, 767–780. https://doi.org/10.1080/02732170701534267

Piest, R.F., 1963. The Role of the Large Storm as a Sediment Contributor, in: Federal Inter-Agency Sedimentation Conference USDA Misc. Pub. 970. pp. 98–108.

Pingree-Shippee, K.A., Zwiers, F.W., Atkinson, D.E., 2018. Representation of mid-latitude North American coastal storm activity by six global reanalyses. Int. J. Climatol. 38, 1041–1059. https://doi.org/10.1002/joc.5235

Piscopia, R., Inghilesi, R., Panizzo, A., Corsini, S., Franco, L., 2003. Analysis of 12-year wave measurements by the italian wave network, in: Coastal Engineering 2002. World Scientific Publishing Company, pp. 121–133. https://doi.org/10.1142/9789812791306_0011

Plomaritis, T.A., Costas, S., Ferreira, Ó., 2018. Use of a Bayesian Network for coastal hazards, impact and disaster risk reduction assessment at a coastal barrier (Ria Formosa, Portugal). Coast. Eng. 134, 134–147. https://doi.org/10.1016/j.coastaleng.2017.07.003

Pouzet, P., Robin, M., Decaulne, A., Gruchet, B., Maanan, M., 2018. Sedimentological and dendrochronological indicators of coastal storm risk in western France. Ecol. Indic. 90, 401–415. https://doi.org/10.1016/j.ecolind.2018.03.022

Powell, E.J., Tyrrell, M.C., Milliken, A., Tirpak, J.M., Staudinger, M.D., 2019. A review of coastal management approaches to support the integration of ecological and human community planning for climate change. J. Coast. Conserv. 23, 1–18. https://doi.org/10.1007/s11852-018-0632-y

Prinos, P., Galiatsatou, P., 2018. Coastal Flooding: Analysis and Assessment of Risk, in: Handbook of Coastal and Ocean Engineering. WORLD SCIENTIFIC, pp. 1521–1550. https://doi.org/10.1142/9789813204027_0054

Puig, M., Del Río, L., Plomaritis, T.A., Benavente, J., 2016. Contribution of storms to shoreline changes in mesotidal dissipative beaches. Case study in the Gulf of Cadiz (SW Spain). Nat.

Hazards Earth Syst. Sci. Discuss. 1–30. https://doi.org/10.5194/nhess-2016-199

Pytharoulis, I., Craig, G.C., Ballard, S.P., 2000. The hurricane-like Mediterranean cyclone of January 1995. Meteorol. Appl. 7, 261–279. https://doi.org/10.1017/S1350482700001511

Quevauviller, P. (Ed.), 2014. Hydrometeorological Hazards. John Wiley & Sons, Ltd, Chichester, UK. https://doi.org/10.1002/9781118629567

Quevauviller, P., Ciavola, P., Garnier, E., 2017. Management of the Effect of Coastal Storms. Policy, Scientific and Historical Perspectives. Wiley.

R Core Team, 2021. R: A language and environment for statistical computing.

Ranasinghe, R., 2016. Assessing climate change impacts on open sandy coasts: A review. Earth-Science Rev. 160, 320–332. https://doi.org/10.1016/j.earscirev.2016.07.011

Rangel Buitrago, N., Anfuso, G., 2015. Risk Assessment of Storms in Coastal Zones: Case Studies from Cartagena (Colombia) and Cadiz (Spain), SpringerBriefs in Earth Sciences. Springer International Publishing, Cham. https://doi.org/10.1007/978-3-319-15844-0

Rangel Buitrago, N., Anfuso, G., 2011a. Coastal storm characterization and morphological impacts on sandy coasts. Earth Surf. Process. Landforms 36, 1997–2010. https://doi.org/10.1002/esp.2221

Rangel Buitrago, N., Anfuso, G., 2011b. An application of Dolan and Davis (1992) classification to coastal storms in SW Spanish littoral. J. Coast. Res. 1891–1895.

Rao, S., Mandal, S., 2005. Hindcasting of storm waves using neural networks. Ocean Eng. 32, 667–684. https://doi.org/10.1016/j.oceaneng.2004.09.003

Regnauld, H., Pirazzoli, P.A., Morvan, G., Ruz, M., 2004. Impacts of storms and evolution of the coastline in western France. Mar. Geol. 210, 325–337. https://doi.org/10.1016/j.margeo.2004.05.014

Rego, J.L., Li, C., 2009. On the importance of the forward speed of hurricanes in storm surge forecasting: A numerical study. Geophys. Res. Lett. 36, 1–5. https://doi.org/10.1029/2008GL036953

Renard, B., Lang, M., 2007. Use of a Gaussian copula for multivariate extreme value analysis: Some case studies in hydrology. Adv. Water Resour. 30, 897–912. https://doi.org/10.1016/j.advwatres.2006.08.001

Roberts, A., Thomas, B., Sewell, P., Khan, Z., Balmain, S., Gillman, J., 2016. Current tidal power technologies and their suitability for applications in coastal and marine areas. J. Ocean Eng. Mar. Energy 2, 227–245. https://doi.org/10.1007/s40722-016-0044-8

Robertson, I.N., Riggs, H.R., Yim, S.C., Young, Y.L., 2007. Lessons from Hurricane Katrina Storm Surge on Bridges and Buildings. J. Waterw. Port, Coastal, Ocean Eng. 133, 463–483. https://doi.org/10.1061/(ASCE)0733-950X(2007)133:6(463)

Romero, R., Emanuel, K., 2013. Medicane risk in a changing climate. J. Geophys. Res. Atmos.

118, 5992–6001. https://doi.org/10.1002/jgrd.50475

Rosa-Santos, P., Taveira-Pinto, F., Clemente, D., Cabral, T., Fiorentin, F., Belga, F., Morais, T., 2019. Experimental Study of a Hybrid Wave Energy Converter Integrated in a Harbor Breakwater. J. Mar. Sci. Eng. 7, 33. https://doi.org/10.3390/jmse7020033

Rosenzweig, C., Solecki, W., 2014. Hurricane Sandy and adaptation pathways in New York: Lessons from a first-responder city. Glob. Environ. Chang. 28, 395–408. https://doi.org/10.1016/j.gloenvcha.2014.05.003

Ross, E., Sam, S., Randell, D., Feld, G., Jonathan, P., 2018. Estimating surge in extreme North Sea storms. Ocean Eng. 154, 430–444. https://doi.org/10.1016/j.oceaneng.2018.01.078

Ruggiero, P., Komar, P.D., Allan, J.C., 2010. Increasing wave heights and extreme value projections: The wave climate of the U.S. Pacific Northwest. Coast. Eng. 57, 539–552. https://doi.org/10.1016/j.coastaleng.2009.12.005

Ruiz de Alegria-Arzaburu, A., Masselink, G., 2010. Storm response and beach rotation on a gravel beach, Slapton Sands, U.K. Mar. Geol. 278, 77–99. https://doi.org/10.1016/j.margeo.2010.09.004

Ruppert, D., Matteson, D.S., 2015. Copulas. pp. 183–215. https://doi.org/10.1007/978-1-4939-2614-5_8

Sadegh, M., Ragno, E., AghaKouchak, A., 2017. Multivariate Copula Analysis Toolbox (MvCAT): Describing dependence and underlying uncertainty using a Bayesian framework. Water Resour. Res. 53, 5166–5183. https://doi.org/10.1002/2016WR020242

Saghafian, B., Sanginabadi, H., 2020. Multivariate groundwater drought analysis using copulas. Hydrol. Res. 51, 666–685. https://doi.org/10.2166/nh.2020.131

Salvadori, G., 2004. Bivariate return periods via 2-Copulas. Stat. Methodol. 1, 129–144. https://doi.org/10.1016/j.stamet.2004.07.002

Salvadori, G., De Michele, C., 2013. Multivariate Extreme Value Methods. pp. 115–162. https://doi.org/10.1007/978-94-007-4479-0_5

Salvadori, G., De Michele, C., 2007. On the Use of Copulas in Hydrology: Theory and Practice. J. Hydrol. Eng. 12, 369–380. https://doi.org/10.1061/(ASCE)1084-0699(2007)12:4(369)

Salvadori, G., De Michele, C., 2004. Frequency analysis via copulas: Theoretical aspects and applications to hydrological events. Water Resour. Res. 40. https://doi.org/10.1029/2004WR003133

Salvadori, G., De Michele, C., Durante, F., 2011. On the return period and design in a multivariate framework. Hydrol. Earth Syst. Sci. 15, 3293–3305. https://doi.org/10.5194/hess-15-3293-2011

Salvadori, G., De Michele, C., Kottegoda, N.T., Rosso, R., 2007. Extremes in Nature, Water Science and Technology Library. Springer Netherlands, Dordrecht.

https://doi.org/10.1007/1-4020-4415-1

Salvadori, G., Durante, F., De Michele, C., Bernardi, M., Petrella, L., 2016. A multivariate copula-based framework for dealing with hazard scenarios and failure probabilities. Water Resour. Res. 52, 3701–3721. https://doi.org/10.1002/2015WR017225

Salvadori, G., Durante, F., Tomasicchio, G.R., D'Alessandro, F., 2015. Practical guidelines for the multivariate assessment of the structural risk in coastal and off-shore engineering. Coast. Eng. 95, 77–83. https://doi.org/10.1016/j.coastaleng.2014.09.007

Salvadori, G., Tomasicchio, G.R., D'Alessandro, F., 2014. Practical guidelines for multivariate analysis and design in coastal and off-shore engineering. Coast. Eng. 88, 1–14. https://doi.org/10.1016/j.coastaleng.2014.01.011

Sanchez-Vidal, A., Canals, M., Calafat, A.M., Lastras, G., Pedrosa-Pàmies, R., Menéndez, M., Medina, R., Company, J.B., Hereu, B., Romero, J., Alcoverro, T., 2012. Impacts on the Deep-Sea Ecosystem by a Severe Coastal Storm. PLoS One 7, e30395. https://doi.org/10.1371/journal.pone.0030395

Sanuy, M., Duo, E., Jäger, W.S., Ciavola, P., Jiménez, J.A., 2018. Linking source with consequences of coastal storm impacts for climate change and risk reduction scenarios for Mediterranean sandy beaches. Nat. Hazards Earth Syst. Sci. 18, 1825–1847. https://doi.org/10.5194/nhess-18-1825-2018

Sartini, L., Besio, G., Cassola, F., 2017. Spatio-temporal modelling of extreme wave heights in the Mediterranean Sea. Ocean Model. 117, 52–69. https://doi.org/10.1016/j.ocemod.2017.07.001

Schepsmeier, U., Stöber, J., 2014. Derivatives and Fisher information of bivariate copulas. Stat. Pap. 55, 525–542. https://doi.org/10.1007/s00362-013-0498-x

Schwartz, S.B., 2015. Sea of storms. Princeton University Press.

Sénéchal, N., Castelle, B., R. Bryan, K., 2017. Storm Clustering and Beach Response, in: Coastal Storms. John Wiley & Sons, Ltd, Chichester, UK, pp. 151–174. https://doi.org/10.1002/9781118937099.ch8

Sénéchal, N., Coco, G., Castelle, B., Marieu, V., 2015. Storm impact on the seasonal shoreline dynamics of a meso- to macrotidal open sandy beach (Biscarrosse, France). Geomorphology 228, 448–461. https://doi.org/10.1016/j.geomorph.2014.09.025

Seneviratne, S.I., Nicholls, N., Easterling, D., Goodess, C.M., Kanae, S., Kossin, J., Luo, Y., Marengo, J., McInnes, K., Rahimi, M., Reichstein, M., Sorteberg, A., Vera, C., Zhang, X., Rusticucci, M., Semenov, V., Alexander, L. V., Allen, S., Benito, G., Cavazos, T., Clague, J., Conway, D., Della-Marta, P.M., Gerber, M., Gong, S., Goswami, B.N., Hemer, M., Huggel, C., van den Hurk, B., Kharin, V. V., Kitoh, A., Tank, A.M.G.K., Li, G., Mason, S., McGuire, W., van Oldenborgh, G.J., Orlowsky, B., Smith, S., Thiaw, W., Velegrakis, A., Yiou, P.,

Zhang, T., Zhou, T., Zwiers, F.W., 2012. Changes in Climate Extremes and their Impacts on the Natural Physical Environment, in: Field, C.B., Barros, V., Stocker, T.F., Dahe, Q. (Eds.), Managing the Risks of Extreme Events and Disasters to Advance Climate Change Adaptation. Cambridge University Press, Cambridge, pp. 109–230. https://doi.org/10.1017/CBO9781139177245.006

Serinaldi, F., 2015. Dismissing return periods! Stoch. Environ. Res. Risk Assess. 29, 1179–1189. https://doi.org/10.1007/s00477-014-0916-1

Serinaldi, F., Bonaccorso, B., Cancelliere, A., Grimaldi, S., 2009. Probabilistic characterization of drought properties through copulas. Phys. Chem. Earth, Parts A/B/C 34, 596–605. https://doi.org/10.1016/j.pce.2008.09.004

Shand, T.D., Cox, R.J., Mole, M.A., Carley, J.T., Peirson, W.L., 2011. Coastal storm data analysis: Provision of extreme wave data for adaptation planning, in: 20th Australasian Coastal and Ocean Engineering Conference 2011 and the 13th Australasian Port and Harbour Conference 2011, COASTS and PORTS 2011. pp. 119–125.

Shao, Z., Liang, B., Li, H., Li, P., Lee, D., 2019. Extreme significant wave height of tropical cyclone waves in the South China Sea. Nat. Hazards Earth Syst. Sci. 19, 2067–2077. https://doi.org/10.5194/nhess-19-2067-2019

Shepherd, J.M., Knutson, T., 2007. The Current Debate on the Linkage Between Global Warming and Hurricanes. Geogr. Compass 1, 1–24. https://doi.org/10.1111/j.1749-8198.2006.00002.x

Shiau, J.T., 2006. Fitting Drought Duration and Severity with Two-Dimensional Copulas. Water Resour. Manag. 20, 795–815. https://doi.org/10.1007/s11269-005-9008-9

Siek, M., 2011. Predicting Storm Surges: Chaos, Computational Intelligence, Data Assimilation and Ensembles. CRC Press. https://doi.org/10.1201/b11573

Singleton, F., 2008. The Beaufort scale of winds - Its relevance, and its use by sailors. Weather 63, 37–41. https://doi.org/10.1002/wea.153

Sklar, A., 1959. Fonctions de Répartition à n Dimensions et Leurs Marges. Publ. L'Institut Stat. L'Université Paris 229–231.

Slobbe, E., Vriend, H.J., Aarninkhof, S., Lulofs, K., Vries, M., Dircke, P., 2013. Building with Nature: in search of resilient storm surge protection strategies. Nat. Hazards 65, 947–966. https://doi.org/10.1007/s11069-012-0342-y

Smyth, M.P., Dunning, N.P., Weaver, E.M., van Beynen, P., Zapata, D.O., 2017. The perfect storm: climate change and ancient Maya response in the Puuc Hills region of Yucatán. Antiquity 91, 490–509. https://doi.org/10.15184/aqy.2016.266

Smythe, T.C., 2016. The impacts of Hurricane Sandy on the Port of New York and New Jersey, in: Ng, A.K.Y., Becker, A., Cahoon, S., Chen, S.-L., Earl, P., Yang, Z. (Eds.), Climate Change

and Adaptation Planning for Ports. pp. 74–88.

Song, S., Singh, V.P., 2010. Meta-elliptical copulas for drought frequency analysis of periodic hydrologic data. Stoch. Environ. Res. Risk Assess. 24, 425–444. https://doi.org/10.1007/s00477-009-0331-1

Sorensen, R.M., 2006. Basic Coastal Engineering, Third. ed. Springer US, Boston. https://doi.org/10.1007/b101261

Spalding, M.D., Ruffo, S., Lacambra, C., Meliane, I., Hale, L.Z., Shepard, C.C., Beck, M.W., 2014. The role of ecosystems in coastal protection: Adapting to climate change and coastal hazards. Ocean Coast. Manag. 90, 50–57. https://doi.org/10.1016/j.ocecoaman.2013.09.007

Spencer, T., Brooks, S.M., Evans, B.R., Tempest, J.A., Möller, I., 2015. Southern North Sea storm surge event of 5 December 2013: Water levels, waves and coastal impacts. Earth-Science Rev. 146, 120–145. https://doi.org/10.1016/j.earscirev.2015.04.002

Splinter, K., Harley, M., Turner, I., 2018. Remote Sensing Is Changing Our View of the Coast: Insights from 40 Years of Monitoring at Narrabeen-Collaroy, Australia. Remote Sens. 10, 1744. https://doi.org/10.3390/rs10111744

Sraj, M., Bezak, N., Brilly, M., 2015. Bivariate flood frequency analysis using the copula function: a case study of the Litija station on the Sava River. Hydrol. Process. 29, 225–238. https://doi.org/10.1002/hyp.10145

Stehr, N., Storch, H. von, 2009. Climate and Society. WORLD SCIENTIFIC. https://doi.org/10.1142/7391

Stöber, J., Czado, C., 2017. Pair Copula Constructions, in: Simulating Copulas. pp. 185–230. https://doi.org/10.1142/9789813149250_0005

Stone, G.W., Liu, B., Pepper, D.A., Wang, P., 2004. The importance of extratropical and tropical cyclones on the short-term evolution of barrier islands along the northern Gulf of Mexico, USA. Mar. Geol. 210, 63–78. https://doi.org/10.1016/j.margeo.2004.05.021

Stone, G.W., Orford, J.D., 2004. Storms and their significance in coastal morpho-sedimentary dynamics. Mar. Geol. 210, 1–5. https://doi.org/10.1016/j.margeo.2004.05.003

Sun, Zhang, Yao, Wen, 2019. Hydrological Drought Regimes of the Huai River Basin, China: Probabilistic Behavior, Causes and Implications. Water 11, 2390. https://doi.org/10.3390/w11112390

Swindles, G., Galloway, J., Macumber, A., Croudace, I., Emery, A., Woulds, C., Bateman, M., Parry, L., Jones, J., Selby, K., Rushby, G., Baird, A., Woodroffe, S., Barlow, N., 2018. Sedimentary records of coastal storm surges: Evidence of the 1953 North Sea event. Mar. Geol. 403, 262–270. https://doi.org/10.1016/j.margeo.2018.06.013

Taddicken, M., Reif, A., Hoppe, I., 2018. What do people know about climate change — and how

confident are they? On measurements and analyses of science related knowledge. J. Sci. Commun. 17, 1–26. https://doi.org/10.22323/2.17030201

Tajima, Y., Yasuda, T., Pacheco, B.M., Cruz, E.C., Kawasaki, K., Nobuoka, H., Miyamoto, M., Asano, Y., Arikawa, T., Ortigas, N.M., Aquino, R., Mata, W., Valdez, J., Briones, F., 2014. Initial Report of JSCE-PICE Joint Survey on the Storm Surge Disaster Caused by Typhoon Haiyan. Coast. Eng. J. 56, 1450006-1-1450006–12. https://doi.org/10.1142/S0578563414500065

Takahashi, S., Shimosako, K., Hanzawa, M., 2014. Performance Design for Maritime Structures, in: Young, K. c. (Ed.), Design of Coastal Structures and Sea Defenses. WORLD SCIENTIFIC, Los Angeles, USA, pp. 77–104. https://doi.org/10.1142/9789814611015_0003

Taub, L., 2004. Ancient Meteorology, Ancient Meteorology. Routledge. https://doi.org/10.4324/9780203634288

Thorp, J.M., Scott, B.C., 1982. Preliminary calculations of average storm duration and seasonal precipitation rates for the northeast sector of the united states. Atmos. Environ. 16, 1763–1774. https://doi.org/10.1016/0004-6981(82)90269-4

Tosunoglu, F., Gürbüz, F., İspirli, M.N., 2020. Multivariate modeling of flood characteristics using Vine copulas. Environ. Earth Sci. 79, 459. https://doi.org/10.1007/s12665-020-09199-6

Trifonova, E. V., Valchev, N.N., Andreeva, N.K., Eftimova, P.T., 2012. Critical storm thresholds for morphological changes in the western Black Sea coastal zone. Geomorphology 143–144, 81–94. https://doi.org/10.1016/j.geomorph.2011.07.036

Trigo, I.F., Bigg, G.R., Davies, T.D., 2002. Climatology of Cyclogenesis Mechanisms in the Mediterranean. Mon. Weather Rev. 130, 549–569. https://doi.org/10.1175/1520-0493(2002)130<0549:COCMIT>2.0.CO;2

Trivedi, P.K., Zimmer, D.M., 2006. Copula Modeling: An Introduction for Practitioners. Found. Trends® Econom. 1, 1–111. https://doi.org/10.1561/0800000005

Tsoukala, V.K., Chondros, M., Kapelonis, Z.G., Martzikos, N., Lykou, A., Belibassakis, K., Makropoulos, C., 2016. An integrated wave modelling framework for extreme and rare events for climate change in coastal areas - The case of Rethymno, Crete. Oceanologia 58. https://doi.org/10.1016/j.oceano.2016.01.002

Úbeda Flores, M., de Amo Artero, E., Durante, F., Fernández Sánchez, J. (Eds.), 2017. Copulas and Dependence Models with Applications. Springer International Publishing, Cham. https://doi.org/10.1007/978-3-319-64221-5

United Nations Framework Convention on Climate Change (UNFCCC), 2016. Report of the Conference of the Parties on COP 21. Conf. Parties its twenty- first Sess. (COP 21) 01192, 1.

USGCRP, 2018. Impacts, Risks, and Adaptation in the United States: The Fourth National Climate Assessment, Volume II. Washington, DC. https://doi.org/10.7930/NCA4.2018

Valchev, N., Andreeva, N., Eftimova, P., Trifonova, E., 2014. Prototype of early warning system for coastal storm hazard (Bulgarian black sea \coast). Comptes Rendus L'Academie Bulg. des Sci. 67, 971–978.

van Dongeren, A., Ciavola, P., Martinez, G., Viavattene, C., Bogaard, T., Ferreira, O., Higgins, R., McCall, R., 2018. Introduction to RISC-KIT: Resilience-increasing strategies for coasts. Coast. Eng. 134, 2–9. https://doi.org/10.1016/j.coastaleng.2017.10.007

Van Dongeren, A., Ciavola, P., Viavattene, C., de Kleermaeker, S., Martinez, G., Ferreira, O., Costa, C., McCall, R., 2014. RISC-KIT: Resilience-Increasing Strategies for Coasts - toolKIT. J. Coast. Res. 70, 366–371. https://doi.org/10.2112/SI70-062.1

Van Doorslaer, K., Romano, A., De Rouck, J., Kortenhaus, A., 2017. Impacts on a storm wall caused by non-breaking waves overtopping a smooth dike slope. Coast. Eng. 120, 93–111. https://doi.org/10.1016/j.coastaleng.2016.11.010

Vasseur, L., Thornbush, M.J., Plante, S., 2018. Adaptation to Coastal Storms in Atlantic Canada, SpringerBriefs in Geography. Springer International Publishing, Cham. https://doi.org/10.1007/978-3-319-63492-0

Verlaan, M., Zijderveld, A., de Vries, H., Kroos, J., 2005. Operational storm surge forecasting in the Netherlands: developments in the last decade. Philos. Trans. R. Soc. A Math. Phys. Eng. Sci. 363, 1441–1453. https://doi.org/10.1098/rsta.2005.1578

Vicinanza, D., Lauro, E. Di, Contestabile, P., Gisonni, C., Lara, J.L., Losada, I.J., 2019. Review of Innovative Harbor Breakwaters for Wave-Energy Conversion. J. Waterw. Port, Coastal, Ocean Eng. 145, 03119001. https://doi.org/10.1061/(ASCE)WW.1943-5460.0000519

Vinoth, J., Young, I.R., 2011. Global Estimates of Extreme Wind Speed and Wave Height. J. Clim. 24, 1647–1665. https://doi.org/10.1175/2010JCLI3680.1

Vousdoukas, M., Almeida, L.P.M., Ferreira, Ó., 2012. Beach erosion and recovery during consecutive storms at a steep-sloping, meso-tidal beach. Earth Surf. Process. Landforms 37, 583–593. https://doi.org/10.1002/esp.2264

Vousdoukas, M.I., Voukouvalas, E., Annunziato, A., Giardino, A., Feyen, L., 2016. Projections of extreme storm surge levels along Europe. Clim. Dyn. 47, 3171–3190. https://doi.org/10.1007/s00382-016-3019-5

Wahl, T., Plant, N.G., Long, J.W., 2016. Probabilistic assessment of erosion and flooding risk in the northern Gulf of Mexico. J. Geophys. Res. Ocean. 121, 3029–3043. https://doi.org/10.1002/2015JC011482

Walker, R.A., Basco, D.R., 2011. Application of Coastal Storm Impulse (Cosi) Parameter to Predict Coastal Erosion. Coast. Eng. Proc. 1, 23. https://doi.org/10.9753/icce.v32.management.23

Wamsley, T., Resio, D., Massey, T., Cialone, M., 2011. Screening Method for Determining Coastal Storm Inundation Limits, in: Solutions to Coastal Disasters 2011. American Society of Civil Engineers, Reston, VA, pp. 41–52. https://doi.org/10.1061/41185(417)5

Wang, J., You, Z.-J., Liang, B., 2020. Laboratory investigation of coastal beach erosion processes under storm waves of slowly varying height. Mar. Geol. 430, 106321. https://doi.org/10.1016/j.margeo.2020.106321

Wang, P., Cheng, J., 2017. Storm Impacts on the Morphology and Sedimentology of Open-coast Tidal Flats, in: Coastal Storms. John Wiley & Sons, Ltd, Chichester, UK, pp. 81–98. https://doi.org/10.1002/9781118937099.ch5

Wang, S., McGrath, R., Hanafin, J., Lynch, P., Semmler, T., Nolan, P., 2008. The impact of climate change on storm surges over Irish waters. Ocean Model. 25, 83–94. https://doi.org/10.1016/j.ocemod.2008.06.009

Wei, K., Shen, Z., Ti, Z., Qin, S., 2021. Trivariate joint probability model of typhoon-induced wind, wave and their time lag based on the numerical simulation of historical typhoons. Stoch. Environ. Res. Risk Assess. 35, 325–344. https://doi.org/10.1007/s00477-020-01922-w

Weisse, R., von Storch, H., 2010. Marine weather phenomena, in: Marine Climate and Climate Change. Springer Berlin Heidelberg, Berlin, Heidelberg, pp. 27–76. https://doi.org/10.1007/978-3-540-68491-6_2

Williams, J., Horsburgh, K.J., Williams, J.A., Proctor, R.N.F., 2016. Tide and skew surge independence: New insights for flood risk. Geophys. Res. Lett. 43, 6410–6417. https://doi.org/10.1002/2016GL069522

WMO, 2019. Tropical Cyclones [WWW Document]. URL https://public.wmo.int/en/About-us/FAQs/faqs-tropical-cyclones

WMO, 2017. Guide to Meteorological Instruments and Methods of Observation. Geneva, Switzerland.

WMO, 2015. Tropical cyclone operational plan for the bay of Bengal and the Arabian sea.

Woth, K., Weisse, R., von Storch, H., 2006. Climate change and North Sea storm surge extremes: an ensemble study of storm surge extremes expected in a changed climate projected by four different regional climate models. Ocean Dyn. 56, 3–15. https://doi.org/10.1007/s10236-005-0024-3

Xu, K., Yang, D., Xu, X., Lei, H., 2015. Copula based drought frequency analysis considering the spatio-temporal variability in Southwest China. J. Hydrol. 527, 630–640. https://doi.org/10.1016/j.jhydrol.2015.05.030

Yakir, B., 2013. Extremes in Random Fields, Wiley Series in Probability and Statistics. John Wiley & Sons, Ltd, Chichester, UK. https://doi.org/10.1002/9781118720608

Yao, Z., Xue, Z., He, R., Bao, X., Xie, J., Ge, Q., 2017. Climate projections of spatial variations in coastal storm surges along the Gulf of Mexico and U.S. east coast. J. Ocean Univ. China 16, 1–7. https://doi.org/10.1007/s11802-017-3012-6

Yevjevich, V.M., 1967. An objective approach to definitions and investigations of continental hydrologic droughts. J. Hydrol. 23.

You, Z.-J., 2011. Extrapolation of historical coastal storm wave data with best-fit distribution function. Aust. J. Civ. Eng. 9, 73–82. https://doi.org/10.1080/14488353.2011.11463965

Zanuttigh, B., 2011. Coastal flood protection: What perspective in a changing climate? The THESEUS approach. Environ. Sci. Policy 14, 845–863. https://doi.org/10.1016/j.envsci.2011.03.015

Zehnder, J.A., 2019. Tropical Cyclone. Brittannica.

Zhang, B., Wang, S., 2021. Probabilistic Characterization of Extreme Storm Surges Induced by Tropical Cyclones. J. Geophys. Res. Atmos. 126. https://doi.org/10.1029/2020JD033557

Zhang, B., Wang, S., Wang, Y., 2021. Probabilistic Projections of Multidimensional Flood Risks at a Convection-Permitting Scale. Water Resour. Res. 57. https://doi.org/10.1029/2020WR028582

Zhang, L., Singh, V.P., 2019a. Copulas and Their Properties, in: Copulas and Their Applications in Water Resources Engineering. Cambridge University Press, pp. 62–122. https://doi.org/10.1017/9781108565103.004

Zhang, L., Singh, V.P., 2019b. Copulas and their Applications in Water Resources Engineering. Cambridge University Press. https://doi.org/10.1017/9781108565103

Zhang, L., Singh, V.P., 2019c. Asymmetric Copulas, in: Copulas and Their Applications in Water Resources Engineering. Cambridge University Press, pp. 172–241. https://doi.org/10.1017/9781108565103.006

Zhang, L., Singh, V.P., 2007. Gumbel–Hougaard Copula for Trivariate Rainfall Frequency Analysis. J. Hydrol. Eng. 12, 409–419. https://doi.org/10.1061/(ASCE)1084-0699(2007)12:4(409)